VOLTAMMETRIC SENSORS FOR THE DETERMINATION OF PHARMACEUTICALS

Thesis submitted to

Cochin University of Science and Technology

in partial fulfilment of the requirements for

the award of the degree of

Doctor of Philosophy

in

Chemistry

by

LAINA A.L

Department of Applied Chemistry

Cochin University of Science and Technology

Kochi - 682 022

April 2013

Voltammetric Sensors for the Determination of Pharmaceuticals

Ph. D. Thesis under the Faculty of Science

Author:

LAINA A.L
Research Fellow, Department of Applied Chemistry
Cochin University of Science and Technology
Kochi, India 682 022
E mail: lainaal@gmail.com

Research Guide:

Dr. K. GIRISH KUMAR
Professor of Analytical Chemistry
Department of Applied Chemistry
Cochin University of Science and Technology
Kochi, India 682 022
Email: giri@cusat.ac.in

Department of Applied Chemistry
Cochin University of Science and Technology
Kochi, India 682 022

April 2013

DEPARTMENT OF APPLIED CHEMISTRY
COCHIN UNIVERSITY OF SCIENCE AND TECHNOLOGY
KOCHI - 682 022, INDIA

Dr. K. Girish Kumar **Tel: 0484-2575804**
Professor of Analytical Chemistry **E-mail:** chem@cusat.ac.in

Date: …….

Certificate

Certified that the present work entitled **"Voltammetric Sensors for the Determination of Pharmaceuticals",** submitted by Ms. Laina A.L., in partial fulfillment of the requirements for the degree of Doctor of Philosophy in Chemistry to Cochin University of Science and Technology, is an authentic and bonafide record of the original research work carried out by her under my supervision at the Department of Applied Chemistry. Further, the results embodied in this thesis, in full or in part, have not been submitted previously for the award of any other degree.

K. Girish Kumar
(Supervising Guide)

Declaration

I hereby declare that the work presented in this thesis entitled **"Voltammetric Sensors for the Determination of Pharmaceuticals"** is based on the original work carried out by me under the guidance of Dr. K. Girish Kumar, Professor of Analytical Chemistry, Department of Applied Chemistry, Cochin University of Science & Technology and has not been included in any other thesis submitted previously for the award of any degree.

Kochi-22 *Laina A.L.*
Date:

Dedicated to

Appachan & Ammachi

Acknowledgements

A piece of work to become perfect, one needs the blessings and help of many. For the completion of this research work, I am indebted to many for their generous contributions, be it in the form of a piece of advice or suggestions for improvement.

First of all, let me bow my head in reverent gratitude to God almighty for the manifold blessings showered on me and for the undeserving grace shown to me for the successful completion of this work.

Let me place on record my profound gratitude to my supervising guide Prof. K. Girish Kumar for admitting me in to the programme. His scholarly assistance, inspiring guidance and amiable demeanor really helped me to complete the work in the stipulated time. Apart from the subject of my research, I learnt a lot from him, which I am sure, will be useful in different stages of my life. His simplicity, moral ethics, behavior towards colleagues and students inspired me a lot. Sir, I consider it as a blessing to work under you.

I would like to thank Prof. K. Sreekumar, Head of the Department and my doctoral committee member for his continuous help and encouragement to pursue my research. I am grateful to all teachers of the department for their help and valuable suggestions. I express my sincere thanks to all the non-teaching staff of the department for the help and support they have rendered to me.

I owe a special thanks to Dr. Anitha I., Associate professor of chemistry for her support and help

I am truly grateful to my seniors Dr. Remalakshmy Poduval, Dr. Pearl, Dr. Sareena, Dr. Beena, Dr. Sindhu, Litha chechi, Dr. Renjini, Dr. Sobhana and Dr. Leena and my friends Theresa chechi, Divya chechi, Ajilesh chettan, Sajitha chechi,

Soumya, Jesny chechi, Anuja, Zafna chechi, Rajitha, Ajith, Shinu, Sreejith, Sruthy and Meera for their whole-hearted support, assistance and suggestive criticisms during my research work. Writing this thesis was not the lonely experience it could have been because of cherished friends who provided enthusiasm and empathy in just the right doses. The wonderful companionship of Dr. Sindhu, Dr. Renjini, Dr. Sobhana, Dr. Leena, Theresa chechi, Divya chechi, Soumya, Jesny chechi, Anuja, Zafna chechi, Sreejith, Sruthy and Sheela miss and many others ensures that I can only think back upon the last few years with feelings of fondness and reminisce. I am grateful to recall a lot of splendid memories I had with Renjini chehi, Soumya, Anuja, Jayalakshmi and Shinitha in the hostel.

My thanks to the friends from other labs in the department for the help and support rendered. I thank Nisha Nandhakumar and Umadevi T. U for their wonderful friendship.

It is my pleasure to put in a word of gratitude to the Cochin University of Science and Technology and Inter University Centre For Nanomaterials and Devices for the fellowship. My thanks also goes to the Directorate of Extramural Research and Property Rights, DRDO, New Delhi for their funding assistance. My sincere thanks to Dr. Devala Rao, Principal, KVSR College of Pharmacy, Vijayawada for providing pure drug samples.

My appachan and ammachi deserves special mention for their consistent support and encouragements. They have shown that persistent hard work and respecting the dignity of fellow beings is the road to success. They sincerely raised me with their caring and constant prayers and never failed to remind me to seek God's will in all things so that He will show which path to take. Hence, this thesis is dedicated to them. It is a pleasure to pay tribute for the care and prayers given by my dearest sister Varsha, when I was very much tensed. I express my extreme

gratitude to my in laws and sister in law Anila for the love and support extended to me.

The unconditional love and encouragement provided by my beloved husband Anil served as a secure anchor during the hard and easy times; thank you. Without his wholehearted support it would not have been possible me to complete this work.

Laina A.L

Preface

Electrochemical sensors are increasingly being investigated to perform measurements for single or multiple analytes. Demanded by modern medical diagnosis, advances in microfabrication technology have led to the development of fast, sensitive and selective electrochemical sensors for drug analysis. Electrochemical sensors for the measurement of analytes of interest in clinical chemistry are ideally suited for these applications, due to their high sensitivity and selectivity, simple-to-operate, rapid response time and low-cost.

As part of the present investigations eight voltammetric sensors have been fabricated for six drugs such as PAM Chloride, Tamsulosin Hydrochloride, Hesperidin Methyl Chalcone, Guaiphenesin, Cephalexin and Amoxicillin trihydrate. The modification techniques adopted as part of the present work include multiwalled carbon nanotube (MWNT) based modifications, electropolymerization, gold nanoparticle (AuNP) based modifications and platinum nanoparticle (PtNP) based modifications.

The thesis is divided into nine chapters. A brief account of the different chapters is given below.

Chapter 1 gives a detailed description about the various electroanalytical techniques and their application. It gives a brief description about the different types of chemical sensors and discusses in detail about electrochemical sensors. The chapter also gives a brief review of the important voltammetric sensors developed for different drugs.

Chapter 2 gives a brief sketch of the materials and methods used in the investigation. This chapter explains the procedure for the fabrication of chemically modified electrodes as voltammetric sensors for the determination of various drugs. It also discusses the procedure for the analysis of drug content in pharmaceutical formulations and also in real samples like urine. The instruments used in the present investigation are also discussed.

Chapter 3 deals with the development of MWNT based sensor for the determination of the drug Pyridine-2- Aldoxime Methochloride (PAM chloride). The electrochemical response characteristics are described in detail and the application study of the developed sensor in the determination of the drug in urine samples have also been dealt with in detail.

Chapter 4 deals with the development of a differential pulse voltammetric sensor for the determination of Tamsulosin Hydrochloride (TAM) using a MWNT modified glassy carbon electrode (GCE). The determination conditions, such as the amount of MWNT- Nafion suspension, pH of the supporting electrolyte and scan rate were optimized. The analytical applications of the developed sensor in the determination of the drug in pharmaceutical formulations and real sample like urine were also investigated.

Chapter 5 presents the fabrication of a Prussain blue (PB)/MWNT nanocomposite film based sensor for the quantitative determination of Hesperidin Methyl Chalcone (HMC). The response parameters of the newly developed sensor as well as its analytical applications have been discussed in this chapter.

Chapter 6 describes the development of four simple electrochemical sensors for the voltammetric determintion of Guaiphenesin (Guai). The sensors fabricated include (1) poly (p-aminobenzenesulphonic acid) [poly (p-ABSA)] modified glassy carbon sensor and (2) MWNT/ poly (p-aminobenzenesulphonic acid) [poly (p-ABSA)] modified glassy carbon sensor. Screen printed carbon electrodes (SPCE) modified with poly (p-ABSA) and MWNT were also used for the determination of Guai. Optimization studies of the developed sensors, response characteristics and analytical applications are dealt with in detail in this chapter.

Chapter 7 details the electrocatalytic oxidation of Cephalexin (Ceph) at a AuNP modified GCE. Electrochemical parameters of Ceph on the modified electrode were analyzed. To evaluate the application potential of the developed sensor, it was successfully applied to determine Ceph in commercial formulation and body fluid.

Chapter 8 is devoted to the detailed description about development and performance characteristics of two sensors for the drug Amoxicillin trihydrate (AMX) viz, (1) MWNT/ AuNP modified glassy carbon sensor and (2) MWNT/ PtNP modified glassy carbon sensor. Optimization studies of the developed sensor, response characteristics and analytical applications are dealt with in detail in this chapter.

Chapter 9 gives the summary and the conclusions of the work done. References are given as a separate section at the end of the thesis.

Contents

Chapter **1**

INTRODUCTION.....01 - 56

1.1 Types of electroanalytical methods---------- 02
1.2 Types of chemical sensors ---------- 05
1.2.1 Optical ---------- 05
1.2.2 Mass sensitive---------- 05
1.2.3 Heat sensitive ---------- 05
1.2.4 Electrochemical---------- 06
1.2.4.1 Amperometric sensors----------07
1.2.4.1.1 Principles----------07
1.2.4.2 Voltammetric Sensors ----------08
1.3 Solution structure; the double layer ---------- 09
1.4 Faradaic and nonfaradaic currents---------- 10
1.5 Diffusion ---------- 11
1.6 Migration---------- 12
1.7 Convection---------- 13
1.8 General theory---------- 14
1.9 Voltammetric instrumentation ---------- 16
1.9.1 The electrodes and cell ---------- 16
1.9.2 Reference Electrodes (RE) ---------- 17
1.9.3 Counter Electrodes (CE)---------- 19
1.9.4 Working Electrodes (WE)---------- 19
1.9.5 Supporting electrolyte ---------- 20
1.9.6 Cell atmosphere---------- 21
1.10 Surface modification for electrode protection---------- 21
1.10.1 Conducting polymers ---------- 23
1.10.2 Nanomaterials---------- 24
1.11 Different voltammetric techniques ---------- 26
1.11.1 Linear Sweep Voltammetry (LSV) ---------- 26
1.11.2 Cyclic Voltammetry (CV)---------- 28
1.11.3 Pulse Methods---------- 29
1.11.3.1 Normal Pulse Voltammetry (NPV) ----------29
1.11.3.2 Differential Pulse Voltammetry (DPV) ----------30
1.11.3.3 Square Wave Voltammetry (SWV)----------30
1.11.4 Preconcentration and stripping techniques---------- 31
1.11.4.1 Anodic Stripping Voltammetry (ASV)----------32
1.11.4.2 Cathodic Stripping Voltammetry (CSV)----------32
1.11.4.3 Adsorptive Stripping Voltammetry (AdSV)----------33
1.12 Selecting the voltammetric technique ---------- 34
1.13 Brief Review on voltammetric sensors for drugs (modifications based on MWNT, prussian blue, poly (p-ABSA), AuNP and PtNP)----------36
1.14 Scope of the present investigation ---------- 52

Chapter **2**

MATERIALS AND METHODS.....57 - 67

2.1 Reagents---------- 57
2.2 Instruments used ---------- 58
2.3 Cleaning of PtE---------- 58
2.4 Cleaning of GCE---------- 59
2.5 Preparation of chemically modified electrodes for pharmaceutical analysis---------- 59
2.5.1 Preparation of MWNT modified PtE---------- 59
2.5.2 Preparation of MWNT modified GCE---------- 60
2.5.3 Preparation of Prussian blue (PB)/MWNT modified GCE----- 60
2.5.4.1 Preparation of poly (p-aminobenzenesulphonic acid) modified GCE---------- 61
2.5.4.2 Preparation of MWNT/poly (p-ABSA) modified GCE
2.5.5 Preparation of gold nanoparticle (AuNP) modified GCE------ 61
2.5.6.1 Preparation of platinum nanoparticle (PtNP) modified GCE---------- 61
2.5.6.2 Preparation of MWNT/AuNP and MWNT/PtNP modified GCE---------- 61
2.6 Preparation of the drug solutions ---------- 62
2.7 Preparation of buffer solutions ---------- 62
2.7.1 Preparation of phosphate buffer solution (PBS)---------- 62
2.7.2 Preparation of acetate buffer solution (ABS)---------- 62
2.8 Analysis of the pharmaceutical formulations ---------- 62
2.8.1 Tablet for Tamsulosin Hydrochloride (Veltam)---------- 62
2.8.2 Tablet for Guaiphenesin (Expal) ---------- 63
2.8.3 Tablet for Cephalexin (Citaceph) ---------- 63
2.8.4 Tablet for Amoxicillin trihydrate (Pressmox) ---------- 64
2.9 Analysis of urine sample---------- 64
2.10 Standard methods---------- 64
2.10.1 PAM Chloride---------- 64
2.10.2 Tamsulosin Hydrochloride---------- 65
2.10.3 Guaiphenesin---------- 65
2.10.4 Cephalexin---------- 65
2.10.5 Amoxicillin trihydrate ---------- 65

Chapter **3**

DEVELOPMENT OF SENSOR FOR PYRIDINE-2- ALDOXIME METHOCHLORIDE .....69 - 87

3.1 Introduction ---------- 69
3.2 Preparation of MWNT-modified Pt electrode---------- 72
3.3 Electrochemical behaviour of PAM chloride ---------- 72

3.4 Evidences of electrode modification ---------- 74
3.4.1 SEM images ---------- 74
3.4.2 Surface area study ---------- 74
3.5 Performance characteristics of the developed sensor ---------- 75
3.5.1 Effect of supporting electrolyte ---------- 75
3.5.2 Effect of pH ---------- 75
3.5.3 Effect of amount of the MWNT-Nafion dispersion ---------- 76
3.5.4 Effect of scan rate ---------- 76
3.5.5 Influence of concentration ---------- 77
3.5.6 Interference study ---------- 78
3.6 Analytical application ---------- 78
3.6.1 Determination of PAM chloride in urine sample ---------- 79
3.7 Conclusions ---------- 79

Chapter **4**

DEVELOPMENT OF SENSOR FOR TAMSULOSIN HYDROCHLORIDE ..... 89 - 107

4.1 Introduction ---------- 89
4.2 Preparation of MWNT-modified GCE ---------- 92
4.3 Electrochemical behaviour of TAM ---------- 92
4.4 Evidences of electrode modification ---------- 94
4.4.1 SEM images ---------- 94
4.4.2 Surface area study ---------- 94
4.5 Performance characteristics of the developed sensor ---------- 95
4.5.1 Influence of supporting electrolyte ---------- 95
4.5.2 Influence of pH ---------- 95
4.5.3 Influence of amount of MWNT-Nafion suspension ---------- 96
4.5.4 Influence of scan rate ---------- 96
4.5.5 Influence of concentration ---------- **97**
4.5.6 Interference study ---------- 97
4.6 Analytical Applications ---------- 98
4.6.1 Determination of TAM in pharmaceutical formulations ---------- 98
4.6.2 Determination of TAM in urine sample ---------- 98
4.7 Conclusions ---------- 99

Chapter **5**

DEVELOPMENT OF SENSOR FOR HESPERIDIN METHYL CHALCONE ..... 109 - 126

5.1 Introduction ---------- 109
5.2 Preparation of PB/MWNT-modified GCE ---------- 112
5.3 Electrochemical behaviour of HMC ---------- 112
5.4 Evidences of electrode modification ---------- 114

5.4.1 SEM images ---------- 114
5.4.2 Surface area study ---------- 114
5.5 Performance characteristics of the developed sensor ---------- 115
5.5.1 Effects of supporting electrolyte and pH ---------- 115
5.5.2 Effect of amount of the PB/MWNT dispersion ---------- 115
5.5.3 Effect of scan rate ---------- 116
5.5.4 Calibration curve ---------- 117
5.5.5 Interference study ---------- 117
5.6 Analytical Applications ---------- 118
5.6.1 Determination of HMC in urine sample ---------- 118
5.7 Conclusions ---------- 118

Chapter **6**

DEVELOPMENT OF SENSOR FOR GUAIPHENESIN ..... 127 - 152

6.1 Introduction ---------- 127
6.2 Preparation of poly (p-ABSA) modified GCE ---------- 130
6.3 Preparation of MWNT/poly (p-ABSA) modified GCE ---------- 131
6.4 Preparation of poly (p-ABSA) / SPCE and MWNT/poly (p-ABSA) / SPCE ---------- 131
6.5 Electrochemical behaviour of Guai ---------- 131
6.6 Evidences of electrode modification ---------- 133
6.6.1 SEM images ---------- 133
6.6.2 Surface area study ---------- 133
6.7 Performance characteristics of the developed sensors ---------- 134
6.7.1 Effect of the supporting electrolyte ---------- 134
6.7.2 Effect of film thickness ---------- 134
6.7.3 Effect of amount of the MWNT-Nafion dispersion ---------- 135
6.7.4 Effect of scan rate ---------- 135
6.7.5 Influence of concentration ---------- 136
6.7.6 Interference study ---------- **137**
6.8 Application potential of the developed sensors ---------- 137
6.8.1 Determination of Guai in pharmaceutical formulations ---------- 137
6.8.2 Determination of Guai in urine sample ---------- 138
6.9 Conclusions ---------- 138

Chapter **7**

DEVELOPMENT OF SENSOR FOR CEPHALEXIN ..... 153 - 172

7.1 Introduction ---------- 153
7.2 Preparation of AuNP modified GCE ---------- 156
7.3 Electrochemical behaviour of Ceph ---------- 156
7.4 Evidences of electrode modification ---------- 157
7.4.1 SEM images ---------- 157

7.4.2 Surface area study ---------- 157
7.5 Performance characteristics of the developed sensor ---------- 158
7.5.1 Choice of supporting electrolyte ---------- 158
7.5.2 Effect of film thickness ---------- 158
7.5.3 Effect of scan rate ---------- 158
7.5.4 Calibration curve ---------- 159
7.5.5 Interference Study ---------- **160**
7.6 Amperometric response of the AuNP/GCE ---------- 160
7.7 Analytical Applications ---------- 161
7.7.1 Determination of Ceph in pharmaceutical formulation ---------- 161
7.7.2 Determination of Ceph in urine sample ---------- 162
7.8 Conclusions ---------- 162

Chapter **8**

DEVELOPMENT OF SENSOR FOR AMOXICILLIN TRIHYDRATE ..... 173 - 200

8.1 Introduction ---------- 173
8.2 Preparation of MWNT/AuNP modified GCE ---------- 178
8.3 Preparation of MWNT/PtNP modified GCE ---------- 179
8.4 Electrochemical behaviour of AMX ---------- 179
8.5 Evidences of electrode modification ---------- 181
8.5.1 SEM images ---------- 181
8.5.2 Surface area study ---------- 181
8.6 Performance characteristics of the developed sensors ---------- 181
8.6.1 Effect of the supporting electrolyte ---------- 181
8.6.2 Effect of pH ---------- 182
8.6.3 Effect of film thickness ---------- 182
8.6.3.1 Effect of number of scan cycles for the electrodeposition of AuNPs ---------- 183
8.6.3.2 Effect of the electrodeposition time of PtNP ---------- 183
8.6.3.3 Influence of amount of MWNT-Nafion dispersion ---------- 183
8.6.4 Effect of scan rate ---------- 184
8.6.5 Calibration curve ---------- 185
8.6.6 Stability and reproducibility ---------- 185
8.6.7 Interference study ---------- 186
8.7 Analytical Applications ---------- 186
8.7.1 Determination of AMX in pharmaceutical formulations ---------- 186
8.7.2 Determination of AMX in urine sample ---------- 187
8.8 Conclusions ---------- 187

Chapter **9**

SUMMARY AND CONCLUSIONS ..... 201 - 205

9.1 The objectives of the work---------- 201
9.2 Summary of the work done---------- 203

REFERENCES..... 207 - 228

LIST OF PUBLICATIONS ..... 229 - 230

RESEARCH PAPERS PUBLISHED IN INTERNATIONAL JOURNALS 229
PAPERS PRESENTED IN NATIONAL / INTERNATIONAL CONFERENCES 230

List of Tables

Table 2.1 Preparation of the drug solutions (0.1 M) ---- 67

Table 2.2 Preparation of PBS of different pH ---- 67

Table 2.3 Preparation of ABS of different pH ---- 67

Table 3.1 Comparison of various methods ---- 80

Table 3.2 Interference study ---- 80

Table 3.3 Determination of PAM chloride in urine sample ---- 80

Table 3.4 Comparison of the results obtained with the developed sensor and the standard method ---- 80

Table 4.1 Comparison of various analytical methods ---- 100

Table 4.2 Interference study ---- 100

Table 4.3 Determination of TAM in tablets ---- 100

Table 4.4 Determination of TAM in urine sample ---- 100

Table 5.1 Interference study ---- 119

Table 5.2 Determination of HMC in urine sample ---- 119

Table 6.1 Concentration studies of the developed sensors ---- 139

Table 6.2 Comparison of the present work with some of the reported works ---- 139

Table 6.3 Study of the effect of foreign species on the anodic peak current of 1×10^{-3} M Guai at poly (p-ABSA)/GCE and MWNT/ Poly (PABSA)/GCE ---- 140

Table 6.4 Determination of Guai in pharmaceutical preparation ---- 140

Table 6.5 Determination of Guai in urine sample ---- 140

Table 7.1 Comparison of the developed method with other reported works for the determination of Ceph ---- 163

Table 7.2 Influence of 10^{-1} M foreign species on the anodic peak current of 1×10^{-3} M Ceph ---- 163

Table 7.3 Determination of Ceph in tablets ---- 164

Table 7.4 Determination of Ceph in urine sample ---- 164

Table 8.1 Comparison of various analytical methods ---- 188

Table 8.2 Study of the effect of foreign species on the anodic peak current of 1×10^{-3} M AMX at MWNT/AuNP/GCE and MWNT/PtNP/GCE ---- 189

Table 8.3 Determination of AMX in pharmaceutical preparation ---- 189

Table 8.4 Determination of AMX in urine sample ---- 189

List of Figures

Figure 1.1 Common electroanalytical methods ---------- 54

Figure 1.2 Electrical double layer formed at electrode surface as a result of an applied potential ---------- 54

Figure 1.3 Typical steps involved in an electrode reaction ---------- 55

Figure 1.4 Modes of mass transfer ---------- 55

Figure 1.5 Excitation signals used in voltammetry ---------- 56

Figure 1.6 Linear sweep voltammogram ---------- 56

Figure 3.1 Structure of PAM chloride ---------- 81

Figure 3.2 Differential pulse voltammmograms of 1×10^{-3} M PAM chloride at (a) bare Pt (b) MWNT- modified Pt electrode ---------- 81

Figure 3.3 SEM images of (a) bare Pt electrode and (b) MWNT modified Pt electrode ---------- 82

Figure 3.4 Surface area study of (a) bare Pt electrode and (b) MWNT modified Pt electrode in $K_3Fe(CN)_6$ solution ---------- 82

Figure 3.5 Effect of pH ---------- 83

Figure 3.6 Amount of MWNT dispersion ---------- 83

Figure 3.7 LSV of PAM chloride at different scan rates (20-180 mV/s) in PBS ---------- 84

Figure 3.8 Plot of peak currents as a function of the square root of scan rates ---------- 84

Figure 3.9 Effect of scan rate ---------- 85

Figure 3.10 Plot of peak potential against ln scan rate ---------- 85

Figure 3.11 Reaction mechanism ---------- 86

Figure 3.12 Differential pulse voltammograms of concentrations 1×10^{-3}, 8×10^{-4}, 5×10^{-4}, 1×10^{-4}, 6×10^{-5}, 1×10^{-5}, 6×10^{-6} and 1×10^{-6} M of PAM chloride (from bottom to top) ---------- 86

Figure 3.13 Calibration graph of PAM chloride at MWNT modified Pt electrode ---------- 87

Figure 4.1 Structure of TAM ---------- 101

Figure 4.2 Voltammograms of 1×10^{-3} M TAM at (a) bare GCE (b) MWNT modified GCE ---------- 101

Figure 4.3 SEM image of (a) bare GCE (b) MWNT modified GCE ---------- 101

Figure 4.4 Overlay of square wave voltammograms of 2 mM $K_3Fe(CN)_6$ solution obtained at (a) bare GCE (b) MWNT modified GCE-------- 102

Figure 4.5 Effect of pH on the anodic peak current of 1×10^{-3} M TAM ---------- 103

Figure 4.6 Effect of the amount of MWNT–Nafion dispersion at MWNT modified GCE ---------- 103

Figure 4.7 Overlay of SWVs of TAM at MWNT/GCE in 0.1 M acetate buffer (pH 5) containing 1×10^{-3} M TAM at different scan rates 20, 40, 60, 80, 100, 120, 140, 160,180, 200 mV/s (from top to bottom).---------- 104

Figure 4.8 Variation of the anodic currents of TAM as a function of square root of scan rates---------- 104

Figure 4.9 Variation of log I_p versus log ν---------- 105

Figure 4.10 Variation of ln scan rate versus anodic potential---------- 105

Figure 4.11 Reaction mechanism---------- 106

Figure 4.12 Differential pulse voltammograms of concentrations of 10^{-7} to 10^{-3} M of TAM (from top to bottom) ---------- 106

Figure 4.13 Dependence of concentration of TAM on peak current---------- 107

Figure 5.1 Structure of HMC ---------- 120

Figure 5.2 (I) Cyclic voltammmograms of 1×10^{-3} M HMC at (a) bare GCE (b) PB/MWNT modified GCE and (II) Differential pulse voltammmograms of 1×10^{-3} M HMC at (a) bare GCE (b) PB/MWNT modified GCE---------- 120

Figure 5.3 SEM images of (A) bare GCE (B) PB/MWNT modified GCE------- 120

Figure 5.4 Surface area studies at (a) bare GCE and (b) PB/MWNT modified GCE and inset are plot of peak currents as a function of the square root of scan rates ---------- 121

Figure 5.5 Variation of cathodic peak current with pH of the medium ---------- 122

Figure 5.6 Effect of the amount of PB/MWNT-Nafion suspension at modified GCE ---------- 122

Figure 5.7 (a) Overlay of linear sweep voltammograms of 1×10^{-3} M HMC at PB/MWNT modified GCE in 0.1 M acetate buffer at different scan rates (20 to 280 mV/s) and (b) Overlay of square wave voltammograms of 1×10^{-3} M HMC at PB/MWNT modified GCE in 0.1 M acetate buffer at different scan rates (20 to 220 mV/s).---------- 123

Figure 5.8 Plot of peak currents as a function of the square root of scan rates obtained from (a) linear sweep voltammetric studies and (b) square wave voltammetric studies. ---------- 124

Figure 5.9 Plot of log I versus log ν ---------- 124

Figure 5.10 Variation of ln scan rate versus cathodic potential from (a) linear sweep voltammetric studies and (b) square wave voltammetric studies. ---------- 125

Figure 5.11 Reaction Mechanism ---------- 125

Figure 5.12 Differential pulse voltammograms of HMC at different concentrations, 10^{-3}-10^{-7} M (top to bottom) ---------- 126

Figure 5.13 Plot of peak currents as a function of concentration of HMC--------- 126

Figure 6.1 Structure of Guai ---------- 141

Figure 6.2 Electropolymerization of p-ABSA---------- 141

Figure 6.3 Electrochemical response of Guai on various modified GCE--------- 142

Figure 6.4 Cyclic Voltammmograms of 1×10^{-3} M Guai at (a) bare SPCE (b) poly (p-ABSA) modified SPCE and (C) MWNT / poly (p-ABSA) modified SPCE ---------- 142

Figure 6.5 SEM images of (a) bare GCE (b) poly (p-ABSA)/GCE and (c) MWNT/poly (p-ABSA)/GCE ---------- 143

Figure 6.6 Surface area studies at (A) bare GCE (B) poly (p-ABSA)/GCE (C) MWNT/poly (p-ABSA)/GCE (D) bare SPCE (E) poly (p-ABSA)/SPCE (F) MWNT/poly (p-ABSA)/SPCE ---------- 144

Figure 6.7 Differential pulse voltammograms of Guai at different polymerization cycles (A) 10 cycles (B) 20 cycles(C) 30 cycles(D) 40 cycles(E) 50 cycles(F) 60 cycles---------- 145

Figure 6.8 Amount of MWNT dispersion---------- 145

Figure 6.9 Overlay of linear sweep voltammograms of 1×10^{-3} M Guai at (A) poly (p-ABSA) modified GCE and (B) MWNT / poly (p-ABSA) modified GCE in 0.1 M HCl at different scan rates and Overlay of square wave voltammograms of 1×10^{-3} M Guai at (C) poly (p-ABSA) modified GCE and (D) MWNT / poly (p-ABSA) modified GCE in 0.1 M HCl at different scan rates. ---------- 146

Figure 6.10 The plot of peak currents as a function of the square root of scan rates from linear sweep voltammetric studies of 1×10^{-3} M Guai at (A) poly (p-ABSA) modified GCE and (B) MWNT / poly (p-ABSA) modified GCE and square wave voltammetric studies of 1×10^{-3} M Guai at (C) poly (p-ABSA) modified GCE and (D) MWNT/poly (p-ABSA) modified GCE.----------147

Figure 6.11 Overlay of cyclic voltammograms of Guai at (A) poly (p-ABSA) modified GCE (B) MWNT/poly (p-ABSA) modified GCE (C) poly (p-ABSA) modified SPCE and (D) MWNT/poly (p-ABSA) modified SPCE in 0.1 M HCl at different scan rates. ----- 148

Figure 6.12 The plot of peak currents as a function of the square root of scan rates from cyclic voltammetric studies of Guai at (A) poly (p-ABSA) modified GCE (B) MWNT/poly (p-ABSA) modified GCE (C) poly (p-ABSA) modified SPCE and (D) MWNT/poly (p-ABSA) modified SPCE in 0.1 M HCl at different scan rates. ---------- 149

Figure 6.13 Plot of peak potential against ln (scan rate) from cyclic voltammetric studies of Guai at (A) poly (p-ABSA) modified GCE (B) MWNT/poly (p-ABSA) modified GCE (C) poly (p-ABSA) modified SPCE and (D) MWNT/poly (p-ABSA) modified SPCE in 0.1 M HCl at different scan rates. ---------- 150

Figure 6.14 Reaction Mechanism---------- 150

Figure 6.15 Differential pulse voltammograms of Guai at different concentrations on (A) poly (p-ABSA) modified GCE and (B) MWNT/poly (p-ABSA) modified GCE and square wave voltammograms of Guai at different concentrations on (C) poly (p-ABSA) modified GCE and (D) MWNT/poly (p-ABSA) modified GCE. Insets are the plot of peak currents as a function of concentration of Guai.---------- 151

Figure 6.16 Cyclic voltammograms of Guai at different concentrations on (A) poly (p-ABSA) modified SPCE and (B) MWNT/poly (p-ABSA) modified SPCE. Insets are the plot of peak currents as a function of concentration of Guai. ---------- 152

Figure 7.1 Structure of Ceph---------- 165

Figure 7.2 Electrodeposition of AuNP ---------- 165

Figure 7.3 Electrochemical response of Ceph on various electrodes (A) Bare gold electrode (B) MWNT/GCE (C) Platinum nanoparticle /GCE (D) Poly p-toluenesulphonic acid/GCE (E) Bare GCE (F) Poly L-cysteine/GCE (G) AuNP/GCE (H) Poly o-phenylenediammine /GCE (I) Manganese porphyrin/GCE (J) Copper nanoparticle/GCE---------- 166

Figure 7.4 SEM images of (A) bare GCE (B) AuNP modified GCE ---------- 166

Figure 7.5 Surface area studies at (a) bare GCE and (b) AuNP modified GCE and inset are plot of peak currents as a function of the square root of scan rates---------- 167

Figure 7.6 Square wave voltammograms of Ceph at different electro deposition cycles (A) 10 cycles (B) 20 cycles (C) 30 cycles (D) 50 cycles (E) 40 cycles (F) 60 cycles ---------- 168

Figure 7.7 Overlay of square wave voltammograms of Ceph at different scan rates 40, 80, 120, 160, 200, 240, 280, 320, 360, 400 mV/s in 0.1 M NaOH ---------- 168

Figure 7.8 Influence of scan rate ---------- 169

Figure 7.9 Plot of potential versus ln ν ---------- 169

Figure 7.10 Reaction mechanism ---------- 170

Figure 7.11 Plot of log I versus log ν ---------- 170

Figure 7.12 Square wave voltammograms of oxidation of Ceph of concentrations of 1×10^{-6}, 4×10^{-6}, 8×10^{-6}, 2×10^{-5}, 5×10^{-5}, 8×10^{-5}, 2×10^{-4}, 5×10^{-4}, 8×10^{-4}, 1×10^{-3} M (from top to bottom) ---------- 171

Figure 7.13 Dependence of concentration of Ceph on peak current ---------- 171

Figure 7.14 Current–time recordings obtained on increasing the Ceph concentration in 1×10^{-4} M steps at AuNP modified GCE. Operating potential, -1050 mV. ---------- 172

Figure 7.15 The calibration curve for the amperometric response ---------- 172

Figure 8.1 Structure of AMX ---------- 190

Figure 8.2 Electrodeposition of PtNP ---------- 190

Figure 8.3 Electrochemical response of AMX on (A) bare GCE (B) MWNT/AuNP modified GCE (C) MWNT/PtNP modified GCE ------- 191

Figure 8.4 SEM images of (A) bare GCE (B) AuNP modified GCE (C) PtNP modified GCE (D) MWNT/AuNP modified GCE (E) MWNT/PtNP modified GCE ---------- 192

Figure 8.5 Surface area studies at (A) bare GCE (B) MWNT/AuNP/GCE (C) MWNT/PtNP/GCE and inset are plot of peak currents as a function of the square root of scan rates ---------- 193

Figure 8.6 Relationship between anodic peak current and pH of the medium at (A) MWNT/AuNP/GCE (B) MWNT/PtNP/GCE --------- 194

Figure 8.7 Plot of anodic peak potential of 1×10^{-3} M AMX versus pH of the medium at (A) MWNT/AuNP/GCE (B)MWNT/PtNP/GCE ----- 194

Figure 8.8 Differential pulse voltammograms of AMX at different electrodeposition cycles (a) 100 cycles (b) 10 cycles (c) 90 cycles (d) 20 cycles (e) 80 cycles (f) 30 cycles (g) 60 cycles (h) 50 cycles (i) 70 cycles (j) 40 cycles ---------- 195

Figure 8.9 Effect of electrodeposition time of PtNP---------- 195

Figure 8.10 Effect of the amount of MWNT dispersion at (A) AuNP/GCE (B) PtNP/GCE ---------- 196

Figure 8.11 Overlay of linear sweep voltammograms of 1×10^{-3} M AMX at (A) MWNT/AuNP/GCE (B) MWNT/PtNP/GCE in 0.1 M PBS at different scan rates. ---------- 197

Figure 8.12 Variance of anodic peak current of AMX with scan rate at (A) MWNT/AuNP/GCE (B) MWNT/PtNP/GCE ---------- 197

Figure 8.13 Plot of log I versus log ν at (A) MWNT/AuNP/GCE (B) MWNT/PtNP/GCE sensors ---------- 198

Figure 8.14 Plot of peak potential against ln scan rate at (A) MWNT/AuNP/GCE (B) MWNT/PtNP/GCE sensors ---------- 198

Figure 8.15 Mechanism of oxidation of AMX---------- 199

Figure 8.16 Differential pulse voltammograms of AMX at different concentrations, 10^{-3} - 10^{-6} M (from bottom to top) on (A) MWNT/AuNP/GCE (B) MWNT/PtNP/GCE ---------- 199

Figure 8.17 Dependence of concentration of AMX on peak current at (A) MWNT/AuNP/GCE (B) MWNT/PtNP/GCE ---------- 200

.....ഌ൹.....

Chapter 1

INTRODUCTION

Contents

1.1 Types of electroanalytical methods
1.2 Types of chemical sensors
1.3 Solution structure; the double layer
1.4 Faradaic and nonfaradaic currents
1.5 Diffusion
1.6 Migration
1.7 Convection
1.8 General theory
1.9 Voltammetric instrumentation
1.10 Surface Modification for Electrode Protection
1.11 Different voltammetric techniques
1.12 Selecting the voltammetric technique
1.13 Brief review on voltammetric sensors for drugs
1.14 Scope of the present investigation

Electroanalytical chemistry is the branch of analytical chemistry that employs electrochemical methods to obtain information related to the amounts, properties, and environments of chemical species. The overlap between electroanalytical chemistry and chemical analysis, on one hand, and electroanalytical chemistry and physical electrochemistry on the other, is considerable. Electroanalytical chemistry has made contributions from the two fields it spans. Isaac Maurits Kolthoff once defined electroanalytical chemistry as the application of electrochemistry to analytical chemistry. It is preferable to consider electroanalytical chemistry as that area of analytical chemistry and electrochemistry in which the electrode is used as a probe, to measure something that directly or indirectly involves the electrode [1].

Electroanalytical techniques are the best known analytical method, which can boast the following advantages:

1) Low detection and determination limits.

2) High sensitivity.

3) Relative simplicity, rapidity.

4) Wide spectrum of the analyte (especially drug compounds).

5) Insignificant effect of the matrix (from endogenous substances in biological media or from excipients in pharmaceutical dosage forms).

6) Low cost of equipment.

1.1 Types of electroanalytical methods

Electroanalytical chemistry encompasses a group of quantitative analytical methods that are based upon the electrical properties of the solution. Many types of electroanalytical methods have been developed. For the purpose of classification, these methods can be divided into interfacial methods and bulk methods. Interfacial methods, which are more widely used than bulk methods, are based on the phenomena that occur at the interface between electrode surface and the thin layer of solution just adjacent to these surface. Bulk methods, in contrast, are based on phenomena that occur in the bulk of the solution: every effort is made to avoid interfacial effects.

Interfacial methods can be divided into two major categories, static methods and dynamic methods, depending on whether there is a current in the electrochemical methods. The static methods, which require potentiometric measurements, are extremely important because of their speed and selectively.

Dynamic interfacial methods, in which electrochemical currents play a vital part, are of several types. In three of the dynamic interfacial methods

except electrogravimetry (Figure **1.1)**, the potential of the cell is controlled while measurements of other variables are made. Generally these methods are sensitive and have relatively wide dynamic ranges (typically 10^{-3} to 10^{-8} M). Furthermore, many of these procedures can be carried out with microliter or even nanoliter volumes of sample. Thus, these methods may achieve detection limits in the picomole range.

In constant-current dynamic methods, the current in the cell is held constant while data are collected. Most of the electroanalytical techniques shown in figure have been used as detectors in various chromatographic procedures [2].

Electroanalytical methods are among the most powerful and popular techniques used in analytical chemistry [3-15]. Electrochemistry affords some of the most sensitive and informative analytical techniques in the pharmaceutical analysis area. Electroanalytical methods such as linear sweep, cyclic, differential pulse, square wave, stripping voltammetric techniques and chronoamperometry are not only capable of determining trace amounts of an electroactive compounds, but also supply useful information concerning its physical and chemical properties. The pharmaceutical and biomedical analysis is among the most important branches of applied analytical chemistry. Analytical measurement procedures should have a critical role in drug analysis as well as in biological samples [3-10]. Electrochemistry has always provided analytical techniques characterized by instrumental simplicity, moderate cost and portability [16].

In many cases, modern electroanalytical methods can be viable alternative to more frequently used spectrometric or separation methods. The knowledge of an electrode process of drug compounds provides a useful aid

for understanding of its enzymatic processes and oxidation/reduction mechanisms after administration in the body. The characteristics of electroanalytical techniques make these trace amount of drug analysis particularly well suited for automatic in situ speciation measurements, with or without minimum sample change. The quantization of trace and ultra-trace components in complex samples of clinical or industrial origin represents an important task of modern electroanalytical chemistry.

The development of chemical and biological sensors is currently one of the most active areas of analytical research. Sensors are small devices that incorporate a recognition element with a signal transducer. Such devices can be used for direct measurement of the analyte in the sample matrix [17].

Chemical sensors have been widely used in applications such as critical care, safety, industrial hygiene, process controls, product quality controls, human comfort controls, emissions monitoring, automotive, clinical diagnostics, home safety alarms, and, more recently, homeland security. In these applications, chemical sensors have resulted in both economic and social benefits. A useful definition for a chemical sensor is ‘‘a small device that as the result of a chemical interaction or process between the analyte and the sensor device, transforms chemical or biochemical information of a quantitative or qualitative type into an analytically useful signal” [18].

The signal from a sensor is typically electronic in nature, being a current, voltage, or impedance/conductance change caused by changing analyte composition or quality. While chemical sensors contain a physical transducer and a chemically sensitive layer or recognition layer, the microinstrument sends out an energy signal, be it optical, mass sensitive, thermal or electrical and reads the change in this same property caused by the intervening chemical.

1.2 Types of chemical sensors

Chemical sensors are categorized into the following groups according to the transducer type.

1.2.1 Optical

It relies on an optical transducer for signal measurement. In optical sensors there is a spectroscopic measurement associated with the chemical reaction. Normally it involve a two phase system in which the reagents are immobilized in or on a solid substrate such as a membrane which changes color in the presence of a solution of the analyte. Optical sensors are often referred to as 'optodes' and the use of optical fibres is a common feature. Absorbance, reflectance and luminescence measurements are used in the different types of optical sensors.

1.2.2 Mass sensitive

These make use of the piezoelectric effect and include devices such as the surface acoustic wave (SAW) sensor and are particularly useful as gas sensors. They rely on a change in mass on the surface of an oscillating crystal which shifts the frequency of oscillation. The extent of the frequency shift is a measure of the amount of material adsorbed on the surface.

1.2.3 Heat sensitive

Chemical reactions produce heat and the quantity of the heat produced depends on the amounts of the reactants. Thus, the measurement of heat of reaction can be related to the amount of a particular reactant. Measurements of the heats of reaction form the basis of the field of calorimetry and this has provided a class of chemical sensors which has gained considerable importance.

Calorimetric sensors, like all other chemical sensors, have a region where a chemical reaction takes place and a transducer which responds to heat. There are three classes of calorimetric sensors which are of particular importance. The first uses a temperature probe such as a thermistor as the transducer to sense the heat involved in a reaction on its surface. The second class of calorimetric sensors is referred to as catalytic sensors and is used for sensing flammable gases. The third class is called thermal conductivity sensors and this sense a change in the thermal conductivity of the atmosphere in the presence of a gas. This is the basis of the thermal conductivity detector which has been used for many years in gas chromatography [19].

1.2.4 Electrochemical.

Electrochemical sensors, in which an electrode is used as the transducer element, represent an important subclass of chemical sensors. Electrochemical sensors are essentially an electrochemical cell which employs a two or three-electrode arrangement. Electrochemical sensor measurement can be made at steady-state or transient. The applied current or potential for electrochemical sensors may vary according to the mode of operation, and the selection of the mode is often intended to enhance the sensitivity and selectivity of a particular sensor.

Electrochemical sensors generally can be categorized as potentiometric, amperometric, and voltammetric sensors. Potentiometric Chemical sensors make use of the development of an electrical potential at the surface of a solid material when it is placed in a solution containing ions which can exchange with the surface. The magnitude of the potential is related to the number of ions in the solution. Measurement of the potential is made under an essentially zero current condition. The amperometric and voltammetric sensors are

characterized by their current-potential relationship with the electrochemical system.

1.2.4.1 Amperometric sensors

Amperometric sensors can also be viewed as a subclass of voltammetric sensors. In amperometric sensors, a fixed potential is applied to the electrochemical cell, and a corresponding current, due to a reduction or oxidation reaction, is then measured. This current can be used to quantify the species involved in the reaction. The key consideration of an amperometric sensor is that it operates at a fixed potential.

1.2.4.1.1 Principles

A potential (the electrochemical driving force) is applied to the working electrode to select the species that will undergo redox reaction(s) and the current (the rate of the reaction(s)) is measured. In the simplest form of amperometry, the current is measured at a fixed potential under steady state conditions. The latter occur when the transport of the species of interest to the electrode or the kinetics of the electrode reaction are independent of time. This is the basis for simple sensors where the current is proportional to the concentration of the species of interest; a typical example is the Clark electrode where the diffusion of oxygen across a membrane imposes steady state mass transport conditions [20]. Many amperometric methods employ potential waveforms to provide additional information. The simplest waveform is a single potential step from a value where no reaction occurs to one where the reaction of interest is mass transport or kinetically controlled. In this case the current is either measured at a fixed time or as a function of time. Integration of the current over time yields the charge passed which thanks to Faraday's law can be directly related to the number of moles that have reacted.

1.2.4.2 Voltammetric Sensors

Historically, the branch of electrochemistry (voltammetry) was developed from the discovery of polarography in 1922 by the Czech chemist Jaroslav Heyrovsky, for which he received the 1959 Nobel Prize in chemistry. The early voltammetric methods experienced a number of difficulties, making them less ideal for routine analytical use. However, in the 1960s and 1970s significant advances were made in all areas of voltammetry (theory, methodology, and instrumentation), which enhanced the sensitivity and expanded the repertoire of analytical methods. The coincidence of these advances with the advent of low-cost operational amplifiers also facilitated the rapid commercial development of relatively inexpensive instrumentation.

The common characteristic of all voltammetric techniques is that, they involve the application of a potential (E) to an electrode and then monitoring the resulting current (i) flowing through the electrochemical cell. In many cases the applied potential is varied or the current is monitored over a period of time (t). Thus, all voltammetric techniques can be described as function of E, i, and t. They are considered as active techniques because the applied potential forces a change in the concentration of an electroactive species at the electrode surface by electrochemically reducing or oxidizing it.

The analytical advantages of the various voltammetric techniques include excellent sensitivity with a very large useful linear concentration range for both inorganic and organic species (10^{-12} to 10^{-1} M), a large number of useful solvents and electrolytes, a wide range of temperatures, rapid analysis times (seconds), simultaneous determination of several analytes, the ability to determine kinetic and mechanistic parameters, a well developed theory and thus the ability to reasonably estimate the values of unknown parameters, and

the ease with which different potential waveforms can be generated and small currents measured [21].

Analytical chemists routinely use voltammetric techniques for the quantitative determination of a variety of dissolved inorganic and organic substances. Inorganic, physical, and biological chemists widely use voltammetric techniques for a variety of purposes, including fundamental studies of oxidation and reduction processes in various media, adsorption processes on surfaces, electron transfer and reaction mechanisms, kinetics of electron transfer processes, and transport, speciation, and thermodynamic properties of solvated species. Voltammetric methods are also applied for the determination of compounds of pharmaceutical interest and, when coupled with HPLC, they are effective tools for the analysis of complex mixtures.

1.3 Solution structure; the double layer

Electroanalytical studies are centered on electrode, which is considered as a probe in the electrolyte. An electrode can only donate or accept electrons from a species that is present in a layer of solution that is immediately adjacent to the electrode. Thus, this layer may have a composition that differs significantly from that of the bulk of the solution. Let us consider the structure of the solution immediately adjacent to that electrode. Immediately after impressing the potential, there will be a momentary surge of current, which rapidly decays to zero if no reactive species is present at the surface of the electrode. This current is a charging current that creates an excess of negative charge at the surface of the two electrodes. As a consequence of ionic mobility, however, the layers of solution immediately adjacent to the electrodes acquire an opposing charge. This effect is illustrated in Figure **1.2**. The surface of the metal electrode is shown as having an excess of positive

charge as a consequence of an applied positive potential. The charged solution layer consists of two parts: (1) a compact inner layer (d_0 to d_1), in which the potential decreases linearly with distance from the electrode surface and (2) a diffuse layer (d_1 to d_2), in which the decrease is exponential. This assemblage of charge at the electrode surface and in the solution adjacent to the surface is termed as electrical double layer.

1.4 Faradaic and nonfaradaic currents

Two types of processes can conduct currents across an electrode/solution interface. One involves a direct transfer of electrons via an oxidation reaction at one electrode and a reduction reaction at the other. Processes of this type are called faradaic processes because they are governed by Faraday's law, which states that the amount of chemical reaction at an electrode is proportional to the current; the resulting currents are called faradaic currents.

Under some conditions a cell will exhibit a range of potentials where faradaic processes are precluded at one or both of the electrodes for thermodynamic or kinetic reasons. Here, conduction of continuous alternating currents can still take place. With such currents, reversal of the charge relationship occurs with each half cycle, as first negative and then positive ions are attracted alternately to the electrode surface. Electrical energy is consumed and converted to heat by friction associated with this ionic movement. Thus, each electrode surface behaves as one plate of a capacitor, the capacitance of which may be large. The capacitive current increases with frequency and with electrode area; by controlling these variables, it is possible to arrange conditions such that essentially all the alternating current in a cell is carried across the electrode interface by this nonfaradaic process [2].

Current in voltammetric experiment is a measure of the rate of the electrode process. When an electrode is placed in an electrolyte solution, different processes may occur. Steps involved in an electrode reaction are (Figure **1.3.)**

1) Mass transfer of species between bulk solution and the electrode surface.
2) Heterogeneous electron transfer at the electrode/solution interface.
3) Chemical reactions, either preceding or following electron transfer.
4) Surface reactions such as adsorption, desorption and electrodeposition – dissolution [1].

The mass transfer rates of the detecting species in the reaction onto the electrode surface and the kinetics of the faradaic or charge transfer reaction at the electrode surface directly affect the current-potential characteristics. This mass transfer can be accomplished through

a) A diffusion under a chemical potential difference or concentration gradient.
b) An ionic migration as a result of an electric potential gradient and
c) A bulk transfer by natural or forced convection.

The electrode reaction kinetics and the mass transfer processes contribute to the rate of the faradaic process in an electrochemical cell. This provides the basis for the operation of the voltammetric sensor.

1.5 Diffusion

When there is a concentration difference between two regions of a solution, ions or molecules move from the more concentrated region to the more dilute.

This process, called diffusion, ultimately leads to a disappearance of the concentration difference. The rate of diffusion is directly proportional to the concentration difference. When ions are deposited at a cathode by a current, the concentration of ions at the electrode surface becomes lower than the bulk concentration. The difference between the concentration at the surface and the concentration in the bulk solution creates a concentration gradient that causes ions to diffuse from the bulk of the solution to the surface film. The rate of diffusion dc/dt is given by

$$\mathbf{dc/dt = k\,(c-c_0)}$$

where **c** is the reactant concentration in the bulk of the solution, $\mathbf{c_0}$ is its equilibrium concentration at the surface of the electrode, and k is a proportionality constant. The value of $\mathbf{c_0}$ at any instant is fixed by the potential of the electrode and can be calculated from the Nernst equation. When higher potentials are applied to the electrode, $\mathbf{c_0}$ becomes smaller and smaller, and the diffusion rate becomes greater and greater. Ultimately, $\mathbf{c_0}$ becomes negligible with respect to **c** ; the rate then becomes constant. That is, when $\mathbf{c_0 \rightarrow 0}$,

$$\mathbf{dc/dt = kc}$$

then the electrode behaves as an ideal polarized electrode.

1.6 Migration

The process by which ions move under the influence of an electric field is called migration. This process, shown schematically in Figure **1.4**, is the primary cause of mass transfer in the bulk of the solution in a cell. The rate at which ions migrate to or away from an electrode surface generally increases as the electrode potential increases. This charge movement constitutes a current, which also increases with potential. Migration of analyte species is

undesirable in most types of electrochemistry, and migration can be minimized by having a high concentration of an inert electrolyte, called a supporting electrolyte, present in the cell. The current in the cell is then primarily due to charges carried by ions from the supporting electrolyte. The supporting electrolyte also serves to reduce the resistance of the cell, which decreases the *IR* drop.

1.7 Convection

Reactants can also be transferred to or from an electrode by mechanical means. Forced convection, such as stirring or agitation, will tend to decrease the thickness of the diffusion layer at the surface of an electrode and thus decrease concentration polarization. Natural convection resulting from temperature or density differences also contributes to the transport of molecules to and from an electrode.

A preferred mass transfer condition is total diffusion, which can be described by Fick's law of diffusion. Under this condition, the cell current, a measure of the rate of the faradaic process at an electrode, usually increases with increases in the electrode potential. The limiting current and the bulk concentration of the detecting species can be related by

$$i = ZFk_mC$$

Where k_m is the mass transfer coefficient and C is the bulk concentration of the detecting species. At the other extreme, when the electrode kinetics are slow compared with the mass transfer rate, the electrochemical system is operated in the reaction kinetic control regime. This usually corresponds to a small overpotential. The limiting current and the bulk concentration of the detecting species can be related as

$$i = ZFk_cC$$

where k_c is the kinetic rate constant for the electrode process. Both Eqs. shows the linear relationship between the limiting current and the bulk concentration of the detecting species. In many cases, the current does not tend to a limiting value with an increase in the electrode potential. This is because other faradaic or nonfaradaic processes become active, and the cell current represents the cumulative rates of all active electrode processes. The relative rates of these processes, expressing current efficiency, depend on the current density of the electrode. Assessment of such a system is rather complicated, and the limiting current technique may become ineffective [22].

1.8 General theory

In voltammetry, the effects of the applied potential and the behavior of the redox current are described by several well-known laws. The applied potential controls the concentrations of the redox species at the electrode surface (C_O^0 and C_R^0) and the rate of the reaction (k^0), as described by the Nernst or Butler–Volmer equations, respectively. In the cases where diffusion plays a controlling part, the current resulting from the redox process (known as the faradaic current) is related to the material flux at the electrode–solution interface and is described by Fick's law. The interplay between these processes is responsible for the characteristic features observed in the voltammograms of the various techniques.

For a reversible electrochemical reaction (that is, a reaction so fast that equilibrium is always reestablished as changes are made), which can be described by $\mathbf{O} + n\mathbf{e}^- \leftrightarrow \mathbf{R}$, the application of a potential E forces the respective concentrations of **O** and **R** at the surface of the electrode (C_O^0 and C_R^0) to a ratio in compliance with the Nernst equation:

$$E=E^0 - (RT/nF) \ln C_R^0 / C_O^0$$

where *R* is the molar gas constant (8.3144 J mol^{-1} K^{-1}), T is the absolute temperature (K), n is the number of electrons transferred, F = Faraday constant (96,485 C/equiv), and E^0 is the standard reduction potential for the redox couple. If the potential applied to the electrode is changed, the ratio C_R^0/C_O^0 at the surface will also change so as to satisfy the above equation.

If the potential is made more negative the ratio becomes larger (that is, **O** is reduced) and, conversely, if the potential is made more positive the ratio becomes smaller (that is, **R** is oxidized).

For some techniques it is useful to use the relationship that links the variables for current, potential, and concentration, known as the Butler–Volmer equation:

$$\frac{i}{nFA} = K^0 \left\{ C_O^0 \exp[-\alpha\theta] - C_R^0 \exp\left[(1-\alpha)\theta\right] \right\}$$

where $\theta = nF(E - E^0)/RT$, k^0 is the heterogeneous rate constant, α is known as the transfer coefficient, and **A** is the area of the electrode. This relationship allows us to obtain the values of the two analytically important parameters, **i** and k^0.

Finally, in most cases the current flow also depends directly on the flux of material to the electrode surface. When new **O** or **R** is created at the surface, the increased concentration provides the force for its diffusion toward the bulk of the solution. Likewise, when **O** or **R** is destroyed, the decreased concentration promotes the diffusion of new material from the bulk solution. The resulting concentration gradient and mass transport is described by Fick's

law, which states that the flux of matter (Φ) is directly proportional to the concentration gradient:

$$\Phi = -AD_o \left(\partial C_o / \partial x \right)$$

where $\mathbf{D_O}$ is the diffusion coefficient of **O** and ***x*** is the distance from the electrode surface. An analogous equation can be written for **R**. The flux of **O** or **R** at the electrode surface controls the rate of reaction, and thus the faradaic current flowing in the cell. In the bulk solution, concentration gradients are generally small and ionic migration carries most of the current. The current is a quantitative measure of how fast a species is being reduced or oxidized at the electrode surface. The actual value of this current is affected by many additional factors, most importantly the concentration of the redox species, the size, shape, and material of the electrode, the solution resistance, the cell volume, and the number of electrons transferred [21].

1.9 Voltammetric instrumentation

1.9.1 The electrodes and cell

A typical electrochemical cell consists of the sample dissolved in a solvent, an ionic electrolyte, and three (or sometimes two) electrodes. These are reference electrode (RE), working electrode (WE), and counter electrode (CE) (also called the secondary or auxiliary electrode). The applied potential is measured against the RE, while the CE closes the electrical circuit for the current to flow. The experiments are performed by a potentiostat that effectively controls the voltage between the RE and WE, while measuring the current through the CE (the WE is connected to the ground).Cells (sample holders) come in a variety of sizes, shapes, and materials. The type used depends on the amount and type of sample, the technique, and the analytical data to be obtained. The material of the cell (glass, Teflon, polyethylene) is

selected to minimize reaction with the sample. In most cases the reference electrode should be as close as possible to the working electrode; in some cases, to avoid contamination, it may be necessary to place the reference electrode in a separate compartment. The unique requirements for each of the voltammetric techniques are described under the individual techniques.

1.9.2 Reference Electrodes (RE)

The purpose of the RE is to provide a stable, reproducible voltage to which the WE of an electrochemical cell. Ideally, if a small current is passed through the electrode, the potential change is negligible, and in any case, returns to the initial value when the current ceases. In addition, the potential value should not vary with time and should be reproducible from electrode to electrode. The reference electrode should provide a reversible half reaction with Nernstian behavior, be constant over time, and be easy to assemble and maintain.

Ideally, the potential of RE should be temperature independent; however, it typically changes by 0.5 - 1 mV per degree Celsius. Consequently, precise potential measurements require the use of a constant temperature apparatus. In addition, the temperature at which the measurements were made should always be reported. The absence of any temperature control limits the accuracy of the measurements to about 5 - 10 mV. Two widely used aqueous reference electrodes are the Ag/AgCl electrode and the saturated calomel electrode.

The redox process for this electrode is:

$$AgCl + e^- \Leftrightarrow Ag + Cl^-$$

This electrode consists of a silver wire, coated with silver chloride, which is immersed in a solution containing chloride ions. The BAS RE uses an

aqueous solution containing 3M sodium chloride. A porous Vycor frit is used for the junction between the RE solution and the sample solution. The potential E for any electrode is determined by the Nernst equation, which relates E to the standard potential E^0 and the activities of the redox components (the standard potential is the potential of the electrode at unit activity under standard conditions). The Nernst equation for the Ag/AgCl electrode is

$$E = E^0 + \frac{RT}{nF} \ln \frac{1}{a_{Cl^-}}$$

(The activities of the solid silver and silver chloride under standard conditions are unity).

It is generally more convenient to consider concentrations rather than activities $\left(a_{Cl^-} = \gamma_{Cl^-}[Cl^-]\right)$, and the Nernst equation can be rewritten as follows:

$$E = E^{0'} + \frac{RT}{nF} \ln \frac{1}{[Cl^-]}$$

where E^0 is the formal potential and is related to the standard potential by the equation:

$$E^{0'} = E^0 + \frac{RT}{nF} \ln \frac{1}{\gamma_{Cl^-}}$$

The above equations show that variations in the chloride ion concentration in the electrode change the redox potential. Since there is generally a large chloride concentration gradient across the RE frit, there is slow diffusion of chloride ions from the RE into the sample solution; that is, the reference potential will gradually change when used.

There are some precautions that can be taken to minimize the reference potential drift. When the electrodes are made, the Vycor frit is covered in plastic to prevent leakage. This plastic should be carefully removed immediately upon receipt, and the Vycor frit should be immersed in a 3M aqueous sodium chloride solution. The RE should also be removed from the electrochemical cell and stored in this solution between experiments. Occasionally, air bubbles will form in the solution next to the Vycor frit; these should be removed by gently flicking the end of the electrode [23].

1.9.3 Counter Electrodes (CE)

The role of the CE is to supply the current required by the WE, without limiting the measured response of the cell. In most voltammetric techniques the analytical reactions at the electrode surfaces occur over very short time periods and rarely produce any appreciable changes in bulk concentrations of **R** or **O**. Thus, isolation of the CE from the sample is not normally necessary. It is usually made of inert materials to avoid its dissolution. Most often the CE consists of a thin Pt wire, although Au and sometimes graphite have also been used. It should have a large area compared to the working electrode.

1.9.4 Working Electrodes (WE)

They are of various geometries and materials, ranging from small Hg drops to flat Pt disks. Often, they are small, flat disks of a conductor that are press fitted into a rod of an inert material, such as Teflon or Kel-F, that has a wire contact imbedded in it. The conductor may be an inert metal, such as platinum or gold; pyrolytic graphite or glassy carbon; a semiconductor, such as tin or indium oxide; or a metal coated with a film of mercury. Mercury microelectrodes have been widely employed in voltammetry for several reasons. One is the relatively large negative potential range that can be

achieved with mercury because of the large overvoltage of hydrogen on mercury. This overvoltage allows the determination of metals such as Cd, Zn, and Pb that are reduced at negative potentials to amalgams at the surface of a mercury electrode. Furthermore, a fresh metallic surface is readily formed by simply producing a new mercury drop. Mercury microelectrodes take several forms. The range of potentials that can be used with these electrodes in aqueous solutions varies; it depends not only on the electrode material but also on the composition of the solution in which it is immersed.

1.9.5 Supporting electrolyte

The supporting electrolyte is an inert soluble ionic salt added to the solvent, generally in 10-fold or 100- fold excess over the concentration of the species being studied. The inertness meant here is the ability to avoid oxidation or reduction at the indicating or reference electrode during the course of the electrochemical measurements.

There are three functions of the supporting electrolyte. First, it carries most of the ionic current of the cell since its concentration is much larger than that of the other species in solution. Thus it serves to complete the circuit of the electrochemical cell and keep the cell resistance at a low value. Second, it maintains a constant ionic strength. This is necessary because the structure of the interphase region should not change significantly if a reaction occurs there. A stable structure is created on the electrolyte side by adding a high concentration of an inert salt. Third, migration current observed is reduced by the presence of large excess of ions that are not electrochemically active at the potentials in use, because they can carry an ionic current without permitting its conversion into electronic, and hence net or measured, current at the electrodes.

1.9.6 Cell atmosphere

Some electroanalytical measurements can be run in cells under an atmosphere of ordinary air. Oxygen, however, is electrochemically active, and the solubility of oxygen in water is sufficiently great that its reduction interferes with most electroanalytical techniques in aqueous media, mixed solvents or even in non aqueous media. Additional complications such as reoxidation of electroreduced species can also be expected if oxygen is present. As a consequence, most electroanalytical measurements are carried out under an atmosphere of inert gas. Normally this is nitrogen, although argon is occasionally used instead. Use of other gases or gas mixtures is rare, and only occurs when mandated by the specific electroanalytical measurements being made.

Nitrogen is preferred to argon only for reasons of cost. Most commercial nitrogen is manufactured by fractional distillation of liquid air and contains enough oxygen that a solution deaerated with it still contains enough residual oxygen to seriously affect sensitive techniques. This oxygen interference can be prevented by use of nitrogen without oxygen, such as high purity commercial nitrogen or preferably nitrogen run through a deoxygenation system. Commercial argon contains much less oxygen than does commercial nitrogen, but deoxygenation is still a worthwhile precaution [1].

1.10 Surface modification for electrode protection

Electrode surfaces need to be protected against non electroactive interferents, which can be irreversibly adsorbed on the surface of the electrode during voltammetric scans. These interferents lead to a decrease in electrode response with time and preclude the possibility of analysis of untreated samples. Such protection can be achieved by using suitable electrode materials

or, alternatively, suitably modified electrode materials. Much attention has been devoted to carbon electrodes and their modification, given their widespread use in electroanalytical chemistry [24].

Surface modification changes the surface layers of the electrode itself or creates a layer with some form of chemical as well as physical selectivity.

Modified electrodes can be prepared in the following ways.

a) Chemical modification: The electrode surface is activated by chemical reaction, such as with silane, which is then used to react with another chemical species that becomes immobilized on the surface.

b) Adsorption: This is used for coating electrode surfaces with solutions of the modifier either by dipping or, more commonly, by applyingf a drop of solution followed by spinning to evaporate the solvent (spin coating). This is particularly used for modifying with soluble polymers. Some polymeric species which have a tendency for self assembly can also be applied through such procedures, leading to self assembled monolayers on the electrode surface.

c) Electroadsorption and electrodeposition: If adsorption is carried out under the influence of an applied potential then thicker modifier layers usually result, but there is probably a greater guarantee of uniformity. Electropolymerisation of monomers is also possible. Such procedures are used for the formation of conducting polymers.

d) Plasma: The electrode surface is cleaned by a plasma leaving the surface with dangling bonds and being highly active. Adsorption of any species, such as amines or ethenes, in the vicinity is very fast [25].

1.10.1 Conducting polymers

Polymer modification is an approach which has been used with success for reducing adsorption phenomena. These polymers can either represent a new electrode surface in themselves, i.e., conducting polymers(CP) or redox polymers, or allow only the electroactive species of interest to reach the electrode substrate underneath. Thus, selectivity can be due to their porosity, excluding large molecules such as proteins, or due to ion exchange characteristics if it is desired to make the membrane selective to charged species, or both of these [26].

The modern development of CP began in 1977 as the American scientists Heeger and MacDiarmid and their Japanese colleague Shirakawa discovered that doping chainlike polyacetylene (PA) with iodine endowed the polymer with metal-like properties, producing copper colored films with an increase of conductivity of 10 orders of magnitude [28]. PA was not stable and was easily destroyed by oxidative degradation. Therefore, numerous other CP with properties similar to those of PA were synthesized, such as polyphenylene (PP), polyphenylenevinylene, polypyrrole (PPy), polythiophene (PTh), and polyaniline (PANI) [28-32].

CP offers a myriad of opportunities to couple analyte receptor interactions, as well as nonspecific interactions, into observable (transducible) responses. A key advantage of CP based sensors over devices using small molecule (chemosensor) elements is the potential of the CP to exhibit collective properties that are sensitive to very minor perturbations. In particular, the CP's transport properties, electrical conductivity or rate of energy migration, provide amplified sensitivity. Polymers are often used in sensory devices as passive supports or structural materials to provide stability [33].

1.10.2 Nanomaterials

Nanomaterials have become an extremely popular theme in recent electrochemical sensing research, due to their electrical conductivity, unique structural and catalytic properties, high loading of biocatalysts, good stability and excellent penetrability [34]. Nanomaterials feature unique physicochemical properties that can be of great utility in creating new recognition and transduction processes for chemical and biological sensors [35−46], as well as improving the S/N ratio by miniaturization of the sensor elements [47].

Carbon nanotubes (CNTs) can be used as electrode materials with useful properties for various potential applications including miniature biological devices. CNTs are expected to exhibit inherent electrochemical properties similar to other carbon electrodes widely used in various electrochemical applications. Unlike other carbon- based nanomaterials such as C_{60} and C_{70}, CNTs show very different electrochemical properties. The subtle electronic properties suggest that CNTs will have the ability to mediate electron transfer reactions with electroactive species in solution when used as the electrode material. CNT based electrodes have been widely used in electrochemical sensing.

First, the CNT modified electrodes catalyze the redox reactions of analytes. It has been reported that the oxidation of analytes such as dopamine, H_2O_2 and NADH are catalyzed at the various types of CNT modified electrodes. Second, the biomacro molecules such as enzymes and DNA can be immobilized on the CNT modified electrodes and maintain their biological activities. Third, the CNTs are a good material for constructing the electrodes. CNTs are small, straight and strong and they also have chemical stability. These characteristics of CNTs are advantageous for constructing CNT modified electrodes. Fourth, CNTs can be functionalized mostly through the carboxyl group on the tips which helps to

immobilize the enzymes, etc. for the development of various types of sensors. The fifth advantage of CNTs is their good electronic conductivity. The conductivity of CNTs is also affected by the structural changes such as twisting and bending of CNTs which may be applied for the sensing purpose.

These advantages combined with others such as the porous structure may contribute to having good wetting property for the solvents, a better electrode-electrolyte interface and a large surface area. The central hollow cores and outside walls are a superior material to adsorb and store gases such as oxygen, hydrogen and nitrogen oxide. The investigation of gas sensors using the adsorptive properties of CNTs to detect oxygen and carbon dioxide has been reported. The CNTs in many cases can serve as molecular wires that connect the electrode surface to the active sites of enzymes [17].

Gold nanoparticles (AuNPs) possess distinct physical and chemical attributes that make them excellent scaffolds for the fabrication of novel chemical and biological sensors [48−56]. First, AuNPs can be synthesized in a straightforward manner and can be made highly stable. Second, they possess unique optoelectronic properties. Third, they provide high surface-to-volume ratio with excellent biocompatibility using appropriate ligands. Fourth, these properties of AuNPs can be readily tuned by varying their size, shape, and the surrounding chemical environment. Finally, AuNPs offer a suitable platform for multifunctionalization with a wide range of organic or biological ligands for the selective binding and detection of small molecules and biological targets. Each of these attributes of AuNPs has allowed researchers to develop novel sensing strategies with improved sensitivity, stability and selectivity. In the past decade of research, the advent of AuNP as a sensory element provided us a broad spectrum of innovative approaches for the detection of metal ions,

small molecules, proteins, nucleic acids, malignant cells, etc., in a rapid and efficient manner [57].

The Pt-nanotubule and macroporous Pt-modified electrodes have been shown to exhibit good sensitivity towards glucose [58]. Some sensors were fabricated by Pt nanoparticles immobilized on CNTs, which facilitated the incorporation of Pt nanoparticles [59-63]. Pt nanoclusters embedded polypyrrole nanowire provided a special porous, biocompatible and highly catalytic activity [64].

1.11 Different voltammetric techniques

Several different voltage-time functions can be applied to the electrode (Figure **1.5)**. The simplest of these is a linear scan in which the potential of the WE is changed linearly with time. Typically, the potential of the WE is varied over a 1- or 2-V range. The current in the cell is then measured as a function of the applied potential. Pulsed waveforms and triangular waveforms can also be applied.

1.11.1 Linear-Sweep Voltammetry (LSV)

LSV involves an increase in the imposed potential linearly at a constant scanning rate from an initial potential to a defined upper potential limit. LSV is of two types: hydrodynamic voltammetry and polarography.

Linear-sweep voltammograms under slow sweep conditions (a few mV/s) with the solution moving past the electrode generally have the shape of a sigmoidal curve called a voltammetric wave. The constant current beyond the steep rise (Figure **1.6**) is called the limiting current i_l, because it is limited by the rate at which the reactant can be brought to the electrode surface by mass transport processes.

Limiting currents are generally directly proportional to reactant concentration. Thus, we may write

$$\mathbf{i_l = Kc_A}$$

where c_A is the analyte concentration and k is a constant. Quantitative LSV is based on this relationship.

The potential at which the current is equal to one half the limiting current is called the half wave potential and is given the symbol $E_{1/2}$. The half wave potential is closely related to the standard potential for the half reaction but is usually not identical to that constant. Half wave potentials are useful for identification of the components of a solution.

To obtain reproducible limiting currents rapidly, it is necessary that either (1) the solution or the microelectrode be in continuous and reproducible motion or (2) a dropping mercury electrode be used. LSV in which the solution is stirred or the electrode is rotated is called **hydrodynamic voltammetry**. Voltammetry with the dropping mercury electrode is called **polarography**.

In the type of LSV discussed above, the potential is changed slowly enough and mass transfer is rapid enough that a steady state is reached at the electrode surface. Hence, the mass transport rate of analyte A to the electrode just balances its reduction rate at the electrode. Likewise, the mass transport of product P away from the electrode is just equal to its production rate at the electrode surface. There is another type of LSV in which fast scan rates (1 V/s or greater) are used with unstirred solutions. In this type of voltammetry, a peak-shaped current-time signal is obtained because of depletion of the analyte in the solution near the electrode. Cyclic voltammetry is an example in which forward

and reverse linear scans are applied. With cyclic voltammetry, products formed on the forward scan can be detected on the reverse scan if they have not moved away from the electrode or have not been altered by a chemical reaction.

1.11.2 Cyclic Voltammetry (CV)

CV has become an important and widely used electroanalytical technique in many areas of chemistry. It is rarely used for quantitative determinations, but it is widely used for the study of redox processes, for understanding reaction intermediates, and for obtaining stability of reaction products.

This technique is based on varying the applied potential at a working electrode in both forward and reverse directions while monitoring the current. For example, the initial scan could be in the negative direction to the switching potential. At that point the scan would be reversed and run in the positive direction. Depending on the analysis, one full cycle, a partial cycle, or a series of cycles can be performed.

The important parameters in a cyclic voltammogram are the peak potentials (E_{pc}, E_{pa}) and peak currents (i_{pc}, i_{pa}) of the cathodic and anodic peaks, respectively. If the electron transfer process is fast compared with other processes (such as diffusion), the reaction is said to be electrochemically reversible, and the peak separation is

$$\mathbf{\Delta E_p = E_{pa} - E_{pc} = 2.303\ RT\ /\ nF}$$

Thus, for a reversible redox reaction at 25 °C with *n* electrons ΔE_p should be 0.0592/*n* V or about 60 mV for one electron. In practice this value is difficult to attain because of such factors as cell resistance. Irreversibility due

to a slow electron transfer rate results in $\Delta E_p > 0.0592/n$ V, greater, say, than 70 mV for a one-electron reaction.

The formal reduction potential (E^o) for a reversible couple is given by

$$\mathbf{E^o = (E_{pc} + E_{pa}) / 2}$$

For a reversible reaction, the concentration is related to peak current by the Randles–Sevcik expression (at 25 °C):

$$\mathbf{i_p = 2.686 \times 10^5 \ n^{3/2} \ Ac \ D^{1/2} \ \upsilon^{1/2}}$$

where i_p is the peak current in Amps, A is the electrode area (cm^2), D is the diffusion coefficient ($cm^2\ s^{-1}$), c is the concentration in mol cm^{-3}, and υ is the scan rate in Vs^{-1}.

CV is carried out in quiescent solution to ensure diffusion control. A three electrode arrangement is used.

1.11.3 Pulse Methods

In order to increase speed and sensitivity, many forms of potential modulation (other than just a simple staircase ramp) have been tried. Three of these pulse techniques are widely used.

1.11.3.1 Normal Pulse Voltammetry (NPV)

This technique uses a series of potential pulses of increasing amplitude. The current measurement is made near the end of each pulse, which allows time for the charging current to decay. It is usually carried out in an unstirred solution at either DME (called normal pulse polarography) or solid electrodes. The potential is pulsed from an initial potential E_i. The duration of the pulse, τ, is usually 1 to 100 milliseconds and the interval between pulses typically 0.1

to 5 seconds. The resulting voltammogram displays the sampled current on the vertical axis and the potential to which the pulse is stepped on the horizontal axis.

1.11.3.2 Differential Pulse Voltammetry (DPV)

This technique is comparable to normal pulse voltammetry in that the potential is also scanned with a series of pulses. However, it differs from NPV because each potential pulse is fixed, of small amplitude (10 to 100 mV), and is superimposed on a slowly changing base potential. Current is measured at two points for each pulse, the first point (1) just before the application of the pulse and the second (2) at the end of the pulse. These sampling points are selected to allow for the decay of the nonfaradaic (charging) current. The difference between current measurements at these points for each pulse is determined and plotted against the base potential.

1.11.3.3 Square Wave Voltammetry (SWV)

The excitation signal in SWV consists of a symmetrical square wave pulse of amplitude E_{sw} superimposed on a staircase waveform of step height ΔE, where the forward pulse of the square wave coincides with the staircase step. The net current, i_{net}, is obtained by taking the difference between the forward and reverse currents ($i_{for} - i_{rev}$) and is centered on the redox potential. The peak height is directly proportional to the concentration of the electroactive species and detection limits as low as possible.

SWV has several advantages. Among these are its excellent sensitivity and the rejection of background currents. Another is the speed. This speed, coupled with computer control and signal averaging, allows for experiments to be performed repetitively and increases the signal to noise ratio. Applications of SWV include the study of electrode kinetics with regard to preceding,

following, or catalytic homogeneous chemical reactions, determination of some species at trace levels, and its use with electrochemical detection in HPLC.

1.11.4 Preconcentration and stripping techniques

The preconcentration techniques have the lowest limits of detection of any of the commonly used electroanalytical techniques. Sample preparation is minimal and sensitivity and selectivity are excellent. The three most commonly used variations are anodic stripping voltammetry (ASV), cathodic stripping voltammetry (CSV), and adsorptive stripping voltammetry (AdSV).

Even though ASV, CSV, and AdSV each have their own unique features, all have two steps in common. First, the analyte species in the sample solution is concentrated onto or into a working electrode. It is this crucial preconcentration step that results in the exceptional sensitivity that can be achieved. During the second step, the preconcentrated analyte is measured or stripped from the electrode by the application of a potential scan. Any number of potential waveforms can be used for the stripping step (that is, differential pulse, square wave, linear sweep, or staircase). The most common are differential pulse and square wave due to the discrimination against charging current. However, square wave has the added advantages of faster scan rate and increased sensitivity relative to differential pulse.

The electrode of choice for stripping voltammetry is generally mercury. The species of interest can be either reduced into the mercury, forming amalgams as in anodic stripping voltammetry, or adsorbed to form an insoluble mercury salt layer, as in cathodic stripping voltammetry. Stripping voltammetry is a very sensitive technique for trace analysis. As with any quantitative technique, care must be taken so that reproducible results are obtainable. Important conditions

that should be held constant include the electrode surface, rate of stirring, and deposition time. Every effort should be made to minimize contamination.

1.11.4.1 Anodic Stripping Voltammetry (ASV)

ASV is one of the most sensitive electroanalytical techniques available. When the potential is held at a negative potential followed by scanning in a positive direction, the technique is called at ASV. The pre-concentration in ASV is based electrolytic deposition (reduction of organic compound or metal ion to amalgam or electrode surface) and its subsequent dissolution (re-oxidation) from the electrode surface by means of an anodic potential scan. This method has been the most widely used from stripping analysis for determination of metals. The pre-concentration is done by cathodic deposition at a controlled potential and time. Usually, 0.3-0.5 V more negative potential than E^o are used for the deposition potential for the least reduced metal ion to be determined. The target compound or metal ions reach to the electrode surface by diffusion or convention where they are reduced and concentrated as amalgams (for mercury electrode) or on the electrode (other solid electrodes). The convection transport is achieved by solution stirring or electrode rotation. This convection force is usually used to facilitate the deposition step. After the pre-concentration period, the convection is stopped. About 15 second rest period is used before the stripping step. The resulting peak current depends on various parameters of the deposition and stripping steps as well as on the characteristics of the metal ion or organic compounds and the electrode geometry. Actually, anodic stripping voltammetry is most frequently used for metals that form amalgams with mercury.

1.11.4.2 Cathodic Stripping Voltammetry (CSV)

It is similar to trace analysis method ASV, except that for the plating step, the potential is held at an oxidizing potential, and the oxidized species are

stripped from the electrode surface by sweeping the potential positively. As a short description it is the mirror image of ASV. CSV can be used to determine substances that form insoluble salts with the mercurous ion. Application of a relatively positive potential to a mercury electrode in a solution containing such substances results in the formation of an insoluble film on the surface of the mercury electrode. A potential scan in the negative direction will then reduce (strip) the deposited film into solution. This method has been used to determine inorganic anions such as halides, selenide, and sulfide, and oxyanions such as MoO_4^{2-} and VO_3^{5-}. In addition, many organic compounds, such as nucleic acid bases, also form insoluble mercury salts and may be determined by CSV. CSV is best suited for the determination a wide range of organic sulfur compounds such as penicillin, thiols and inorganic anions, halides, sulfides etc that form insoluble salts with the electrode material. In addition, many other organic compounds, such as nucleic acid bases also form insoluble salts and can be determined using this technique. CSV has been less used in general, but the fact that it can be carried out without use of mercury is advantageous and this technique is not effect from dissolved oxygen. Solid electrodes such as silver, copper are less commonly used in CSV.

1.11.4.3 Adsorptive Stripping Voltammetry (AdSV)

In drug analysis, AdSV is popular because of the low limit of determination ($ng.mL^{-1}$ or ppb level concentrations), its accuracy and precision, as well as the low cost of instrumentation relative to other analytical methods of analysis. For trace analysis of pharmaceutically active organic compounds that cannot be accumulated by electroanalysis another stripping method was proposed: Adsorptive stripping voltammetry (AdSV). In this technique, the analyte is adsorbed on working electrode by means of a non-electrolytic process prior to the voltammetric scan. AdSV technique involves

the formation, adsorptive accumulation and reduction (potential cathodic scan) of a surface-active complex of the metal. The voltammetric response of such a complex is directly linked to its surface concentration: this is described by an isotherm function, which provides the relationship between the surface and bulk concentration of the adsorbate.

The principle of AdSV can be compared to the other stripping techniques such as ASV or CSV except that no change is transferred during the pre-concentration step. Accumulation of the analyte at the electrode surface is performed at open circuit by applying a suitable potential at which no electrochemical reactions occur for set time. After the equilibrium time, the potential is scanned by anodic or cathodic direction depending on the redox properties of the investigated compounds. The adsorptive approach may offer improvements in selectivity or sensitivity for organic compounds and metals that are measurable also by conventional stripping analysis and they exhibit surface active properties. The adsorptive accumulation scheme results in very effective pre-concentration, allowing highly sensitive measurements (about 10^{-10}-10^{-11} M levels) following short adsorption times. To attain such high sensitivity, it is essential to optimize operational variables such as nature of the supporting electrolyte, pH, accumulation potential and time etc favoring strong adsorption [16].

1.12 Selecting the voltammetric technique

The choice of which voltammetric technique to use depends on the sample's characteristics, including the analyte's expected concentration and the sample's location. For example, amperometry is ideally suited for detecting analytes in flow systems, including the in vivo analysis of a patient's blood, or as a selective sensor for the rapid analysis of a single analyte. The

portability of amperometric sensors, which are similar to potentiometric sensors, also make them ideal for field studies. Although cyclic voltammetry can be used to determine an analyte's concentration, other methods described are better suited for quantitative work.

Pulse and stripping voltammetry frequently are interchangeable. The choice of which technique to use often depends on the analyte's concentration, and the desired accuracy and precision. Detection limits for NPV generally are on the order of 10^{-6} M to 10^{-7} M, and those for DPV, and SWV are between 10^{-7} M and 10^{-9} M. Because we concentrate the analyte in stripping voltammetry, the detection limit for many analytes is as little as 10^{-10} M to 10^{-12} M. On the other hand, the current in stripping voltammetry is much more sensitive than pulse methods to changes in experimental conditions, which may lead to poorer precision and accuracy. Pulse techniques can use to analyze a wider range of inorganic and organic analytes because there is no need to first deposit the analyte at the electrode surface.

Stripping voltammetry also suffers from occasional interferences when two metals, such as Cu and Zn, combine to form an intermetallic compound in the mercury amalgam. The deposition potential for Zn^{2+} is sufficiently negative that any Cu^{2+} in the sample also deposits into the mercury drop or film, leading to the formation of intermetallic compounds such as CuZn and $CuZn_2$. During the stripping step, zinc in the intermetallic compounds strips at potentials near that of copper, decreasing the current for zinc and increasing the apparent current for copper. It is often possible to overcome this problem by adding an element that forms a stronger intermetallic compound with the interfering metal. Thus, adding Ga^{3+} minimizes the interference of Cu when analyzing for Zn by forming an intermetallic compound of Cu and Ga [65].

1.13 Brief Review on voltammetric sensors for drugs (modifications based on MWNT, prussian blue, poly (p-ABSA), AuNP and PtNP)

Electrochemistry is a well established and fast growing area with a number of possible applications in pharmaceutical field. The power and scope of this analysis have grown dramatically during the past decade. Electrochemical methods are routinely used in analytical chemistry. The improvement of quality of life has stimulated considerable research in drug design bioavailability and safety. Voltammetry is an extremely sensitive electrochemical technique for measuring trace amount of pharmaceutically active compound either in dosage forms or in biological samples. In drug analysis, voltammetric techniques are very popular because of the low quantification limit, its accuracy and precision, as well as the low cost of equipment compared to other analytical methods.

AuNPs immobilized on an amine terminated self assembled monolayer (SAM) on a polycrystalline Au electrode were successfully used for the selective determination of dopamine (DA) in the presence of ascorbate (AA) by T. Ohsaka et al. Well separated voltammetric peaks were observed for DA and AA at the nano Au electrode. The oxidation potential of AA is shifted to less positive potential due to the high catalytic activity of AuNP. The reversibility of the electrode reaction of DA is significantly improved at the AuNP electrode, which results in a large increase in the SWV peak current with a detection limit of 0.13 mM. The coexistence of a large excess of AA does not interfere with the voltammetric sensing of DA [66].

Electrocatalytic oxidation of morphine (MO) at an optically transparent indium tin oxide (ITO) electrode modified by an electrodeposited Prussian blue (PB) thin film is first demonstrated by K. C. Ho et al. The rate of the

electrocatalytic reaction is pH dependent with the highest value at pH 5. A linear calibration curve, displaying the relationship between steady state currents and MO concentrations (ranging from 0.09 to 1.0 mM), was obtained [67].

G. C. Zhao et al studied the electrocatalytic response of the MWNT modified GCE towards tryptophan (Trp) by CV and DPV. Compared with a bare electrode, the peak current had obviously increased, and the peak potential had shifted in a negative direction. Under the chosen conditions, the DPV peak current is linear to the concentration of Trp in the range of 2.5×10^{-7} to 1.0×10^{-4} M, and the detection limit is 2.7×10^{-8} M [68].

The electrochemical behavior of L-tyrosine was investigated at a MWNT modified GCE. L-tyrosine itself showed a poor electrochemical response at the bare GCE; however, a MWNT film fabricated on the GCE can directly enhance the electrochemical signal of L-tyrosine when applying CV and square wave stripping voltammetry without any mediator. The square wave stripping voltammetry currents of L-tyrosine at the MWNT modified electrodes increased linearly with the concentration in the range of 2.0×10^{-6}-5.0×10^{-4} M. The detection limit was 4.0×10^{-7} M [69].

A voltammetric method for the direct determination of 10-hydroxycamptothecin (HCPT) have been developed by S. Dong et al. At MWNT modified electrode, HCPT yields a very sensitive and well shaped oxidation peak, which can be used as analytical signal for HCPT determination. This developed sensor possesses very low detection limit (2×10^{-9} M) and wider linear range (from 1×10^{-8} to 4×10^{-6} M) [70].

A novel method for fabricating AuNP combining the dithiothreitol (DTT) and dodecanethiol (DDT) mixed self assembled approach is proposed by L. Wang et al. The mixed self assembled monolayers were first formed by

the assembly of DTT and DDT from solution onto gold electrode. When these thiol rich surfaces are exposed to Au colloid, the sulfur form strong bonds to AuNPs, anchoring the clusters to the electrode surface and a new nano Au surface was obtained. The nano Au electrode is demonstrated to promote the electrochemical response of epinephrine (EP) by CV [71].

AuNP were self assembled to the modified GCE with cysteamine (CA) to prepare the nano-Au/CA/GC modified electrode. The electrochemical behavior of epinephrine (EP) on the modified electrode was explored with CV and DPV. EP gave a pair of redox peaks at *E*pa = 190 mV and *E*pc =−224 mV (vs SCE), respectively. The modified electrode could be used to determine EP in the presence of ascorbic acid (AA). The response of catalytic current with EP concentration shows a linear relation in the range of 1.0×10^{-7} to 5.0×10^{-4} M with the correlation coefficient of 0.998. The detection limit is 4.0×10^{-8} M [72].

L. Wang et al have reported the selective detection of epinephrine (EP) in the presence of ascorbic acid using Poly (*p*-aminobenzenesulphonic acid) Poly (*p*-ABSA) modified GCE. In PBS of pH 7.0 oxidation peak current was proportional to the concentration of EP in the ranges: 1.0×10^{-6} to1.0×10^{-5} M and 2.0×10^{-5} to 2.0×10^{-4} M. Detection limit was 8.0×10^{-7} M. DPV was used to determine EP in the presence of excess of ascorbic acid (AA) at the modified electrode. Potentials of the recorded peaks (obtained in PBS, pH 7.0) were 138 and 66 mV (vs SCE) for EP and AA, respectively. High selectivity and sensitivity for the determination of EP was due to the favorable electrostatic interactions between the EP cations and the negatively charged Poly (*p*-ABSA) film in PBS of pH 7.0 [73].

A composite film of polyaniline (PAN) nano-networks/poly (p-ABSA) modified GCE has been fabricated via an electrochemical oxidation procedure

and applied to the electrocatalytic oxidation of uric acid (UA) and ascorbic acid (AA). Due to its different catalytic effects towards the electrooxidation of UA and AA, the modified GCE can resolve the overlapped voltammetric response of UA and AA into two well defined voltammetric peaks with both CV and DPV, which can be used for the selective and simultaneous determination of these species in a mixture. The catalytic peak currents are linearly dependent on the concentrations of UA and AA in the range of 50–250 and 35–175 μM. The detection limits for UA and AA are 12.0 and 7.5 μM, respectively [74].

Electrochemical behaviors of tryptophan at the poly (*p*-ABSA) film electrode were investigated by C. Li et al. The results indicate that the electrochemical response of tryptophan is improved significantly in the presence of poly (*p*-ABSA) film. Compared with the bare GCE, the poly (*p*-ABSA) film electrode remarkably enhances the irreversible oxidation peak current of tryptophan. Some parameters such as voltammetric sweeping segments for the electrochemical polymerization, pH, accumulation potential and accumulation time are optimized. Under the optimal conditions, the oxidation peak current is proportional to tryptophan concentration in the range of 1.0×10^{-7} to 1.0×10^{-6} M, and 2.0×10^{-6} to 1.0×10^{-5} M with a detection limit of 7.0×10^{-8} M [75].

The MWNTs/Nafion film coated GCE is constructed and the electrochemical behavior of norfloxacin (NFX) at the electrode is investigated in detail by K. J. Huang et al. Under conditions of CV, the current for oxidation of selected analyte is enhanced significantly in comparison to the bare GCE. Under optimized conditions the concentration calibration range and detection limit are 0.1–100 μM and 0.05 μM for NFX [76].

A novel conductive composite film containing MWNTs with poly (methylene blue) (PMB) has been synthesized on GCE, gold and indium tin oxide electrodes by S. M. Chen et al. The composite film exhibits a promising higher electrocatalytic activity towards the oxidation of ascorbic acid (AA), epinephrine (EP) and dopamine (DA) present in pH 7.4 aqueous solution. Both, the CV and SWV have been used for the measurement of electroanalytical properties of analytes by means of composite film modified electrodes. In CV, well separated voltammetric peaks have been obtained at the composite film modified GCEs for AA–EP and AA–DA mixture with a peak separation of 144.36 and 164.00 mV, respectively. The detection limit values obtained are equivalent to the concentrations found in physiological conditions [77].

A rapid, sensitive and simple electrochemical method was developed by K. J. Huang et al for the determination of trace level ofloxacin, based on the excellent properties of MWNT. The MWNT/Nafion film coated GCE is constructed and the electrochemical behavior of ofloxacin at the electrode is investigated in detail. The determination conditions, such as the amount of MWNT-Nafion suspension, the pH values of the supporting electrolyte, accumulation potential and time, as well as scan rate were optimized. Under the chosen conditions, the concentration of ofloxacin shows excellent linear relationships with the oxidation peak current, with a low detection limit of 1×10^{-7} M for 20 sec accumulation at -1200 mV [78].

The electrochemical behavior of ofloxacin on the MWNTs-Nafion film-coated GCE was investigated by CV, LSV and electrochemical impedance spectroscopy (EIS). The oxidation peak current of ofloxacin increased significantly on the MWNTs-Nafion film modified GCE compared with that using a bare GCE. A well defined oxidation peak was observed at 970 mV and

was applied to the determination of ofloxacin. The oxidation peak current was proportional to ofloxacin concentration in the ranges 1.0×10^{-8} to 1.0×10^{-6} M and 1.0×10^{-6} to 2.0×10^{-5} M. A detection limit of 8.0×10^{-9} M was obtained for 400 s accumulation at open circuit [79].

Platinum nanoparticles (PtNP) supported on polyaniline coated MWNT were fabricated by G. P. Jin et al using electrochemical method at paraffin-impregnated graphite electrode (Pt/PAN/MWCNTs). The electrode has been effectively applied for formaldehyde (HCHO) sensing. A good linear response curves from 1×10^{-9} to 1×10^{-3} M was obtained with a lower detection limit of 4.6×10^{-11} M. The successful preparation of nanocomposites opens a new path to fabricate the promising sensor for HCHO [80].

S. Issac et al reported the voltammetric analysis of Sulfamethoxazole (SMX) at a (MWNT)-Nafion modified GCE. SMX gave a well defined oxidation peak at 740 mV in 0.1 M PBS of pH 8.0. Various experimental parameters were optimized. Under optimum conditions the oxidation peak current is linear to the concentration of SMX in the range $1\times10^{-2} - 5\times10^{-5}$ M with a detection limit of 1×10^{-5} M. The MWNT/GCE showed good stability, selectivity and was successfully used to quantify SMX in pharmaceutical formulations and urine sample [81].

S. Yang et al have investigated the electrochemical behavior of rutin on AuNPs/ethylenediamine/MWNT modified GCE (AuNPs/en/MWNTs/GCE) in 0.1 M PBS of pH 3.5. Rutin effectively accumulated on the AuNPs/en/MWNTs/GCE and caused a pair of redox peaks at around 487 mV and 432 mV (vs. SCE) in 0.1 M PBS (pH 3.5). Under optimized conditions, the anodic peak current was linear to the rutin concentration in the range of 4.8×10^{-8} M - 9.6×10^{-7} M. The regression equation was: $i_{pa} = 2.3728C_{rutin} - 0.1782$ (i_{pa}: 10^{-5} A, C_{rutin}: μM, r = 0.9973). The detection limit of 3.2×10^{-8} M was obtained [82].

A gold nanoparticles carbon paste electrode (AuNP-CPE) has been used for the determination of atenolol (ATN) in drug formulations by CV, DPV and chronocoulometric methods. The results revealed that the modified electrode showed an electrocatalytic activity towards the anodic oxidation of atenolol by a marked enhancement in the current response in a buffered solution at pH 10.0. The anodic peak potential shifts by −80.0 mV when compared with the potential using bare carbon paste electrode. A linear analytical curve was observed in the range of 1.96×10^{-6} to 9.09×10^{-4} M. The detection limit for this method is 7.3×10^{-8} M [83].

M. Behpour et al have reported a sensitive electrochemical method for simultaneous determination of acetaminophen and atenolol on a AuNP-CPE in Britton-Robinson buffer solution. DPV was used for determination of both drugs. The modified electrode exhibited electrocatalytic properties toward acetaminophen and atenolol oxidation with a peak potential of 20.0 and 50.0 mV lower than that at the bare carbon paste electrode, respectively. Also the enhanced peak current response is a clear evidence of the catalytic action of the AuNP modified CPE towards oxidation of acetaminophen and atenolol. Linear calibration curves were obtained in the range of 0.770 μM – 0.375 mM and 0.990 μM – 0.167 mM with detection limits of 0.058 μM and 0.073 μM for acetaminophen and atenolol, respectively [84].

The electrochemical behaviors of rutin at poly (p-ABSA)/GCE have been investigated by X. Chen et al. Rutin can generate a pair of well defined redox peaks on the poly (p-ABSA)/GCE at 440 mV (*E*pa) and 396 mV (*E*pc) (vs SCE) respectively. The electrochemical parameters of rutin on the modified electrode were calculated with the results of the charge transfer coefficient (a), the number of electron transfer (*n*) and the electrode reaction rate constant (*k*s) as 0.61, 2.08 and 2.18 s^{-1} respectively. Under the selected

conditions, the oxidation peak current was linear to the rutin concentration over the range of 2.5×10^{-7}-1.0×10^{-5} M with a detection limit of 1.0×10^{-7} M [85].

S. Yang et al reported a sensitive method for voltammetric determination of paeonol in drug samples and human biological samples. Nafion/MWNTs composite film was coated on the GCE. The adsorptive voltammetric behavior of paeonol on the Nafion/MWNTs-modified electrode was investigated using CV and differential pulse anodic stripping voltammetry (DPASV). Under the optimum conditions, the anodic peak current was proportional to paeonol concentration in the range of 6.0×10^{-7}-6.0×10^{-5} M with a detection limit of 4.0×10^{-7} M [86].

R. C. Carvalho et al developed electrochemical sensor for the determination of ascorbate. The MWNT and poly (neutral red) (PNR)/MWNT modified electrodes were applied to the oxidative determination of ascorbate. Comparison was made with electrodes surface modified by graphite powder. All modified electrode configurations with and without PNR were successfully employed for ascorbate oxidation at 50 mV vs saturated calomel electrode [87].

B. Habibi et al reported a simple procedure to prepare a carbon ceramic electrode (CCE) modified with MWNT. The electrochemical behavior of pyridoxine was investigated on the obtained electrode in phosphate buffer solution (PBS), pH 7.0. During oxidation of pyridoxine on the MWCNT/CCE, one irreversible anodic peak at a potential of 716 mV (vs. SCE) appeared. The number of exchanged electrons in the electro oxidation process was obtained, and the data indicated that pyridoxine is oxidized via two one-electron steps. Using the proposed method, pyridoxine can be determined with a detection limit of 95 nM [88].

Theophylline [TP],(1,3-dimethylxanthine) has been commonly used as an additional treatment drug in the asthmatic acute phase in children and asthma and bronchospasm in adults. L. Qu et al have fabricated a Nafion/ MWNTs composite film-modified electrode and applied to the sensitive and convenient determination of TP. TP could effectively accumulate at the modified electrode and cause a sensitive anodic peak at around 1180 mV (vs SCE) in 0.01 M H_2SO_4 medium (pH 1.8). Under the optimized conditions, the anodic peak current was proportional to TP concentration in the range of 8.0×10^{-8} $–6.0\times10^{-5}$ M, with a detection limit of 2.0×10^{-8} M [89].

A ferrocene modified carbon nanotubes paste electrode (FCMCNTPE) was constructed by H. K. Maleh et al and used as a fast and sensitive tool for the determination of *N*-acetylcysteine (NAC) at trace level. It has been shown that by direct current CV and double step chronoamperometry, FCMCNTPE can catalyze the oxidation of NAC in phosphate buffer solution (PBS) and produces a sharp oxidation peak current. Linear calibration ranges were 1.0-400.0 μM with detections limit of 0.6 μM for DPV [90].

H. M. Moghaddam et al used a modified carbon nanotube paste electrode for the voltammetric determination of norepinephrine (NE). The mediated oxidation of NE at the modified electrode was investigated by CV. Under optimum conditions, the calibration curve for NE was obtained in the range of 0.03-500.0 μM with a detection limit (3s) of 22.0 nM using DPV [91].

Modified GCEs have been made by deposition of functionalised MWNTs followed by formation of poly(Nile blue) (PNB) films by electropolymerisation, using potential cycling in 0.1M PBS at pH 6.0. The electrochemical oxidation of carbidopa (CD) and benserazide (BS) on the

MWNTs/PNB modified electrodes was investigated using CV and DPV in 0.1M PBS, pH 5.0. Peak currents in DPV were linear over the concentration range of 1×10^{-5} to 1×10^{-4} M for CD and 4×10^{-6} to 4×10^{-5}M for BS. Higher sensitivities and lower detection limits, of 1.17 μM for CD and 0.50 μM for BS, were obtained with the modified electrode [92].

Atta et al have investigated a highly sensitive and simple method for the determination of acetaminophen (ACOP) using AuNP modified carbon paste electrode (GNMCPE). GNMCPE displayed excellent electrochemical catalytic activities towards the oxidation of ACOP. Under optimized experimental conditions in DPV technique, the sensitivity of ACOP was improved greatly and gave a linear response over the ranges 5.0×10^{-8} to 2.7×10^{-4} M with a detection limit of 1.46×10^{-8} M. This method could readily discriminate ACOP from dopamine (DA) [93].

A. S. Adekunle et al investigated the electrochemical response and impedimetric behaviour of Dopamine (DA) and Epinephrine (EP) at Platinum (Pt) electrode modified with Carbon Nanotubes-Gold Nanocomposite. Results showed that Pt-MWCNT-Au electrode gave the best DA and EP current response at lower charge transfer resistance. The electrode was easy to prepare and was also electrochemically stable such that it could be used for the detection of DA and EP in the presence of interfering species such as ascorbic acid (AA) [94].

A GCE modified with MWNT and bimetallic inorganic-organic nanofiber hybrid nanocomposite was prepared by M. B. Gholivand et al and was used for determination of trace levels of guaifenesin. Oxidation of guaifenesin on the surface of the modified electrode was investigated with DPV and the results showed that the modified electrode remarkably improved

sensitivity and selectivity for the electrochemical assay of guaifenesin. Detection limit and quantitation limit were found to be 0.0175 μM and 0.0583 μM, respectively [95].

An electrochemical sensor for determination of L-cysteine (CySH) was presented by Ye et al. It was based on vertically aligned MWNT modified with Pt nanoparticles by magnetron sputtering deposition. The electrochemistry of CySH was investigated by CV, DPV and chronoamperometry. It displays a linear dependence on the concentration of CySH at an applied potential of 450 mV. The electrode is found to be highly inert towards other amino acids, creatinine and urea [96].

PtNP were electrodeposited on graphene modified GCE to form a modified electrode. At the modified electrode, rutin, shows a couple of well defined redox peaks, which is corresponds to the reduction and reoxidation of rutin. Under the optimal conditions, the peak currents of DPV increased linearly with the rutin concentration in the range from 2.0×10^{-8} to 8.0×10^{-5} M with a limit of detection of 6.7×10^{-9} M. The as prepared electrode was successfully used for the selective determination of rutin in tablet, displaying a potential application of graphene composite modified electrode [97].

The use of a MWNT, ionic liquid and AuNP film GCE to determine oxytetracycline (OTC), one of the mostly used antibiotics in salmon industry, by amperometry and adsorptive stripping voltammetry (AdSV) is reported by E. Nagles et al. Using AdSV, variables like pH, scan rate (ν), accumulation potential, and time (E_{acc}, t_{acc}) were optimized. The best experimental conditions were: pH = 7.0; ν = 0.60 Vs^{-1}; E_{acc} = 0.40 V, and t_{acc} = 70 s. Using AdSV and amperometric techniques, the linear calibration curves ranged up to 8.0×10^{-6} M and the detection limits were 1.5×10^{-7} and 2.0×10^{-8} M, respectively [98].

S. Shahrokhiana et al studied the electrochemical reduction of tinidazole (TNZ) on AuNP/MWNT modified GCE using the LSV. An electrochemical procedure was used for the deposition of AuNP onto the MWNT film precast on a GCE surface. Under the optimal conditions, the modified electrode showed a wide linear response toward the concentration of TNZ in the range of 0.1–50 μM with a detection limit of 10 nM [99].

K. Li et al have developed a AuNP/SWNT Composite film Modified GCE for the determination of Meclofenoxate Hydrochloride (MFX). The AuNP/SWNT modified electrode exhibited a linear voltammetric response for MFX in the concentration range of 5.0×10^{-7} - 2.0×10^{-5} M. The sensor exhibited good sensitivity of MFX with the detection limit of 1.0×10^{-7} M by SWV under accumulation time of 200 s. The proposed method was further applied for the detection of MFX in real sample with satisfactory results [100].

Graphene decorated with AuNPs (AuNPs/β-CD/Gra) has been synthesized by in situ thermal reduction of graphene oxide and $HAuCl_4$ with β-cyclodextrin (β-CD) under alkaline condition. This material was used to fabricate an AuNPs/β-CD/Gra/GCE which showed excellent electrooxidation of L-ascorbic acid (AA), dopamine (DA) and uric acid (UA) in 0.10 M NaH_2PO_4–HCl buffer solution (pH 2.0) by SWV. Three well resolved oxidation peaks of AA and DA and UA were obtained. The modified GCE exhibits linear responses to AA, DA and UA in the ranges 30–2000, 0.5–150 and 0.5–60 μM, respectively. The detection limits for AA, DA and UA are 10, 0.15 and 0.21 μM, respectively [101].

A stable modified GCE based on (*p*-ABSA) film was prepared by electrochemical polymerization technique in PBS (pH 7.0) and its electrochemical behavior were studied by CV. The polymer film-modified

electrode has been used for investigation of the dermination of uric acid (UA). The peak potential values for the oxidation processes of 5×10^{-5} M UA on a bare GCE and the *p*-ABSA modified GCE surfaces has been obtained at about 509 mV and 309 mV by DPV, respectively. A linear calibration curve for DPV analysis was constructed in the concentration range of 1×10^{-5}-1×10^{-4} M. Limit of detection (LOD) and limit of quantification (LOQ) at *p*-ABSA modified electrode were obtained as 1.125×10^{-6} M and 3.750×10^{-6} M respectively [102].

An electrochemical immunosensor has been developed by X. Sun et al, for the determination of carbofuran based on AuNP, prussian blue-multiwalled carbon nanotubes-chitosan (PB-MWNTs-CTS) nanocomposite film. AuNP and PB-MWNTs-CTS incorporated films were used to enhance the electroactivity and stability of the immunosensor. Effects of experimental variables were investigated in details. Under optimum operating conditions, the system provided a wide linear range between 0.1 and 1 ng/mL with a detection limit of 0.021 ng/mL[103].

A highly sensitive method was investigated by H. Beitollahi et al for the simultaneous determination of dopamine (DA), uric acid (UA), and tryptophan (TRP) using a MWNT/5-amino-3',4'-dimethoxy-biphenyl-2-ol modified carbon paste electrode (5ADMBCNPE). The electrochemical profile of the proposed modified electrode was analyzed by CV, which showed a shift in the oxidation peak potential of DA at 160 mV to a less positive value compared with an unmodified carbon paste electrode. SWV in 0.1 M PBS at pH 7.0 was performed to determine DA in the range from 1.2 to 800.0 μM, with a detection limit of 0.16 μM [104].

S. Kumar et al used MWNT modified GCE to develop an analytical method for the analysis of ascorbic acid (AA) by SWV. The oxidation of

ascorbic acid at the modified GCE showed a peak potential at 315 mV, about 80 mV lower than that observed at the bare electrode. The peak current was about threefold higher than the response at the bare electrode. The limit of detection was 1.4 μM AA, while the limit of quantitation was 4.7 μM AA [105].

B. Unnikrishnan et al reported the fabrication and characterization of a voltammetric sensor for the determination of chlorpromazine (CPM) based on MWNT-polyethyleneimine (MWNT-PEI) composite modified GCE. CPM shows irreversible oxidation peak at MWCNT and MWNT-PEI modified GCE in pH 7 at 685 mV. MWNT-PEI shows excellent electroanalytical properties towards CPM and can detect as low as 10 nM level DPV. The MWCNT-PEI film shows well defined and well separate peaks for dopamine, uric acid, acetaminophen and CPM in the same solution. Therefore, this sensor may be used for the determination of all these compounds individually or simultaneously [106].

H. K. Maleh et al proposed isoprenaline (ISPT) as a new mediator for the voltammetric determination of glutathione (GSH) using multiwall carbon nanotubes paste electrode (MWCNTPE). The kinetic parameters of the system including electron transfer coefficient, and catalytic rate constant were also determined using the electrochemical approaches [107].

J. Zhou et al reported the voltammetric determination of the Baicalein by using a CPE doped with MWNT. The resulting sensor exhibits excellent redox activity towards Baicalein due to the large surface area and good conductivity of the electrode. CV at various scan rates was used to investigate the redox properties of Baicalein. At the optimum conditions, the sensor displays a linear current response to Baicalein in the 0.02-10 μM concentration range, with a limit of detection 4.2 nM [108].

The electrocatalytic study of ascorbic acid using single walled carbon nanotube/tungsten oxide ($SWCNT/WO_3$) modified GCE was conducted by K. S. Ngai et al. The oxidation peaks obtained indicate that the modified GCE has good electrochemical behavior in terms of sensitivity. The oxidation peak of $SWCNT/WO_3$ modified electrode was considerably enhanced by 2.5 times with about a 230 mV peak shift towards a lower potential when the $SWCNT/WO_3$ modified electrode was used in comparison with a bare GCE [109].

G. Ziyatdinova et al created MWNT modified graphite electrodes (MWNT-GE) for the voltammetric determination of α-tocopherol and retinol. α-Tocopherol and retinol are oxidized on bare GE and MWNT-GE in 0.1 M $HClO_4$ in acetonitrile. For α-tocopherol and retinol decrease in the overpotential and increase in oxidation currents have been observed at the MWNT-GE in comparison with unmodified electrode. The calibration graphs are linear in the range of 0.065-2.00 mM for α-tocopherol and 0.05-1.50 mM for retinol. The detection limits was found to be 0.05 and 0.04 mM for α-tocopherol and retinol, respectively [110].

W. Guo et al developed an electrochemical method for the determination of metoclopramide (MCP) with a MWNT modified GCE. Compared with the bare GCE, the MWNT-modified electrode exhibits electrocatalytic activity to the oxidation of MCP because of the significant oxidation peak current enhancement. Furthermore, various experimental parameters, such as the solution pH, the amount of MWNT-PAA suspension and accumulation conditions were optimized for the determination of MCP. The developed sensor exhibited a linear response in the range from 1.0×10^{-7} to 1.0×10^{-5} M and detection limit of 5.0×10^{-8} M [111].

A. Mohadesi used the modified carbon nanotubes paste electrode (MCNTPE) for the sensitive voltammetric determination of carbidopa (CD) in buffer solution using CV, SWV and chronoamperometry (CHA). The diffusion coefficient (D = 2.62 $\times 10^{-5}$ cm^2/s), and the kinetic parameter such as the electron transfer coefficient (α=0.37) of CD oxidation at the surface of MCNTPE was determined using electrochemical approaches. It has been found that under an optimum condition (pH 9.0), the oxidation of CD at the surface of the modified electrode occurs at a potential about 100 mV less positive than that of an unmodified carbon nanotubes paste electrode. SWV of CD at the modified electrode exhibited linear dynamic range with a detection limit of 0.4 μM [112].

Isoniazid (ISN) is used worldwide as an effective drug in the treatment of tuberculosis. W. C. Chen et al have reported the fabrication of an electrochemical sensor for the amperometric determination of ISN based on functionalized multiwalled carbon nanotube (f-MWNT) modified GCE. f-MWNT has been synthesized by acid treatment of MWNT by ultrasonication. ISN undergoes an irreversible oxidation at f-MWNT film in pH 4 at 400 mV which is well defined and it can be utilized for electroanalytical purposes. ISN showed fast amperometric response at f-MWNT modified GCE with a good linear range of detection 1 to 70 μM ISN [113].

A MWNT modified gold electrode (MWNT/Au) was prepared and its external morphology was characterised by scanning electron microscope and surface area study. The electrochemical behaviour of pyridine-2-aldoxime methochloride (PAM chloride) at this electrode was examined by SWV. At the MWNT/Au electrode, PAM chloride exhibited a well-defined anodic peak at 584 mV in pH 8 phosphate buffer solution with a 15 times enhancement in anodic peak current. The peak current was linear to PAM chloride

concentration over the range of 8×10^{-7}–1×10^{-5} M with a detection limit of 1×10^{-7} M [114].

A. Bahari et al described the use of a carbon paste electrode modified by ethynylferrocene (EF) and NiO/MWNT nanocomposite for the electrocatalytic oxidization of glutathione (GSH) and acetaminophen (AC). For the mixture containing GSH and AC, the peak potential were separated from each other. Their SWV peak currents increased linearly with concentration at the ranges of 0.01–200 and 0.8–600 μM respectively with the detection limits of 0.006 and 0.5 μM, respectively [115].

S. Kazemi studied the electrochemistry of norepinephrine (NE) by CV, chronoamperometry and SWV at a carbon paste electrode modified by MWNTs and room temperature ionic liquid, 1-methyl-3-butylimidazolium chloride (MBIDZCl). The cyclic voltammogram showed an irreversible oxidation peak at 360 mV (vs. Ag/AgCl), which corresponded to the oxidation of NE. Under the optimized conditions, the oxidation peak current of NE showed linear dynamic range (0.2–500 μM) with a detection limit of 0.08 μM, using SWV method [116].

1.14 Scope of the present investigation

Quality control in pharmaceuticals is an area of immense interest. Quantitative determination of very low concentration say in nanomolar ranges is an important aspect of quality control. Electrochemical methods are suited for such concentration studies. Among the electrochemical methods, voltammetry has been widely utilized for the development of pharmaceutical sensors due to its high accuracy and sensitivity, short analysis time, simple sample preparation, compact equipment, relatively low investment and running costs. With the aid of chemically modified electrodes, their efficiency can be further enhanced. From

the time of its discovery, nanoparticles have found its niche in every field of research. Voltammetry is no exception. As a continuation of work done in our lab on development of sensors for drug analysis [81, 114, 117-134], various nanoparticles like gold, platinum and MWNTs are used for the development of voltammetric sensors for the determination of drugs like PAM Chloride, Tamsulosin Hydrochloride, Hesperidin Methyl Chalcone, Guaiphenesin, Cephalexin and Amoxicillin trihydrate.

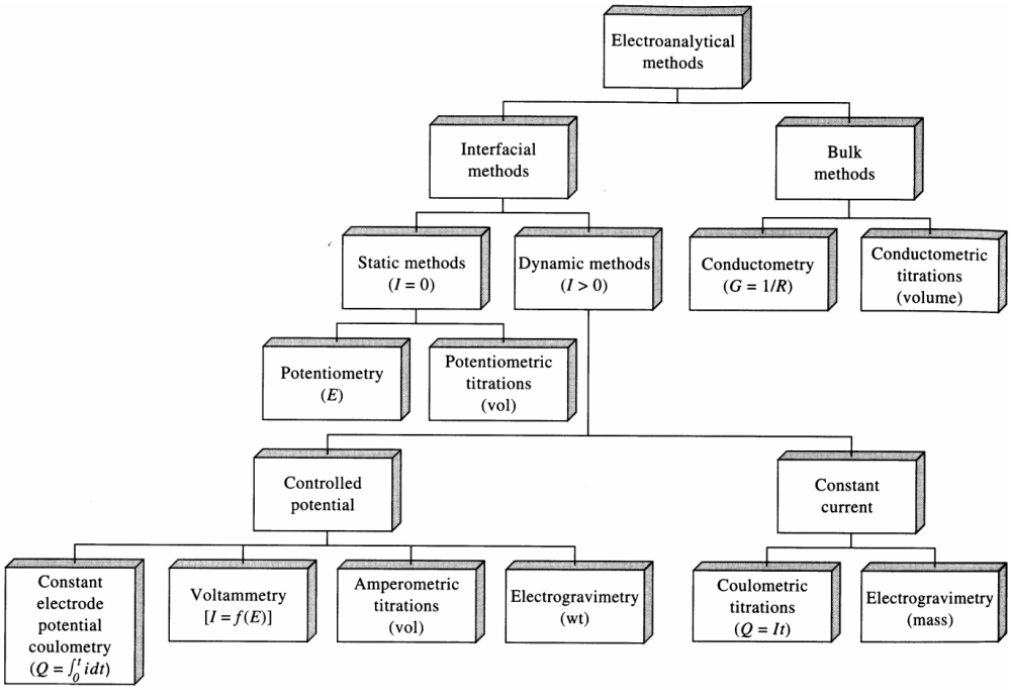

Figure1.1 Common electroanalytical methods

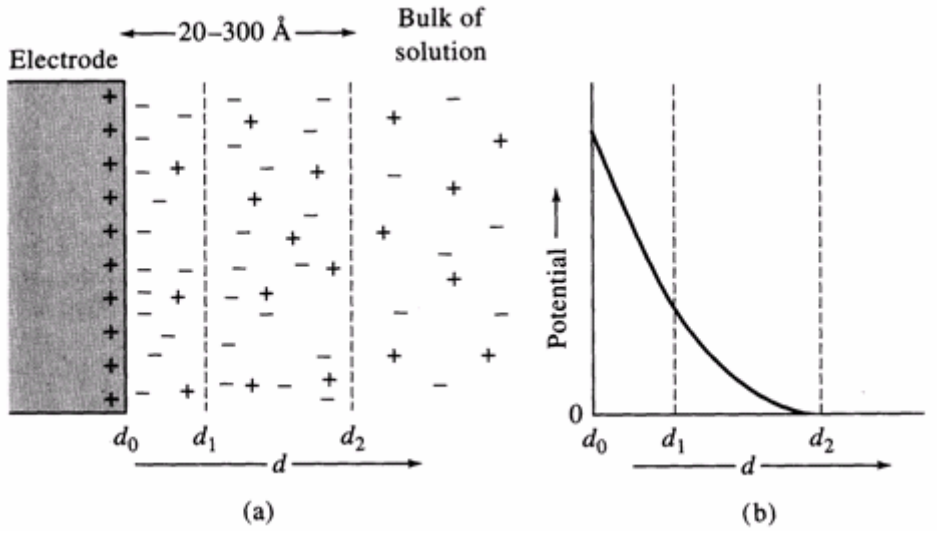

Figure 1.2 Electrical double layer formed at electrode surface as a result of an applied potential

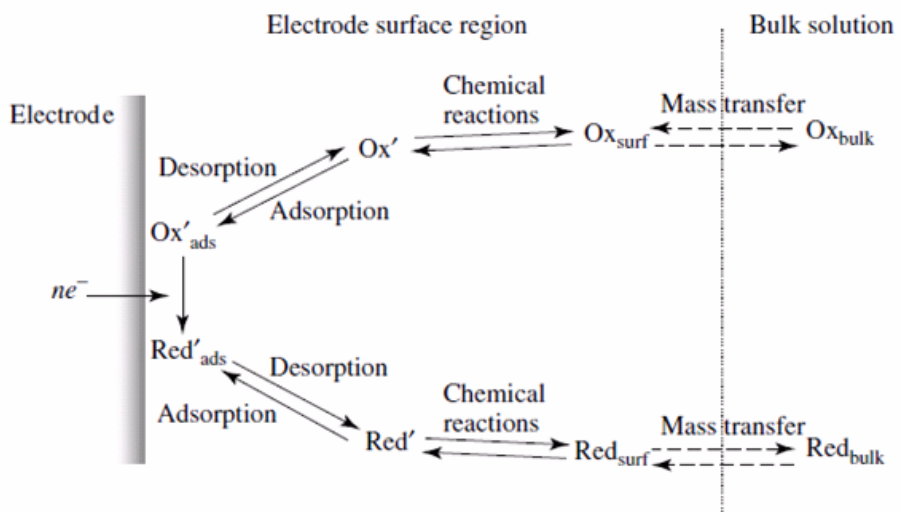

Figure 1.3 Typical steps involved in an electrode reaction

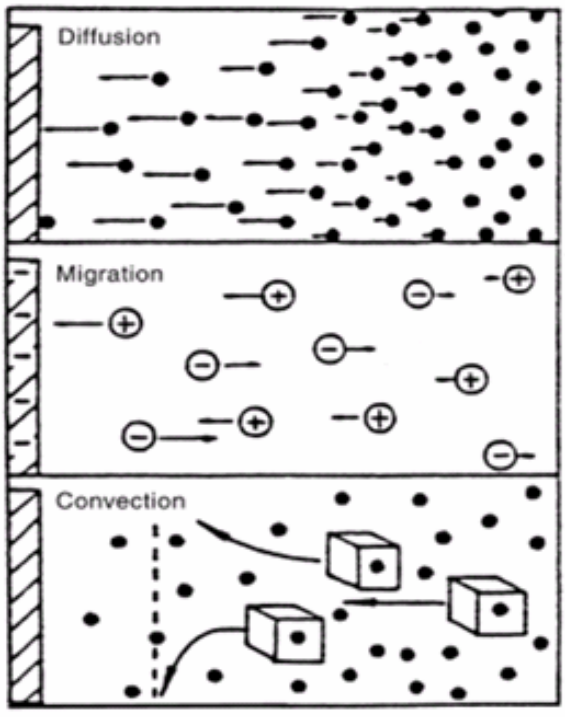

Figure 1.4 Modes of mass transfer

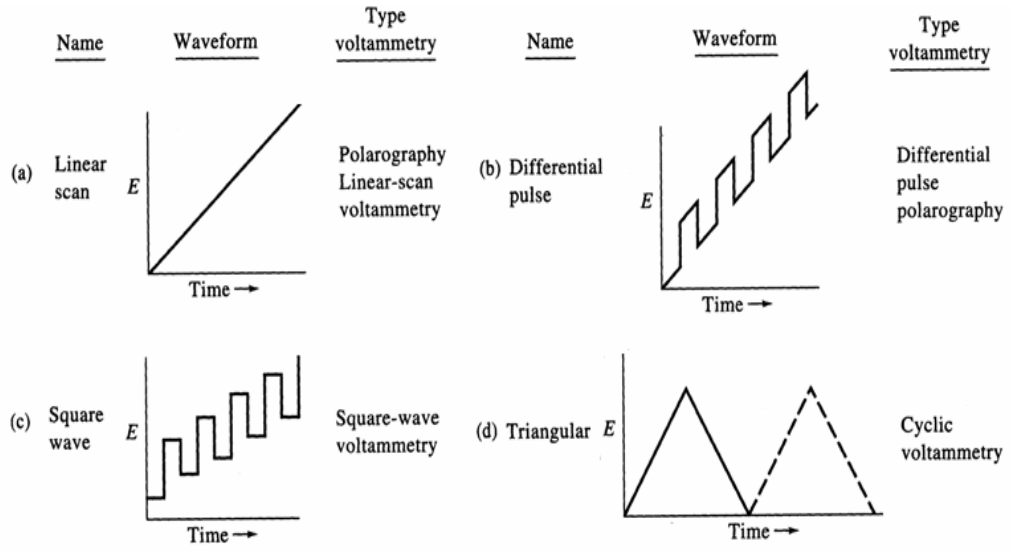

Figure 1.5 Excitation signals used in voltammetry

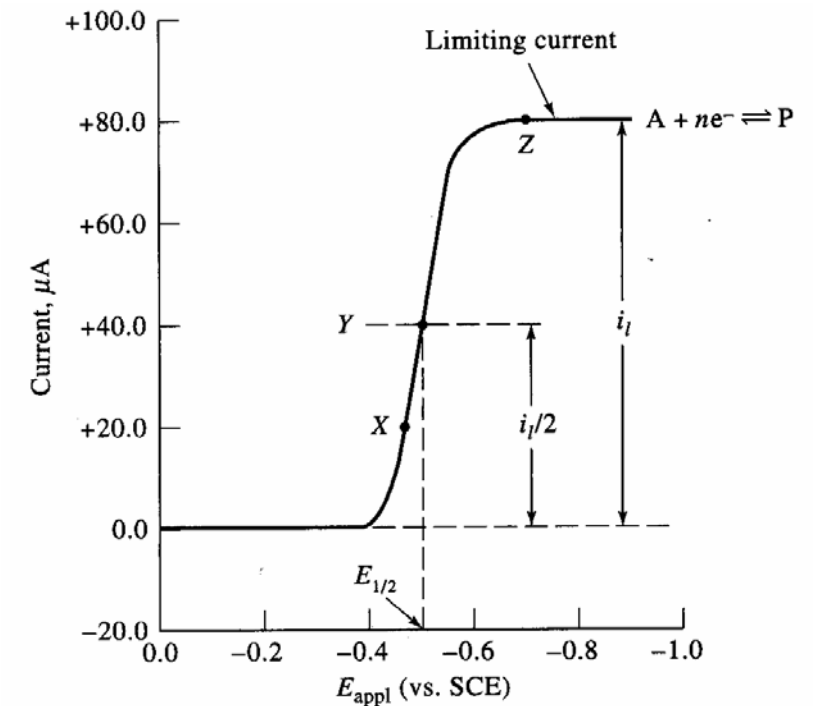

Figure 1.6 Linear sweep voltammogram

.....ꕥ.....

Chapter 2

MATERIALS AND METHODS

Contents

2.1 Reagents
2.2 Instruments Used
2.3 Cleaning of PtE
2.4 Cleaning of GCE
2.5 Preparation of chemically modified electrodes for pharmaceutical analysis
2.6 Preparation of the drug solutions
2.7 Preparation of buffer solutions
2.8 Analysis of the pharmaceutical formulations
2.9 Analysis of Urine Sample
2.10 Standard methods

This chapter explains the materials and methods used in the investigations. The general method for the fabrication of the modified electrodes is described in this chapter. Details about the general reagents and the instruments used in the investigations are also discussed in this chapter. The chapter also discusses the general procedure for the analysis of the pharmaceutical formulations and real samples employed in the studies.

2.1 Reagents

All reagents and solvents used for the investigations were of analytical grade and millipore water was used throughout the studies. Multiwalled carbon nanotube (MWNT), Nafion, alumina and PAM Chloride were purchased from Sigma Aldrich Corporation, USA. Except MWNT, other chemicals were used as received. Ethanol was purchased from Changshu Yangyuan Chemicals, China. Chloroauric acid was purchased from SRL Chemicals, India. Chloroplatinic acid was obtained from Spectrochem. Ltd, India. Sodium dihydrogen orthophosphate, disodium hydrogen orthophosphate, and sodium acetate trihydrate were

purchased from Merck, Germany and were used as received. All other common reagents were obtained from s.d fine chemicals Pvt. Ltd, Mumbai, India. Pure drugs such as Tamsulosin hydrochloride (TAM), Hesperidin methylchalcone (HMC), Guaiphenesin (Guai), Cephalexin (Ceph) and Amoxycillin trihydrate (AMX) were obtained as gift samples. Dosage forms containing the drugs were purchased from local drug stores. Disposable screen-printed carbon electrodes were purchased from DROPSENS, Spain.

2.2 Instruments Used

Electrochemical measurements were performed on a BAS Epsilon electrochemical analyzer (Bioanalytical system, USA) and an electrochemical workstation from CH Instruments, Austin, TX with a conventional three-electrode system. Working electrode used was platinum (PtE)/glassy carbon electrode (GCE) modified with suitable chemical modifications, an Ag/AgCl was used as the reference electrode, and a platinum wire as the counter-electrode. All voltammograms were recorded in the polarographic mode. The pH measurements were carried out in a Metrohm pH meter. Scanning Electron Microscopic (SEM) images were recorded using JOEL 6300 LV. Ultrasonic cleaning of the electrode was carried out in an Ultrasonicator (Oscar Ultrasonics, Pvt. Ltd. Mumbai). FTIR spectra were recorded on JASCO-4100 FTIR Spectrometer using KBr discs. The UV-Visible spectrum was recorded using Spectro UV-Visible Double Beam UVD-3500 instrument.

2.3 Cleaning of PtE

The working PtE was mechanically polished with aqueous slurries of alumina (50 nm) on a flat pad prior to surface modification. After polishing, it was rinsed ultrasonically with absolute ethanol to remove residual alumina particles from the surface and then cleaned with a piranha solution

(H_2O_2:H_2SO_4 = 1:3, v/v) for 10 minutes. Following this mechanical process, an electrochemical cleaning process was carried out using cyclic voltammetry (CV) performed from 0 to 1500 mV in 0.5 M sulphuric acid solution at a scan rate of 100 mV/s until a stable cyclic voltammogram was obtained.

2.4 Cleaning of GCE

Prior to modification, the GCE was mechanically polished with alumina slurry down to 0.05 μm on a polishing cloth. The electrode was then rinsed with millipore water thoroughly. In order to remove any adsorbed substances on the electrode surface, it was sonicated in methanol, water, aqueous HNO_3 (1:1, v/v) and acetone respectively.

2.5 Preparation of chemically modified electrodes for pharmaceutical analysis

2.5.1 Preparation of MWNT modified PtE

MWNT was refluxed in concentrated HNO_3 for 48 hrs to cause segmentation and carboxylation [135]. The resulting suspension was then diluted with 200 mL water. MWNT was then filtered and washed with double distilled water. The washed nanotube was collected and dried. As a result of this treatment, length of MWNT got shortened and they gained functional groups which made them hydrophilic. The peaks at 1703 cm^{-1} and 1564 cm^{-1} of the FTIR Spectrum demonstrated that carboxy groups and carboxylate groups are present on the surface of treated MWNTs.

Because of their large aspect ratio, MWNT are subject to large van der Waals forces, which cause them to stick together, forming large bundles. Therefore, one of the major challenges in fabricating a MWNT film is to separate the tubes, without using covalent chemistries or other harsh conditions, which could lower their electrical conductivity. While there has been

tremendous research and several reviews on the dispersion of MWNTs, we focused on the fabrication of MWNT dispersion in Nafion. Major barrier of developing MWNT-film based sensing devices is the insolubility of MWNT in most solvents. Because of the unique-ion exchange characteristics, thermal stability, chemical inertness, and mechanical strength, Nafion, a sulphonated tetra fluoro ethylene copolymer, was selected as the suitable solvent for the studies.

5 mg of the acid treated MWNT was dispersed in 13% (v/v) Nafion-water solution (2.3 mL) to give a 0.22 % (w/v) black homogenous suspension. Then the PtE was coated with an adequate amount of the resulting MWNT/Nafion suspension and the solvent was evaporated at room temperature in air to get MWNT modified PtE.

2.5.2 Preparation of MWNT modified GCE

A black homogenous suspension of MWNT in Nafion was prepared as explained in section 2.5.1. MWNT modified GCE was prepared by dropping 4 µL of this dark suspension (5 mg of MWNT in a mixture of 300 µL Nafion and 2 mL water) onto the clean GCE surface and evaporating the solvent at room temperature.

2.5.3 Preparation of Prussian blue (PB)/MWNT modified GCE

10 mg of the acid treated MWNT was dispersed in 13% (v/v) Nafion-water solution (4.6 mL) to give a 0.22 % (w/v) black homogenous suspension with the aid of ultrasonic agitation and it was added to 50 mL of the acidic mixture (pH 1.5) of $FeCl_3 \cdot 6H_2O$ (0.0654 g), $K_3Fe(CN)_6$ (0.0849 g) and KCl (0.3720 g) with stirring. After 12 h, excess ions were removed by filtration. The PB/MWNT hybrids were redispersed in deionized water by sonication. 4 µL of the dark suspension was dropped on to the surface of cleaned GCE. The electrode was then allowed to dry in air to obtain the PB/MWNT modified GCE.

2.5.4.1 Preparation of poly (p-aminobenzenesulphonic acid) modified GCE

After being cleaned, the GCE was immersed in 0.1 M HNO_3 containing 2.0 mM p-aminobenzenesulphonic acid (p-ABSA). CV was carried out between -0.5 and 2.0 V at a scan rate of 0.1 V/s [136]. This resulted in the electrochemical polymerization of p-ABSA on the electrode surface. The electrode was washed with millipore water to remove the remaining p-ABSA monomers. After drying in air, a blue thin film of poly (p-ABSA) was formed at the electrode surface.

2.5.4.2 Preparation of MWNT/poly (p-ABSA) modified GCE

The poly (p-ABSA) modified GCE was coated with an adequate amount of the MWNT/Nafion suspension (5 mg of the MWNT in a mixture of 300 µL Nafion and 2 mL water). Solvent was evaporated at room temperature in air to get the modified GCE.

2.5.5 Preparation of gold nanoparticle (AuNP) modified GCE

The cleaned GCE, reference electrode and auxiliary electrode were immersed in 0.05 M H_2SO_4 solution containing 1 mM $HAuCl_4$. 40 cyclic scans were carried out between 1.3 and 0 V at a scan rate of 0.1 V/s [137]. This resulted in the electrochemical deposition of AuNP on the electrode surface.

2.5.6.1 Preparation of platinum nanoparticle (PtNP) modified GCE

The electrochemical deposition of PtNP was performed in 0.1 M HCl solution containing 2 mM H_2PtCl_6. The deposition time was 9 minutes and the potential was -250 mV vs an Ag/AgCl electrode. The modified electrode was washed with millipore water and allowed to dry to get (PtNP) modified GCE.

2.5.6.2 Preparation of MWNT/AuNP and MWNT/PtNP modified GCE

The nanoparticles modified GCE were coated with an optimum amount of MWNT/Nafion dispersion (5 mg of MWNT in a mixture of 300 µL Nafion and 2 mL water). Then solvent was evaporated at room temperature in air to get the MWNT/ nanoparticles modified electrodes.

2.6 Preparation of the drug solutions

A 10^{-1} M stock solution in suitable solvents was prepared for each of the drugs. Solutions of different concentrations were obtained by the serial dilution of the stock solution. Table **2.1** details the amount of drugs required to prepare 10^{-1} M stock solution.

2.7 Preparation of buffer solutions

2.7.1 Preparation of phosphate buffer solution (PBS)

PBS of different pH was prepared by mixing NaH_2PO_4 and Na_2HPO_4 in varying amounts. Table **2.2** shows the amount of NaH_2PO_4 and Na_2HPO_4 required to prepare PBS of different pH.

2.7.2 Preparation of acetate buffer solution (ABS)

The buffer solutions of different pH were prepared by mixing sodium acetate trihydrate and acetic acid in different amounts. Table **2.3** gives an illustration of the amount of sodium acetate trihydrate and acetic acid required to prepare ABS of various pH.

2.8 Analysis of the pharmaceutical formulations

2.8.1 Tablet for Tamsulosin Hydrochloride (Veltam)

Ten tablets (‘Veltam’, Intas pharmaceuticals, India) were weighed and ground to a fine powder. To prepare approximately 1×10^{-4} M solution of TAM,

0.23 g of this powder was transferred to a 10 mL standard flask and made upto the mark with water. Solutions of different concentrations were prepared by serial dilution of the stock with supporting electrolyte. Voltammetric studies were carried out and the unknown concentrations were determined from the calibration graph.

2.8.2 Tablet for Guaiphenesin (Expal)

Ten tablets (Expal, Mech pharma, India) were weighed and finely powdered. Then 0.03 g of the powdered drug was weighed to prepare a solution of approximately 1×10^{-3} M Guai and was transferred to a beaker. The powder was dissolved in methanol and filtered to a titrimetric flask (100 mL). The beaker was washed several times and the washings were collected in the volumetric flask and then it was quantitatively diluted. Solutions of different concentrations were prepared by serial dilution of the stock with supporting electrolyte. Differential pulse voltammogram were recorded and the unknown concentrations were determined from the calibration graph.

2.8.3 Tablet for Cephalexin (Citaceph)

Ten tablets ('Citaceph', Citadel Aurobindo Biotech Ltd.) were weighed, crushed and finely powdered. Then 0.02 g of the powdered drug was weighed to prepare a solution of approximately 1×10^{-3} M and was transferred to a beaker. The beaker was washed a number of times with NaOH and the washings were collected in the 50 mL titrimetric flask and then it was quantitatively diluted. Solutions of different concentrations were prepared by serial dilution of the stock with supporting electrolyte. The sample solution was then taken and the voltammetric studies were carried out.

2.8.4 Tablet for Amoxicillin trihydrate (Pressmox)

Ten tablets ('Pressmox', Citadel Aurobindo Biotech Ltd.) were weighed, crushed and finely powdered. Then 0.02 g of the powdered drug (corresponding to the concentration approximately 1×10^{-3} M AMX) was weighed and transferred to a beaker. The powder was dissolved in ethanol and filtered to a 50 mL titrimetric flask through a Whatman 41 filter paper. The beaker was washed several times with ethanol and the contents were filtered into the flask. The solution was made upto the mark and shaken well. Solutions of different concentrations were prepared by serial dilution of the stock with supporting electrolyte. The sample solution was then taken in the electrochemical cell and the voltammetric studies were carried out.

2.9 Analysis of Urine Sample

The developed sensors were applied for the determination of the drug in spiked urine samples. Different quantities of drug were added to a fixed volume of urine sample and then quantitatively diluted using the supporting electrolyte. The voltammograms were recorded and the unknown concentrations were determined from the calibration graph.

2.10 Standard methods

2.10.1 PAM Chloride [138]

0.5 g of PAM Chloride was accurately weighed and dissolved in 250 mL water. 5 mL of this solution was then diluted to 100 mL with water. 5 mL of this solution was then transferred to a 50 mL titrimetric flask. Adequate amount of urine sample was added and then diluted to 40 mL with water. To this 5 mL of 1 M NaOH was added and made up to the mark. The absorbance of the resulting solution with various concentrations was measured.

2.10.2 Tamsulosin Hydrochloride [139]

Ten tablets of ('Veltam', Intas pharmaceuticals, India), were weighed and finely powdered. An adequate amount of this powder containing 0.3 g of TAM was weighed. It was dissolved in 5 mL formic acid, 75 mL of a mixture of glacial acetic acid and acetic anhydride. Then it was titrated against 0.1 N perchloric acid. The end point was determined potentiometrically.

2.10.3 Guaiphenesin [140]

Ten tablets ('Expal', Mech pharma, India), were accurately weighed and finely powdered. An adequate amount of this powder containing 0.01 g of Guai was weighed and dissolved in 10 mL methanol. 1 mL of the solution was taken in a 100 mL volumetric flask and the volume was made upto the mark with chloroform. The absorbance of the resulting solution with various concentrations was measured.

2.10.4 Cephalexin [141]

Ten tablets ('Citaceph', Citadel Aurobindo Biotech Ltd.), were accurately weighed and finely powdered. An adequate amount of this powder containing 0.2 g of Ceph was weighed, dissolved in 5 mL 1 M NaOH and transferred to a stoppered conical flask. 20 mL acetate buffer solution was added to it. To this 5 mL 1 M HCl was added and mix thoroughly. Then 25 mL 0.02 M I_2 was added to it and close the flask immediately and wet the cover by water. Keep the flask away from the light for 20 min. Titrate the excess Iodine with 0.02 M $Na_2S_2O_3$ using starch as indicator and the end point was determined.

2.10.5 Amoxicillin trihydrate [142]

Ten tablets ('Pressmox', Citadel Aurobindo Biotech Ltd.), were accurately weighed and finely powdered. An adequate amount of this powder

containing 0.17 g of AMX was weighed and dissolved in sufficient ethanol to produce 500 mL. Now transfer 10 mL of this solution into a 100 mL volumetric flask and add 10 mL of borate buffer solution (pH 9.0) followed by 1 mL of acetic anhydride-dioxan solution, allow to stand for 5 minutes and add sufficient water to produce 100 mL. Pipette 2 mL of the resulting solution into a stoppered tube. Add 10 mL of imidazole-mercury reagent, (dissolve 8.25 g of recrystallised imidazole in 60 mL of water and add 10 mL of 5 N HCl. Stir the solution magnetically and add dropwise, 10 mL of a 0.27% w/v solution of Hg_2Cl_2. Adjust the pH to 6.8 with 5 N HCl and add sufficient water to produce 100 mL) mix, stopper the tube and immerse it in a water bath previously maintained at 60^0c for exactly 25 minutes, with occasional swirling. Remove the tube from the water bath and cool rapidly to 20^0c. The absorbance of the resulting solutions was measured.

Table 2.1 Preparation of the drug solutions (0.1 M)

Drug	Amount	Solvent	Volume (mL)
PAM Chloride	1.726 g	water	100
TAM	4.449 g	water	100
HMC	6.246 g	water	100
Guai	1.982 g	methanol	100
Ceph	3.654 g	NaOH	100
AMX	4.194 g	ethanol	100

Table 2.2 Preparation of PBS of different pH

pH	NaH_2PO_4 (in grams/100 mL)	Na_2HPO_4 (in grams/100 mL)
2	1.3799	0.0001
3	1.3790	0.0003
4	1.3780	0.0036
5	1.3615	0.0360
6	1.2143	0.3218
7	0.5836	1.5466
8	0.0940	2.4970
9	0.0100	2.6605
10	0.0010	2.6781

Table 2.3 Preparation of ABS of different pH

pH	NaH_2PO_4 (in grams/100 mL)	Na_2HPO_4 (in grams/100 mL)
2	0.5994	0.0024
3	0.5900	0.0237
4	0.5098	0.2054
5	0.2161	0.8711
6	0.0319	1.2885
7	0.0336	1.3534
8	0.0034	1.3602
9	0.0004	1.3609
10	0	1.3609

.....ஜ۞ஜ.....

Chapter 3

DEVELOPMENT OF SENSOR FOR PYRIDINE-2-ALDOXIME METHOCHLORIDE

Contents

3.1 Introduction
3.2 Preparation of MWNT-modified Pt electrode
3.3 Electrochemical behaviour of PAM chloride
3.4 Evidences of electrode modification
3.5 Performance characteristics of the developed sensor
3.6 Analytical application
3.7 Conclusions

This chapter deals with the development of a differential pulse voltammetric sensor for the determination of pyridine-2-aldoximemethochloride (PAM chloride) using a multiwalled carbon nanotube (MWNT) modified platinum (Pt) electrode. PAM chloride is a cholinesterase reactivator, used as an antidote in the treatment of organophosphate poisoning. At MWNT modified electrode, PAM chloride gave a well defined oxidation peak at a potential of 536 mV. Compared to the bare electrode, the peak current of PAM chloride showed marked increase, and the peak potential showed a negative deviation. Various determination conditions were optimized. The concentration of PAM chloride showed excellent linear relationships with the oxidation peak current in the concentration range 1×10^{-6}-2×10^{-5} M, with a detection limit of 3.03×10^{-7} M. The developed sensor exhibits good stability and reproducibility, and was successfully applied for the determination of PAM chloride in urine samples.

3.1 Introduction

Nerve agents are manmade organophosphorus compounds that have been manufactured for use in chemical warfare. These agents are known to be present in military stockpiles of several nations. Nerve agents inhibit cholinesterase enzymes in plasma, erythrocytes and at cholinergic nerve

endings in tissues. Once tissue cholinesterase is inhibited by the nerve agent, the enzyme cannot hydrolyze the neurotransmitter acetylcholine. Consequently, acetylcholine accumulates and causes prolonged stimulation of the affected tissues. Excess acetylcholine on nerve agent poisoning leads to pupils contraction, profuse salivation, convulsions, involuntary urination and defecation, and eventual death by asphyxiation as control is lost over respiratory muscles. The bond between the nerve agent and the enzyme is permanent unless antidotes are administered. Enzyme activity will slowly return to normal without antidotes, but only as new cholinesterase is synthesized or with erythrocyte turnover [143].

PAM chloride, chemically 2-formyl-1 methylpyridinium chloride oxime (Figure **3.1**), is an antidote approved for reactivation of inhibited acetylcholinesterase (AChE) in organophosphate poisoning [144]. It reactivates the poisoned enzyme (AChE) by scavenging the phosphoryl group attached on the functional hydroxyl group of the enzyme. This is known as "regenerating" or "reactivating" acetylcholinesterase, which allows the breakdown of acetylcholin at the synapse. The specific activity of the drug resides in the 2-formyl-1 methylpyridinium ion and is independent of the particular salt employed.

Detection of PAM chloride is highly significant from the point of view of its application in defence. The drug is rapidly excreted in the urine partly unchanged, and partly as a metabolite produced by the liver. One of the major applications of this work is to determine PAM chloride in urine using the developed sensor.

Only very limited methods are available for the determination of PAM chloride. K. K Rajic et al have developed a spectrophotometric method for the deiermination of PAM chloride in aqueous solutions using Pd (II) as the

analytical reagent [145]. A capillary zone electrophoresis method for the fast and reliable determination of PAM chloride in serum, cerebrospinal fluid and brain was described by H. Kalasz et al [146]. An isotachophoresis method for the determination of PAM chloride in dosage forms was developed by M. Bodiroga et al [147]. These methods are time consuming and require expensive and sophisticated instruments. Modern electrochemical methods are sensitive, selective, rapid and easy techniques which are applicable to analysis in the pharmaceutical fields. Hence these electroanalytical techniques can easily be adopted to solve many problems of pharmaceutical interest with a high degree of accuracy and precision. A search through the literature reveals no data on the development of an electrochemical sensor for PAM chloride using a MWNT modified Pt electrode.

Carbon nanotubes (CNT) are extremely promising for applications in materials science and medicinal chemistry. Although nanotubes are produced from the graphite precursor, their structure and topology differ from that of the parent graphite; the structure is tubular and of nanometer dimensions [148]. They are expected to find important applications in various fields such as gas sensing [149-150], nano electronic devices [151-153], hydrogen energy storage [154], field emission materials [155] etc. The special structure and subtle electronic properties suggest that CNT may have the ability to promote electron-transfer when it is used as electrode material. Many researchers have confirmed this point, and it has been widely used as modifying material in electrochemical area. Certainly, in studies of the electrochemical properties of biologically relevant molecules such as hydrogen peroxide [156–157], NADH [158–159], and dopamine [160–161], etc., MWNT-modified electrodes have shown superior performances as compared to other carbon electrodes. Also, their subtle electronic properties suggest that MWNTs have the stability to promote the direct electron

transfer reaction of some important biomolecules such as microperoxidase [162], horseradish peroxidase [163], hemoglobin [164], and glucose oxidase [165].

As part of the present investigations, Pt electrode modified with MWNT was employed for the study of the electrocatalytic oxidation and determination of PAM chloride. Modified Pt electrode was fabricated by drop drying the homogeneous suspension of MWNT-Nafion mixture onto the cleaned Pt electrode surface. Electrochemical and surface characterization by square wave voltammetry (SWV) and scanning electron microscopy (SEM) confirmed the presence of MWNT on Pt electrode. At modified electrode, PAM chloride gave an irreversible oxidation peak at 536 mV. Under the optimized condition, oxidation peak current of PAM chloride increases with increase in the concentration. The developed sensor can be used to quantify PAM chloride in urine samples.

3.2 Preparation of MWNT-modified Pt electrode

Prior to modification, the Pt electrode was polished and electrochemically cleaned as explained in section 2.3 of chapter 2. A detailed procedure for the fabrication of MWNT-Nafion / Pt electrode was given in section 2.5.1 of chapter 2. Acid treated MWNT was dispersed in Nafion-water solution (5 mg of MWNT in a mixture of 300 μL Nafion and 2 mL water) with the aid of ultrasonic agitation to form a black homogenous suspension. 4 μL of the darkish suspension was dropped onto the cleaned Pt surface and the solvent was evaporated at room temperature in air.

3.3 Electrochemical behaviour of PAM chloride

Electrochemical data were obtained with a three electrode system using a BAS Epsilon electrochemical analyzer (Bio-analytical system USA)

interfaced to a PC. MWNT-Nafion modified Pt electrode and a Pt wire were served as the working electrode and the counter electrode respectively. Ag/AgCl electrode served as the reference electrode.

Stock solution of PAM chloride was prepared as described in section 2.6 of Chapter 2. Standard solutions of the analyte (1×10^{-3}-1×10^{-6} M) were prepared by serial dilution of stock solution with appropriate supporting electrolyte (phosphate buffer solution (PBS), pH 8). A 10 mL PBS (0.1 M) containing a specific amount of sample solution was transferred to a voltammetric cell, and then purged with purified nitrogen for 3 min to remove oxygen. Differential Pulse Voltammogram was recorded from 0 – 1.0 V at a scan rate of 100 mV/s. The peak current for the oxidation of PAM chloride at 536 mV was measured. After each measurement the modified electrode was subjected to successive sweeping at pH 8 to give reproducible electrode surface.

The electrochemical behavior of PAM chloride was first studied on bare Pt electrode. PAM chloride gave an oxidation peak at 624 mV with a peak current of 1.32 μA. In order to reduce the overpotential, we tried various chemical modifications on Pt electrode. At a chitosan modified Pt electrode, an oxidation peak appeared at 420 mV and the peak current was 1.4099 μA. However, the electrochemical behavior of PAM chloride at a MWNT-Nafion modified Pt electrode has been investigated by differential pulse voltammetry (DPV). At the MWNT modified electrode, the oxidation peak appeared at 536 mV and the peak current was found to be 31.3 μA. Since electrochemical response of PAM chloride at MWNT-Nafion modified Pt electrode was obtained with high peak current, the choice is justified. Figure **3.2** displays the comparison of oxidation peak of 1×10^{-3} M PAM chloride in PBS at bare and MWNT-Nafion modified Pt electrodes. Compared with the bare Pt electrode,

the oxidation potential of PAM chloride has shifted negatively by about 90 mV and also there is a 30 fold increase in peak current. It undoubtedly proved the electrocatalytic activity of MWNT towards the oxidation of PAM chloride.

3.4 Evidences of electrode modification

3.4.1 SEM images

SEM images of both bare and MWNT modified electrodes are given in Figure **3.3**. Electrode modification is evidenced from the SEM images. The SEM image of MWNT modified electrode showed that electrode surface contains aggregates of MWNTs. It has been reported that drying a droplet of MWNT solution at room temperature on a wettable surface led to redistribution, accumulation, and organization of MWNTs along the perimeter of the droplet [166].

3.4.2 Surface area study

2 mM $K_3Fe(CN)_6$ was taken as a probe to measure the microscopic areas of the MWNT- modified and bare Pt electrodes. Square wave voltammograms were recorded at different scan rates for both bare and modified Pt electrodes (Figure **3.4**). For a reversible system the relationship between the current and scan rate is given by the Randles-Sevcik equation [167],

$$I_p = 2.69 \times 10^5 A n^{3/2} D_R^{1/2} C \nu^{1/2}$$

where I_p refers to the peak current, n is the number of electron transferred, A is the surface area of the electrode, D_R is the diffusion coefficient, C is the concentration of $K_3Fe(CN)_6$ and ν refers to the scan rate. For $K_3Fe(CN)_6$, n =1 and $D_R = 7.6\times10^{-6}$ cm/s. Graphs were plotted with current vs square root of scan rate for both electrodes (I_p versus $\nu^{1/2}$). The regression equations obtained from SWV analysis for the bare and modified electrodes are:

I_p =0.950 $\nu^{½}$ +2.097 (r^2=0.999, ν in mV/s, I_p in μA) and I_p =2.580 $\nu^{½}$ +0.772 (r^2=0.998, ν in mV/s, I_p in μA) respectively.

The surface area can be calculated from the slope of these linear graphs. Surface area for bare electrode was found to be 0.0668 cm^2. On modification with MWNT the effective surface area was increased to 0.2510 cm^2, ie there is a 4 fold increase in surface area. This is a strong evidence for the successful and effective modification of Pt electrode surface using MWNT.

3.5 Performance characteristics of the developed sensor

Several parameters were investigated in order to evaluate the performance of the MWNT based PAM chloride sensor, in terms of effect of supporting electrolyte, effect of pH, effect of amount of the MWNT-Nafion dispersion, effect of scan rate, influence of concentration, detection limit and influence of foreign species. The next sections explain in detail each of these parameters.

3.5.1 Effect of supporting electrolyte

The electrochemical oxidation signals of PAM chloride at MWNT-Nafion film coated Pt electrode has been examined in various electrolytes. The supporting electrolytes include KNO_3, H_2SO_4, NaOH, NaCl, tetra-n-butyl ammonium chloride, KCl and PBS (0.1 M). The results showed that a well defined oxidation peak is appeared in PBS. Therefore 0.1 M PBS was used as the supporting electrolyte for the determination of PAM chloride.

3.5.2 Effect of pH

The influence of pH on the oxidation peak current of 1×10^{-3} M PAM chloride at the MWNT-Nafion modified Pt was investigated from pH, 3 to 10. An anodic peak was appeared when pH reaches 7. The plot of anodic peak

current versus pH of the supporting electrolyte in the range of 7 to 10 for PAM chloride is presented in Figure **3.5**. Experimental results shows that the pH had a strong influence on the anodic peak current. Peak current showed gradual increase with maxima at pH 8. An increase of pH beyond this value caused a marked decrease in the peak current. Hence the optimal pH for the buffer medium was selected to be 8.

3.5.3 Effect of amount of the MWNT-Nafion dispersion

The relationship between the amount of the MWNT-Nafion dispersion (5 mg of MWNT in a mixture of 300 μL Nafion and 2 mL water) and the oxidation peak current of PAM chloride was studied. As the amount of MWNT was increased upto 4 μL, the oxidation peak current greatly enhanced Figure **3.6**. The enhancement of current indicates that the surface area and the number of catalytic site increases with increasing volume of MWNT. With further increase in the amount of MWNT-Nafion dispersion, the oxidation peak current showed a drastic decrease. This indicates the hindrance to the electron transfer of PAM chloride due to excessive MWNT.

3.5.4 Effect of scan rate

The influence of scan rate on the oxidation peak potential and the peak current of 1×10^{-3} M PAM chloride at the MWNT-Nafion film coated Pt electrode was investigated by linear sweep voltammetry (LSV) in the range of (20-180 mV/s) (Figure **3.7**). The regression equation obtained from LSV analysis is: $I_p = 1.485\ \nu^{1/2} + 1.800$ ($r^2=0.990$, ν in mV/s, I_p in μA). It was found that the oxidation peak current varies linearly with square root of scan rate which indicate that the electrochemical oxidation process of PAM chloride at the modified electrode is diffusion controlled (Figure **3.8**).

The effect of scan rate on peak current was also examined under the above conditions with a plot of log I versus log ν, giving a straight line within the same scan rate range (Figure **3.9**). The regression equation obtained is log I = 0.423 log ν + 0.375 (r^2=0.998). The slope (0.4) of the curve was close to the theoretically expected value (0.5) for an ideal reaction of solution species (diffusion controlled electrodic process) [168].

Number of electrons involved in the reaction (n_a) can be calculated from the scan rate study using the Laviron's equation [169] which is given by E = 0.028 ln ν + 0.500 (r^2=0.996). It was found that E varies linearly with the logarithm of ν (Figure **3.10**). The slope of this plot (b) is equal to $RT/\alpha n_a F$, where b is the slope, R is the Universal Gas Constant, T is the temperature, α is a constant (for a totally irreversible electrode process the value of α is assumed to be 0.5) and the value of F (Faraday) is 96500 C. For the irreversible oxidation of PAM chloride n_a value was calculated to be around 2. It indicates that two electrons were involved in the oxidation process of PAM chloride.

The oxidation site of PAM chloride is the aldoxime functionality. Mechanistic evidence exist for the oxidation of aldoxime involving one-electron oxidation of aldoxime to the iminoxy radical, followed by a second one-electron oxidation step to the α-hydroxy nitroso compound. This on dimerization and elimination of hyponitrous acid gives the carbonyl compound [170] (Figure **3.11**).

3.5.5 Influence of concentration

The relationship between the anodic peak current with its concentration was investigated by DPV. Under optimized conditions, with PAM chloride concentrations varying in the range of 1×10^{-6}-1×10^{-3} M, the oxidation peak

current varied proportionally with the concentration of the drug (Figure **3.12**). The detection limit of PAM chloride was found to be 3.03×10^{-7} M (Figure **3.13**). Comparison of the developed sensor with the previously reported methods demonstrates that the presently developed sensor method is a good method for the determination of PAM chloride (Table **3.1**).

The determination of PAM chloride at a concentration level of 1×10^{-3} M was carried out repeatedly at a MWNT-Nafion film coated Pt electrode for several times. The relative standard deviation (RSD) of peak current was obtained as 1.69 % when 5 parallel determinations were made (ie n=5). This result demonstrated the good reproducibility of the developed sensor. The storage stability of the modified electrodes was evaluated by measuring the current response of PAM chloride once in every day. It was found that the electrode surface showed stability for 10 days.

3.5.6 Interference study

The most important characteristic of any sensor is its response to the analyte in the presence of other ions present in solution. To evaluate the interference of foreign compounds on the determination of PAM chloride at the 1×10^{-3} M level, a systematic study was carried out. It was found that upto 100 fold excess molar concentration of urea, glucose, lactose, Na^+, K^+, Cl^-, and SO_4^{2-} did not interfere the current response of 1×10^{-3} M PAM chloride (signal change below 5%), however ascorbic acid interferes severely in the PAM chloride determination.(Table **3.2**).

3.6 Analytical application

The application of the developed sensor was further investigated by using the sensor in the determination of PAM chloride in the spiked urine samples.

3.6.1 Determination of PAM chloride in urine sample

The developed sensor was applied for the determination of PAM chloride in urine samples. 2 mL of the urine sample and 8 mL PBS were transferred to the voltammetric cell. An adequate amount of PAM chloride corresponding to 1×10^{-3} M was added. This solution was quantitatively diluted using PBS to obtain various concentrations. Then purified nitrogen was purged for 3 min to remove oxygen. DPV was recorded and the unknown concentrations were determined from the calibration graph. The recoveries obtained are shown in Table **3.3**. The recovery obtained with the developed sensor was compared with that obtained using the standard method (spectrophotometric method) [138] Table **3.4**. It was found that there is a satisfactory agreement between the PAM chloride content determined by the developed sensor and by the reported standard method.

3.7 Conclusions

Voltammetric behaviour of PAM chloride was investigated at MWNT modified Pt electrode by DPV and LSV. The MWNT modified Pt electrode showed electrocatalytic action for the oxidation of PAM chloride, characterized by the enhancement of the peak current and the reduction of peak potential. The electrochemical oxidation of PAM chloride at modified electrode involves transfer of two electrons and was diffusion controlled one. The proposed method is a better method for the analytical determination of PAM chloride, because it is simple, fast and it has sufficient precision, accuracy and sensitivity. The developed method was successfully applied for the determination of PAM chloride in urine samples.

Table 3.1 Comparison of various methods

Method adopted	Detection limit
Capillary zone electrophoresis (CZE)[146]	1.0×10^{-7}M
Isotachophoresis [147]	1.5×10^{-7} M
Spectrophotometry(Indian pharmacopeia method) [138]	1.0×10^{-5} M
Present method	3.0×10^{-7} M

Table 3.2 Interference study

Foreign species	Signal change*(%)	S.D*
Urea	- 0.3	0.10
Glucose	- 3.4	0.39
Lactose	- 3.0	0.82
Na^+	- 3.6	0.60
K^+	+ 2.6	0.46
Cl^-	- 3.6	0.60
SO_4^{2-}	+ 2.6	0.46
Ascorbic acid	- 32.0	3.8

* Average of three replicates

Table 3.3 Determination of PAM chloride in urine sample

PAM chloride added (M)	PAM chloride found (M)	Recovery (%)
3.00×10^{-6}	2.96×10^{-6}	99
5.00×10^{-6}	5.03×10^{-6}	101
7.00×10^{-6}	7.03×10^{-6}	100

Table 3.4 Comparison of the results obtained with the developed sensor and the standard method

Developed sensor		Standard method	
Recovery (%)*	CV*	Recovery*	CV*
99.7	1.24	99.4	1.91

*Average of six replicates

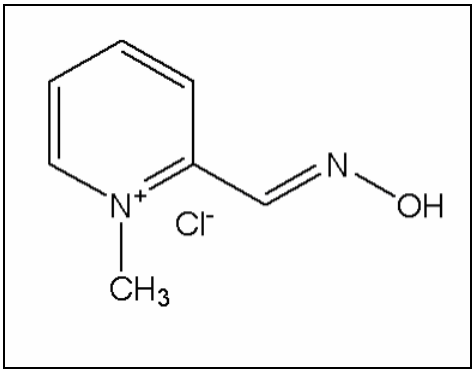

Figure 3.1 Structure of PAM chloride

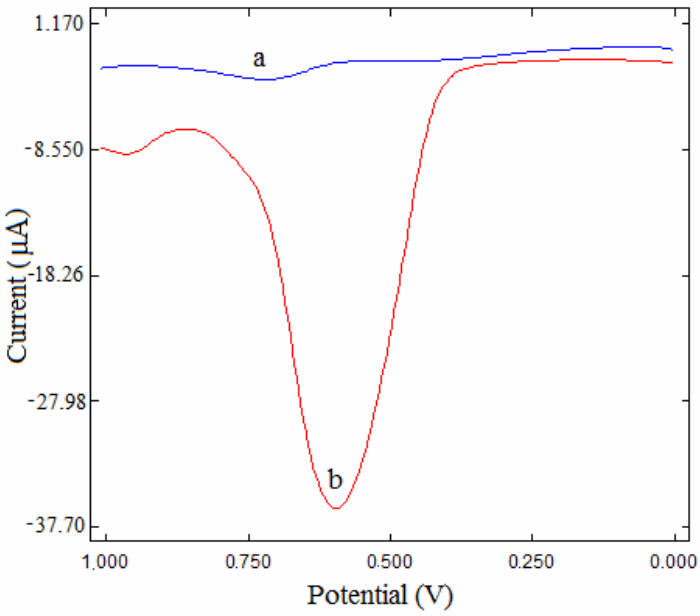

Figure 3.2 Differential pulse voltammmograms of 1×10^{-3} M PAM chloride at (a) bare Pt (b) MWNT- modified Pt electrode

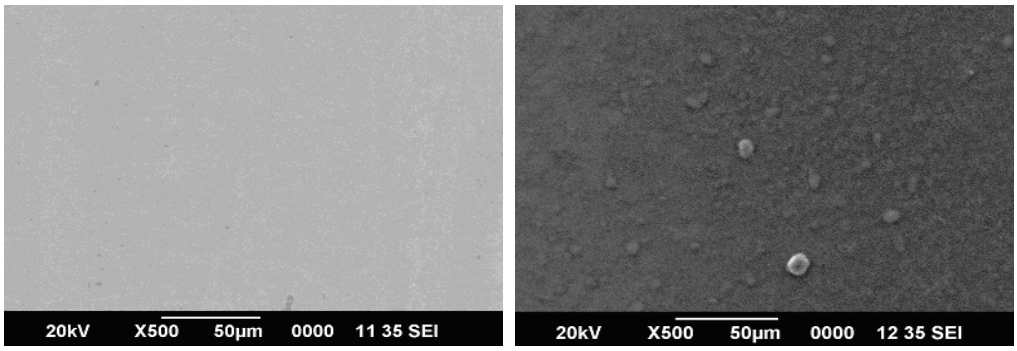

(a) (b)

Figure 3.3 SEM images of (a) bare Pt electrode and (b) MWNT modified Pt electrode

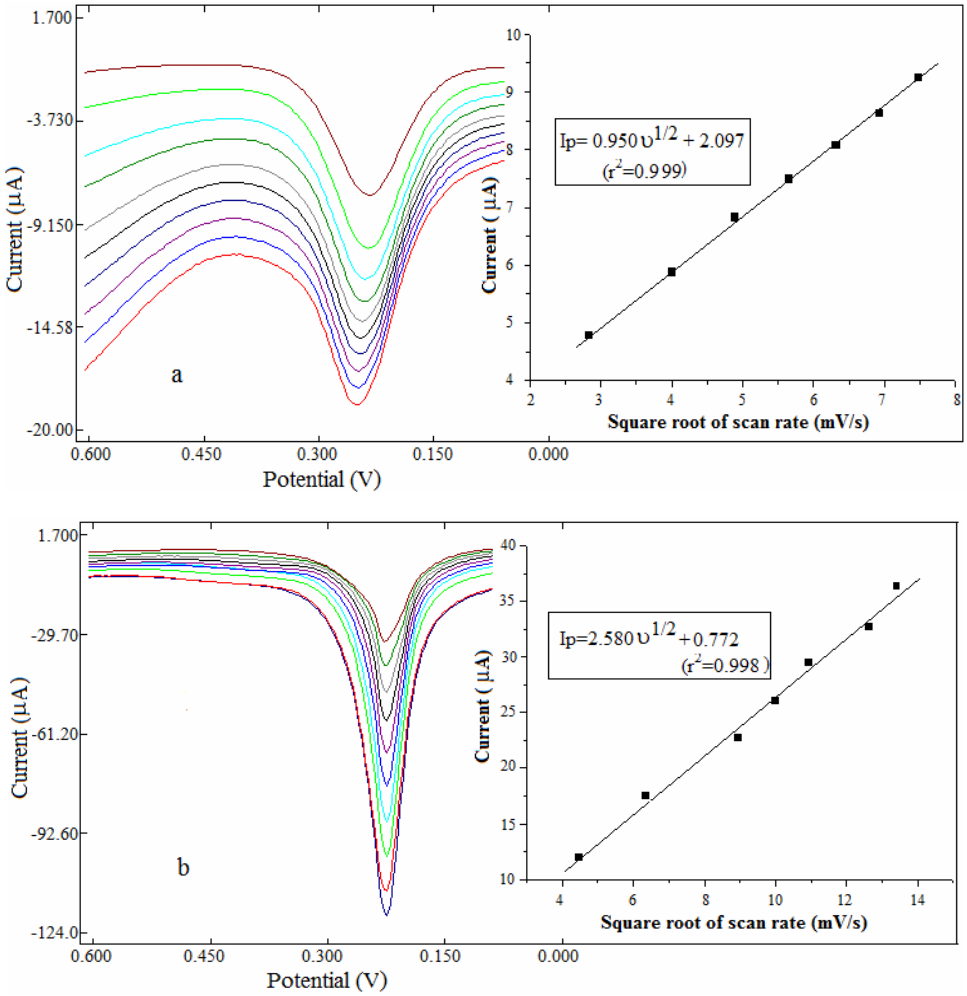

Figure 3.4 Surface area study of (a) bare Pt electrode and (b) MWNT modified Pt electrode in $K_3Fe(CN)_6$ solution

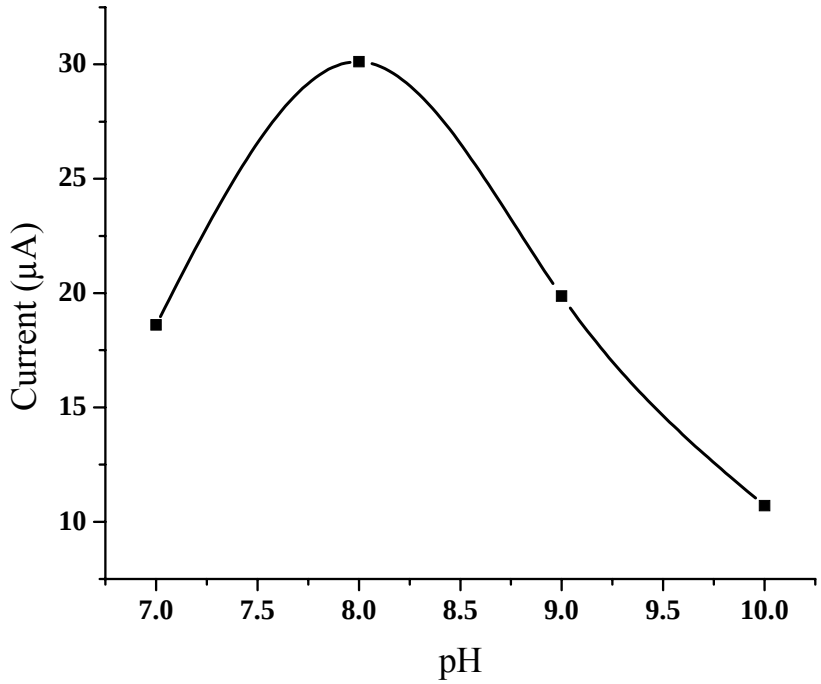

Figure 3.5 Effect of pH

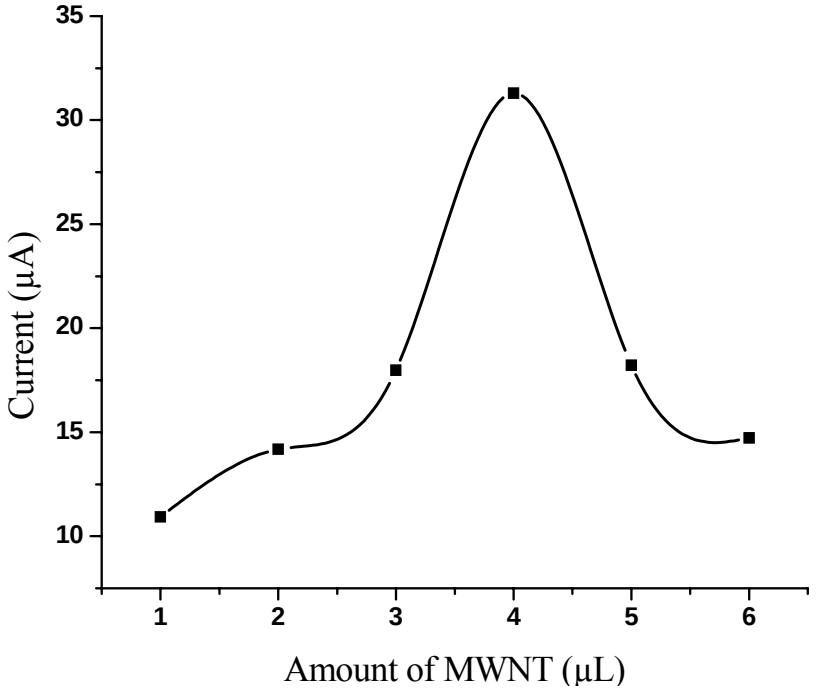

Figure 3.6 Amount of MWNT dispersion

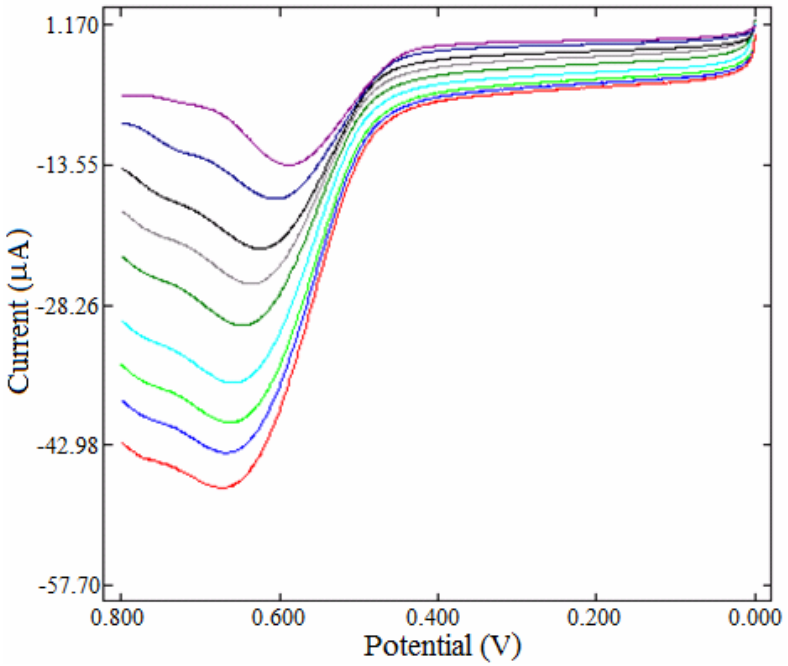

Figure 3.7 LSV of PAM chloride at different scan rates (20-180 mV/s) in PBS

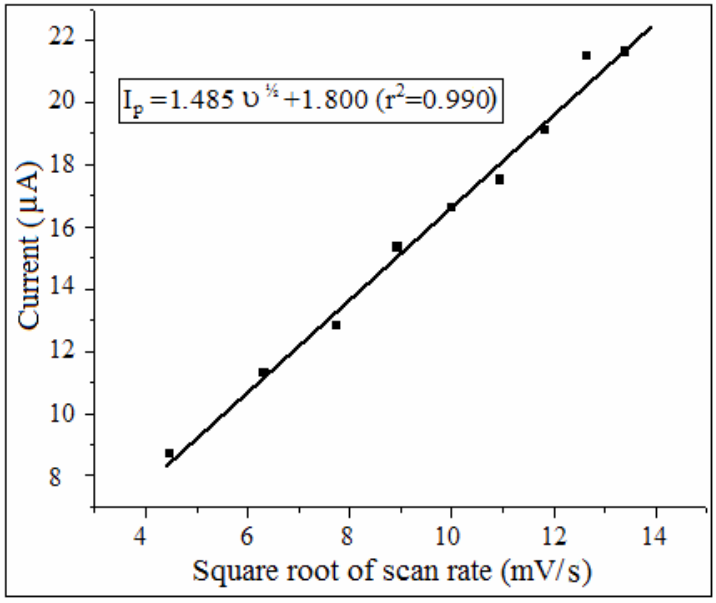

Figure 3.8 Plot of peak currents as a function of the square root of scan rates.

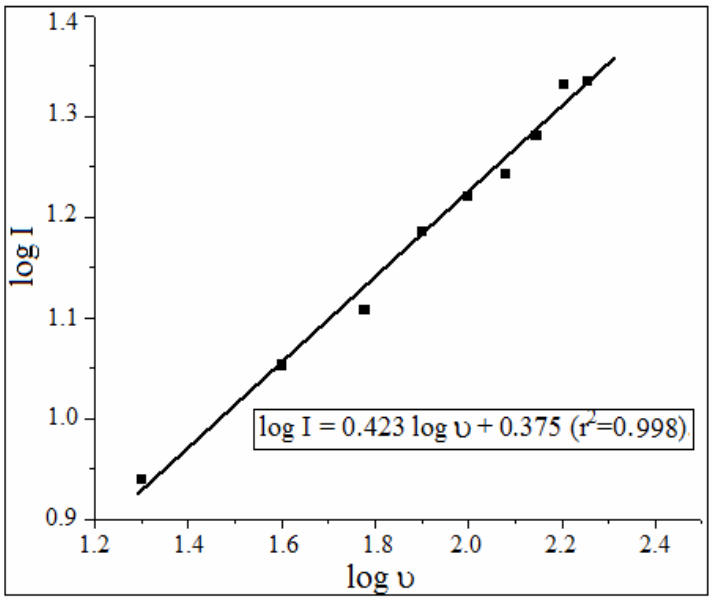

Figure 3.9 Effect of scan rate

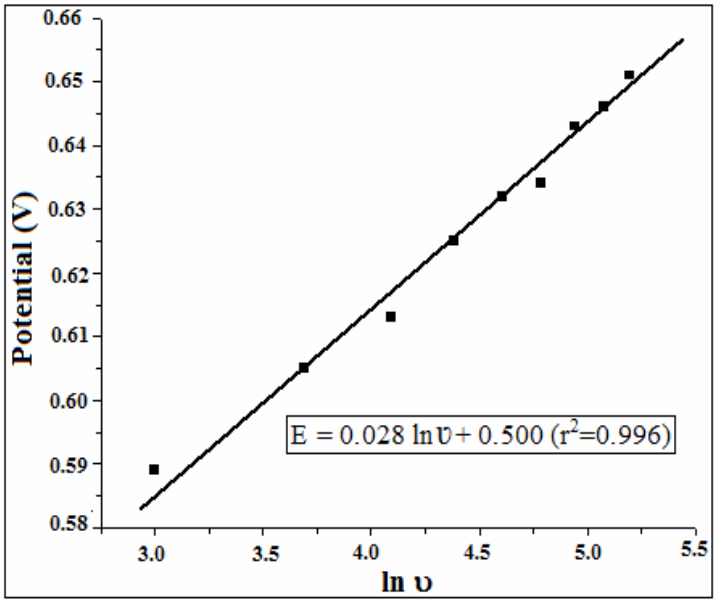

Figure 3.10 Plot of peak potential against ln scan rate

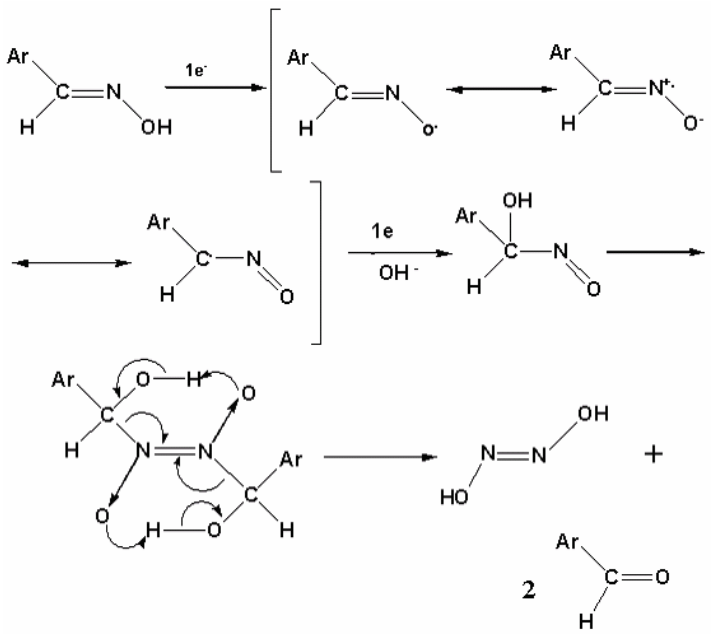

Figure 3.11 Reaction mechanism

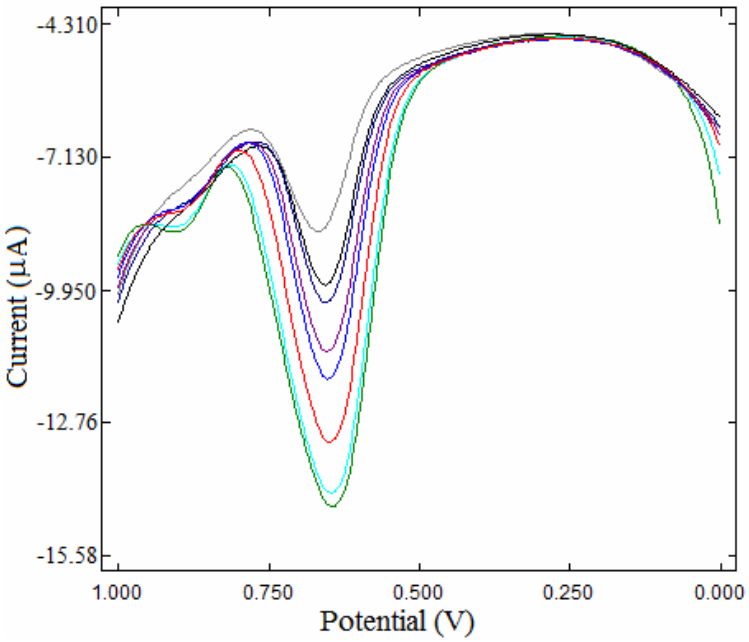

Figure 3.12 Differential pulse voltammograms of concentrations 1×10^{-3}, 8×10^{-4}, 5×10^{-4}, 1×10^{-4}, 6×10^{-5}, 1×10^{-5}, 6×10^{-6} and 1×10^{-6} M of PAM chloride (from bottom to top)

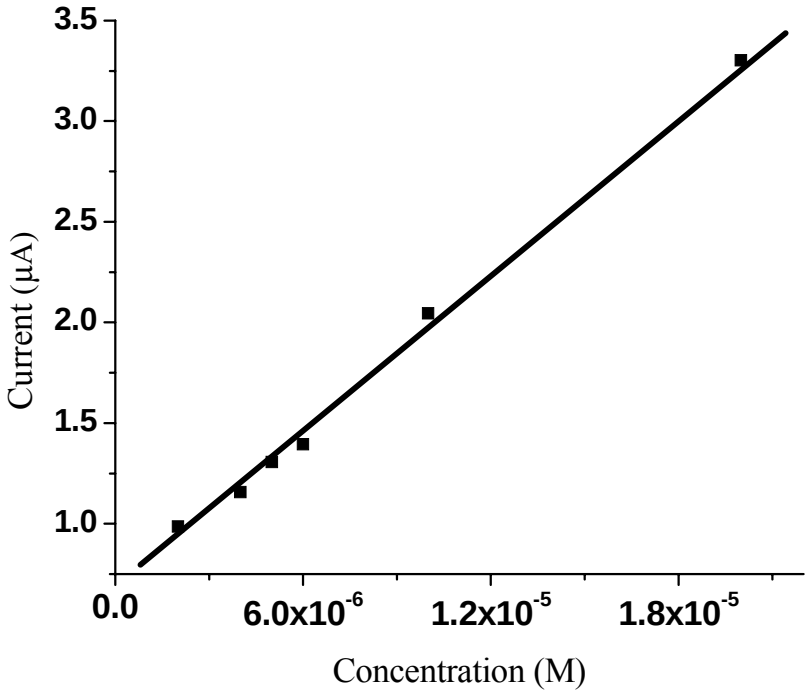

Figure 3.13 Calibration graph of PAM chloride at MWNT modified Pt electrode

.....ஜ۞ஜ.....

Chapter 4

DEVELOPMENT OF SENSOR FOR TAMSULOSIN HYDROCHLORIDE

Contents

4.1 Introduction
4.2 Preparation of MWNT-modified GCE
4.3 Electrochemical behaviour of TAM
4.4 Evidences of electrode modification
4.5 Performance characteristics of the developed sensor
4.6 Analytical applications
4.7 Conclusions

This chapter details the electrocatalytic oxidation of Tamsulosin Hydrochloride (TAM) at a multiwalled carbon nanotubes (MWNT) - Nafion modified glassy carbon electrode (GCE). MWNT were dispersed in water with the help of Nafion, and was used to modify the surface of GCE via solvent evaporation. Experimental results showed that MWNT, can serve as an excellent electrocatalyst which facilitates electron transfer and considerably lowers the overpotential required, as compared to a bare electrode. The determination conditions, such as the amount of MWNT- Nafion suspension, pH of the supporting electrolyte and scan rate were optimized. Under optimum conditions the oxidation peak current was propotional to the concentration of TAM in the range 1×10^{-3} M - 3×10^{-7} M with a detection limit of 9.8×10^{-8} M. From the electrochemical response, the main oxidation step was found to be related to the methoxy group on the phenyl ring. The method was extended to the determination of TAM in pharmaceutical formulations and in spiked urine sample.

4.1 Introduction

Prostatic and urethral smooth muscle tone is maintained by stimulation of postjunctional α_1-adrenoceptors through the release of noradrenaline from the adrenergic nerves in both animals and humans [171]. Benign prostatic hyperplasia (BPH) is associated with a bladder outlet obstruction that has been

postulated to occur via both mechanical compression exerted by the increased bulk of the prostate and alterations in the neural control of the prostatic smooth muscle. TAM is a new type of highly selective α1A adrenergic receptor antagonist for treatment of BPH. TAM is [(-)-(R)-5-[2-[[2-(o-ethoxyphenoxy) ethyl]amino]propyl]-2-methoxybenzenesulfonamide] monohydrochloride [Figure **4.1**]. It is a white crystalline powder that melts with decomposition at approximately 230°C. It is sparingly soluble in water and methanol, slightly soluble in glacial acetic acid and ethanol, and practically insoluble in ether [172]. It exits in two enantiomeric forms, in which R-isomer is the pharmaceutically active component. It blocks α-receptors that are found in the muscle of the prostate gland, which causes the muscle in the prostate to relax. This allows urine to flow freely post the prostate and relieves the urinary symptoms [173]. This drug is extensively metabolized by cytochrome P450 enzymes in the liver and is used as an oral medication to ameliorate the bladder-outlet obstruction associated with prostatichypertrophy. In recent years, α_1-adrenoceptor antagonists have been increasingly used for the symptomatic treatment of lower urinary tract symptoms (LUTS), suggestive of benign prostatic obstruction [174].

Receptor cloning and pharmacological analysis have identified the existence at least three α_1 adrenoceptor subtypes which are designated as α_{1A}, α_{1B}, and α_{1D} [175, 176]. Their distribution differs between human organs and tissue. Approximately 70% of the α_1 receptors in the human prostate are of the α_{1A} subtype. In vitro studies of TAM show that it has a greater affinity for α_{1A} -adrenoceptors than for α_{1B} - and α_{1D} -adrenoceptors [177-179]. Compared to other α-antagonists, TAM has greater specificity for α_1 receptors in the human prostate [180, 181] and does not affect receptors on blood vessels [182,183].

A thorough literature search has revealed that several analytical methods are available for determination of TAM. M. K. Thimmaraju et al has reported a reverse phase high performance liquid chromatographic (RP-HPLC) method for the determination of TAM in bulk and tablet dosage forms [184]. Another RP-HPLC method for evaluation of purity of TAM in bulk drugs and pharmaceuticals was developed by R. N. Rao et al [185]. Also G.S. Kumar et al described a stability indicating RP-HPLC method for determination of TAM [186]. A spectrofluorimetric method for the determination of TAM in tablet dosage form was developed by D. B. Patel using methanol as solvent [187]. Major drawbacks of these reported methods include lengthy, tedious and time-consuming sample preparation, extraction processes and interference of endogenous substances. Also, these methods require sophisticated and expensive instrumentation. In this context electrochemical detection methods are often advantageous since they offer high sensitivity, ease of use, portability and relatively less expensive equipment. The electrooxidative behavior and determination of TAM, on a glassy carbon disc electrode were investigated using various voltammetric techniques by S. A. Ozkan et al [188].

Chemically modified electrodes (CMEs) comprise a relatively modern approach to electrode systems. Carbon nanotubes (CNTs) have been at the forefront of novel nanoscale investigations owing to their unique structure dependent electronic and mechanical properties. Their small dimensions, closed topology and lattice helicity have enabled nanotubes to influence broad areas of science and technology, ranging from super strong nanocomposites to nanoelectronics [189, 190].

This chapter describes the details of the development and analytical applications of TAM sensor using MWNT-Nafion modified GCE. For that, MWNT-Nafion dispersion was drop dried at the surface of GCE and the

electrochemical behavior of TAM at this modified electrode was investigated. Surface modification was characterized by scanning electron microscopy (SEM) and square wave voltammetry (SWV). Differential pulse voltammetry (DPV) was employed for the studies. The performance of the modified electrode with respect to sensitivity, linear range, and selectivity toward TAM was evaluated and discussed. The applicability of the GCE modified by MWNT was demonstrated for the determination of TAM in pharmaceutical formulations and in urine sample.

4.2 Preparation of MWNT-modified GCE

First, acid treatment of MWNT was carried out as explained under section 2.5.1 of chapter 2. Section 2.4 of chapter 2 explains the detailed procedure for cleaning of GCE.

MWNT- Nafion / GCE was fabricated as described in section 2.5.2 of chapter 2. The surface of the cleaned GCE was treated by dropping the blackish suspension (4 μL) of MWNT in Nafion- water solution (5 mg of MWNT in a mixture of 300 μL Nafion and 2 mL water) and then dried in air to obtain the MWNT modified GCE.

4.3 Electrochemical behaviour of TAM

Voltammetric measurements were performed with a PC- controlled BAS Epsilon electrochemical analyzer (Bio- analytical system, USA). A three electrode cell system incorporating the MWNT- Nafion modified GCE as working electrode, an Ag/AgCl reference electrode and a platinum wire auxiliary electrode were used.

Preparation of TAM stock solution was carried out as explained in section 2.6 of Chapter 2. Standard solutions of the analyte (1×10^{-3} M - 3×10^{-7}

M) were prepared by serial dilution of the stock solution using supporting electrolyte. Sample solution was taken in the electrochemical cell. The solution was then deaerated with purified nitrogen for 3 minutes. Differential pulse voltammograms from 800 to 1300 mV, at a scan rate of 100 mV/s were recorded and finally the oxidation peak current at 1084 mV was measured for TAM. For electrode regeneration, several cyclic scans were carried out in the blank electrolyte solution until a stable voltammogram was obtained.

As the development of a sensor for TAM is interesting due to its importance in pharmaceutical application we tried different types of sensor fabrication methods. It was first studied on a MWNT modified gold electrode but no response was obtained. The electrochemical response of TAM was further studied using platinum electrode modified with polyaniline. Compared to bare electrode, the peak current of TAM showed marked decrease, and the peak potential showed a positive deviation. Prussian blue- MWNT colloid modified GCE was also used to study the electrochemical behavior of TAM. An oxidation peak was obtained at 1164 mV with a peak current of 10 μA. However at MWNT- Nafion modified GCE, TAM gave a well defined oxidation peak at 1084 mV with a peak current of 36.7 μA. Since a better sensitivity for TAM was obtained with MWNT- Nafion modified GCE, the choice is justified.

The cyclic voltammograms of TAM at the bare GCE and MWNT–Nafion modified GCE are shown in Figure **4.2**. It can be seen that the oxidation peak at the bare GCE was weak while the response was considerably improved at the MWNT-modified GCE. The peak potentials of TAM at the bare electrode and the MWNT modified GCE were almost the same. However, the peak was sharper and the peak current increased significantly, for the latter.

DPV was also applied to investigate the electrochemical behavior of TAM at the bare and modified GCEs. Figure **4.2** shows the differential pulse voltammograms obtained for 1×10^{-3} M TAM at bare and MWNT modified GCEs. As can be seen, the oxidation peak of TAM at bare GCE was broad may be due to slow electron transfer [191] whereas at MWNT modified electrode, an improved response was observed. In the case of the bare GCE, TAM gave an oxidation peak at 1232 mV and the peak current was about 1.87 μA, whereas at the MWNT modified GCE, the oxidation peak was at 1084 mV with a peak current of 36.7 μA. Compared with the bare GCE, the oxidation potential of TAM showed a negative shift of about 148 mV and also, a 36 fold increase in peak current. These results undoubtedly proved the electrocatalytic activity of MWNT- Nafion GCE towards the oxidation of TAM.

4.4 Evidences of electrode modification

4.4.1 SEM images

SEM images of the bare and MWNT modified electrode (Figure **4.3**) clearly showed that the electrode surface was effectively modified with MWNT.

4.4.2 Surface area study

Further proof for the effective modification of GCE was obtained from surface area studies. The surface area of both bare and MWNT-Nafion GCE were determined by recording the square wave voltammograms at different scan rates (Figure **4.4**). 2 mM $K_3Fe(CN)_6$ was taken as a probe to measure the microscopic areas. For a reversible system, the peak current should follow Randles Sevcik equation [167]

$$I_p = 2.69\times10^5 An^{3/2}D_R^{1/2} C \nu^{1/2}$$

From the slope of I_p versus $\nu^{1/2}$, the regression equations obtained for both the bare and modified GCEs are I_p =2.851 $\nu^{1/2}$ – 11.47 (r^2=0.991, ν in mV/s, I_p in μA) and Modified I_p =4.249 $\nu^{1/2}$ – 10.05 (r^2=0.992, ν in mV/s, I_p in μA) respectively (Figure **4.4**). Surface areas of bare and MWNT modified electrodes were estimated and found to be 0.129 cm^2 and 0.287 cm^2 respectively. This enhancement in surface area resulted in the remarkable catalytic activity of the modified electrode.

4.5 Performance characteristics of the developed sensor

The response characteristics of the developed sensor depend on various parameters such as influence of supporting electrolyte, influence of pH, influence of amount of MWNT-Nafion suspension, influence of scan rate and influence of concentration.

4.5.1 Influence of supporting electrolyte

The electrochemical behavior of TAM in various media such as 0.1 M solutions of phosphate buffer, acetate buffer, H_2SO_4, NaOH, and tetra-n-butyl ammonium chloride were studied by DPV. The best oxidation response was obtained in acetate buffer solution as the peak current is the highest. So 0.1 M acetate buffer was taken as the experimental medium for the determination of TAM.

4.5.2 Influence of pH

The electrochemical studies of 1×10^{-3} M TAM in acetate buffer were carried out in the pH range of 3 to 9 using DPV. Figure **4.5** clearly depict the effect of pH on the anodic peak current of TAM at the MWNT modified GCE. The best oxidation response was obtained in pH 5 as the peak current is the highest. Thus pH 5 was fixed as optimal pH.

4.5.3 Influence of amount of MWNT-Nafion suspension

When the amount of MWNT-Nafion suspension was 1- 4 μL (5 mg of MWNT in a mixture of 300 μL Nafion and 2 mL water), the peak current increased gradually (Figure **4.6**). This may be due to that the specific surface area and the number of catalytic sites increases with an increasing volume of MWNT. Further increase in the amount of MWNT-Nafion suspension caused a decrease in the anodic peak current. This is because Nafion is an insulator and this along with excess of MWNT blocks electron transfer. As a result, the peak current decreases when the MWNT-Nafion film is too thick. So the amount of MWNT-Nafion dispersion was fixed to be 4 μL.

4.5.4 Influence of scan rate

Scan rate studies were carried out to assess whether the processes at the MWNT-Nafion modified GCE was under diffusion or adsorption controlled (Figure **4.7**). When the scan rate was varied from 20 to 200 mV/s in 1×10^{-3} M solutions of TAM, (Figure **4.8**) a linear dependence of the peak current upon the square root of the scan rate was found, demonstrating a diffusional behavior. The regression equation obtained from SWV analysis is: $I_p = 1.636\ \nu^{1/2} - 3.617$ (r^2=0.996, ν in mV/s, I_p in μA).

A linear relationship was observed between log I_p and log ν over the scan range 20 and 200 mV/s (Figure **4.9**) and corresponds to equation: $\log I_p = 1.577 \log \nu + 0.261$, ($r^2$=0.997). The slope of 0.61 is close to the theoretically expected value of 0.5 for a diffusive process [168].

The effect of scan rate ν, on the peak potential was investigated (Figure **4.10**). It was found that the peak potential was shifted linearly with the increase of scan rate, ν in accordance with the equation $E= 0.034 \ln \nu + 0.992$

(r^2 =0.998). From the slope of E-ln ν plot [169], the electron transfer number was calculated to be 2, assuming the transfer coefficient α = 0.5. For the irreversible oxidation of TAM, n_a value was calculated to be around 2.

The anodic oxidative behavior of TAM may be due to oxidation of alkoxybenzene [192, 193]. The alkoxybenzene is converted into quinone by undergoing a 2 e^-, 2 H^+ oxidation as explained in Figure **4.11**.

4.5.5 Influence of concentration

Under the optimized experimental conditions, the anodic peak current of TAM increased linearly with its concentration (Figure **4.12**). The experimental results showed that the peak current was linear with the concentration of TAM in the range 2×10^{-6} - 3×10^{-7} M, (Figure **4.13**).The detection limit was found to be 9.8×10^{-8} M. The reproducibility of peak potentials was confirmed by repeating the experiments over different days with 3×10^{-6}, 4×10^{-5}, 1×10^{-4} and 1×10^{-3} M TAM concentrations. The relative standard deviations (RSD) of peak potentials were obtained as 1.4 %, 2.7 %, 2.3 %, and 2.0 % respectively (n=5). After each determination, the modified electrode was run in acetate buffer (pH 5). Modified electrode exhibited stable behavior for 12 days.

The Table **4.1** gives a comparative study of response characteristics of the newly developed method with some of the reported methods. It is obvious that the developed method is superior in terms of detection limit.

4.5.6 Interference study

In order to investigate the selectivity of the method, the interference effects of some biologically important species on the electrochemical oxidation of $l\times l0^{-3}$ M TAM have been evaluated. The results are given in Table **4.2**. It was found that up to 100 fold excess concentration of urea,

glucose, lactose, Na^+, K^+, Cl^- and SO_4^{2-} have almost no influence on the current response of 1×10^{-3} M TAM (Signal change below 5%). However, ascorbic acid interferes severely with the oxidation signal of TAM.

4.6 Analytical applications

The sensor developed for TAM was employed for its determination in tablet form. The utility of the developed sensor in the determination of TAM in real sample like urine was also studied.

4.6.1 Determination of TAM in pharmaceutical formulations

The developed sensor was successfully applied for the determination of TAM in commercially available pharmaceutical formulation, Veltam (Intas pharmaceuticals, India). The TAM content in the tablet was determined by calibration method. The detailed procedure for the determination is given in section 2.8.1 of chapter 2. The results obtained are summarized in Table **4.3**. The results obtained are in good agreement with the declared TAM content and showed a high degree of precision.

In order to test the reliability of this method, results obtained by MWNT/ GCE sensor were compared with those obtained by standard pharmacopoeia method [139] (Table **4.3)**. The results show that the developed sensor is highly reliable for the determination of TAM in pharmaceutical formulations.

4.6.2 Determination of TAM in urine sample

The applicability of MWNT modified electrode for the determination of TAM in urine was also investigated. Various concentrations of the drug solution in acetate buffer solution containing fixed amount of urine sample was prepared. The electrochemical behavior of the prepared solution on

MWNT modified GCE was studied by DPV (Table **4.4**) and the unknown concentrations were determined from the calibration graph.

4.7 Conclusions

In this work, a MWNT modified GCE has been successfully developed for electrocatalytic oxidation of TAM in acetate buffer solution. The results indicated that the modified electrode facilitated the determination of TAM with good sensitivity and reproducibility. MWNT showed electrocatalytic action for the oxidation of TAM, characterized by the enhancement of the peak current, which was probably due to the larger effective surface area of MWNT. MWNT-Nafion GCE provided a good platform for the determination of TAM in pure form, dosage forms, and in urine sample.

Table 4.1 Comparison of various analytical methods

	Analytical method	Detection limit
1	Reverse phase high performance liquid Chromatography (RPHPLC) [184]	0.495 µg/mL
2	RPHPLC [185]	0.06–0.11 µg/mL
3	RPHPLC [186]	0.360 µg/mL
4	Spectrofluorimetry [187]	1.360 µg/mL
5	Voltammetry [188]	0.1479 µg/mL (DPV) 0.1085 µg/mL (SWV)
6	Voltammetry (present method)	0.040 µg/mL

Table 4.2 Interference study

Foreign species	Signal change,%
Urea	+ 1.50
Glucose	- 1.30
Lactose	- 3.00
Na^+	- 0.62
K^+	+ 3.00
Cl^-	- 0.62
SO_4^{2-}	+ 3.00
Ascorbic acid	- 20.0

* Average of three replicates

Table 4.3 Determination of TAM in tablets

Sample	Declared amount (mg /tablet)	Method adopted	Found* (mg / tablet)	S.D*	C.V*
Veltam	0.20	MWNT / GCE	0.190	1.40	0.71
		Standard Method	0.202	3.86	1.91

*Average of six replicates

Table 4.4 Determination of TAM in urine sample

TAM added (M)	TAM found (M)	Recovery %
2.00×10^{-6}	1.95×10^{-6}	97.5
4.00×10^{-6}	4.08×10^{-6}	102
6.00×10^{-6}	5.99×10^{-6}	100

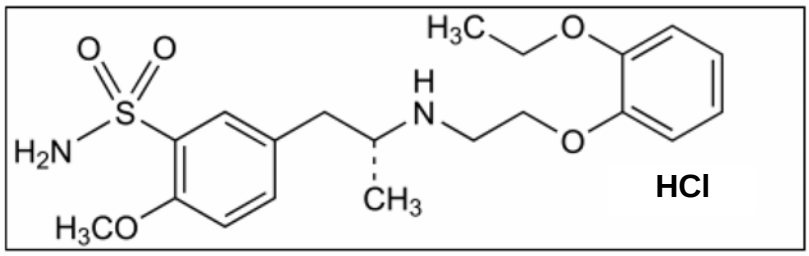

Figure 4.1 Structure of TAM

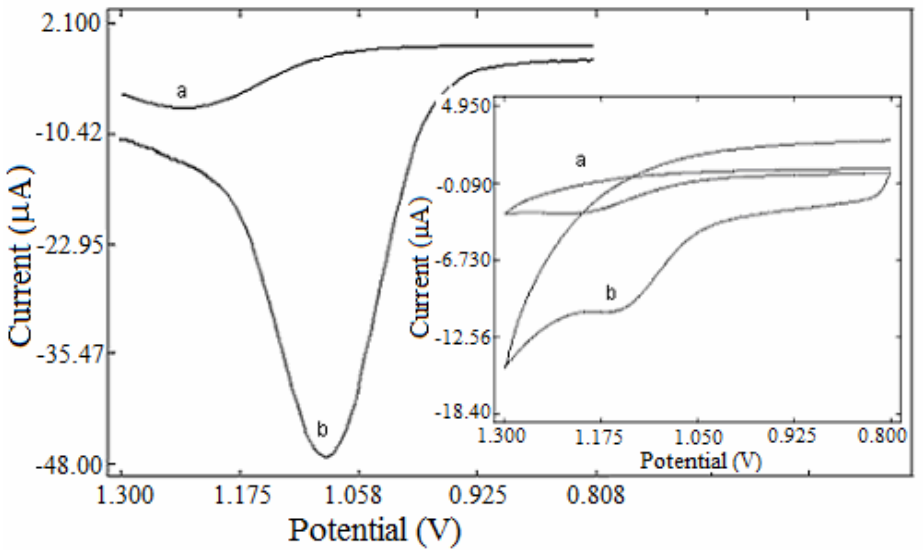

Figure 4.2 Voltammograms of 1×10^{-3} M TAM at (a) bare GCE (b) MWNT modified GCE

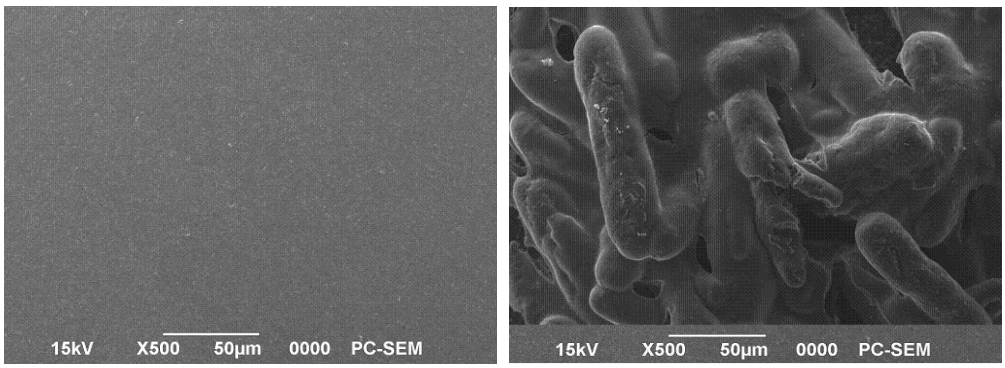

(a) **(b)**

Figure 4.3 SEM image of (a) bare GCE (b) MWNT modified GCE

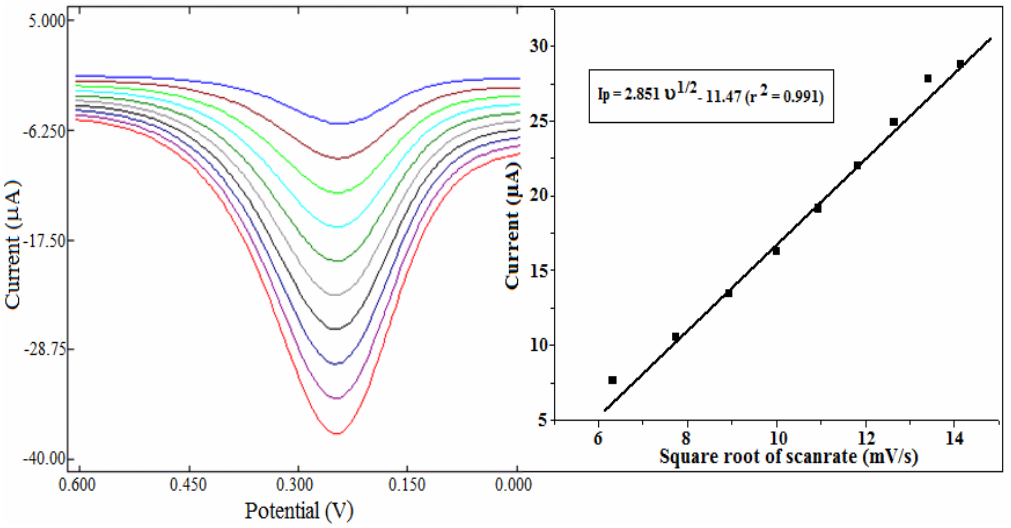

(a)

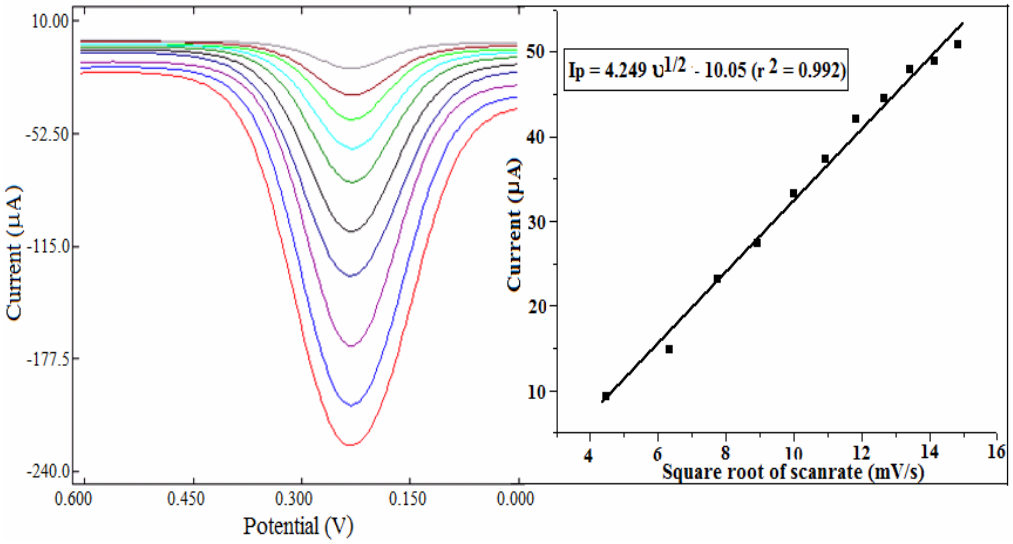

(b)

Figure 4.4 Overlay of square wave voltammograms of 2 mM $K_3Fe(CN)_6$ solution obtained at (a) bare GCE (b) MWNT modified GCE

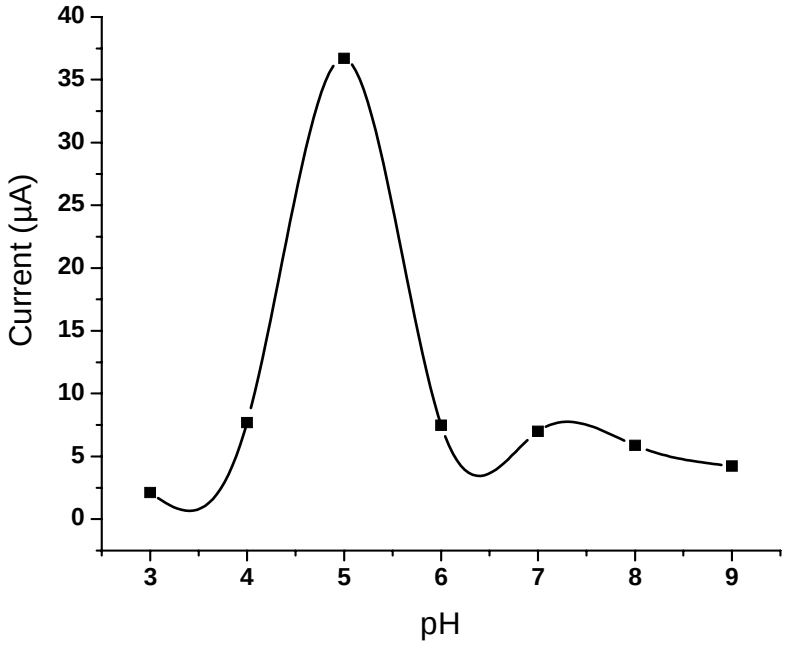

Figure 4.5 Effect of pH on the anodic peak current of 1×10^{-3} M TAM

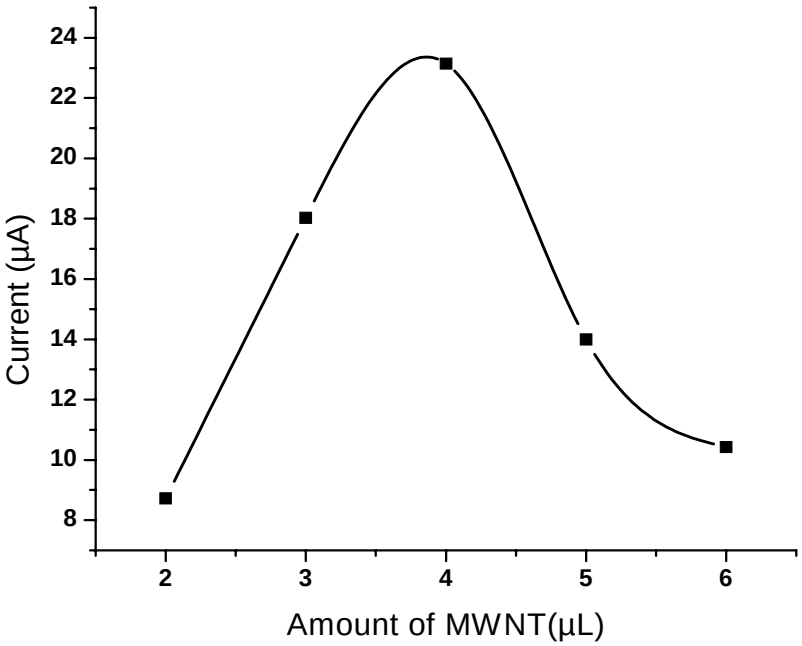

Figure 4.6 Effect of the amount of MWNT–Nafion dispersion at MWNT modified GCE

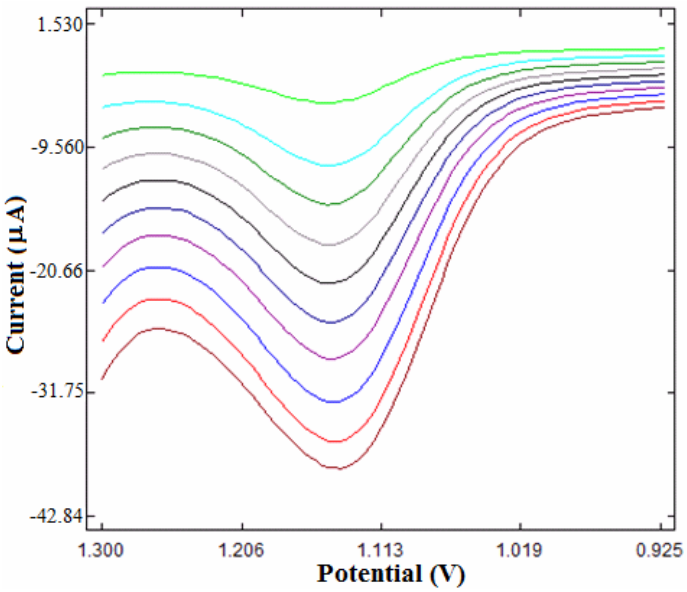

Figure 4.7 Overlay of SWVs of TAM at MWNT/GCE in 0.1 M acetate buffer (pH 5)
containing 1×10^{-3} M TAM at different scan rates 20, 40, 60, 80, 100, 120, 140, 160,180, 200 mV/s (from top to bottom).

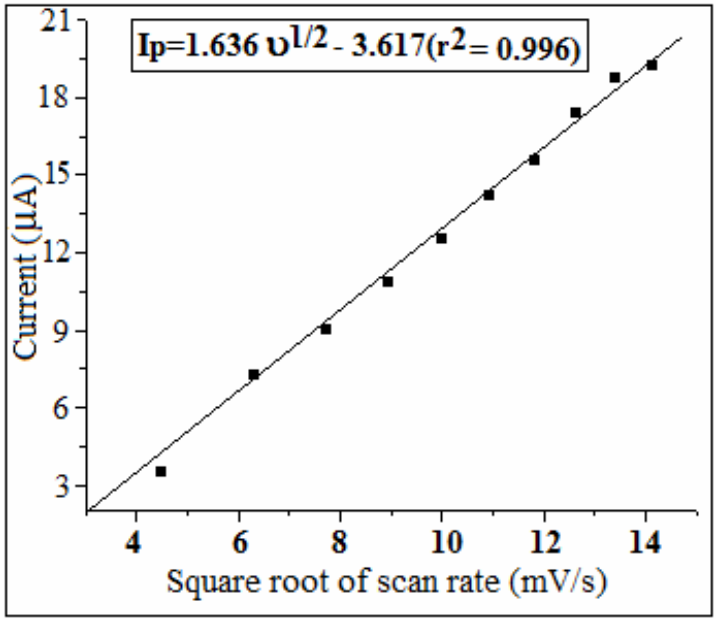

Figure 4.8 Variation of the anodic currents of TAM as a function of square root of scan rates

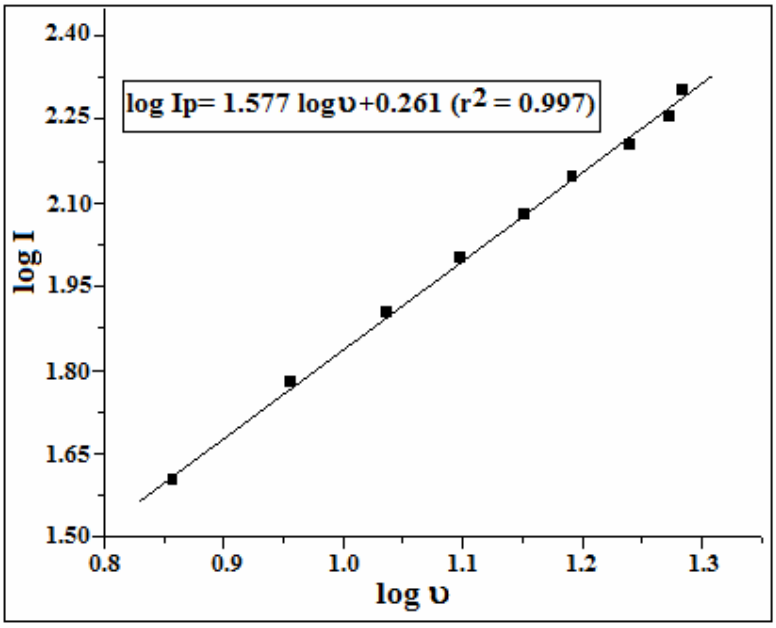

Figure 4.9 Variation of log I_p versus log ν

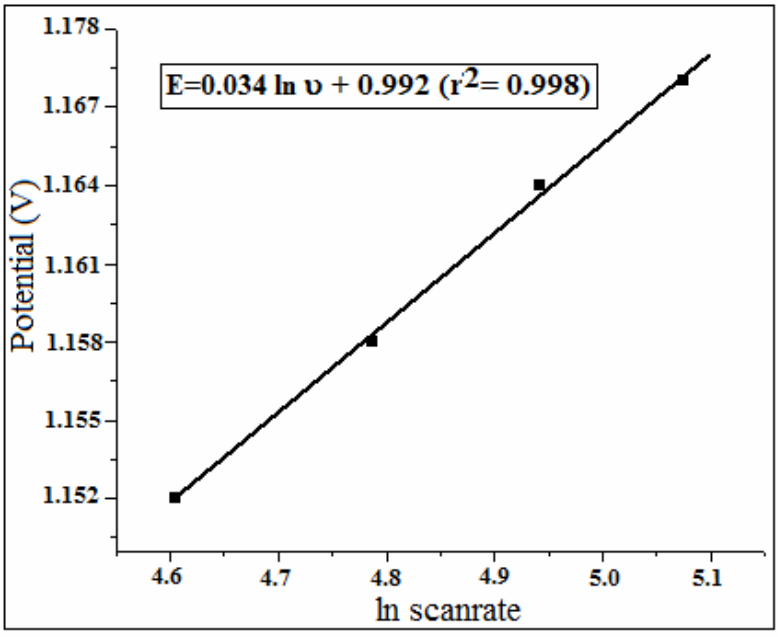

Figure 4.10 Variation of ln scan rate versus anodic potential

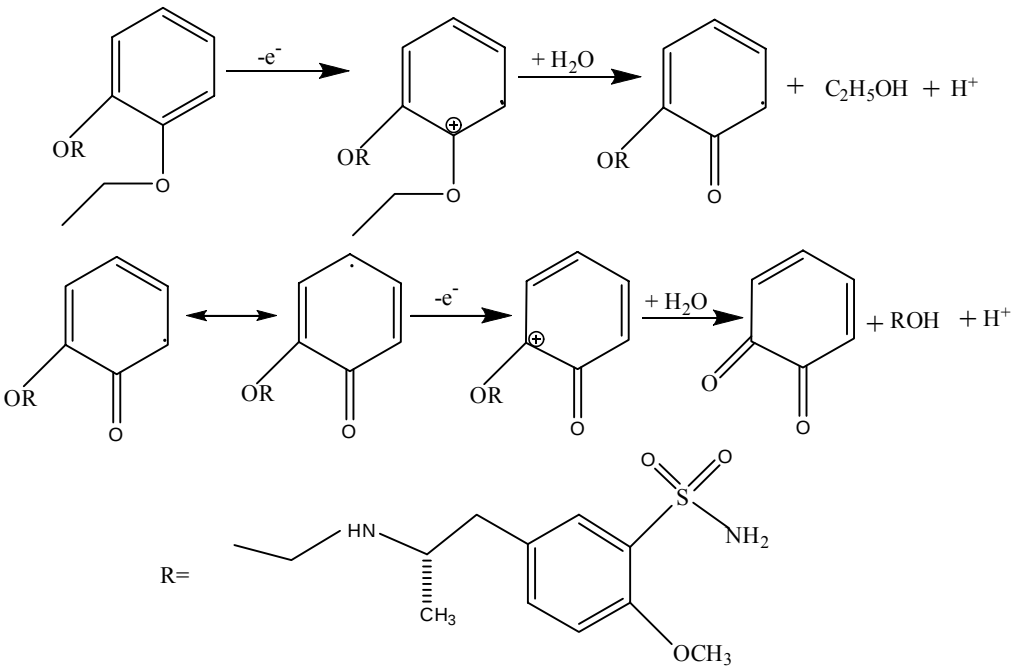

Figure 4.11 Reaction mechanism

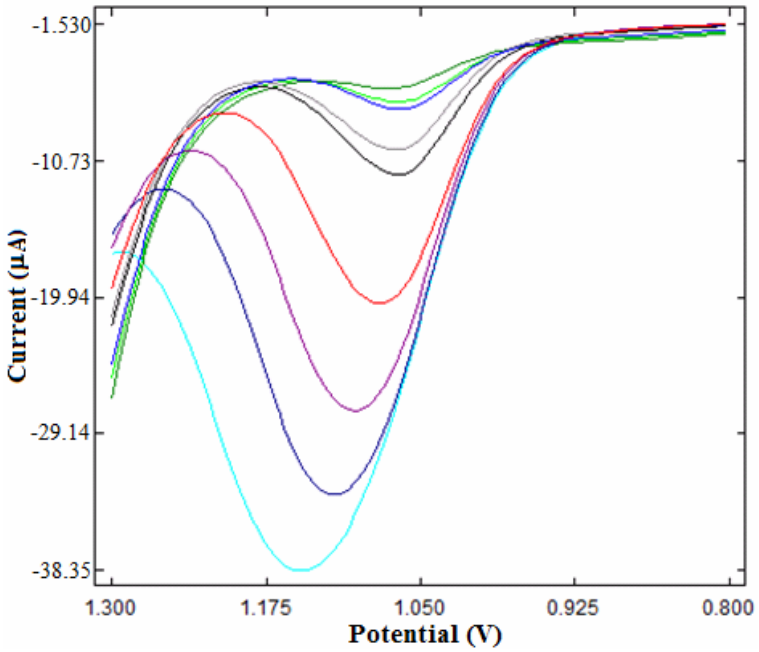

Figure 4.12 Differential pulse voltammograms of concentrations of 10^{-7} to 10^{-3} M of TAM (from top to bottom)

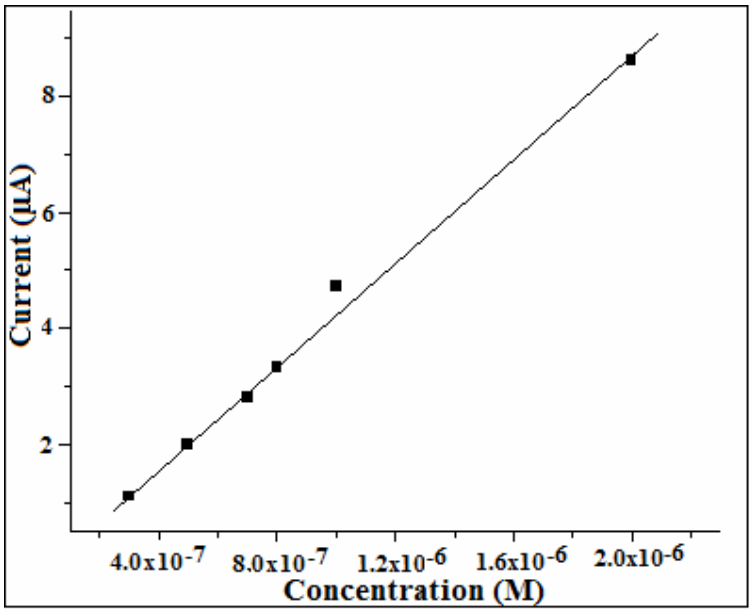

Figure 4.13 Dependence of concentration of TAM on peak current

.....ꕥ.....

Chapter 5

DEVELOPMENT OF SENSOR FOR HESPERIDIN METHYL CHALCONE

Contents

5.1 Introduction
5.2 Preparation of PB/MWNT-modified GCE
5.3 Electrochemical behaviour of HMC
5.4 Evidences of electrode modification
5.5 Performance characteristics of the developed sensor
5.6 Analytical Applications
5.7 Conclusions

An easy and convenient technique to fabricate a prussain blue (PB)/ multi walled carbon nanotube (MWNT) nanocomposite film on a glassy carbon electrode (GCE) is described in this chapter. The electrochemical behavior of Hesperidin Methyl Chalcone (HMC) at a PB/ MWNT coated GCE various experimental conditions was conducted by using differential pulse voltammetry (DPV). The number of electrons transferred was calculated by using cyclic voltammetric technique. Under the optimized conditions, the concentration of HMC showed excellent linear relationships with the reduction peak current, with a detection limit of 7.16×10^{-8} *M. The developed sensor was successfully applied for the determination of HMC in urine samples.*

5.1 Introduction

Hesperidin, 3′,5,7-trihydroxy-4′-methoxy-flavanone-7-o-ß-rutinoside, is a bioflavonoid found in high concentrations in the skins of citrus fruits, and in substantially lower concentrations in the juices of these fruits [194,195]. The hesperidin concentration can be related to the quality, or "freshness" of the fruit juice. Higher concentrations of hesperidin (higher ratio of the 2S/2R diastereoisomers of hesperidin) is found in freshly squeezed orange juice compared to less fresh commercial orange juices [196,197]. Because of its

poor aqueous solubility, the partially methylated derivatives of hesperidin have been synthesized. These derivatives are called hesperidin methyl chalcone (HMC) (Figure **5.1**). HMC supports and protects the integrity of the vascular system with particular activity in the capillaries and veins. HMC has been shown to help strengthen capillaries by increasing capillary resistance and decreasing capillary permeability. Increased venous motility, tone, and the ability of vessels to dilate are also enhanced by HMC. Also they possess anti-inflammatory [198], antihypertensive, diuretic [199], analgesic [200], hypocholestrolemic [201], anticancer [202] and antioxidant activities [203]. The methods available for the determination of HMC are thin layer chromatography [204] and high performance liquid chromatography [205]. As such these detection methods are limited in comparison to direct electroanalytical techniques by their expense, lack of portability, complex sample pre-treatment requirements and their inability to perform rapid in-field measurements. Zheng et al. [206] developed a method for the determination of HMC based on the voltammetric techniques. However, this report involves the use of mercury electrodes, which is undesirable due to toxicity. An attempt has been made to develop a convenient and sensitive method for the determination of HMC by DPV using PB/ MWNT modified GCE.

Prussain blue (PB), is an ancient coordination material and can be used as an electron transfer mediator. Due to the unique properties, synthetic versatility and the ability of the bridging cyanide ligands to efficiently mediate its properties, PB has wide applications in electrochromism [207,208] photoresponse [209], electrocatalysis [210], sensors [211] and even batteries [212]. PB and its analogues are the prototype of a number of polynuclear transition-metal hexacyanometalates having an open, zeolite-like structure. Prussian white, the peculiar reduction product of PB is able to catalyze the

electrochemical reduction of hydrogen peroxide at low potentials. Due to its high activity and selectivity toward the reduction of hydrogen peroxide, PB is usually considered as an "artificial peroxidase" and has been extensively used in the construction of electrochemical biosensors [213, 214]. Recently, various electrodes modified by a film of electrodeposited PB is used in the development of biosensors for the detection of glucose [215, 216], glutamate [217], amino acid [218], alcohol [219], acetylcholine [220], cholesterol [221] etc. Electrochemical deposition [222, 223] chemical deposition [224] and self-assembling method [225] have been used to fabricate PB modified electrodes. Therefore, the study on a new method to fix chemically prepared PB without binders has great significance for expanding the application of the PB-modified electrode.

The combination of PB and MWNT has received more attention [226-228]. CNTs are considered to be good mediators for PB-modified electrodes. Their unique electronic and chemical properties and tubular structure make them ideal supports for inorganic nanoparticles. Because of large specific surface area and good capability of electron transfer, MWNT opens a new door for electroanalytical chemistry field. MWNTs could impart strong electrocatalytic activity and minimization of surface fouling onto electrochemical devices [229]. Modifications of the CNTs with polymers or biomolecules are usually used to improve their dispersion and orientation in aqueous solutions.

Several solvents such as concentrated sulfuric acid, acetone, dihexadecyl hydrogen phosphate (DHP), N,N- dimethylformamide (DMF) and chitosan can be used to disperse MWNT. However, the biological incompatibility of these solvents restrained the development of their applications. The novelty of this work is to suggest a new nanocomposite, which was formed by

combination of PB nanoparticles and MWNT in the presence of Nafion. Because of the unique-ion exchange characteristics, thermal stability, chemical inertness, and mechanical strength, Nafion, a sulphonated tetra fluoro ethylene copolymer, was selected as the suitable solvent for this study.

The PB/MWNT modified GCE was prepared by using drop drying method. At bare GCE, no voltammetric response was obtained. But on modification of GCE with PB/MWNT, a well defined and sensitive reduction peak was obtained at -972 mV for HMC. The developed sensor has also been successfully applied for the determination of HMC in urine sample.

5.2 Preparation of PB/MWNT-modified GCE

Before each experiment, GCE was cleaned as described under section 2.4 of chapter 2. PB/MWNT-modified GCE was fabricated as given in the section 2.5.3 of chapter 2. To obtain PB/MWNT hybrids, the MWNTs were added to the mixture of $FeCl_3$, $K_3Fe(CN)_6$ and KCl. 4 μL of the dark suspension was dropped on the surface of the GCE. The PB/MWNT modified GCE was obtained just after evaporation of the solvent.

5.3 Electrochemical behaviour of HMC

Electrochemical measurements were carried out on a BAS Epsilon electrochemical analyzer (Bio-analytical system, USA) controlled by a personal computer. A three-electrode system was employed, including a PB/MWNT modified GCE working electrode, an Ag/AgCl reference electrode and a platinum wire counter electrode.

Stock solution of HMC was prepared as given in section 2.6 of Chapter 2. Standard solutions of the analyte were prepared by serial dilution of stock solution with appropriate supporting electrolyte (0.1 M acetate buffer solution

(pH=2)). A 10 mL of supporting electrolyte with appropriate amount of HMC for various concentrations was transferred into a cell, and then the electrode system was immersed into the solution and then purged with purified nitrogen for 3 min to remove oxygen. DPV was recorded from -700 to -1100 mV, at a scan rate of 100 mV/s. All the voltammetric experiments were carried out at room temperature. After each measurement the modified electrode was subjected to successive sweeping at pH 2 to give reproducible electrode surface.

We tried different modification techniques for various electrodes to study the electrochemical behavior of HMC. It was first studied on bare gold and platinum electrodes, but no response was obtained. PB/MWNT modified gold and platinum electrodes were then tried and it also gave no response for HMC. Also, HMC gave no response at the bare GCE. In order to get an electrochemical response of HMC, we tried various chemical modifications on GCE. Modifications using gold nanoparticles, copper nanoparticles and p-toluenesulphonic acid were also found to be failure. HMC gave a reduction peak at -1300 mV on an electrochemically deposited PB modified GCE and the peak current was 9.9886 μA. A reduction peak at -1292 mV with a peak current of 2.6429 μA was obtained using MWNT modified GCE. However at PB/MWNT modified GCE, HMC gave a well defined reduction peak at -972 mV. 1×10^{-3} M solution of HMC was used for all these studies. Since a better electrochemical response of HMC was obtained with PB/MWNT modified GCE, the choice is justified.

Figure **5.2.I** shows the cyclic voltammograms of HMC at a bare GCE and PB/MWNT modified GCE. HMC gave no response at the bare GCE. It can be seen that on modification of GCE with PB/MWNT, a reduction peak appeared at -1105 mV with a peak current of 8.4779 μA. It also showed that

no oxidation peak was observed in the reverse scan, suggesting that the electrochemical reaction was a totally irreversible process. DPV was also applied to investigate the electrochemical behavior of HMC at the bare and modified GCE (Figure **5.2.II**). As can be seen, a well defined reduction peak at -972 mV with a peak current of 34.6532 μA appeared at PB/MWNT modified GCEs. These results undoubtedly proved the electrocatalytic activity of PB/MWNT modified GCE towards the oxidation of HMC. Since DPV showed a better response, this technique was selected for further studies.

5.4 Evidences of electrode modification

5.4.1 SEM images

Surface morphology of bare and modified GCEs was studied by SEM. SEM images (Figure **5.3**) clearly indicated that the effective modification of GCE surface has taken place.

5.4.2 Surface area study

Surface area study gave a clear evidence for the effective modification of GCE with PB/MWNT. 2 mM $K_3Fe(CN)_6$ was taken as a probe to measure the effective surface areas of both bare and modified GCE by CV at different scan rates (Figure **5.4**).

For a reversible system, the peak current should follow Randles Sevcik equation [167]. From the slope of I_p vs $\nu^{1/2}$ plot, the areas of bare GCE and PB/MWNT modified GCE were estimated and was found to be 0.1244 cm^2 and 0.8848 cm^2 respectively. Thus, there was an enhancement in the effective surface area when GCE was modified with PB/MWNT, which is a strong evidence for the successful and effective modification of GCE using PB/MWNTs.

5.5 Performance characteristics of the developed sensor

The performance of the developed sensor depends on many analytical parameters including effect of supporting electrolyte and pH, effect of amount of the PB/MWNT dispersion, effect of scan rate, and interference of other materials.

5.5.1 Effects of supporting electrolyte and pH

The electrode reaction might be affected by the buffer solution and the pH of the medium. The effect of different electrolytes on the current responses of 1×10^{-3} M HMC was investigated by DPV. Some electrolytes including phosphate buffer solution, H_2SO_4, HCl, KCl, tetra-n-butyl ammonium chloride, KNO_3, acetate buffer, and NaOH (0.1 M) were studied. It was observed that the peak current is highest and the peak shape is well defined in acetate buffer. Hence acetate buffer was chosen as the experimental medium for the voltammetric studies of HMC.

The effect of the solution pH on the cathodic peak current of 1×10^{-3} M HMC was investigated by DPV. The peak current against pH over the range of 1 to 7 was studied (Figure **5.5**). The results showed that the highest peak current was obtained in acetate buffer solution at a pH value of 2. Therefore, acetate buffer of pH 2 was chosen for the subsequent analytical experiments.

5.5.2 Effect of amount of the PB/MWNT dispersion

The electrochemical reduction of 1×10^{-3} M HMC was studied with GCE modified with different amounts of PB/MWNT dispersion (Figure **5.6**). The current first increased when the amount of the PB/MWNT dispersion was increased up to 4 μL, thereafter the current decreased. The lowest potential for HMC reduction, with maximum current was observed for 4 μL dispersion. Hence 4 μL PB/MWNT dispersion was used to modify the GCE for further studies.

5.5.3 Effect of scan rate

Useful information involving electrochemical mechanism can be acquired from the relationship between peak current and scan rate. Therefore, the electrochemical behaviors of HMC at different scan rates were also investigated on the surface of the PB/MWNT modified GCE by LSV and SWV (Figure **5.7**). A linear relationship was observed between the peak current and the square root of scan rate in the range 20 to 280 mV/s in LSV and 20 to 220 mV/s in SWV, which revealed that the reduction of HMC was a diffusion controlled process (Figure **5.8**). The regression equation obtained from LSV analysis is: I_p=0.966 $\nu^{1/2}$+6.910 (r^2=0.998, ν in mV/s, I_p in μA) and SWV gave a regression equation, I_p =0.968 $\nu^{1/2}$-1.870 (r^2=0.995, ν in mV/s, I_p in μA).

A plot of logarithm of peak current (log I_p) versus logarithm of scan rate (log ν) gives a straight line (Figure **5.9**). The linear relationship obtained from LSV and SWV analysis are log I_p = 0.511 log ν + 0.165 (r^2=0.996) and log I_p = 0.637 log ν - 0.387 (r^2=0.998) respectively. Slope of the plots clearly confirms that the reduction at the electrode surface is an irreversible diffusion controlled process [168]. According to the Laviron's conclusion [169], the relationship between the peak potential (E_p) and ν was examined. It was found that E_p varies linearly with ln ν and is shown in Figure **5.10**. The no. of electrons (n_a) involved in the reaction can be calculated from the slope of the plot. The obtained values for n_a is around 2, which confirms that 2 electrons are involved in the reduction of HMC. The cathodic reductive behavior of HMC may be due to reduction of keto group [206]. The keto group is converted into hydroxyl group by undergoing a $2H^+$, $2e^-$ reduction as explained in Figure **5.11**.

5.5.4 Calibration curve

Dependence of peak current on the concentration of HMC was studied using DPV. Figure **5.12** shows DPV of HMC on PB/MWNT modified GCE at various concentrations (10^{-3}–10^{-7} M). The results show that the cathodic peak current has a linear relationship with the concentration in the range 1.0×10^{-6}-3.0×10^{-7} M which is shown in Figure **5.13**. The regression equation is: $I_p = 1.0\times10^{-7}C - 1.870$ (r^2=0.988, C in M, I_p in μA). The detection limit of HMC was 7.16×10^{-8} M. The reproducibility of the electrode was examined by repetitive measurement of 1×10^{-3} M HMC using the same PB/MWNT modified GCE. After five successive measurements, comparable results with relative standard deviation (RSD) 1.9 % were obtained suggesting that the PB/MWNT modified GCE has good reproducibility. The long term stability of modified electrode was evaluated by measuring the current responses at a fixed HMC concentration of 1×10^{-3} M over a period of 2 weeks. The electrode was used daily and was stored in distilled water after use. The experimental results showed that the current responses deviated only 6.2 % revealing that the fabricated sensor possesses long term stability.

5.5.5 Interference study

Selectivity of the sensor was examined by studying the effects of foreign species on the determination of HMC. Table **5.1** lists the influence of foreign species on the reduction signal of HMC. Up to 100-fold excess concentrations of urea, glucose, lactose, Na^+, K^+, Cl^- and SO_4^{2-} have no influences on 1×10^{-3} M HMC signals (deviation below 5%).

5.6 Analytical Applications

Analytical application studies were conducted using the fabricated sensor. The application of the developed sensor in the determination of HMC in real sample like urine was studied.

5.6.1 Determination of HMC in urine sample

To validate the possibility of practical application of the sensor, it was applied for the determination of HMC in urine sample. The results are given in Table **5.2**. These results demonstrated the ability of PB/MWNT modified GCE for voltammetric determination of HMC with high accuracy and high percentage recovery.

5.7 Conclusions

The electrochemical reduction behavior and determination of HMC in urine samples with acetate buffer on PB/MWNT modified GCE using CV, DPV, SWV and LSV is studied. Experimental data clearly confirms that HMC undergoes an irreversible diffusion controlled reduction process at the electrode surface. The PB/MWNT modified GCE showed electrocatalytic action for the reduction of HMC. Well-defined DP voltammograms are obtained in PB/MWNT modified GCE with high sensitivity and reproducibility.

Table 5.1 Interference study

Foreign species	Signal change (%)
Urea	-3.53
Glucose	+2.78
Lactose	+2.92
Na^+	+0.80
K^+	+1.22
Cl^-	+0.80
SO_4^{2-}	+1.22

*Average of three replicates.

Table 5.2 Determination of HMC in urine sample

Added (M)	Found (M)	Recovery (%)
2.00×10^{-6}	2.02×10^{-6}	101
4.00×10^{-6}	3.97×10^{-6}	99.3
6.00×10^{-6}	5.86×10^{-6}	97.7

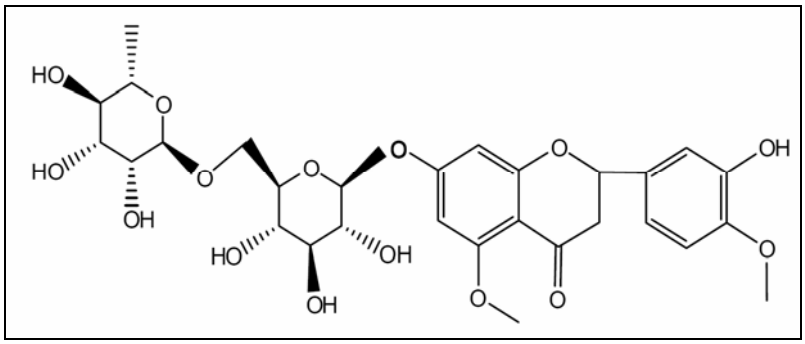

Figure 5.1 Structure of HMC

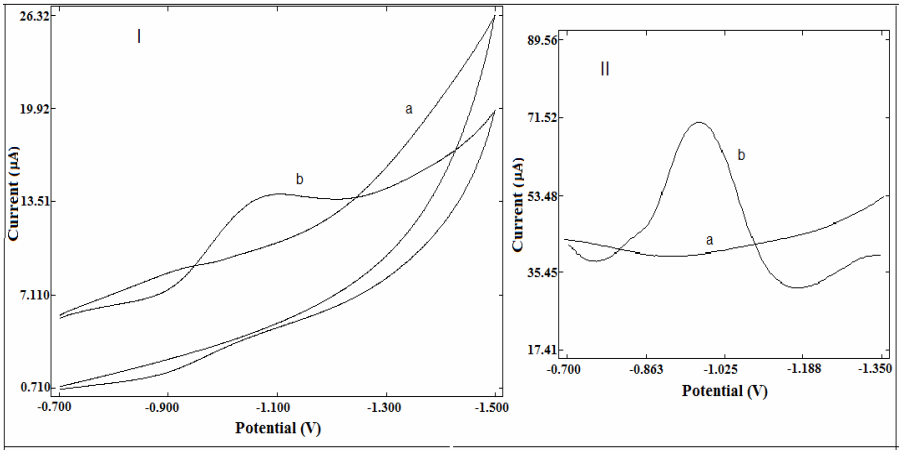

Figure 5.2 (I) Cyclic voltammmograms of 1×10^{-3} M HMC at (a) bare GCE (b) PB/MWNT modified GCE and (II) Differential pulse voltammmograms of 1×10^{-3} M HMC at (a) bare GCE (b) PB/MWNT modified GCE

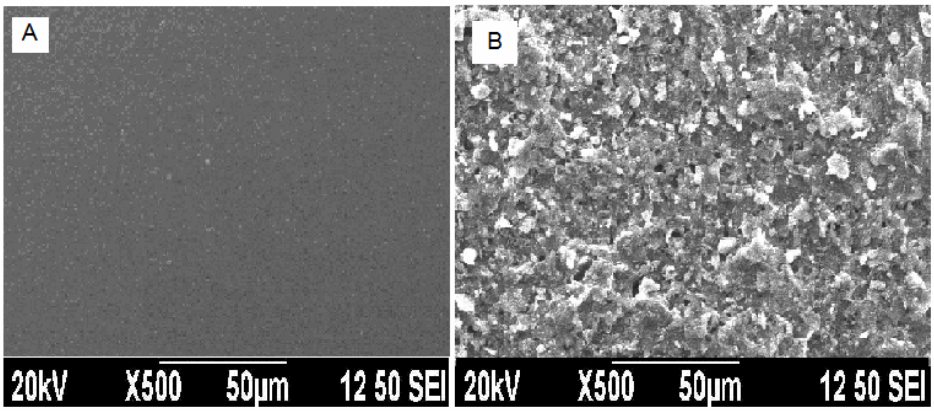

Figure 5.3 SEM images of (A) bare GCE (B) PB/MWNT modified GCE

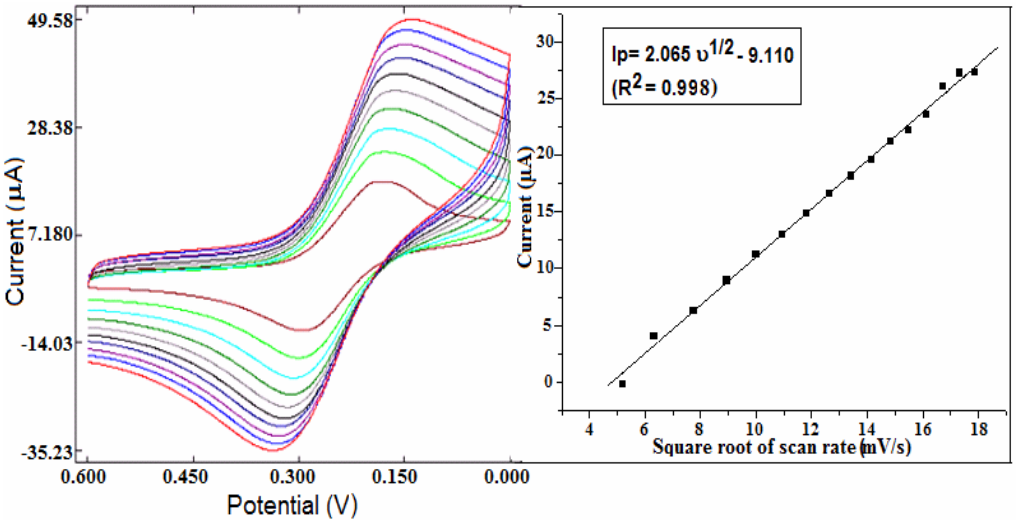

(a)

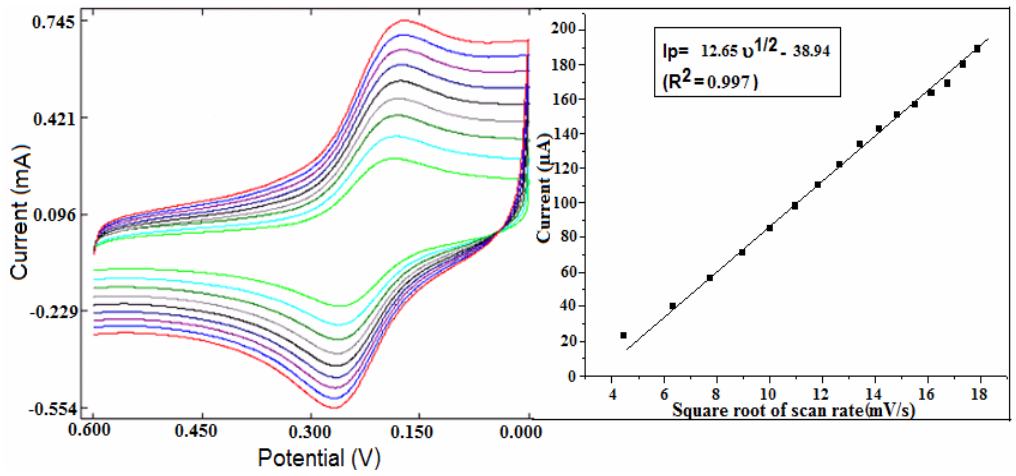

(b)

Figure 5.4 Surface area studies at (a) bare GCE and (b) PB/MWNT modified GCE and inset are plot of peak currents as a function of the square root of scan rates

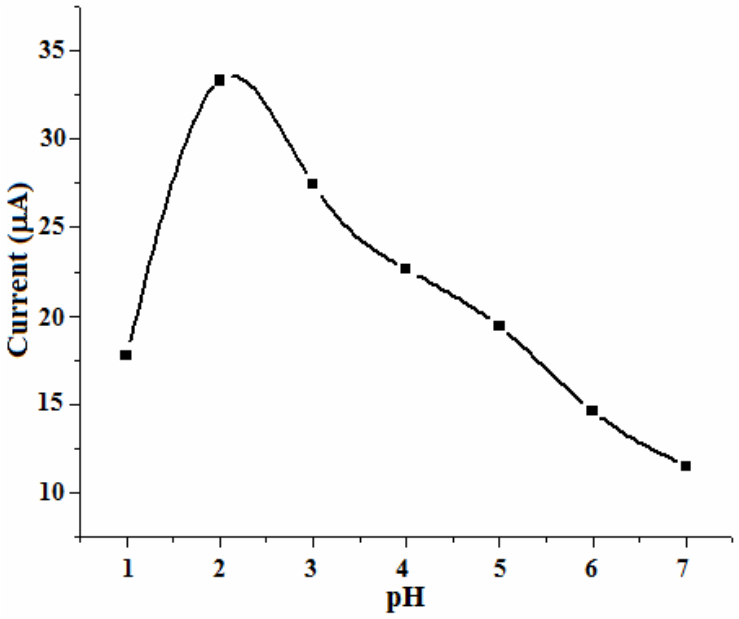

Figure 5.5 Variation of cathodic peak current with pH of the medium

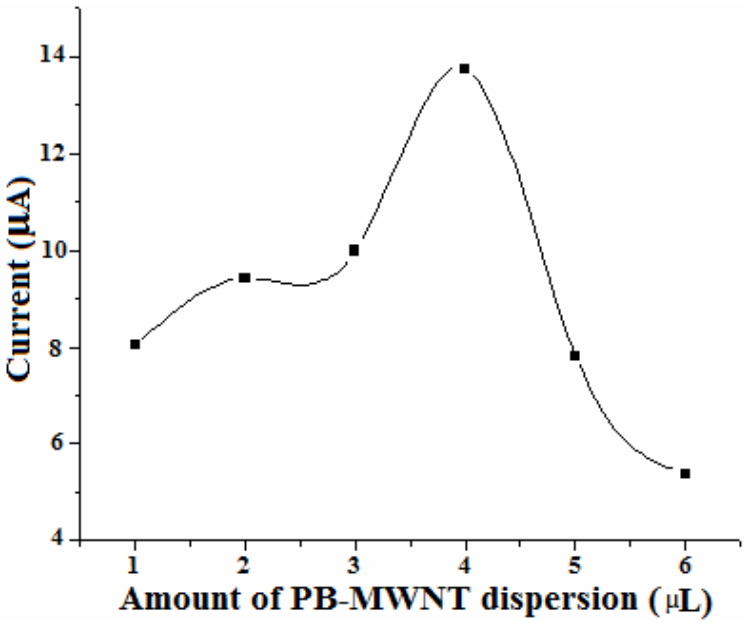

Figure 5.6 Effect of the amount of PB/MWNT-Nafion suspension at modified GCE

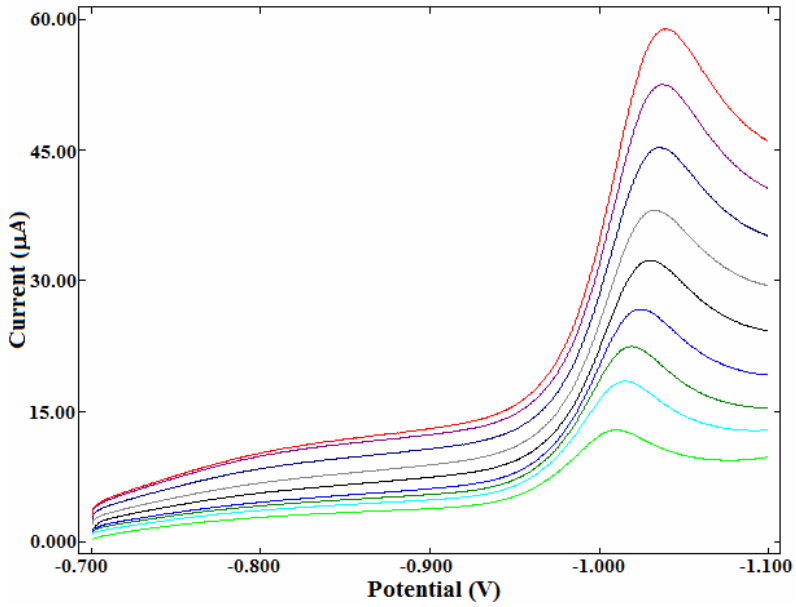

(a)

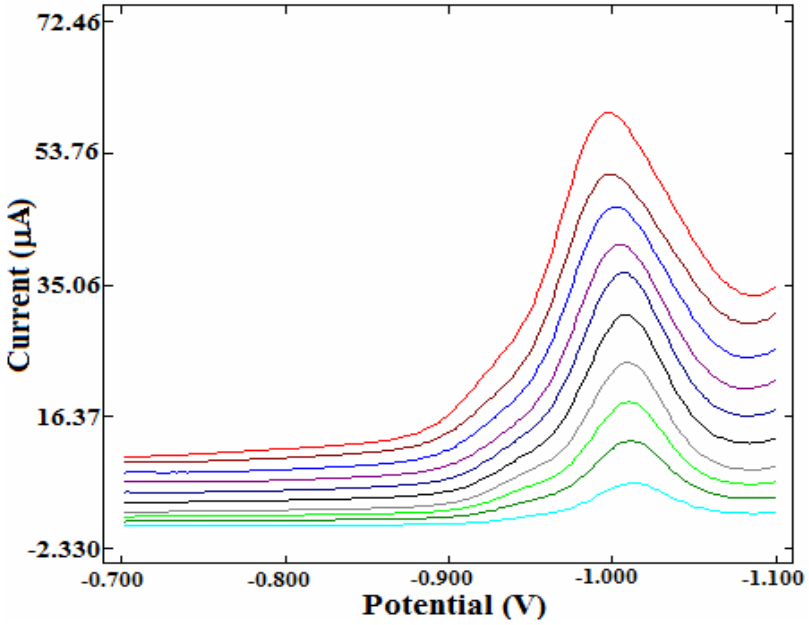

(b)

Figure 5.7 (a) Overlay of linear sweep voltammograms of 1×10^{-3} M HMC at PB/MWNT modified GCE in 0.1 M acetate buffer at different scan rates (20 to 280 mV/s) and (b) Overlay of square wave voltammograms of 1×10^{-3} M HMC at PB/MWNT modified GCE in 0.1 M acetate buffer at different scan rates (20 to 220 mV/s).

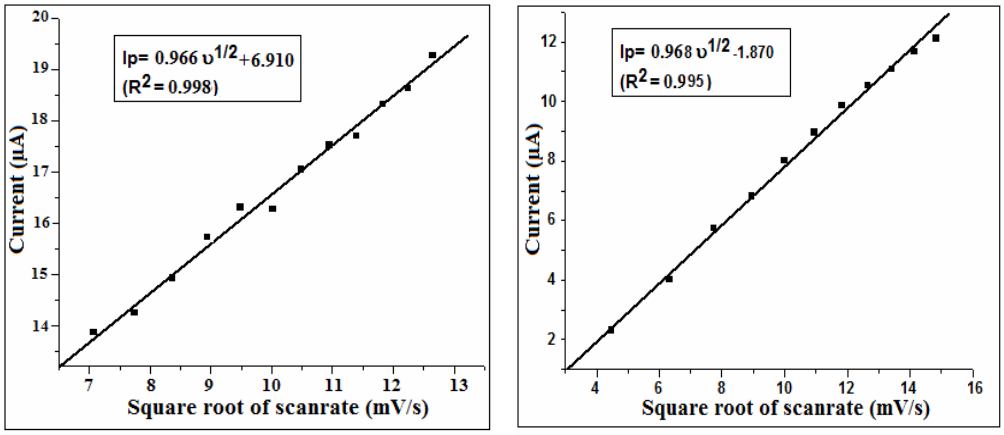

(a) (b)

Figure 5.8 Plot of peak currents as a function of the square root of scan rates obtained from (a) linear sweep voltammetric studies and (b) square wave voltammetric studies.

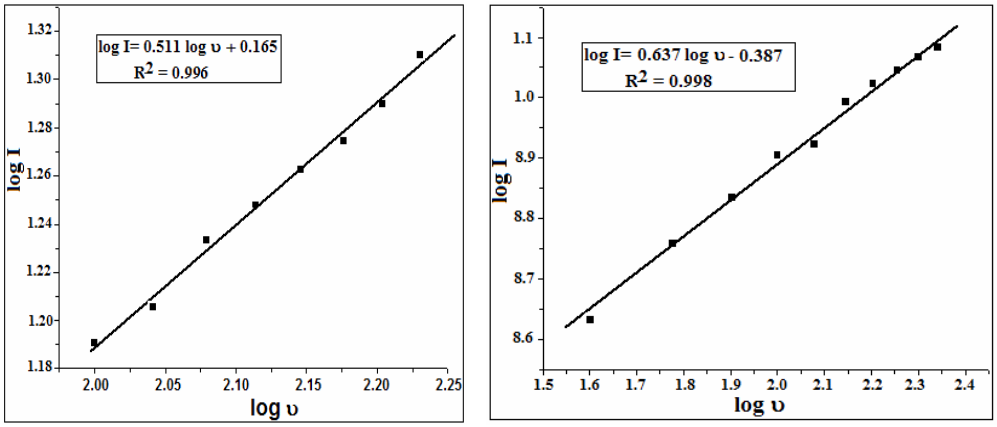

(a) (b)

Figure 5.9 Plot of log I versus log ν

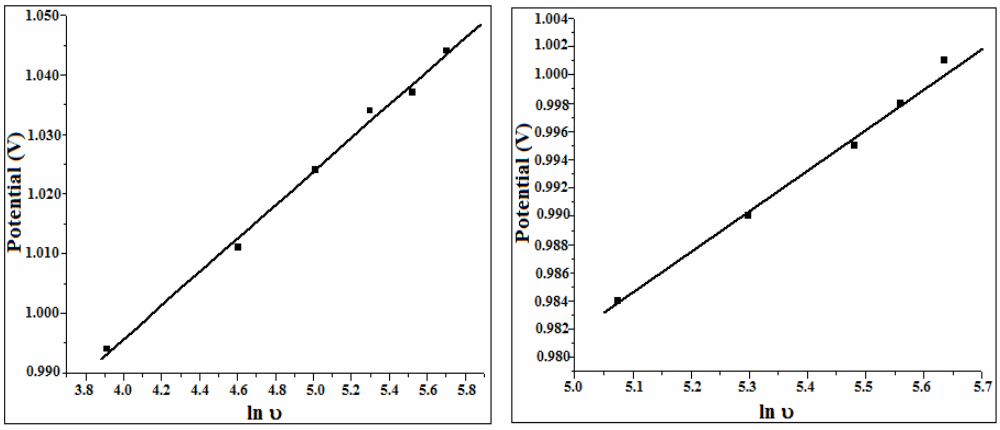

(a) (b)

Figure 5.10 Variation of ln scan rate versus cathodic potential from (a) linear sweep voltammetric studies and (b) square wave voltammetric studies.

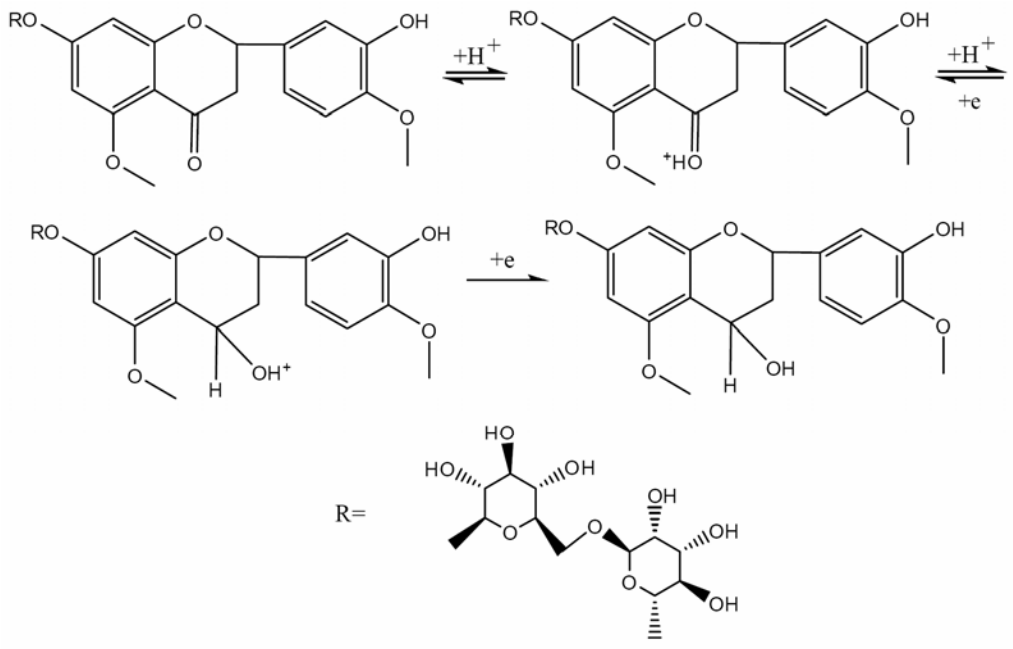

Figure 5.11 Reaction Mechanism

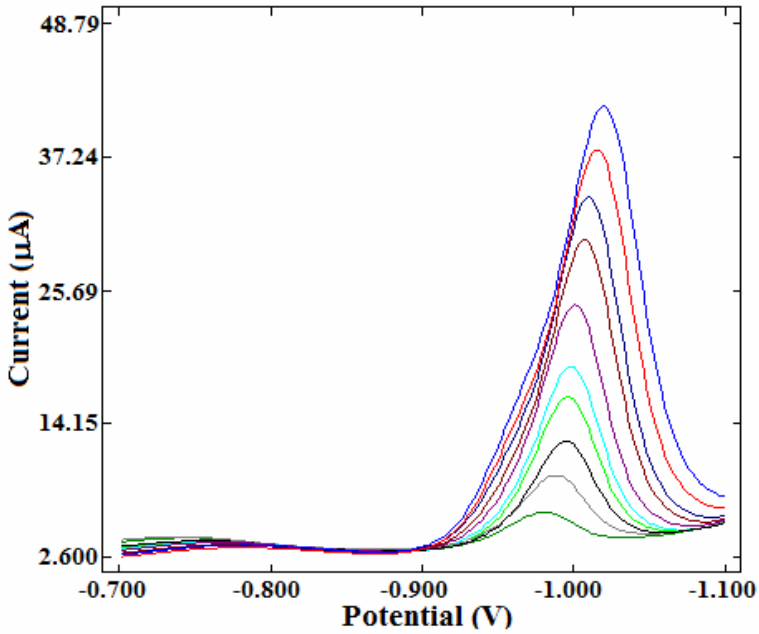

Figure 5.12 Differential pulse voltammograms of HMC at different concentrations, 10^{-3}- 10^{-7} M (top to bottom)

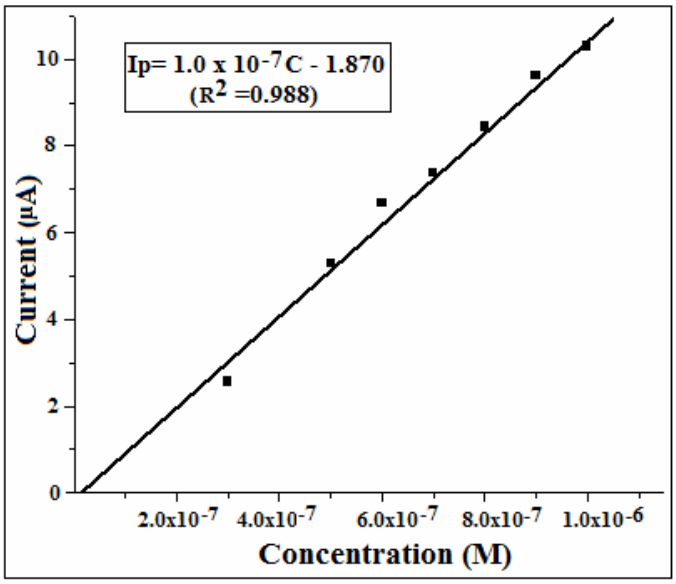

Figure 5.13 Plot of peak currents as a function of concentration of HMC

Chapter 6

DEVELOPMENT OF SENSOR FOR GUAIPHENESIN

Contents

6.1 Introduction
6.2 Preparation of poly (p-ABSA) modified GCE
6.3 Preparation of MWNT/poly (p-ABSA) modified GCE
6.4 Preparation of poly (p-ABSA) / SPCE and MWNT/poly (p-ABSA) / SPCE
6.5 Electrochemical behaviour of Guai
6.6 Evidences of electrode modification
6.7 Performance characteristics of the developed sensors
6.8 Application potential of the developed sensors
6.9 Conclusions

Four simple electrochemical sensors have been developed for the voltammetric determintion of Guaiphenesin (Guai). Screen printed carbon electrodes (SPCE) modified with poly (p-aminobenzenesulphonic acid) [poly (p-ABSA)] and multiwalled carbon nanotube (MWNT) was constructed. The electrochemical behavior of Guai on poly (p-ABSA) modified glassy carbon electrode (GCE) and MWNT/ poly (p-ABSA) modified GCE was investigated using various voltammetric techniques such as Cyclic Voltammetry (CV), Differential Pulse Voltammetry (DPV), Square Wave Voltammetry (SWV) and Linear Sweep Voltammetry (LSV). The determination conditions, such as the amount of MWNT-Nafion suspension, thickness of poly (p-ABSA) film, supporting electrolyte and scan rate were optimized.

6.1 Introduction

Guaiphenesin (Guai) (Figure **6.1**), chemically named as (R,S)-3-(2-methoxyphenoxy)propane-1,2-diol, is one of the most widely used sedative expectorant that reduces the viscosity of tenacious sputum and thins bronchial secretions. It also stimulates the flow of respiratory tract secretions, allowing ciliary movement to carry the loosened secretions upward toward the pharynx. It is used to treat symptoms of allergy, cold and upper respiratory infections. It

is present in a variety of pharmaceutical formulations [230,231]. Methods available for the determination of Guai are spectrophotometry [232-234], high performance liquid chromatography [235-238], chemometrics [239] and capillary electrophoresis [240]. But most of these reported methods are time consuming and also require expensive and sophisticated instruments.

The poor reproducibility of electrochemical oxidation of Guai on bare GCE has led to the use of mediators and modified electrodes to catalyze the electrochemical oxidation of Guai [241]. For example, electrode surfaces modified with bimetallic inorganic-organic nanofiber hybrid nanocomposite [242] has been used.

For past two decades, conducting polymers (CPs) have been widely used as electrode modifiers. The extended p-conjugated system of the CPs has single and double bonds alternating along the polymer chains. CPs are particularly appealing because they exhibit electrical, magnetic, and optical properties of metals or semiconductors while retaining the attractive mechanical properties and processing advantages of polymers. Because of the unusual electronic and optical properties, CPs are very attractive materials in various applications including solar cells, light weight batteries, electrochromic devices, sensors and molecular electronic devices. Electropolymerization is a good method to immobilize polymers on electrodes. Because of its selectivity, sensitivity and homogeneity in electrochemical deposition, polymers modified electrodes (PMEs) have many advantages in the detection of bio-molecules. Recently, poly (p-ABSA) modified electrodes have been reported for the electrochemical study of several compounds, including dopamine [243], uric acid [244], H_2O_2 [245], tyrosine [246], trifluoperazine [247], phenylephrine and chlorprothixene [248]. Nevertheless, there is no report about electrochemical determination of Guai by using poly (p-ABSA) modified electrodes.

On the other hand, carbon nanotubes (CNTs) have also aggravated enormous interest in wide variety of potential applications. Depending on their helicity, CNTs can be either metallic or semiconducting [249]. Composite materials based on the coupling of CPs and CNTs have been shown to possess properties of the individual components with a synergistic effect [250].The coupling of polymers with CNTs is of increasing importance due to its simplicity of construction and its ability to incorporate conducting materials into porous polymers in order to form electrochemical sensors. In this chapter MWNT/ poly (p-ABSA) modified GCE is utilized for the determination of Guai.

Screen printing technology is one of the most promising routes for mass production of inexpensive, reproducible and reliable electrochemical sensors. Use of SPCEs is a growing and attractive electroanalytical tool for quality control of pharmaceuticals. Some of the reports available for the use of SPCEs in the determination of pharmaceuticals are; the quantitative analysis of paracetamol on an untreated SPCE using amperometric detection coupled to a flow injection analysis system [251], the lamotrigine determination by differential pulse adsorptive stripping voltammetry (DPAdSTV) using SPCE [252], and the electrochemical determination of nitrazepam at a SPCE using AdSV [253].

Appropriate modification of the electrode substrate with electron mediators enhances the selectivity of these devices [254]. Ascorbic acid determination using the 7,7,8,8-tetracyanoquinodimethane (TCNQ) [255] or cobalt phthalocyanine [256] modified SPCE have also been reported. However, these modifiers serve as general electrocatalysts to a wide range of analytes [257]. This chapter also describes the development of MWNT and poly (p-ABSA) modified screenprinted electrode sensors that allows the Guai

determination at low potential and holds out the possibility for portable testing. The electrochemical behaviour on SPCEs was studied by CV. The combination of MWNT and poly (p-ABSA) results in a novel composite material, consisting of an interconnected MWNT–polymer network, and possessing mechanical flexibility, high toughness, and high porosity, while retaining the attractive electrochemical behaviour of MWNT electrodes and biocompatibility of polymer.

In this chapter voltammetric methods based on modified GCEs and SPCEs was developed for the determination of Guai. Compared with bare electrodes, modified electrodes exhibits a remarkable shift of the oxidation potentials of Guai in the negative direction and a drastic enhancement of the anodic current response. The performance characteristics of the developed sensors were studied in detail. The modified electrodes have been successfully applied for the determination of Guai in pharmaceutical formulations and in urine sample.

6.2 Preparation of poly (p-ABSA) modified GCE

Preparation of poly (p-ABSA)/GCE was carried out using a BAS Epsilon electrochemical workstation with a conventional three electrode system, including GC working electrode, a platinum wire counter electrode and an Ag/AgCl reference electrode.

GCE was cleaned as explained under section 2.4 of Chapter 2. The poly (p-ABSA)/GCE was prepared by electropolymerisation. The detailed procedure for the fabrication of poly (p-ABSA)/GCE is given in section 2.5.4.1 of Chapter 2.

Voltammograms of 2×10^{-3} M p-ABSA in 0.1 M HNO_3 at the GCE are shown in Figure **6.2**. As shown in Figure **6.2**, an anodic peak at 1037 mV and

a cathodic peak at -145 mV were observed in the first scan. From the second scan, an anodic peak at 465 mV and a cathodic peak at -442 mV appeared. Then larger peaks were observed on continuous scanning, reflecting the continuous growth of the film. These facts indicated that p-ABSA was deposited on the surface of GCE by electropolymerization [258]. After modification, the poly (p-ABSA) film electrode was carefully washed with redistilled water to remove the physically adsorbed materials and dried in air. A blue film was found to be formed on the electrode surface.

6.3 Preparation of MWNT/poly (p-ABSA) modified GCE

4 μL of MWNT/Nafion suspension was deposited onto the surface of poly (p-ABSA) modified GCE. The composite was then dried in air before it was used as a working electrode in the experiment. A uniform thin film of nanotube was formed on GCE. The detailed procedure for the fabrication of MWNT/ poly (p-ABSA) modified GCE is given in section 2.5.4.2 of Chapter 2.

6.4 Preparation of poly (p-ABSA)/SPCE and MWNT/poly (p-ABSA)/SPCE

Modification of SPCEs was carried out in the same manner as explained in above section.

6.5 Electrochemical behaviour of Guai

Stock solution of Guai was prepared as described in section 2.6 of Chapter 2. Appropriate dilutions of the standard solution of Guai, was performed with 0.1 M HCl to obtain final concentrations of Guai. Sample solution was taken in the voltammetric cell, and nitrogen was purged for 3 min to remove oxygen. Voltammograms from 600 to 1300 mV, at 100 mV/s were

recorded. Prior to each measurement, the modified electrodes were activated by sweeping in 0.1 M HCl until the voltammograms kept unchangeable.

Guai gave an oxidation peak on bare GCE at 1152 mV with a peak current of 0.0290 mA. In order to reduce the oxidation potential of Guai, various chemical modifications on GCE was tried (Figure **6.3**). At poly (p-ABSA) modified GCE, Guai oxidizes at 1088 mV and the peak current was increased to 0.0826 mA. Further on modifying the poly (p-ABSA) / GCE surface with MWNT, oxidation potential was reduced to 1004 mV with a peak current of 0.1814 mA. Compared with the bare GCE, there was a reduction in the anodic potential by about 148 mV and 6 times enhancement in the peak current at MWNT / poly (p-ABSA) / GCE. Also when compared with poly (p-ABSA) / GCE, there was a reduction in the potential by about 84 mV and 2 times increase in the peak current at MWNT / poly (p-ABSA) / GCE.

The electrochemical oxidation of Guai was studied on the modified SPCE in the same experimental conditions (Figure **6.4**). The determination of Guai on bare SPCEs, poly (p-ABSA) / SPCE and MWNT / poly (p-ABSA) / SPCE were also conducted. Though the oxidation potential obtained in these cases are almost the same as that obtained with modified GCEs, the peak current has greatly enhanced. At bare SPCE, oxidation of Guai occurs with a peak current of 0.1147 mA. Upon modification of the electrode surface with poly (p-ABSA), peak current was increased to 0.6320 mA. The enhancement in the peak current suggests that poly (p-ABSA) film can accelerate the electron transfer of Guai. Further on modifying the poly (p-ABSA) / SPCE surface with MWNT, the observed peak current was 1.2027 mA. The ability of MWNT to promote electron transfer also resulted in the tremendous enhancement of peak current.

6.6 Evidences of electrode modification

6.6.1 SEM images

Surface morphological observations of modified electrodes were carried out by SEM. Figures **6.5a, 6.5b** and **6.5c** depict the SEM images of the bare GCE, poly (p-ABSA)/GCE and MWNT/ poly (p-ABSA)/GCE at 500 times magnification respectively. The comparison points to the effective modification of the GCE.

6.6.2 Surface area study

Cyclic voltammetry of 2 mM potassium ferricyanide solution was carried out at both bare and modified electrodes at different scan rates to calculate the effective surface area (Figures **6.6**). The obtained current were plotted against the square root of scan rates in both the cases. From the slope of the straight line, the obtained regression equations are as given below.

At bare GCE: $I_p = 0.866\ \nu^{1/2} + 5.263$ ($r^2 = 0.996$)

At poly (p-ABSA) / GCE: $I_p = 6.839\ \nu^{1/2} - 11.56$ ($r^2 = 0.998$)

At MWNT / poly (p-ABSA) / GCE: $I_p = 1.767\ \nu^{1/2} + 2.000$ ($r^2 = 0.983$)

At bare SPCE: $I_p = 1.332\ \nu^{1/2} + 5.356$ ($r^2 = 0.992$)

At poly (p-ABSA) / SPCE: $I_p = 2.396\ \nu^{1/2} + 0.793$ ($r^2 = 0.995$)

At MWNT / poly (p-ABSA) / SPCE: $I_p = 9.634\ \nu^{1/2} - 37.96$ ($r^2 = 0.993$)

By using the Randles-Sevcik equation [167], effective surface area of bare and modified electrodes were calculated. Surface area for bare GCE was found to be 0.0620 cm^2. On modification with poly (p-ABSA) and MWNT / poly (p-ABSA), the effective surface area increased to 0.1151 cm^2

and 0.4498 cm^2 respectively. In the case of SPCE, surface area without modification was 0.0904 cm^2. On modification with poly (p-ABSA) and MWNT / poly (p-ABSA), surface area increased to 0.6499 cm^2 and 0.8942 cm^2.

6.7 Performance characteristics of the developed sensors

The functional potential of the developed sensors depend on many factors including effect of the supporting electrolyte, effect of amount of the MWNT-Nafion dispersion, effect of scan rate, range of linear response, detection limit and interference study. Each of these parameters are discussed in detail in the next section.

6.7.1 Effect of the supporting electrolyte

The electrochemical behavior of Guai in various media were studied by DPV. The supporting electrolytes include KNO_3, HCl, NaOH, NaCl, tetra-n-butyl ammonium chloride, KCl, phosphate buffer and acetate buffer (0.1 M). The oxidation peak obtained for Guai at all the developed sensors was best defined in 0.1 M HCl.

6.7.2 Effect of film thickness

Optimization of the thickness of poly (p-ABSA) film on the oxidation peak current of 1×10^{-3} M Guai was also investigated (Figures **6.7**). As the number of polymerization cycles increases, the electrochemical response of Guai increased at first, but when the number of cycles was more than 40, the current decreases. This may be due to the fact that increase in thickness of the film would prevent the electron transfer. It was also observed that when the number of cycles was less than 40, poly (p-ABSA) modified electrode showed poor repeatability and stability. Therefore, 40 cycles was used throughout the experiment.

6.7.3 Effect of amount of the MWNT-Nafion dispersion

The effect of using an increasing concentration of MWNT dispersion (5 mg of MWNT in a mixture of 300 μL Nafion and 2 mL water) to modify the GCE is depicted in the Figure **6.8**. From the figure it is clear that the lowest Nafion concentration was apparently unable to keep the MWNTs attached to the GCE, whereas at the highest concentration, the Nafion membrane was probably too thick with the result that it inhibited access of the analyte to the electrode. So the amount of MWNT-Nafion dispersion was fixed to be 4 μL.

6.7.4 Effect of scan rate

The effect of scan rate was investigated in 0.1 M HCl solution containing 1×10^{-3} M Guai using LSV and SWV (Figure **6.9**). When the scan rate was increased, a linear dependence of the peak current upon the square root of the scan rate was found, demonstrating a diffusional behavior (Figure **6.10**). At a poly (p-ABSA) / GCE, the regression equations obtained from LSV and SWV analysis are: $I_p = 0.077\ \nu^{1/2} - 0.023$ ($r^2=0.998$, ν in mV/s, I_p in mA) and $I_p = 0.031\ \nu^{1/2} - 0.008$ ($r^2=0.990$) respectively. Regression equation obtained from LSV and SWV analysis on the MWNT / poly (p-ABSA) / GCE are $I_p = 0.006\ \nu^{1/2} - 0.019$ ($r^2=0.991$) and $I_p = 0.006\ \nu^{1/2} - 0.013$ ($r^2=0.997$) respectively. Cyclic voltammograms illustrating the relationship between I_p and $\nu^{1/2}$ is depicted in Figure **6.11** and **6.12**. The obtained regression equations are given below.

At poly (p-ABSA) / GCE: $I_p = 0.012\ \nu^{1/2} - 0.008$ ($r^2=0.994$)

At MWNT / poly (p-ABSA) / GCE: $I_p = 0.009\ \nu^{1/2} - 0.016$ ($r^2=0.990$)

At poly (p-ABSA) / SPCE: $I_p = 0.101\ \nu^{1/2} - 0.307$ ($r^2=0.991$)

At MWNT / poly p-ABSA / SPCE: $I_p = 0.042\ \nu^{1/2} - 0.042$ ($r^2=0.997$)

Laviron's equation [169] can be used to calculate the number of electrons (n_a) involved in the reaction. From the scan rate study it was found that E varies linearly with ln ν (Figure **6.13**). The regression equations for the linear graphs are,

At poly (p-ABSA) / GCE: $E = 32.66 \ln \nu + 1031$ (r^2=0.998)

At MWNT / poly (p-ABSA) / GCE: $E = 32.54 \ln \nu + 977.8$ (r^2=0.996)

At poly (p-ABSA) / SPCE: $E = 32.56 \ln \nu + 926.5$ (r^2=0.996)

At MWNT / poly (p-ABSA) / SPCE: $E = 27.65 \ln \nu + 966$ (r^2=0.994)

n_a values for poly (p-ABSA) / GCE, MWNT / poly (p-ABSA) / GCE, poly (p-ABSA) / SPCE, and MWNT / poly p-ABSA / SPCE sensors, from the CV studies were found to be 1.7, 1.7, 1.6 and 2.1 (around 2) respectively. This confirms that 2 electrons are involved in the oxidation of Guai (Figure **6.14**).

6.7.5 Influence of concentration

The relationship between concentration and the anodic peak current of Guai was investigated by DPV and SWV (Figure **6.15**). In the case of modified SPCE sensors, concentration study was carried out by CV (Figure **6.16**). The oxidation peak current was found to increase with increase in the concentration of Guai. From the calibration curves, detection limits was obtained and tabulated (Table **6.1**). The reproducibility of the developed sensor was examined by repetitive measurement of the oxidation peak current of 1×10^{-3} M Guai using the same electrode. After several successive measurements, stable electrochemical responses were obtained suggesting that all the developed sensors have excellent reproducibility.

A comparison of the present work with the already reported works is tabulated in Table **6.2**. It can be inferred that the present work is comparable with the reported works.

6.7.6 Interference study

As shown in Table **6.3**, the additions upto 10^{-1} M of urea, glucose, lactose, Na^+, K^+, Cl^- and SO_4^{2-} do not interfere with the voltammetric response of 1×10^{-3} M Guai. These results indicate that the film electrode has good selectivity for the determination of Guai. However, ascorbic acid interferes with the oxidation signal of Guai.

6.8 Application potential of the developed sensors

The sensors developed for Guai were employed for its determination in tablet forms and in spiked urine samples.

6.8.1 Determination of Guai in pharmaceutical formulations

Experiments were performed analyzing commercial formulation containing Guai namely, Expal Capsules (Mech pharma, India).

The Guai content in the tablet was determined using the developed sensors by calibration method. The detailed procedure for the determination is given in section 2.8.2 of Chapter 2. The results obtained are summarized in Table **6.4**. The close agreement of the found values with the declared amount is indicative of non-interference of the other ingredients and excipients present in the formulation.

The results were compared with those obtained by the standard method [140]. The results show that there is a good agreement between the developed method and the standard method.

6.8.2 Determination of Guai in urine sample

The developed sensor was applied for the determination of Guai in urine samples. Suitable aliquot of Guai was added to the above solution. The solution was then thoroughly stirred. DPV was then recorded and the anodic peak current obtained was measured. This procedure was repeated for several additions of Guai and the unknown concentrations were determined from the calibration graph. The results summarized in Table **6.5**, shows a very good recovery indicating the practical utility of the developed sensor.

6.9 Conclusions

Four novel voltammetric sensors were fabricated for the determination of Guai using modified GCEs and SPCEs. The voltammetric behavior of Guai was investigated at the modified electrodes by CV, DPV, SWV and LSV. The oxidation of Guai was found to be an irreversible process. Compared with the bare electrode, the electrochemical response of Guai at the modified electrodes exhibited a tremendous increase in the peak current and considerable decrease in the peak potential. The developed sensors have been successfully applied for the voltammetric determination of Guai in urine samples and in pharmaceutical formulation.

Table 6.1 Concentration studies of the developed sensors

Type of sensor	Technique	Linear range	Detection limit	
			M	g/mL
poly (p-ABSA) / GCE	DPV	2×10^{-6}–1×10^{-5}	9.554×10^{-7}	1.844×10^{-7}
	SWV	3×10^{-6}–2×10^{-5}	1.060×10^{-6}	0.210×10^{-6}
MWNT / poly (p-ABSA) / GCE	DPV	2×10^{-6}–1×10^{-5}	1.466×10^{-8}	0.291×10^{-8}
	SWV	3×10^{-6}–1×10^{-5}	1.540×10^{-6}	0.305×10^{-6}
poly (p-ABSA) / SPCE	CV	2×10^{-4}–1×10^{-3}	9.353×10^{-5}	1.853×10^{-6}
MWNT / poly p-ABSA / SPCE	CV	7×10^{-6}–2×10^{-6}	1.533×10^{-6}	0.304×10^{-6}

Table 6.2 Comparison of the present work with some of the reported works

Method adopted	Detection limit
Colorimetric method [232]	2.500 µg/mL
First and second derivative ultraviolet spectrophotometry [233]	0.350 and 1.890 µg/mL
Derivative spectrophotometry [234]	0.048 µg/mL
High Performance Liquid Chromatography (HPLC) [235]	0.160 µg/mL
HPLC with fluorometric detection [236]	1.134 µg /mL
HPLC method with spectrophotometric detection [237]	3.700 µg/mL
Reverse phase HPLC method [238]	0.180 µg/mL
Chemometric method [239]	0.280 µg/mL
Capillary electrophoretic method [240]	1.982 µg/mL
Differential pulse Voltammetric method [241]	0.003 µg/mL
Cyclic voltammetric method [242]	3.000 µg/mL
DPV using poly (p-ABSA) / GCE	0.184 µg/mL
SWV using poly (p-ABSA) / GCE	0.210 µg/mL
DPV using MWNT/poly(p-ABSA)/GCE	0.003 µg/mL
SWV using MWNT/poly(p-ABSA)/GCE	0.305 µg/mL
CV using poly (p-ABSA) / SPCE	18.53 µg/mL
CV using MWNT/poly p-ABSA/SPCE	0.304 µg/mL

Table 6.3 Study of the effect of foreign species on the anodic peak current of 1×10^{-3} M Guai at poly (p-ABSA)/GCE and MWNT/ poly (PABSA)/GCE

Foreign species	Signal change (%)	
	poly (PABSA) sensor	MWNT/ poly (PABSA) sensor
Urea	+1.852	-1.181
Glucose	-1.278	+0.940
Lactose	+3.509	-3.846
Na^+	+1.946	+2.614
K^+	+0.968	-1.584
Cl^-	+1.946	+2.614
SO_4^{2-}	+0.968	-1.584
Ascorbic acid	+12.89	-11.65

Table 6.4 Determination of Guai in pharmaceutical preparation

Sample	Declared amount (mg/tablet)	Method adopted	Found* (mg/tablet)	S.D*	C.V*
Expal (Mech pharma, India)	100	poly (p-ABSA) / GCE	97	1.54	1.24
		MWNT / poly (p-ABSA) / GCE	98	1.86	1.41
		Standard method	102	2.11	1.55

*Average of six replicates

Table 6.5 Determination of Guai in urine sample

Type of sensor	Added (M)	Found (M)	Recovery (%)
poly (p-ABSA) / GCE	3.00×10^{-6}	3.15×10^{-6}	104.9
	5.00×10^{-6}	4.97×10^{-6}	99.35
	7.00×10^{-6}	6.88×10^{-6}	98.23
MWNT / poly (p-ABSA) / GCE	6.00×10^{-6}	5.86×10^{-6}	97.68
	8.00×10^{-6}	7.88×10^{-6}	98.53
	1.00×10^{-5}	1.02×10^{-5}	102.4

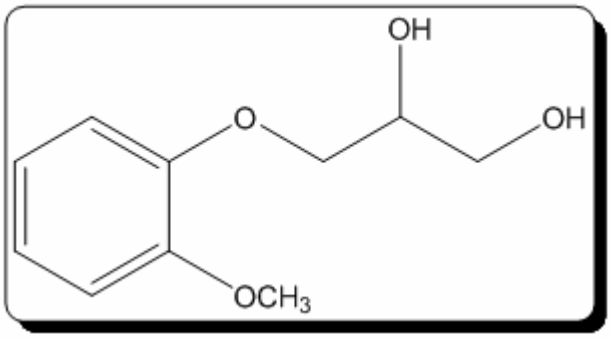

Figure 6.1 Structure of Guai

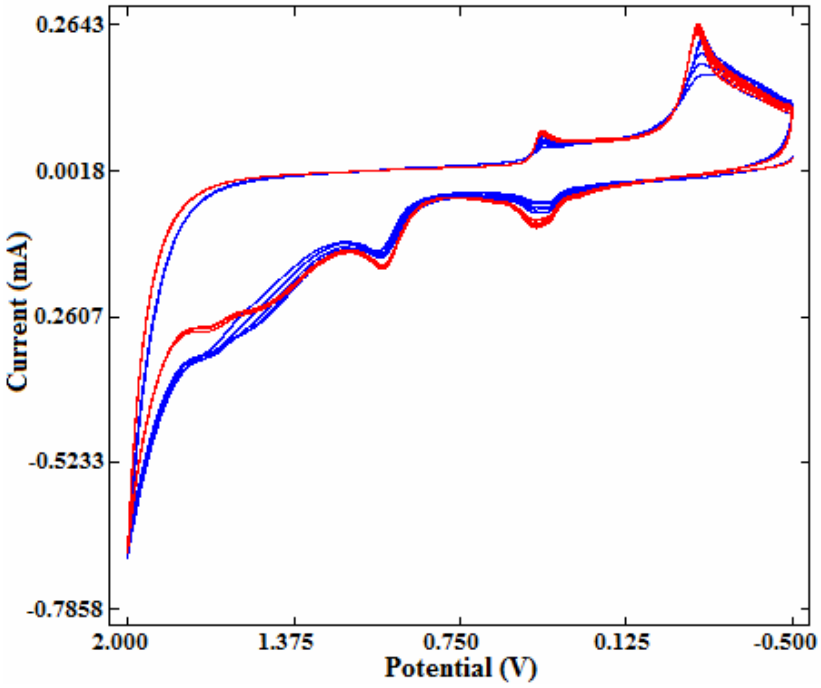

Figure 6.2 Electropolymerization of p-ABSA

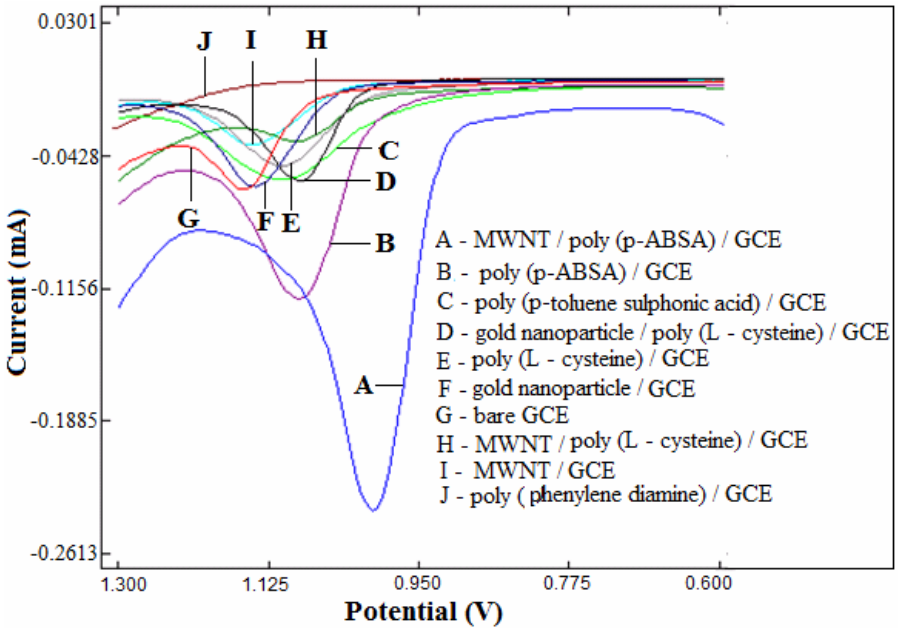

Figure 6.3 Electrochemical response of Guai on various modified GCE

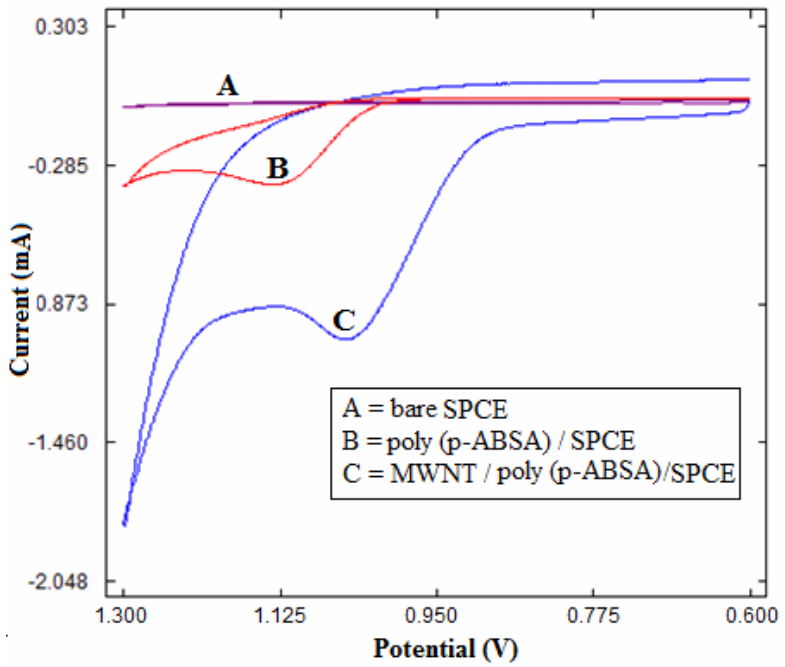

Figure 6.4 Cyclic voltammmograms of 1×10^{-3} M Guai at (a) bare SPCE (b) poly (p-ABSA) modified SPCE and (C) MWNT / poly (p-ABSA) modified SPCE

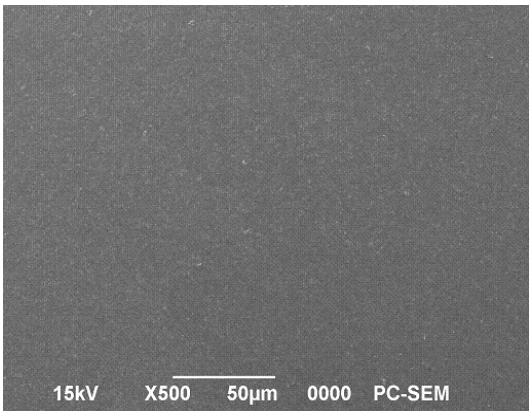

(a)

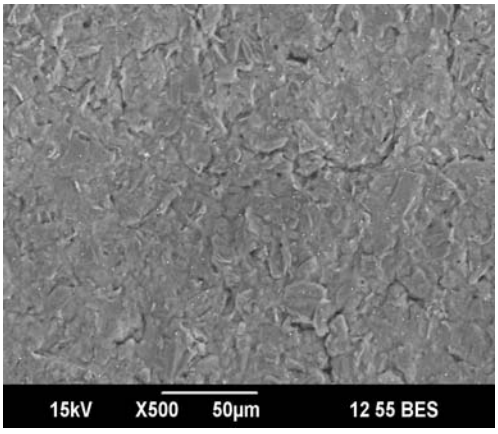

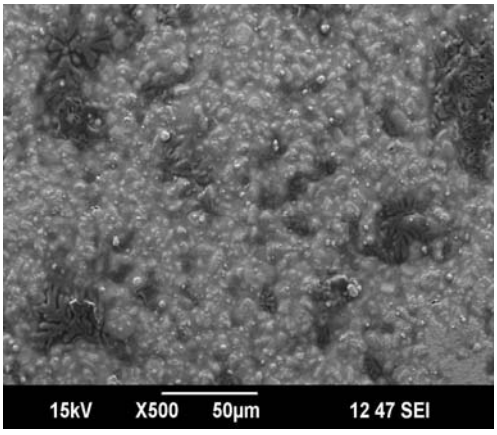

(b) (c)

Figures 6.5: SEM images of (a) bare GCE (b) poly (p-ABSA)/GCE and (c) MWNT/poly (p-ABSA)/GCE

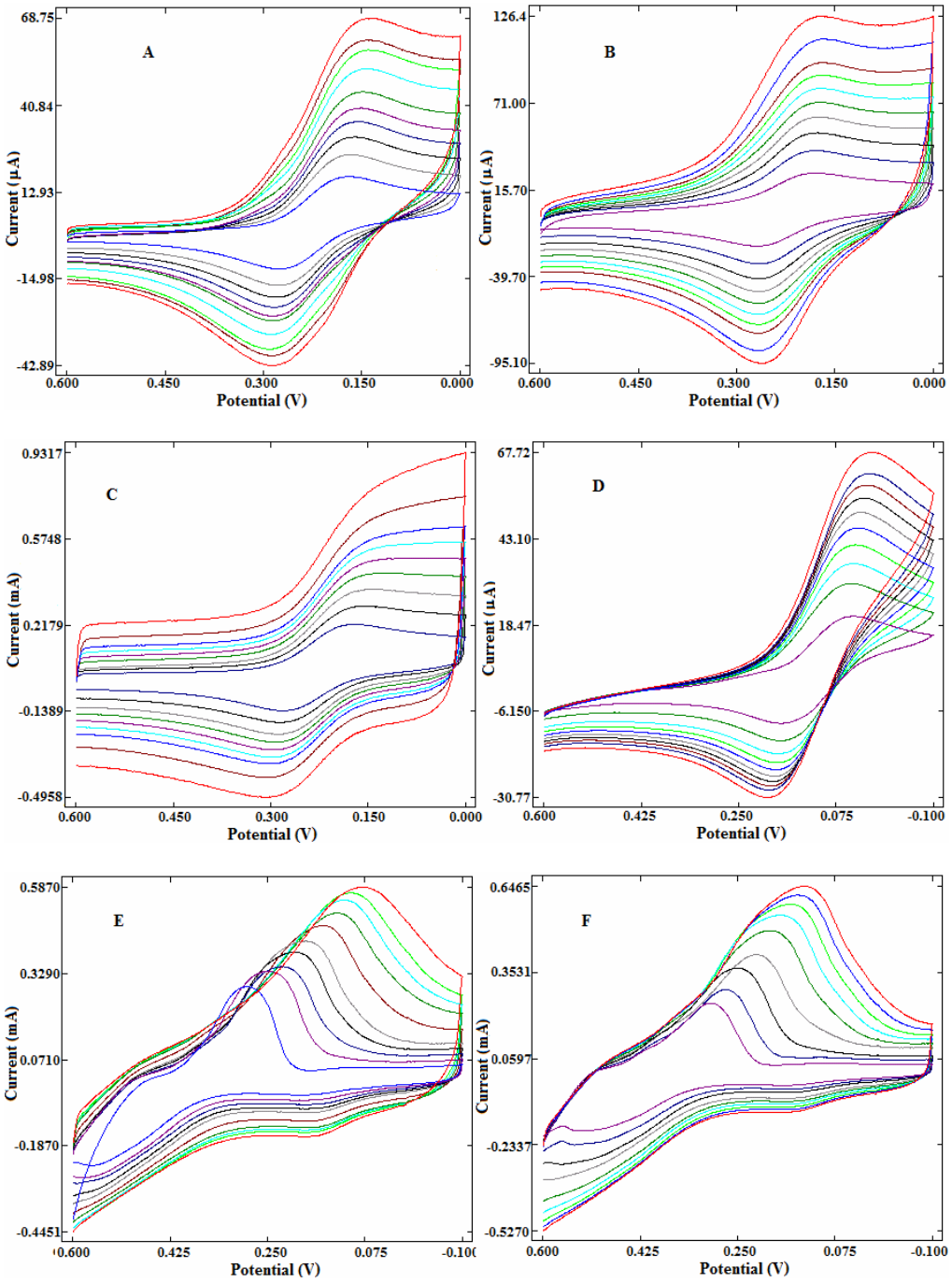

Figure 6.6 Surface area studies at (A) bare GCE (B) poly (p-ABSA)/GCE (C) MWNT/ poly (p-ABSA)/GCE (D) bare SPCE (E) poly (p-ABSA)/SPCE (F) MWNT / poly (p- ABSA) / SPCE

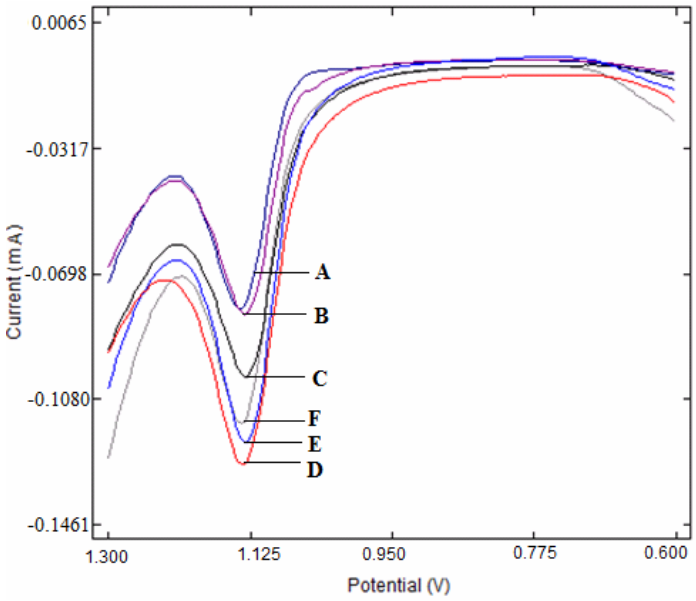

Figure 6.7 Differential pulse voltammograms of Guai at different polymerization cycles (A) 10 cycles (B) 20 cycles(C) 30 cycles(D) 40 cycles(E) 50 cycles(F) 60 cycles

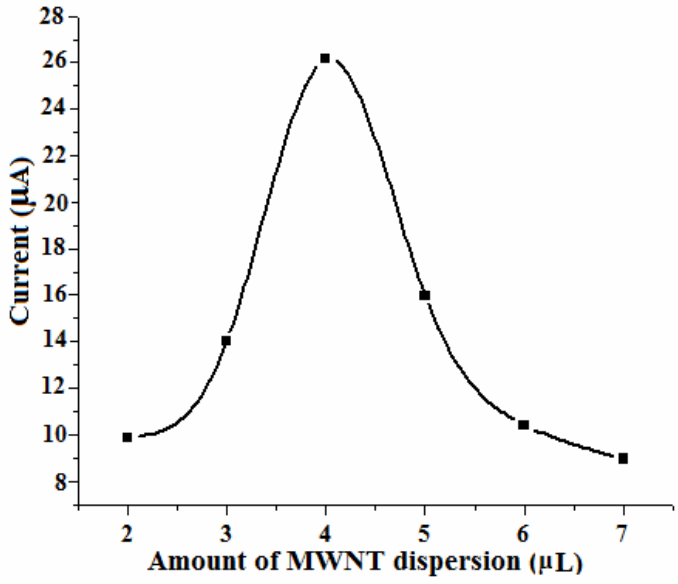

Figure 6.8 Amount of MWNT dispersion

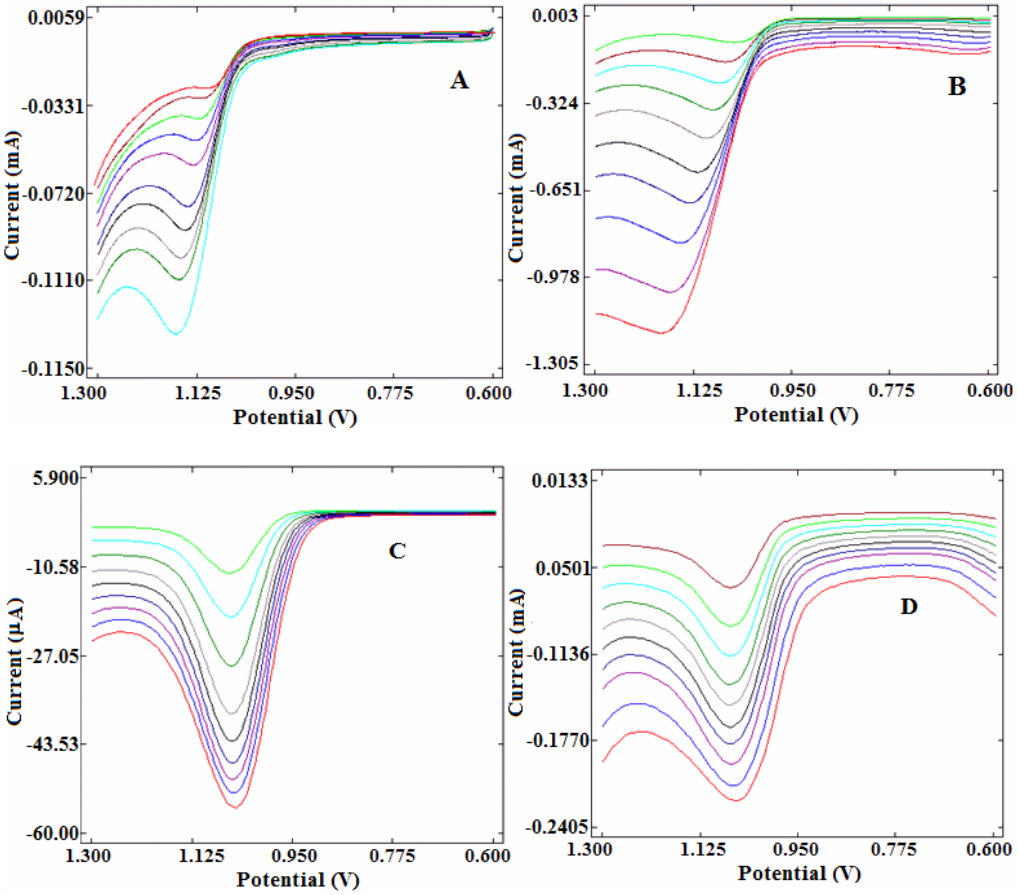

Figure 6.9 Overlay of linear sweep voltammograms of 1×10^{-3} M Guai at (A) poly (p-ABSA) modified GCE and (B) MWNT / poly (p-ABSA) modified GCE in 0.1 M HCl at different scan rates and Overlay of square wave voltammograms of 1×10^{-3} M Guai at (C) poly (p-ABSA) modified GCE and (D) MWNT / poly (p-ABSA) modified GCE in 0.1 M HCl at different scan rates.

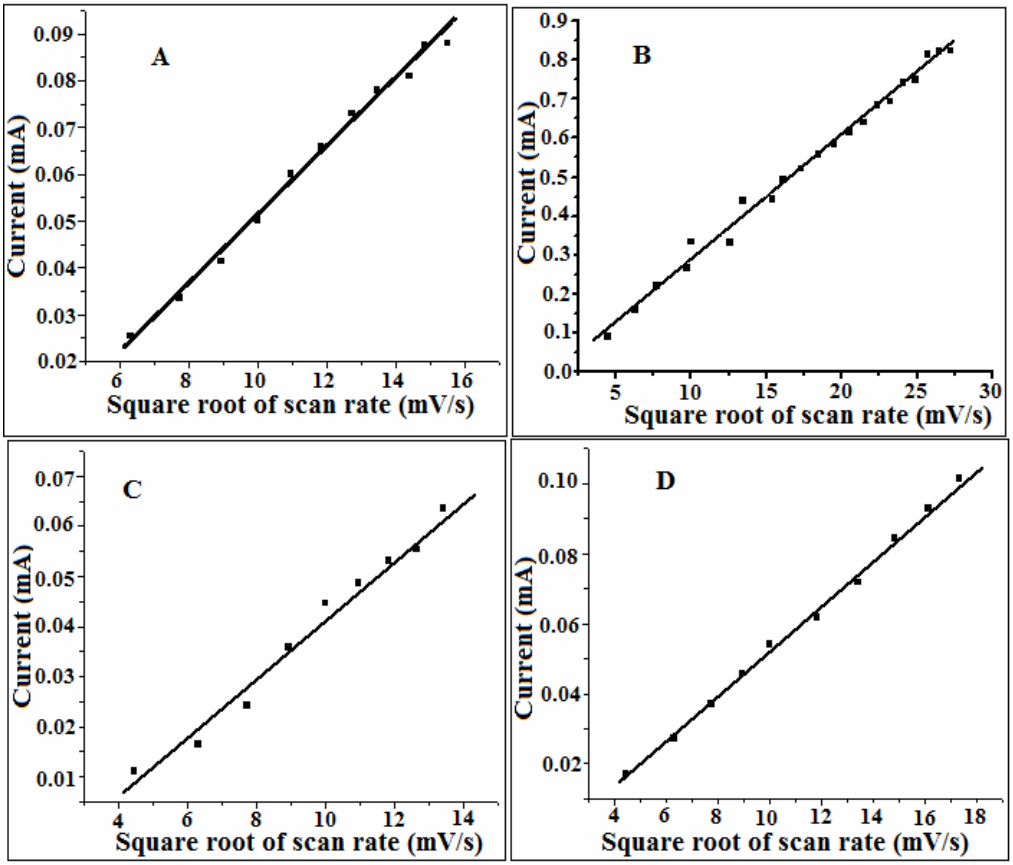

Figure 6.10 The plot of peak currents as a function of the square root of scan rates from linear sweep voltammetric studies of 1×10^{-3} M Guai at (A) poly (p-ABSA) modified GCE and (B) MWNT / poly (p-ABSA) modified GCE and square wave voltammetric studies of 1×10^{-3} M Guai at (C) poly (p-ABSA) modified GCE and (D) MWNT /poly (p-ABSA) modified GCE.

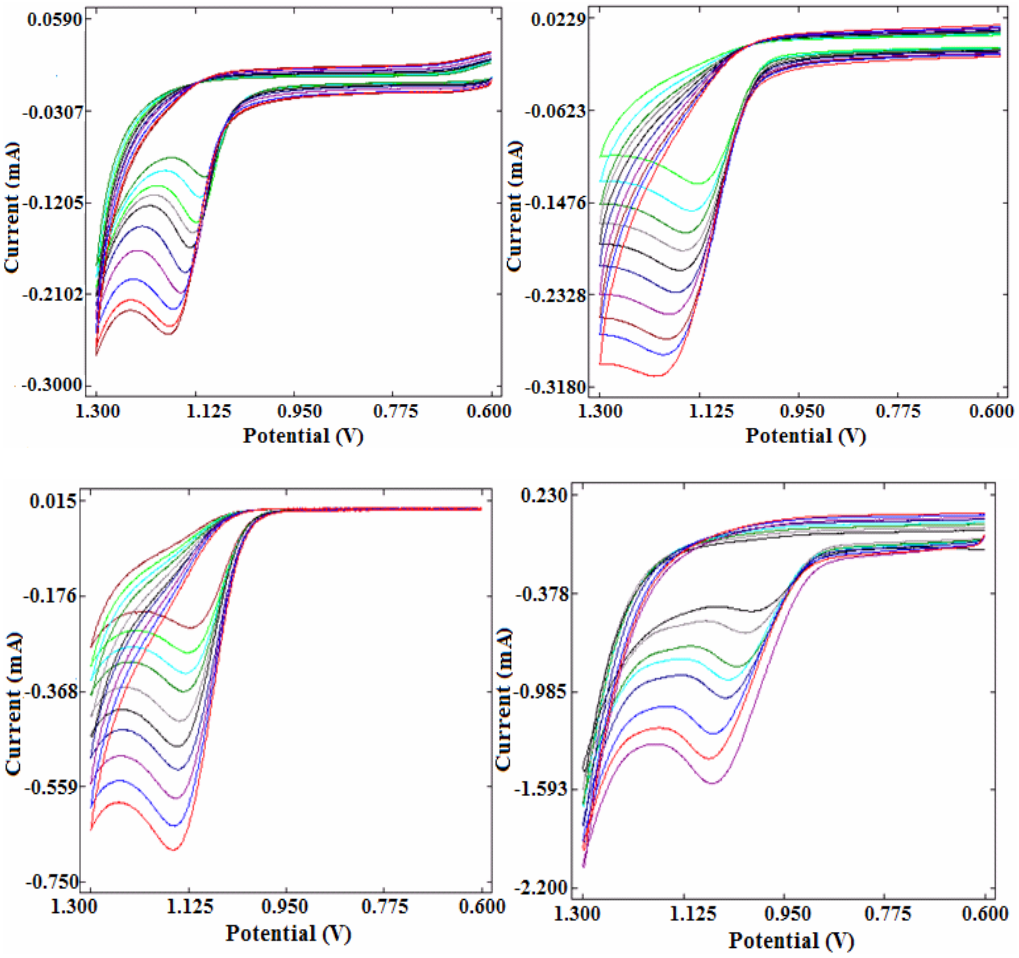

Figure 6.11 Overlay of cyclic voltammograms of Guai at (A) poly (p-ABSA) modified GCE (B) MWNT/poly (p-ABSA) modified GCE (C) poly (p-ABSA) modified SPCE and (D) MWNT / poly (p-ABSA) modified SPCE in 0.1 M HCl at different scan rates.

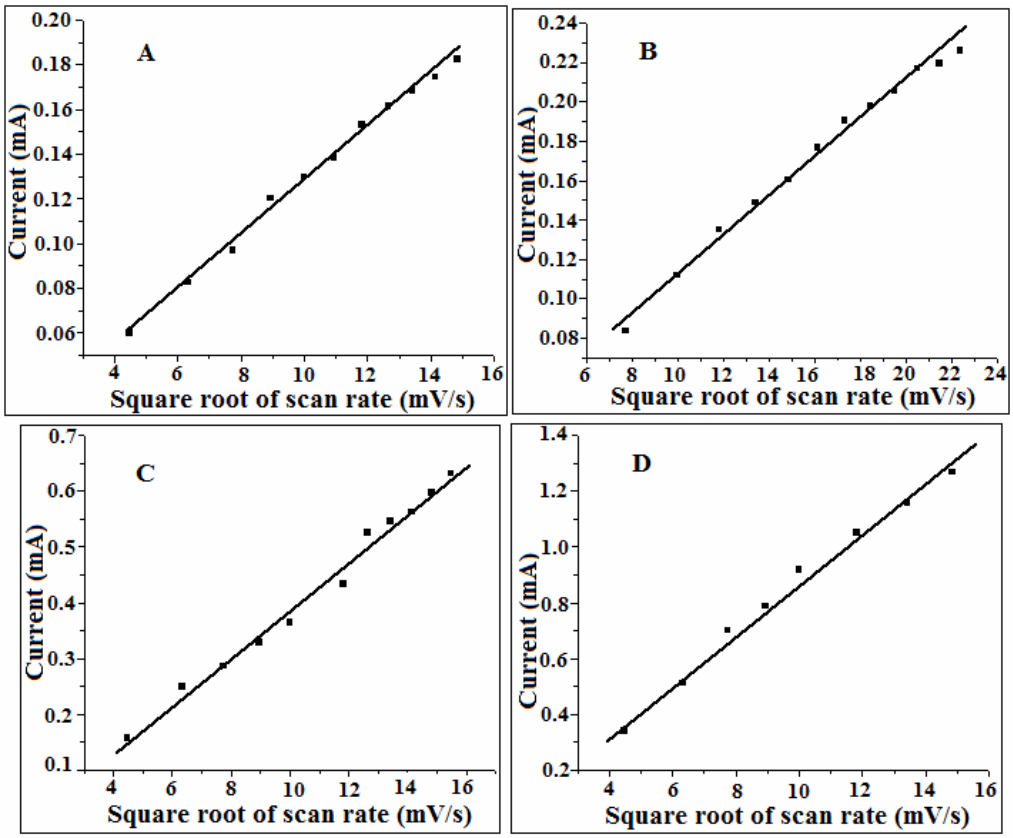

Figure 6.12 The plot of peak currents as a function of the square root of scan rates from cyclic voltammetric studies of Guai at (A) poly (p-ABSA) modified GCE (B) MWNT/poly (p-ABSA) modified GCE (C) poly (p-ABSA) modified SPCE and (D) MWNT / poly (p-ABSA) modified SPCE in 0.1 M HCl at different scan rates.

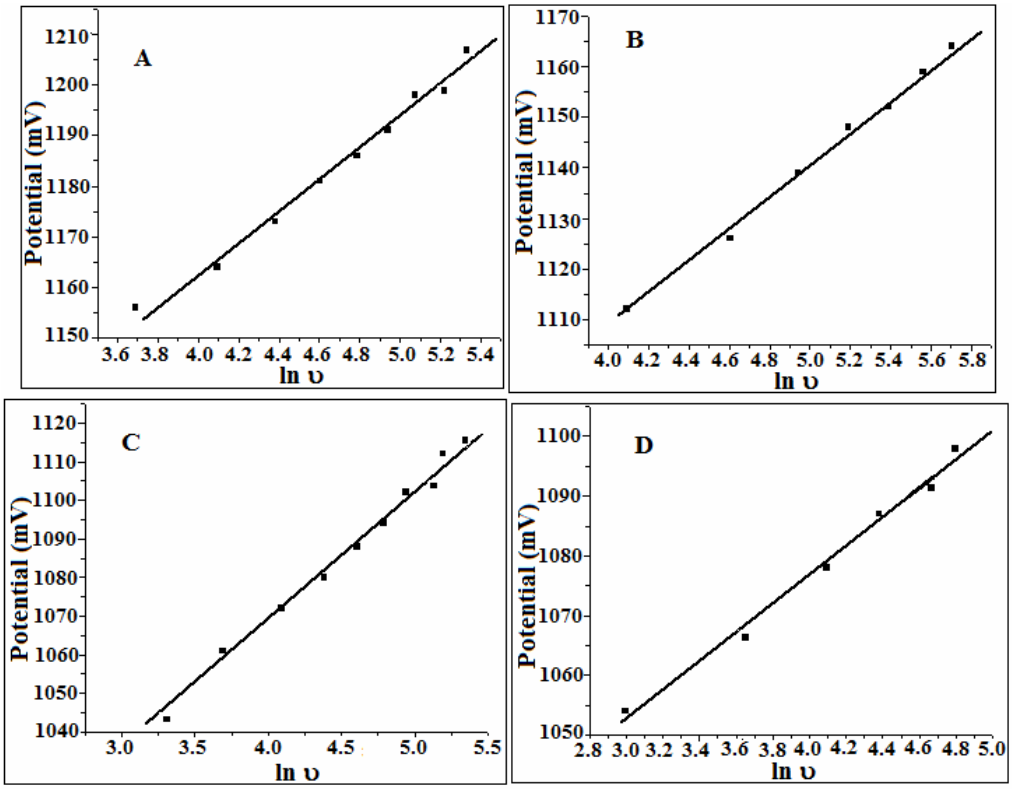

Figure 6.13 Plot of peak potential against ln (scan rate) from cyclic voltammetric studies of Guai at (A) poly (p-ABSA) modified GCE (B) MWNT/poly (p-ABSA) modified GCE (C) poly (p-ABSA) modified SPCE and (D) MWNT / poly (p-ABSA) modified SPCE in 0.1 M HCl at different scan rates.

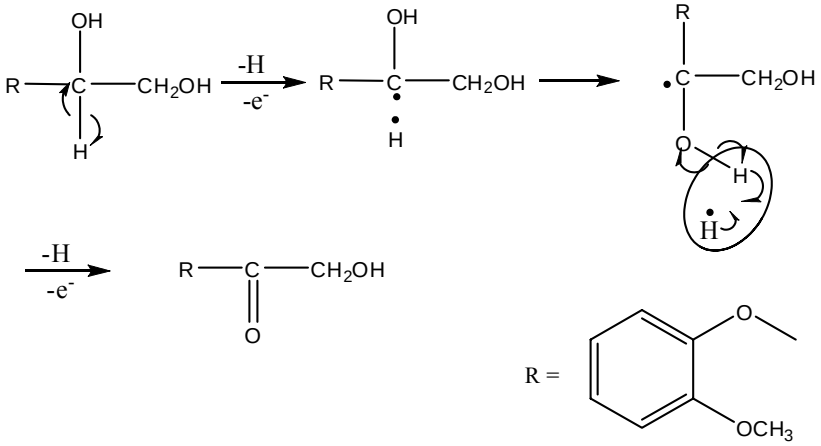

Figure 6.14 Reaction Mechanism

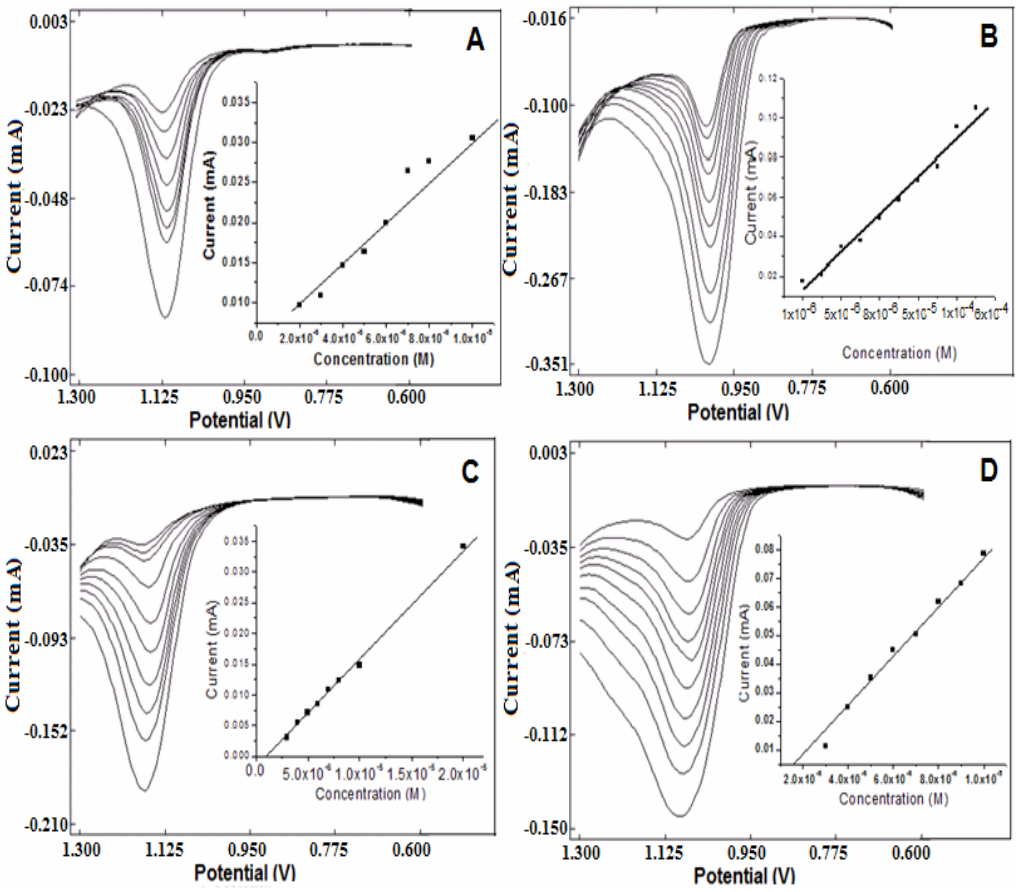

Figure 6.15 Differential pulse voltammograms of Guai at different concentrations on (A) poly (p-ABSA) modified GCE and (B) MWNT / poly (p-ABSA) modified GCE and square wave voltammograms of Guai at different concentrations on (C) poly (p ABSA) modified GCE and (D) MWNT / poly (p-ABSA) modified GCE. Insets are the plot of peak currents as a function of concentration of Guai.

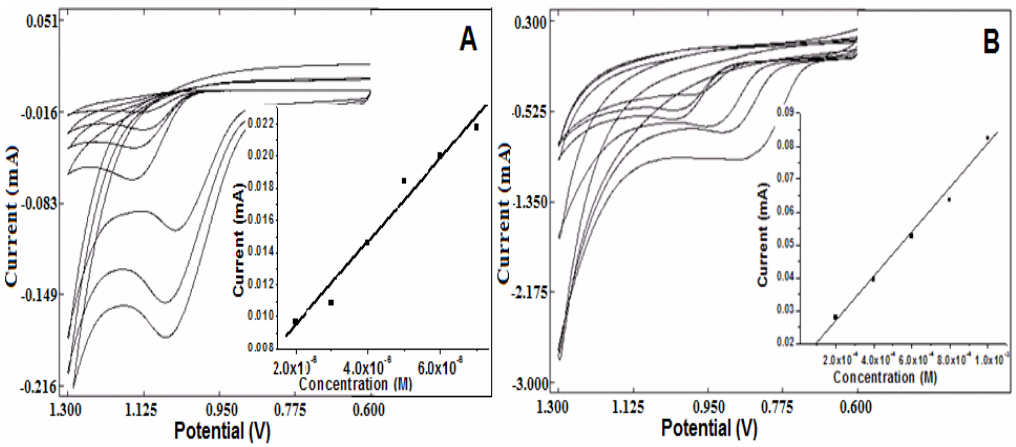

Figure 6.16 Cyclic voltammograms of Guai at different concentrations on (A) poly (p-ABSA) modified SPCE and (B) MWNT / poly (p-ABSA) modified SPCE. Insets are the plot of peak currents as a function of concentration of Guai.

Chapter 7

DEVELOPMENT OF SENSOR FOR CEPHALEXIN

Contents

7.1 Introduction
7.2 Preparation of AuNP modified GCE
7.3 Electrochemical behaviour of Ceph
7.4 Evidences of electrode modification
7.5 Performance characteristics of the developed sensor
7.6 Amperometric response of the AuNP/GCE
7.7 Analytical applications
7.8 Conclusions

This chapter discusses the fabrication of an electrochemical sensor for Cephalexin (Ceph) based on a gold nanoparticle (AuNP) modified glassy carbon electrode (GCE). The electrochemical response of the AuNP film towards the oxidation of Ceph at 0.1 M NaOH was studied by means of square wave voltammetry (SWV). Electrochemical parameters of the oxidation of Ceph on the modified electrode were analyzed. The detection limit of Ceph was found to be 1.333×10^{-8} *M. To evaluate the application potential of the developed sensor, it was successfully applied to determine Ceph in commercial formulation and body fluid.*

7.1 Introduction

Cephalexin ((6*R*,7*R*)-7-{[(2*R*)-2-amino-2-phenylacetyl]amino}-3-methyl-8-oxo-5-thia-1-azabicyclo[4.2.0]oct-2-ene-2-carboxylic acid)(Ceph), (Figure **7.1**) is an effective broad spectrum antibiotic which have a structure similar to that of the penicillins. It is a semi-synthetic antibiotic of the cephalosporins group, which are mainly used in the treatment of various bacterial infections, caused by gram positive and gram negative microorganisms [259]. It interfers the bacteria's cell wall formation and hence ruptures the cell wall and kills the bacteria. Cephalosporins are a series of antibiotics containing a β lactam ring

fused to a six-membered ring with a sulfur atom. Ceph has been used in the treatment of urinary tract infections, respiratory tract infections (including sinusitis, otitis media, pharyngitis, tonsillitis, pneumonia, and bronchitis), skin and soft tissue infections.

Several methods have been reported for Ceph determination. A.P. Argekar et al developed a reverse phase high performance liquid chromatographic (RPHPLC) method for the simultaneous determination of Ceph and Carbocisteine from capsules, using 0.025 M monobasic sodium phosphate : acetonitrile (87 : 13, v/v) as a mobile phase, and a C_8 Shodex column as the stationary phase [260]. A colorimetric method has been developed for the estimation of Ceph in capsules by P. Priyanka and P. Suresh [261]. A.B.C. Yu et al have described a fluorescence method for the determination of Ceph [262]. Spectrofluorometric determination of Ceph was reported by D. R. El-Wasseef [263]. T. Nakagawa et al have developed a high speed liquid chromatographic (HSLC) method for the determination of Ceph in human plasma and urine [264]. This method involves the HSLC separation on a bonded reverse phase column utilizing a mobile phase of methanol-water containing acetic acid. D. Zendelovska et al measured the concentration of cefaclor and Ceph simultaneously in blood plasma after protein precipitation, using a newly developed RPHPLC method on C_8 colum [265]. J. H. Mtindez et al reported the differential pulse polarographic determination of Ceph based on the catalytic pre wave of Nickel (II) [266]. P. C. Falc et al have reported a comparative Study on the Determination of Ceph in its Dosage Forms by Spectrophotometry and HPLC with UV-vis Detection [267]. Y. Chen et al used the heated glassy carbon electrode (HGCE) to hydrolyze and detect the Ceph without oil/water bath setup [268]. Determination of Ceph was carried out by detecting degradation products using square wave voltammetry (SWV).

O. Chailapakul et al reported the determination of glutathione and Ceph using high-quality boron-doped diamond thin-film electrodes [269].

Carbon electrodes are characterized by their high chemical inertness as well as low oxidation rate in addition to small gas and liquid permeability [270]. These properties render the GCE to be a suitable substrate material for the loading of various metals and polymer thin films onto its surface aiming to improve its electrocatalytic activity toward the electrochemical reactions [271–273]. During the last two decades, interests have focused on nanoscaled materials and their use in analytical chemistry because of their specific physico-chemical properties for a wide range of applications including electronics, optics, catalysis and biological sensors. When used for electroanalysis, nanoparticles can display many unique advantages over macroelectrodes such as enhancement of mass transport, catalysis, high effective surface area, and control over electrode microenvironment. AuNP are of wide interest as they display unusual optical, electronic, magnetic, and electrocatalytic properties from the bulk material [274]. Therefore AuNP have been extensively studied in electrochemistry [275–281]. AuNP can be prepared using different chemical methods, such as direct electrodeposition, deposition-precipitation, sol-gel technique, impregnation, coprecipitation, metal organic-chemical vapor deposition, incipient wetness and dip-coating [282-287].

This chapter deals with the electrodeposition of AuNP on the surface of GCE and the investigation of electrochemical bahaviors of Ceph at the modified electrodes. Out of the voltammetric techniques, SWV only produces an oxidation peak of Ceph. At bare GCE, no voltammetric response was obtained. But on AuNP modified GCE, a well defined and sensitive oxidation peak was obtained at -992 mV for Ceph. AuNP modified GCE was used for

the voltammetric determination of Ceph in pharmaceutical dosage form and in spiked urine sample.

7.2 Preparation of AuNP modified GCE

At first, the GCE was cleaned as explained in section 2.4 of Chapter 2. The AuNP modified GCE was prepared by electrochemical deposition. The detailed procedure for the fabrication of AuNP modified GCE is given in section 2.5.5 of Chapter 2. The electrochemical deposition of AuNP on the GCE surface was conducted in a three electrode cell with GCE as the working electrode, Ag/AgCl as the reference electrode and platinum wire as the counter electrode. Electrodeposition was carried out by cyclic voltammetry (CV) (between 1.3 V to 0 V at 0.1 V/s) in 0.05 M H_2SO_4 solution containing 1 mM $HAuCl_4$.

During the electrodeposition process, an anodic peak at 1112 mV and a cathodic peak at 793 mV were observed (Figure **7.2**). The oxidation and reduction peak currents increases with an increase in the number of voltammetric scans, indicating that an AuNP film has been formed on the surface of GCE. After modification, the AuNP/GCE was carefully rinsed with millipore water and then stored in air.

7.3 Electrochemical behaviour of Ceph

Stock solution of Ceph was prepared as described in section 2.6 of Chapter 2. Standard solutions of the analyte were prepared by serial dilution of stock solution with the supporting electrolyte (0.1 M NaOH). 10 mL of 0.1 M NaOH containing required volume of stock solution, was added to the electrochemical cell. Before experiment, the solution was purged with nitrogen for 3 minutes. Then square wave voltammograms from -400 to -1300 mV, at 100 mV/s were recorded.

Electrochemical behavior of Ceph at various modified electrode were investigated by Square wave voltammetric technique. Figure **7.3** showed that there is no voltammetric response at bare GCE. In order to get an electrochemical response of Ceph, we tried various chemical modifications on GCE. At the AuNP modified GCE, the oxidation peak appeared at -992 mV, and the peak current has increased to 26.1112 μA. This clearly depicted the electrocatalytic activity of nanoparticle film on the voltammetric determination of Ceph.

7.4 Evidences of electrode modification

7.4.1 SEM images

The surface morphology of the electrodes was characterized by scanning electron microscopy (SEM). As shown in Figure **7.4**, the surface morphology of AuNP modified GCE was significantly different from that of bare GCE.

7.4.2 Surface area study

Surface area study gave a strong evidence for the effective modification of GCE with AuNP film. 2 mM $K_3Fe(CN)_6$ was taken as a probe to measure the effective surface areas of both bare GCE and AuNP /GCE by CV at different scan rates [167] (Figure **7.5**). The regression equations obtained from SWV analysis for the bare and modified electrodes are: $I_p = 1.357\ \nu^{½} - 3.462$ (r^2=0.997, ν in mV/s, I_p in μA) and $I_p = 2.454\ \nu^{½} + 6.401$ (r^2=0.996, ν in mV/s, I_p in μA) respectively. From the slope of I_p vs. $\nu^{1/2}$ plot, the areas of bare GCE and AuNP /GCE were estimated and was found to be 0.0609 cm^2 and 0.1655 cm^2 respectively. A higher peak current value also illustrated an increase in the electroactive surface area for the AuNP/GCE, mainly due to smaller size of AuNP distributed on the surface of GCE, which increased the large local rates of mass transport to the AuNP/GCE.

7.5 Performance characteristics of the developed sensor

The performance of the developed sensor depends on many factors including effect of the supporting electrolyte, effect of film thickness, effect of scan rate, range of linear response, detection limit and interference study.

7.5.1 Choice of supporting electrolyte

The effect of the supporting electrolyte on the voltammetric behavior of Ceph was also determined, which included 0.1 M solutions of KNO_3, HCl, NaOH, NaCl, phosphate buffer and acetate buffer. A well defined voltammogram was obtained in 0.1 M NaOH. Therefore 0.1 M NaOH was chosen as the supporting electrolyte for further experiments.

7.5.2 Effect of film thickness

The influence of film thickness on the anodic peak current of Ceph was studied. It was found that the anodic peak current of Ceph (1×10^{-3} M) is dependent on the thickness of AuNP film (Figure **7.6**). As shown in the Figure, when the scan cycles were 40, the anodic peak current reached its maximum value. But when the scan cycles were more than 40, the current begins to fall. This may be due to the decreased electron transfer rate of Ceph with an increase in film thickness. Also, the repeatability and stability for the film modified electrode were poor when the voltammetric sweeping segments were less than 40. Film thickness obtained with 40 segment sweeping was selected as the optimal condition in the further experiments.

7.5.3 Effect of Scan rate

The effect of scan rate on the electrochemical response of 1×10^{-3} M Ceph was shown in Figure **7.7**. The anodic peak currents increased gradually along with the increase of the scan rate. A good linearity between the square

root of scan rate and anodic peak current was obtained within the range of 20 to 400 mV/s (Figure **7.8**) and the linear regression equation is given as I_p =1.644 $\nu^{1/2}$ - 9.455 (r^2=0.998, ν in mV/s, I_p in μA). This confirms the electrooxidation of Ceph to be diffusion controlled.

In this experiment, the relationship between the oxidation peak potential and scan rate can be described as following: E = 27.15 ln ν + 868.5, (r^2 = 0.986) (Figure **7.9**). According to Laviron's theory [169], the n_a was calculated to be 1.93 which indicated that two electrons are involved in the oxidation process of Ceph on the film electrode. The electrochemical reaction process for Ceph at AuNP/GCE can therefore be summarized as in Figure **7.10**.The anodic peak generated for the Ceph may be due to the oxidation of amino group present in Ceph to the hydroxyl amine.

The dependence of logarithm of the peak current of 1×10^{-3} M Ceph in 0.1 M NaOH on the logarithm of the scan rate was linear (Figure **7.11**). Linear relationship obtained is log I = 0.675 log ν - 0.383 (r^2=0.997). The slope of 0.6 is close to the theoretically expected value of 0.5 for a diffusion controlled process [168].

7.5.4 Calibration curve

To study the concentration range of Ceph that can be determined with AuNP/GCE, a series of SWVs were recorded at various concentrations of Ceph (Figure **7.12)**. Under the optimum instrumental conditions, when the concentration of Ceph changed from 1.0×10^{-6} to 1.0×10^{-5} M, the anodic peak current and Ceph concentration declared linear relationship (Figure **7.13**). The linear regression equation was I=1×10^{-6} C + 0.897(r^2=0.998, C in M) with the detection limit of 1.333×10^{-8} M.

A comparison of the reported works with the present work is tabulated in Table **7.1**. Lowest detection limit was obtained using the present method compared to the other reported works.

Regeneration and reproducibility are two important characteristics for the modified electrode, which should be investigated. The same modified GCE was used for five times successive measurements of 1×10^{-3} M Ceph. After each measurement, the surface of the AuNP/ GCE was regenerated by successively cycling between -400 mV and -1300 mV (vs. Ag/AgCl) in 0.1 M NaOH for six cycles. The relative standard deviation (RSD) of the anodic peak current was 3.3 %, which suggested good regeneration and reproducibility of the modified electrode. When using three different electrodes, the RSD for five measurements of 1×10^{-3} M Ceph was 1.9 %. The response of the modified electrode retained 97 % of its initial response value after 2 weeks. These results indicate that AuNP/ GCE has good stability and reproducibility.

7.5.5 Interference study

Analytical selectivity is one of the important parameters affecting the accuracy of the analysis. In order to evaluate the selectivity of the proposed method for the determination of Ceph, the influence of various foreign species on the determination of Ceph was investigated. As can be seen from Table **7.2** upto hundred fold excess concentrations of the listed foreign species other than ascorbic acid did not interfere in the anodic response of 1×10^{-3} M Ceph (deviation below 5 %), indicating the good selectivity of the sensor.

7.6 Amperometric response of the AuNP/GCE

AuNP modified GCE was also used for the amperometric determination of Ceph. Amperometric experiments were performed with a BAS Epsilon electrochemical analyzer (Bioanalytical system, USA) interfaced to a PC. A

conventional three electrode system, including working electrode, counter electrode and reference electrode was employed. Working electrode used was AuNP modified GCE, counter electrode used was platinum wire and Ag/AgCl was used as the reference electrode. A magnetic stirrer provided the convective transport during the amperometric measurement.

The amperometric responses of AuNP modified GCEs were studied at the applied potential of -1050 mV vs. Ag/AgCl on successive addition of Ceph, which are 0.1, 0.2, 0.3, 0.4, 0.5, 0.6, 0.7, 0.8 and 0.9 mM, respectively, as shown in Figure **7.14**. Experiments showed that the resulting Ceph sensor exhibited a rapid and sensitive response to the change of Ceph concentration. The response current increased with increasing the concentration of Ceph in the range from 0.1 to 0.9 mM and reached a saturation value at high Ceph concentration.

The calibration curve under the optimized experimental conditions was shown in Figure **7.15**. A good linear relation was observed in the range from 0.1 to 0.9 mM Ceph with a correlation coefficient of 0.991. Linear regression equation was I = 7706 C + 3.712 (C in mM) with the detection limit of 7.33 μM.

7.7 Analytical applications

The analytical utility of the developed sensor in the determination of Ceph in pharmaceutical preparations and in urine sample was investigated.

7.7.1 Determination of Ceph in pharmaceutical formulation

Commercial formulation containing Ceph, "Citaceph tablet" was analysed by SWV. The detailed procedure for the determination is given in section 2.8.3 of Chapter 2. The obtained results are shown in Table **7.3**. The

results obtained are in good agreement with the declared Ceph content and showed a high degree of precision.

The results were compared with those obtained by the standard method [141]. The results show that there is a good agreement between the Ceph content determined by the developed method and the standard method.

7.7.2 Determination of Ceph in urine sample

In order to test the applicability of the proposed method, several aliquots of Ceph were spiked into urine samples in different proportion to get various concentration of Ceph. The SW Voltammograms were recorded applying the optimal conditions for their analytical determination. Recoveries lie in the range of 97-101 % as can be seen from Table **7.4**.

7.8 Conclusions

In summary, a square wave voltammetric method has been developed for the determination of Ceph using AuNP/GCE, evaluated the electrochemical performance and achieved a sensitive determination of Ceph in nanomolar concentrations. A lower detection limit of 13.33 nM was obtained on the modified electrode. The electrocatalytic nature of AuNP/GCE for the determination of Ceph is evident from the favorable reduction in oxidation overpotential of Ceph. It is also shown that the developed sensor can be used for the determination of Ceph in human urine and in pharmaceutical products.

Table 7.1 Comparison of the developed method with other reported works for the determination of Ceph

Method adopted	Detection limit
RP- HPLC method [260]	20.00 µg/mL
colorimetric method [261]	0.140 µg/mL
fluorescence method [262]	0.010 µg/mL
Spectrofluorometry [263]	7.760 ng/mL
High speed liquid chromatography [264]	0.500 µg/mL
High-performance liquid chromatography [265]	0.250 mg/mL
Spectrophotometry and HPLC with UV-vis Detection [266]	1.042 µg/mL
Differential pulse polarography [267]	0.880 µg/mL
The heated glassy carbon electrode (HGCE) using SWV [268]	52.10 ng/mL
BDD electrodes by cyclic voltammetry [269]	1.737 mg/mL
Present method	4.630 ng/mL

Table 7.2 Influence of 10^{-1} M foreign species on the anodic peak current of 1×10^{-3} M Ceph

Foreign species	Signal Change,%
Urea	+ 3.75
Glucose	- 0.978
Lactose	+ 2.610
Na^+	- 0.567
K^+	- 0.430
Cl^-	- 0.567
SO_4^{2-}	- 0.430
Ascorbic acid	- 39.0

Table 7.3 Determination of Ceph in tablets

Sample	Declared amount (mg/tablet)	Method adopted	Found* (mg/tablet)	S.D*	C.V*
Citaceph (Citadel Aurobindo Biotech Ltd.)	250	AuNP/GCE	247	1.60	0.41
		Standard Method	251	2.45	1.05

*Average of six replicates

Table 7.4 Determination of Ceph in urine sample

Ceph Added (M)	Ceph Found (M)	Recovery %
2.00×10^{-6}	1.94×10^{-6}	97.0
4.00×10^{-6}	4.05×10^{-6}	101
6.00×10^{-6}	5.90×10^{-6}	98.3

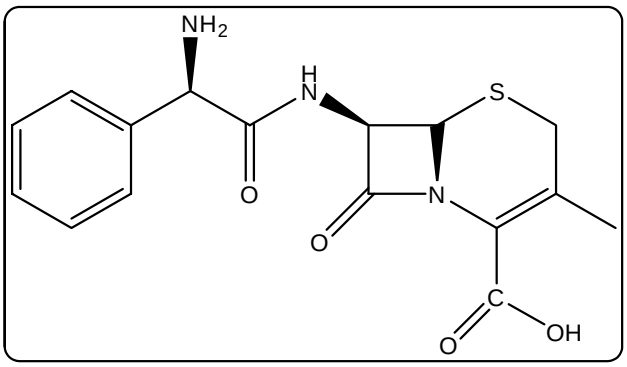

Figure 7.1 Structure of Ceph

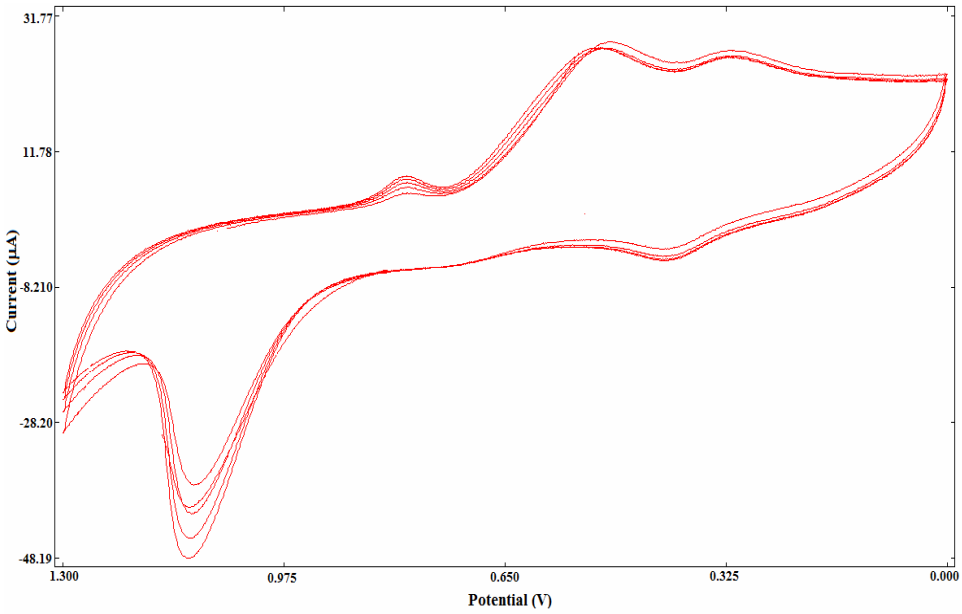

Figure 7.2 Electrodeposition of AuNP

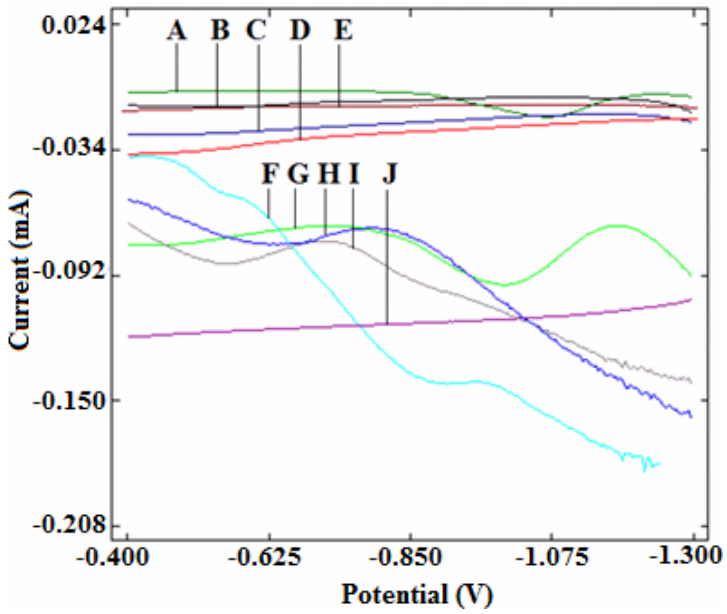

Figure 7.3 Electrochemical response of Ceph on various electrodes (A) Bare gold electrode (B) MWNT/GCE (C) Platinum nano particle/GCE (D) Poly p-toluenesulphonic acid/GCE (E) Bare GCE (F) Poly L-cysteine/GCE (G) AuNP/GCE (H) Poly o-phenylenediammine/GCE (I) Manganese porphyrin/GCE (J) Copper nano particle/GCE.

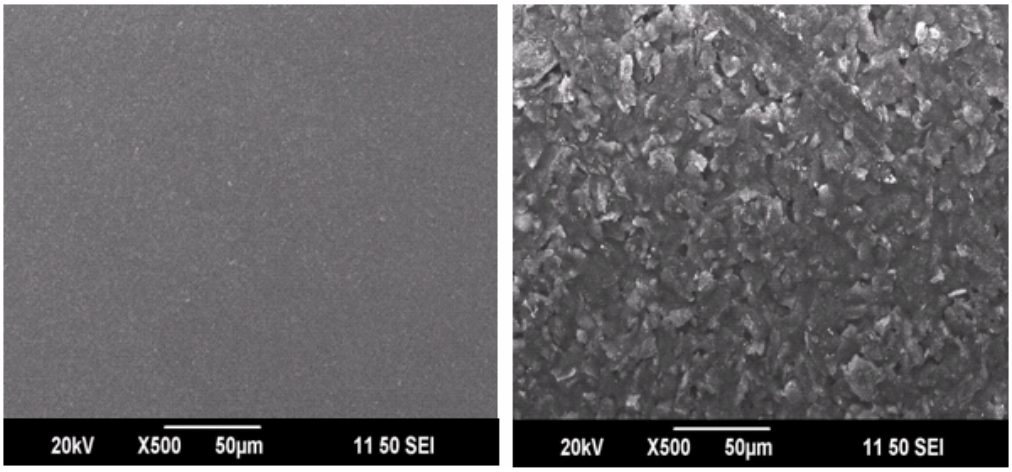

(a) (b)

Figure 7.4 SEM images of (a) bare GCE (b) AuNP modified GCE

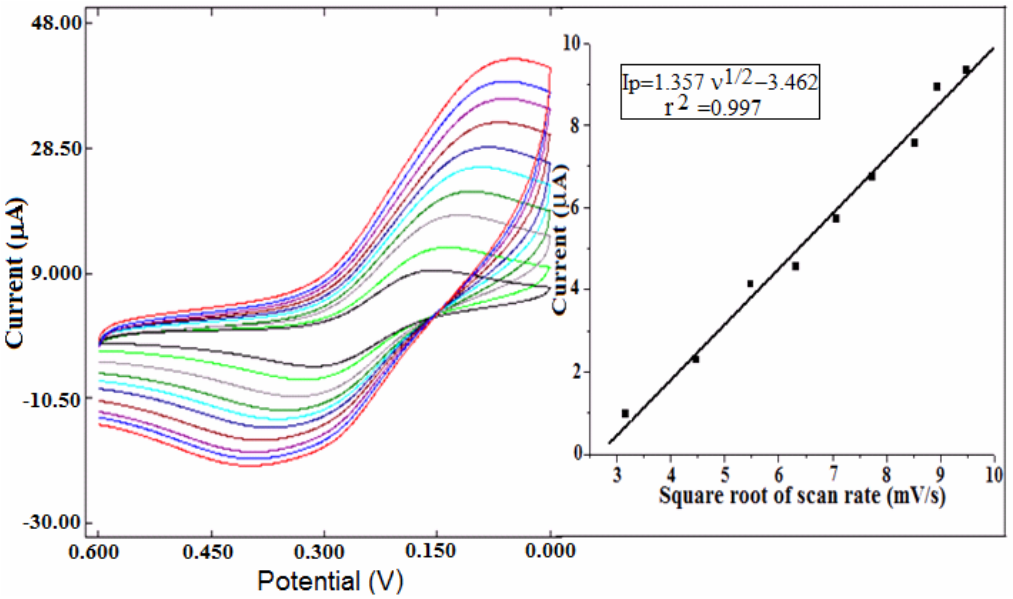

(a)

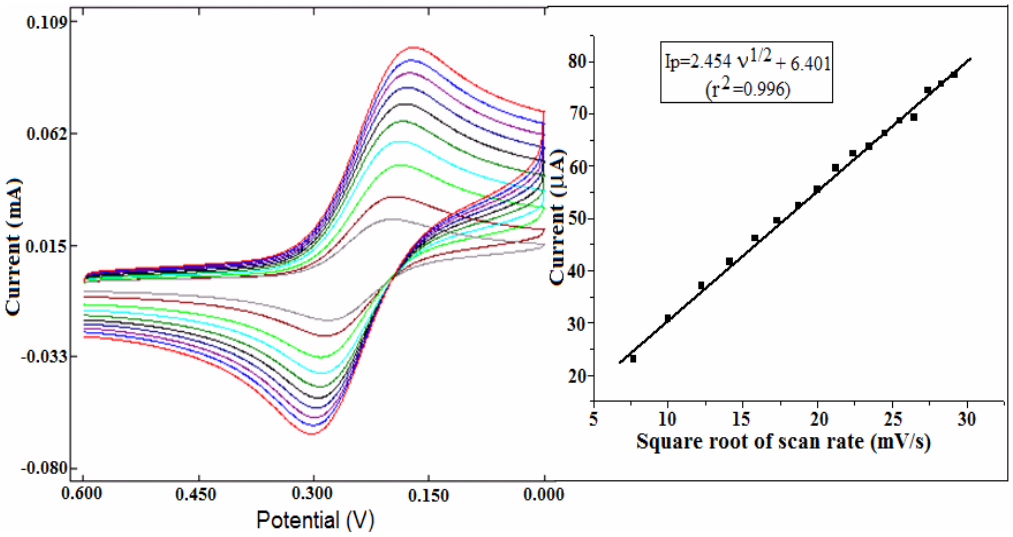

(b)

Figure 7.5 Surface area studies at a) bare GCE and b) AuNP modified GCE and inset are plot of peak currents as a function of the square root of scan rates

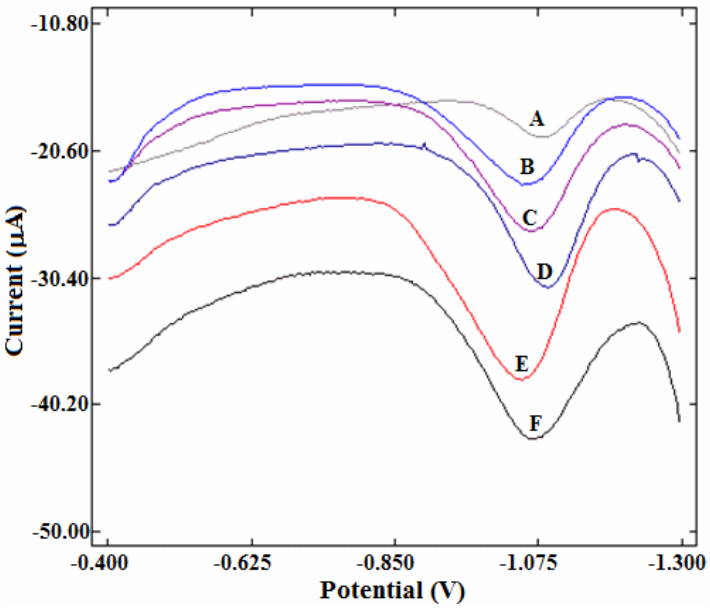

Figure 7.6 Square wave voltammograms of Ceph at different electrodeposition cycles (A) 10 cycles (B) 20 cycles (C) 30 cycles (D) 50 cycles (E) 40 cycles (F) 60 cycles

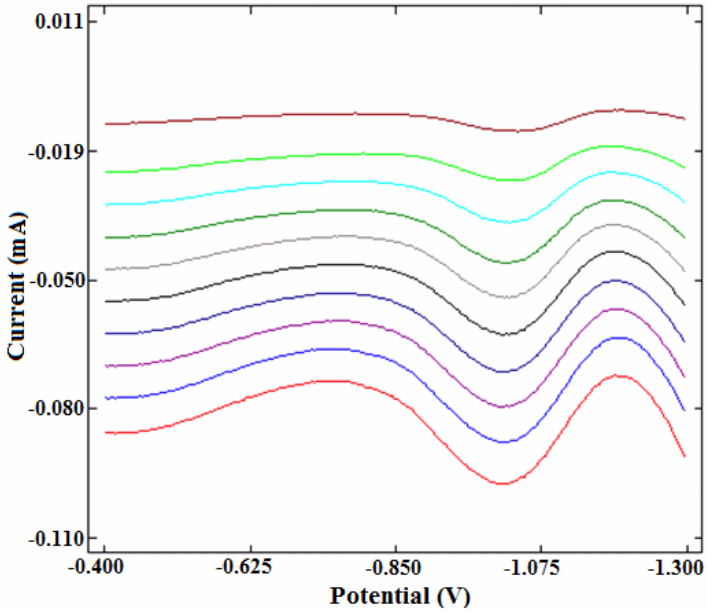

Figure 7.7 Overlay of square wave voltammograms of Ceph at different scan rates 40, 80, 120, 160, 200, 240, 280, 320, 360, 400 mV/s in 0.1 M NaOH

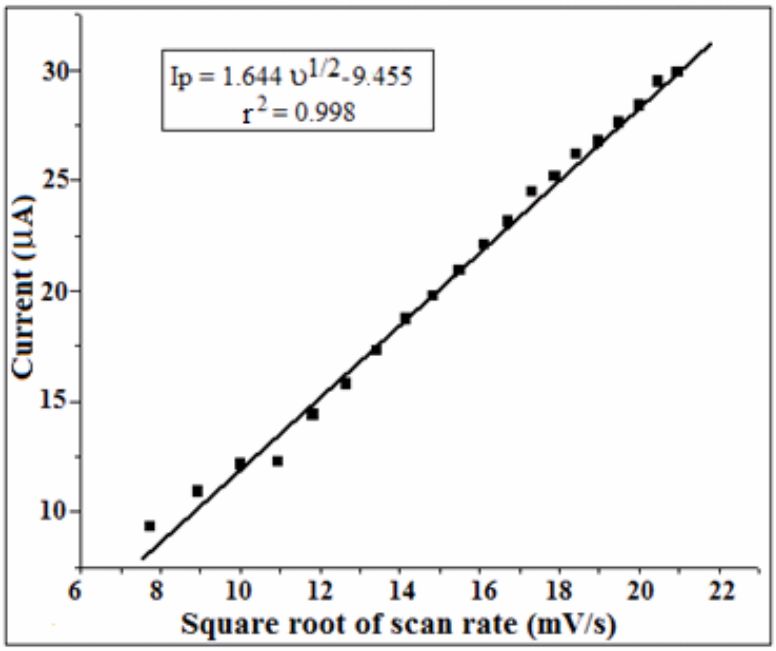

Figure 7.8 Influence of scan rate

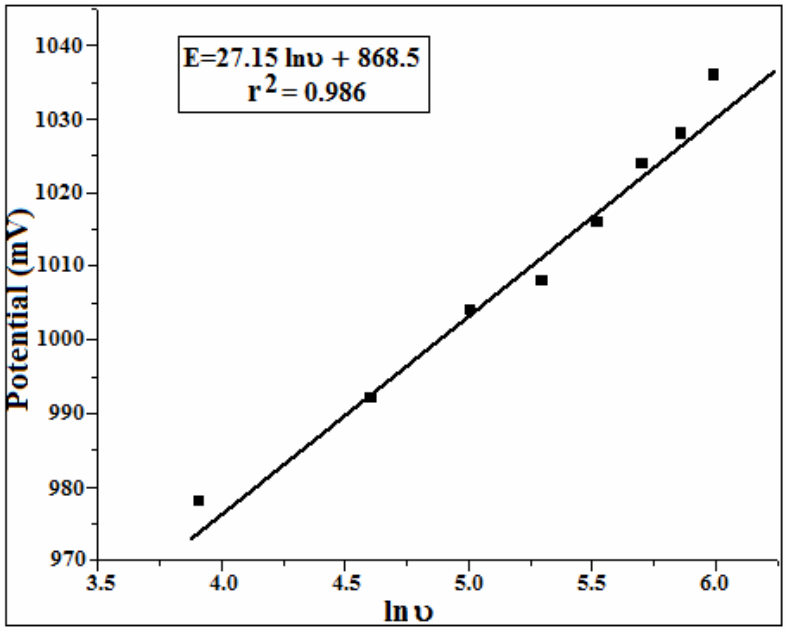

Figure 7.9 Plot of potential versus ln ν

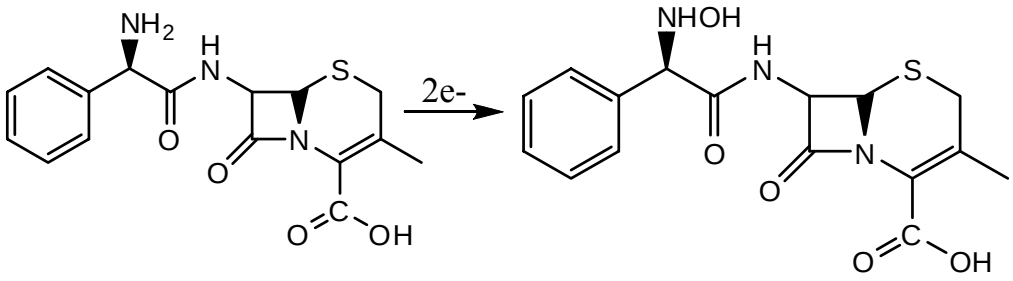

Figure 7.10 Reaction mechanism

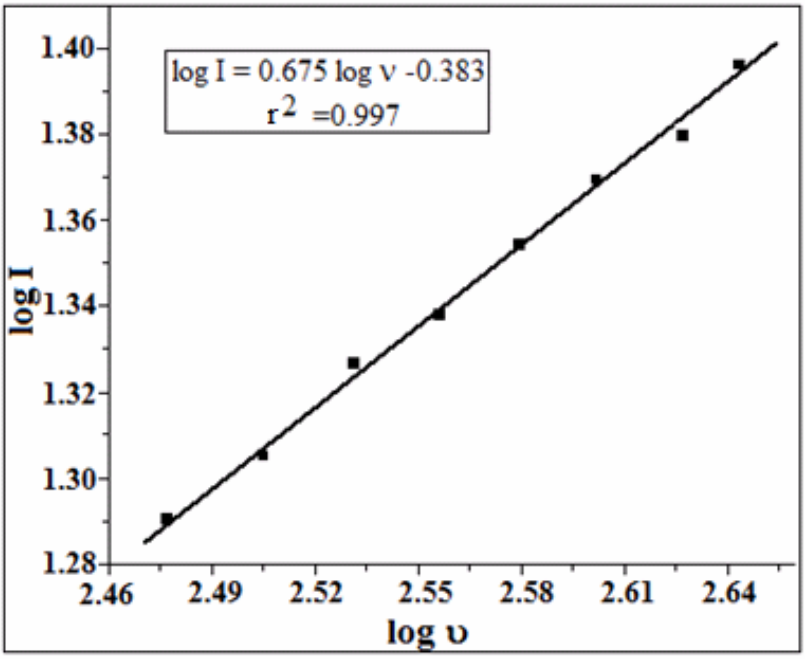

Figure 7.11 Plot of log I versus log ν

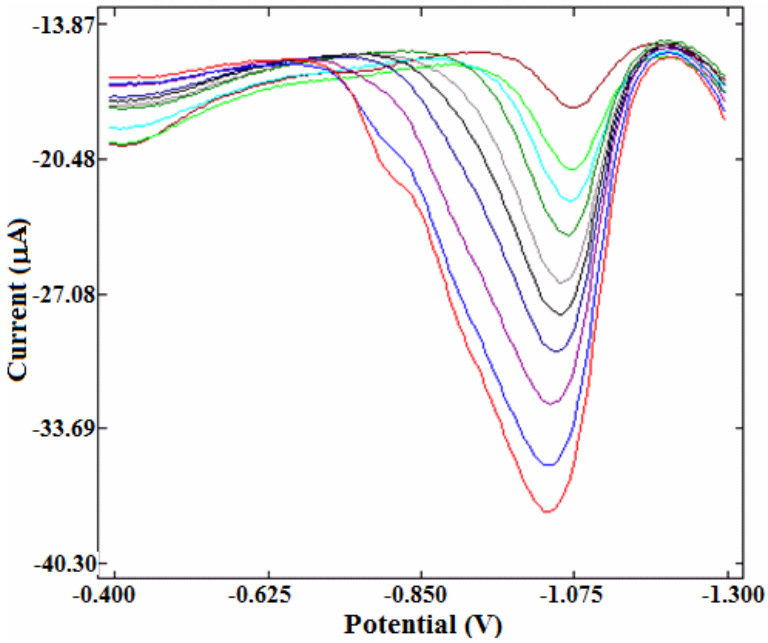

Figure 7.12 Square wave voltammograms of oxidation of Ceph of concentrations of 1×10^{-6}, 4×10^{-6}, 8×10^{-6}, 2×10^{-5}, 5×10^{-5}, 8×10^{-5}, 2×10^{-4}, 5×10^{-4}, 8×10^{-4}, 1×10^{-3} M (from top to bottom)

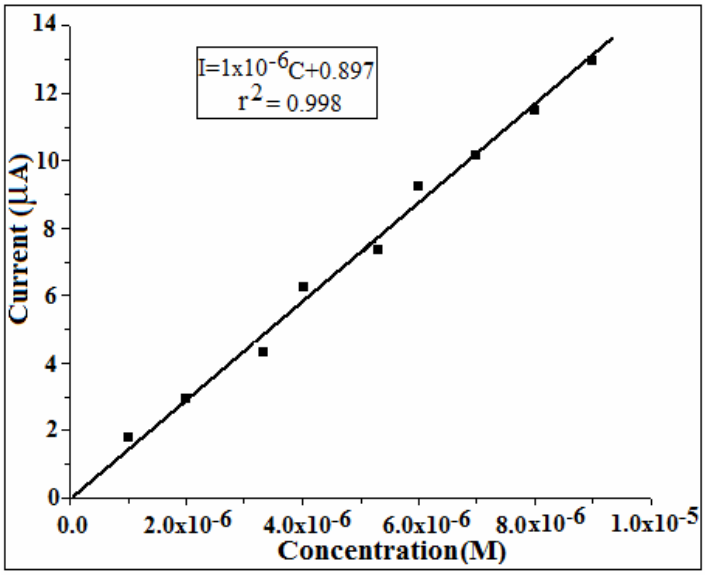

Figure 7.13 Dependence of concentration of Ceph on peak current

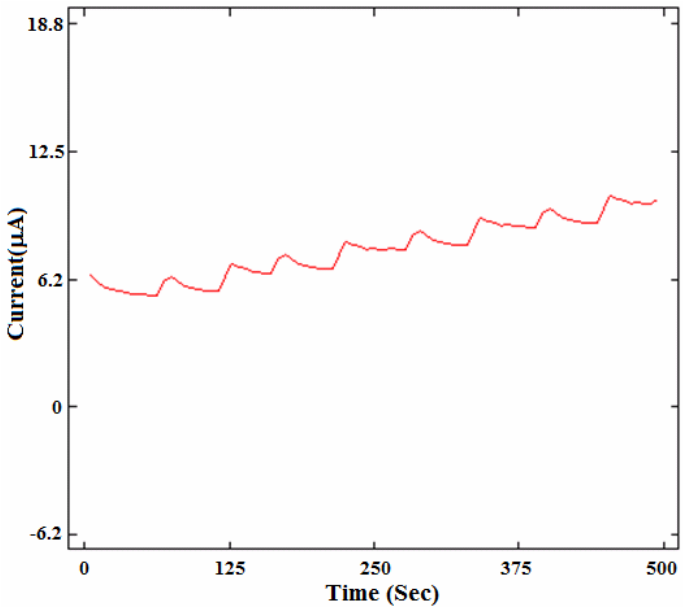

Figure 7.14 Current–time recordings obtained on increasing the Ceph concentration in 1×10^{-4} M steps at AuNP modified GCE. Operating potential, -1050 mV.

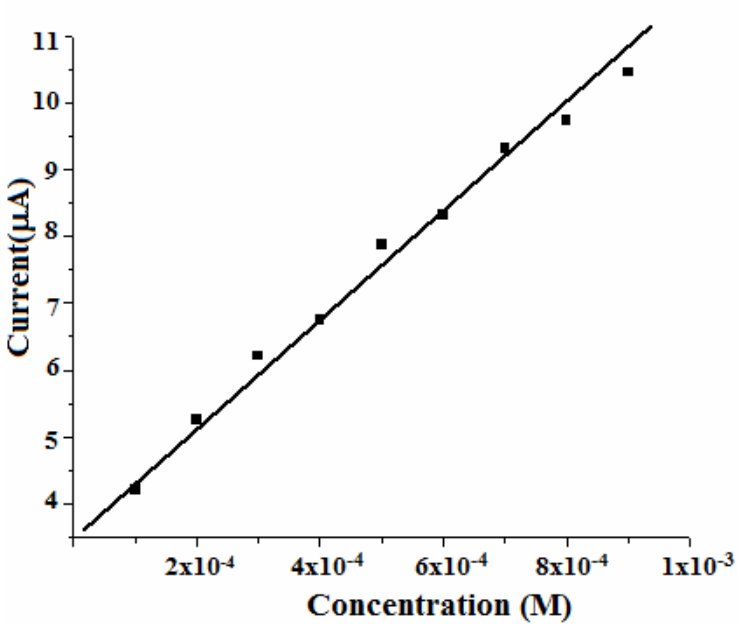

Figure 7.15 The calibration curve for the amperometric response

.....ꕥ.....

Chapter 8

DEVELOPMENT OF SENSOR FOR AMOXICILLIN TRIHYDRATE

Contents

8.1 Introduction
8.2 Preparation of MWNT/AuNP modified GCE
8.3 Preparation of MWNT/PtNP modified GCE
8.4 Electrochemical behaviour of AMX
8.5 Evidences of electrode modification
8.6 Performance characteristics of the developed sensors
8.7 Analytical applications
8.8 Conclusions

The electrochemical oxidation of Amoxicillin trihydrate (AMX) is studied on multiwalled carbon nanotubes (MWNT)/nanoparticles modified glassy carbon electrodes (GCE) using voltammetry. Gold (AuNP) and platinum nanoparticles (PtNP) are firstly electrodeposited on the surface of the GCE. MWNT were subsequently introduced to the surface of nanoparticle film. The resulting electrodes were characterized by scanning electron microscopy and voltammetry. The effect of the electrodeposition conditions, such as deposition time and number of scan cycles on the response of the electrode were studied. Also, the effects of experimental parameters, such as supporting electrolyte, pH, film thickness and scan rate on the response were examined. The prepared electrodes were successfully applied for the determination of AMX in pharmaceutical and in urine samples.

8.1 Introduction

Amoxicillin trihydrate, [4-Thia-1-azabicyclo[3,2,1]heptane-2-carboxylicacid, 6{[amino(4-hydroxyphenyl)acetyl]amino}-3,3-dimethyl-7-oxo-,trihydrate{2s-[2alpha;5alpha,6beta(s*)]}-] (AMX) (Figure **8.1**), is one of the new types of important penicillin antibiotics with a wide spectrum, which is usually used for treating hemolytic streptococcus, pneumococcus, and diphtheria bacteria. AMX is used to treat infections caused by bacteria, such as pneumonia,

bronchitis, gonorrhea and infection of the ears, nose, throat, urinary tract, and skin [288] by inhibiting bacterial cell wall synthesis. AMX is a commonly used β-lactam antibiotic, which is highly active against both gram-positive and gram-negative bacteria. AMX is usually produced by a semisynthetic route using reactive groups of 6-aminopenicillanic acid (6-APA). Also, various hydrated forms of AMX, including monohydrate, dihydrate, and trihydrate, have been reported, among which, the trihydrate is the most stable hydrated form.

AMX is a white, or almost white crystalline powder, slightly soluble in water and in alcohol, practically insoluble in ether and in fatty oils. It dissolves in dilute acids and dilute solutions of alkali hydroxides. The empirical formula of AMX is $C_{16}H_{19}N_3O_5S_{.3}.H_2O$, and the molecular weight is equal to 419.4 g/mol [289]. AMX, presents a structure based on a β -lactam ring responsible for the antibacterial activity and variable side chains that account for the major differences in their chemical and pharmacological properties. AMX has been proven to be unstable in a pH below 2 [290–294], though it is considered to be stable in the pH range of 4 to 7.

As the clinical use of AMX became common, methods for its quantification have attracted the attention of investigators. Several methods were used for the determination of AMX. M. Q. A. Abachi et al have developed a batch and flow injection analysis (FIA) spectrophotometric methods for the determination of AMX in aqueous solution and in pharmaceutical preparations [295]. The methods are based on the reaction of AMX with *N*,*N*-dimethyl-*p*-phenylenediamine in the presence of potassium hexacyanoferrate (III) in alkaline medium. G. G. Mohamed has reported a spectrophotometric method which involves the formation of ion-pair between AMX and inorganic complex of Mo (V)–thiocyanate followed by its

extraction with methylene chloride [296]. A spectrophotometric method based on a nucleophilic substitution reaction to measure the pink compound produced by the reaction of AMX with sodium 1,2-naphthoquinone-4-sulfonate in pH 9.00 buffer solution has been developed by Q. Li et al [297]. Derivatives spectrophotometric techniques were developed for the determination of AMX with potassium clavulanate (PC) by K. H. A. Saidi et al [298].

G. Pajchel et al evaluated a capillary electrophoresis method for determination of AMX and clavulanic acid in Augmentin preparations [299]. A method based on the direct chemiluminescence reaction of AMX with $KMnO_4$ in acidic medium in presence of quinine sulfate was developed by J. Du et al [300]. A method for direct determination of AMX in pharmaceuticals using flow injection analysis (FIA) with UV detection adjusted at 228 nm, along with potentiometer and condoptometric methods are described by G. Altiokka et al. [301]. Sun et al described a chemiluminescence method using flow injection [302]. Q. Peia et al have developed a high performance liquid chromatography with diode array detection based (HPLCDAD) method for simultaneous determination of AMX and sulbactam in human plasma [303]. High-performance liquid chromatographic (HPLC) method for the simultaneous determination of AMX and clavulanic acid in human plasma with ultraviolet detection at 220 nm has also been reported by G. Hoizey et al [304]. Another HPLC method was developed for the determination of AMX in human serum and plasma by H. J. Mascher et al [305]. J.I.D. Wibawa et al have developed a HPLC assay with fluorimetric detection for the routine analysis of AMX in rat plasma, gastric juice aspirate [306]. W. Li et al also developed a HPLC method using ultraviolet detection at 230 nm for the simultaneous determination of AMX and ranitidine in rat plasma [307]. HPLC - electrospray ionization mass spectrometric method for the simultaneous

determination of AMX and clavulanic acid in human plasma using terbutaline as internal standard has been reported by K. H. Yoon et al [308]. An isocratic reversed phase HPLC method with UV detection has been developed for simultaneous determination of AMX and clavulanic acid in human plasma by S. M. Foroutan et al [309].

H. J. Nelis et al reported a means of determining AMX in bovine plasma by liquid chromatography with UV detection at 235 nm. Purification and concentration of extracts were accomplished by a tandem solid phase extraction procedure with two reversed-phase columns [310]. Lee et al. developed, a method for determining AMX in urine with a determination limit of 2.5 µg/mL using the postcolumn derivatisation principle [311]. A voltammetric sensor based on a glutaraldehyde cross-linked polyglutamic acid modified GCE was developed by D. P. Santos et al [312]. Another voltammetric determination of AMX using a poly (*N*-vinyl imidazole) modified carbon paste electrode has been reported by B. Uslu et al [313]. B. Rezaei et al reported an adsorptive stripping voltammetric determination of AMX on a multiwalled carbon nanotubes modified GCE [314]. Most of the reported methods suffer from disadvantages such as complicated procedure, time consuming, requirement of expensive instruments and low detection sensitivity.

The integration of nanotechnology with electrochemistry is expected to produce major advances in the field of electrochemical sensors. Nanomaterials are a new class of materials exhibiting unique and special properties that are differ from the bulk materials, originating from their quantum scale dimensions [315]. So far gold [316–318], silver [319,320], platinum [321, 322], and palladium [323] nanomaterials have attracted considerable interests and studies in the past two decades. Properties of carbon nanotube (CNT) such as

high specific surface area, thermal conductivity, and chemical stability, render them very attractive candidates for use as nano templates for the dispersion and stabilization of metal nanoparticles (NPs) [324]. NPs have been proposed for many potential applications ranging from magnetism and biomedicine [325] up to cancer therapy [326] and catalysis [327]. Those properties are closely related to their size and shape [328-330]. By combining, the two classes of nano materials (CNTs and NPs) novel hybrid materials can be synthesized that successfully incorporate the properties of the two counter components. CNT-NP hybrids materials have been reported to exhibit catalytic activity, enhanced electrical conductivity, and hydrogen-sensing capability [331], suggesting broad potential application in optoelectronics [332], molecular sensors [333] and heterogeneous catalysis.

The formation of CNT-NP hybrids involves the absorption of CNT mainly to the NPs surface or alternatively. In general, there are two main pathways for the preparation of CNT-NP hybrids [334]. In the first strategy, CNT can be linked to the pre-formed NPs surface via covalent or weaker bonds. Therefore, the NPs are prepared and modified with suitable functional groups for the connection to the functionalized CNT surface. An alternative pathway for the formation of CNT-NP hybrids, involves the direct reduction/deposition of the suitable NP precursor to CNT [335, 336].

Taking account of the advantages of AuNP and CNTs, AuNP/CNT has more potential applications in the generation of the electrochemical sensors, because of the greatly promoted electron transfer rate and electrocatalytic ability [337–347]. Electrodeposition offers many advantages over high temperature metal deposition for the metal nanoparticle formation on MWNTs. One of the most significant advantages of electrochemical

deposition is the ability to controlling size and distribution of nanoparticles by varying potential, time or solution concentration.

Recently, Pt-based nanostructures have been widely investigated in electrocatalytic oxidation of small organic molecules [348–350]. In the last several decades, Platinum nanoparticles (PtNP) with a variety of shapes have been explored, including nanocubes [351–354], nanorods [355], nanotubes [356], dendritic NPs [357, 358], and nanowires [359]. Several procedures have been employed to prepare Pt-supported nanoparticles on different supports, including wet impregnation [360, 361], microwave irradiation [362], microemulsion [363, 364], polyol process [365, 366], micro-wave assisted polyol process [367] or two step spray pyrolysis [368]. On the other hand, the electrodeposition of PtNP has received more and more attention due to its advantages, such as high purity of deposits and simple procedure for deposition. Furthermore, electrodeposition method can control the amount of metal deposited, the number of metallic sites and their size to a fairly small scale [369].

This chapter describes the fabrication and characterization of two voltammetric sensors for the determination of AMX based on MWNT/AuNP and MWNT/PtNP modified GCEs.

8.2 Preparation of MWNT/AuNP modified GCE

Before the modification, the GCE was cleaned as explained in section 2.4 of chapter 2. The AuNP modified GCE were obtained by cyclic voltammetry (CV) in 0.05 M H_2SO_4 solution containing 1 mM $HAuCl_4$ for a given number of scans as detailed in section 2.5.5 of Chapter 2. An appropriate amount of pure MWNT was functionalized by concentrated nitric acid treatment process to obtain more edge sites and better dispersion of nanotubes

by the creation of carboxylate groups. Functionalized MWNT was dispersed in Nafion-water solution and homogenized ultrasonically. Then, 4 μL of the suspension (5 mg of MWNT in a mixture of 300 μL Nafion and 2 mL water) was placed on the GCE surface by micropipette and the solvent was evaporated to obtain MWNT/AuNP/GCE.

8.3 Preparation of MWNT/PtNP modified GCE

The electrochemical deposition of PtNP on a cleaned GCE was performed in 0.1 M HCl solution containing 2 mM H_2PtCl_6 (Figure 8.**2**). Detailed procedure is given in section 2.5.6.1 of Chapter 2. Then 4 μL of MWNT dispersion (5 mg of MWNT in a mixture of 300 μL Nafion and 2 mL water) was cast on the surface of a PtNP modified GCE and dried in the air to form a MWNT/PtNP modified electrode.

8.4 Electrochemical behaviour of AMX

Electrochemical experiments were conducted on a electrochemical workstation (CH Instruments, Austin, TX). A conventional single compartment three electrode system was employed, in which nanoparticle modified GCE and a platinum wire were used as the working electrode and counter electrode, respectively. All potentials are quoted vs. an Ag/AgCl reference electrode. A personal computer was used for data storage and processing. The experiments were carried out at room temperature under a N_2 atmosphere, after de-aerating solutions with high purity nitrogen.

Stock solution of AMX was prepared as described in section 2.6 of Chapter 2. Standard solutions of the analyte (1×10^{-3}- 1×10^{-6} M) were prepared by serial dilution of stock solution using phosphate buffer solution (PBS) of pH 7. Sample solution was taken in the electrochemical cell. The solution was

then de-aerated with nitrogen for 5 min. The voltammetric behavior of AMX in PBS was studied by sweeping the potential from 300 mV to 1000 mV at a scan rate of 100 mV/s. Modified electrodes were activated by successive voltammetric sweeps between 300 mV to 1000 mV until the voltammograms kept unchangeable.

AMX gave an oxidation peak on bare GCE at 788 mV with a peak current of 1.829 μA. In order to reduce the oxidation potential of AMX, we tried various chemical modifications on GCE. At poly o-phenylenediammine modified GCE, an oxidation peak appeared at 832 mV with a peak current of 1.038 μA. The electrochemical response of AMX was further studied using different NP modified electrodes. It was first studied on copper nanoparticle modified electrodes, but no response was obtained. At MWNT modified GCE, AMX oxidizes at 644 mV but the peak current was only 0.886 μA. Further AuNP and PtNP modified electrodes were tried. At AuNP and PtNP modified GCEs, oxidation peak were obtained at 708 mV with a peak current of 2.006 μA and at 712 mV with a peak current of 2.576 μA respectively. Then MWNT-NP hybrids modified electrodes were tried. AMX gave no response at the MWNT/ copper nanoparticle modified GCE. (Figure 8.**3**) However at MWNT-AuNP modified GCE, AMX gave a well defined oxidation peak at 656 mV with a peak current of 18.7 μA and at MWNT- PtNP modified GCE AMX gave a well defined oxidation peak at 650 mV with a peak current of 18.5 μA. The results indicate that the incorporation of MWNT could significantly improve the electron transfer behaviour of NP films due to its excellent electronic conductivity. Thus the combination of NPs with MWNT has a greater effect on electrocatalytic activity towards the oxidation of AMX, resulting in a much higher current response. Since a better electrochemical response of AMX was obtained with MWNT-NP hybrids modified electrodes, the choice is justified.

8.5 Evidences of electrode modification

8.5.1 SEM images

The morphology of the MWNT/AuNP/GCE and MWNT/PtNP/GCE were studied by SEM and depicted in Figure 8.**4**.

8.5.2 Surface area study

CV of 2 mM potassium ferricyanide solution was carried out at bare GCE, MWNT/AuNP/GCE and MWNT/PtNP/GCE at different scan rates to calculate the effective surface area of them (Figure 8.**5)**. The obtained peak current was plotted against the square root of scan rates. The regression equations obtained from CV analysis for the bare GCE, MWNT/AuNP/GCE and MWNT/PtNP/GCE are: I_p =0.772 $\nu^{1/2}$+4.230 (r^2=0.989, ν in mV/s, I_p in μA), I_p =1.757 $\nu^{1/2}$ +6.746 (r^2=0.994, ν in mV/s, I_p in μA) and I_p =1.511 $\nu^{1/2}$ +3.427 (r^2=0.994, ν in mV/s, I_p in μA) respectively. By using the Randles Sevcik equation for reversible reaction [167], effective surface area of bare GCE, MWNT/AuNP/GCE and MWNT/PtNP/GCE were calculated from the slope of the I_p versus $\nu^{1/2}$ plot. It was found to be 0.0669 cm^2, 0.1204 cm^2 and 0.1439 cm^2 respectively. The large surface area of the modified GCEs compared to the bare GCE is evident from the resultant values.

8.6 Performance characteristics of the developed sensors

Various electrochemical parameters were optimized. The next sections discuss in detail each of these parameters.

8.6.1 Effect of the supporting electrolyte

The medium in which the electrochemical reaction takes place might have a pronounced effect on the response of the analyte and therefore the oxidation process of 1×10^{-3} M of AMX was monitored in various electrolytes

like KNO_3, HCl, NaOH, NaCl, phosphate buffer and acetate buffer by DPV. On the basis of higher peak current and better peak shape, it is inferred that the oxidation response of AMX at both modified electrodes are much better in phosphate buffer solution (PBS) than that in other medium. Thus PBS was used as the experimental medium for the further studies of AMX.

8.6.2 Effect of pH

The electrochemical studies of 1×10^{-3} M AMX in PBS at modified electrodes were carried out in pH range of 3 to 10 using DPV, the graphical representation of which is shown in Figure 8.**6**. The best oxidation response was obtained in pH 7 as the peak currents are the highest. Thus pH 7 was fixed as optimal pH. As can be seen in Figure 8.**7**, the anodic peak potential shows a negative shift by increasing the solution pH with a slope value of -57.38 mV/pH and -57.45 mV/pH at AuNP based sensors and PtNP based sensors respectively. These observations suggest that equal numbers of electrons and protons are involved in the electro oxidation of AMX on the surface of the MWNT/AuNP/GCE and MWNT/PtNP/GCE [370]. The regression equations for the linear graphs are,

At MWNT/AuNP/GCE: $E = -55.57\ pH + 1054$ ($r^2=0.984$)

At MWNT/PtNP/GCE: $E = -52.67\ pH + 1009$ ($r^2=0.990$)

8.6.3 Effect of film thickness

To investigate the effect of film thickness on the electrochemical response towards AMX, the parameters influencing the film thickness including the number of cycles and time during electrodeposition were studied. Also the influence of amount of MWNT-Nafion dispersion on peak current was studied.

8.6.3.1 Effect of number of scan cycles for the electrodeposition of AuNPs

The influence of the number of scan cycles for the electrodeposition of AuNPs on the anodic peak current of AMX was investigated. The amount and the size of the deposited AuNPs can be controlled by changing the cycle number (N) in electrodeposition process. The anodic peak current slowly increased with increase of scan cycles. The optimum current was obtained when N was 40 (Figure 8.**8)**. When the cycles were beyond 40, the peak current decreased, may be due to the decreased electron transfer with an increase in film thickness. Also, the repeatability and stability for the film modified electrode were not good when the cycles were less than 40. Considering the results, 40 cycles was chosen as the optimum cycle number in gold electrodeposition process.

8.6.3.2 Effect of the electrodeposition time of PtNP

The amount and particle size of the PtNP depend on the electrodeposition time. As shown in Figure 8.**9**, the oxidation peak current increased gradually as deposition time increased. However, when increasing deposition time continuously, the oxidation current decreased slightly, which might be associated with the decrease of the surface area resulting from the aggregation of PtNPs on the electrode surface. So, electrodeposition time was optimized to 9 minutes.

8.6.3.3 Influence of amount of MWNT-Nafion dispersion

The amount of MWNT-Nafion dispersion on the metal nanoparticle modified GCEs, directly determines the thickness of the MWNT film. It is found that the oxidation peak current of AMX increases, while gradually increasing the volume of MWNT-Nafion dispersion (5 mg MWNT in 300 μL Nafion and 2 mL water) from 1μL to 4 μL. The observations are shown in Figure 8.**10**. The

enhancement of current indicates that the number of catalytic sites increases with increase of the amount of MWNT-Nafion dispersion. Further increasing the volume of MWNT dispersion, results in the decrease of the peak current. This is because Nafion, used as one of the solvents, is a kind of insulator that blocks the electron transfer. Hence, the volume of MWNT dispersion was fixed to be 4 μL.

8.6.4 Effect of scan rate

In order to study the effect of scan rate (ν) on the peak current (I_p), linear sweep voltammograms of 1×10^{-3} M AMX were recorded at different scan rates (Figure 8.**11**). It was found that the anodic peak currents increased gradually along with the increase of the scan rate. Figure 8.**12** shows the linear behavior of anodic peak current with the square root of scan rate ($\nu^{1/2}$), which points to the fact that the electrode reaction of AMX on the modified GCEs is controlled by diffusion rather than adsorption. The obtained regression equations are given below.

At MWNT/AuNP/GCE: $I_p = 1.291\ \nu^{1/2} + 4.761$ (r^2=0.990, ν in mV/s, I_p in μA)

At MWNT/PtNP/GCE: $I_p = 2.137\ \nu^{1/2} + 3.863$ (r^2=0.988, ν in mV/s, I_p in μA)

A slope of 0.44 was obtained for the linear relation between the log I_p and log ν, which can be due to the diffusion of AMX on both the modified electrode surfaces [168] (Figure 8.**13)**. Regression equation obtained from linear sweep voltammetric (LSV) analysis on the MWNT/AuNP/GCE and MWNT/PtNP/GCE are log I= 0.407 log ν + 0.437 (r^2=0.989), log I = 0.449 log ν + 0.499 (r^2=0.989) respectively.

In order to have an insight into the mechanism of the electrochemical oxidation of AMX at modified GCEs, the anodic peak potential E was plotted

against ln scan rate as shown in Figure 8.**14.** The regression equations for the linear graphs are,

At MWNT/AuNP/GCE: $E = 54.59 \ln \nu + 586.3$ (r^2=0.990)

At MWNT/PtNP/GCE: $E = 39.50 \ln \nu + 691.5$ (r^2=0.989)

The slopes of the linear graphs were determined. Based on the Laviron's equation [169], the number of electrons involved in the electrochemical reaction (n) was found to be 0.99, 1.20 (close to 1) at MWNT/AuNP/GCE and MWNT/PtNP/GCE respectively. Thus AMX follows a one electron path for its electrochemical oxidation at modified GCEs. From the mentioned results the overall reaction mechanism can be attributed to the contribution of one electron and one proton for oxidation of phenolic group of AMOX to generate the related quinone as shown in Figure 8.**15**.

8.6.5 Calibration curve

The determination of 1×10^{-3} M AMX at MWNT/AuNP/GCE and MWNT/PtNP/GCE was performed under the optimal differential pulse voltammetric conditions. Figure 8.**16** shows the DPVs of AMX on modified electrodes at different concentrations. The results show that the oxidative peak current has a linear relationship with the concentration in the range 1×10^{-6}-1×10^{-5} M which is shown in the Figure 8.**17.** The lower detection limit of AMX at MWNT/AuNP/GCE and MWNT/PtNP/GCE was found to be 1.710×10^{-8} M and 4.642×10^{-8} M respectively.

8.6.6 Stability and Reproducibility

The successive stability of the proposed sensors was evaluated. Five successive scans in the solution containing 1×10^{-3} M AMX were performed. The relative standard deviation value obtained for AuNP & PtNP sensors was

found to be 2.33 % & 2.14 %, indicating excellent stability of the modified electrodes. Moreover, after the modified electrodes were stored for two weeks, only a small decrease of the oxidation peak current was observed, demonstrating that the electrodes had good stability.

Table **8.1** represents comparative study of characteristics of the developed methods with some of the reported methods. The presently developed methods are highly comparable with all the reported methods.

8.6.7 Interference study

In order to examine the effect of foreign bodies on the anodic current of AMX, 100 fold excess concentrations of urea, lactose, fructose, K^+, Na^+, SO_4^{2-} ,Cl^- and ascorbic acid were added to 10^{-3} M AMX. It is found that upto 100 fold excess concentration of urea, lactose, fructose, K^+, Na^+, SO_4^{2-} and Cl^- have no influence on the signals of 1×10^{-3} M AMX, with deviation below 5 %. However ascorbic acid interferes. Table **8.2** lists the influence of foreign substances on the oxidation signal of AMX. The results showed the good selectivity of the modified electrodes.

8.7 Analytical applications

The analytical utility of the developed sensors in the determination of AMX in pharmaceutical preparations and in urine samples were determined.

8.7.1 Determination of AMX in pharmaceutical formulations

Experiments were performed analyzing commercial formulation containing AMX, Pressmox (500 mg) manufactured by Citadel Aurobindo Biotech Ltd. (CABL). Detailed procedure for the determination is given in section 2.8.4 of chapter 2. DP voltammograms of the oxidation of AMX in the tablet were recorded and the unknown concentrations were determined from the calibration

graph. The results are shown in Table **8.3.** The results obtained are in good agreement with the declared AMX content and showed a high degree of precision.

The results were compared with those obtained by the standard method [142]. The results show that the developed methods are comparable to the standard method.

8.7.2 Determination of AMX in urine sample

The urine sample was spiked with AMX by adding several aliquots of AMX in different proportion to get various concentration of AMX. The DPVs were recorded applying the optimal conditions for their analytical determination. Recoveries lie in the range of 97-103 %. The results of the voltammetric analysis of spiked samples of urine shows good recovery as can be seen from Table **8.4.**

8.8 Conclusions

AuNP and PtNP modified electrodes were prepared by elctrodeposition and MWNTs are easily cast onto its surface to form MWNT/AuNP/GCE and MWNT/PtNP/GCE. Both modified electrodes display a strong electrocatalytic activity towards the oxidation of AMX. The proposed methods could be applied to the determination of AMX in pharmaceutical preparations and in urine samples with quite promising results.

Table 8.1 Comparison of various analytical methods

Method adopted	Detection limit
Batch and Flow Injection Aanalysis (FIA) spectrophotometry [295]	0.637 and 4.90 µg /mL
Spectrophotometry [296]	0.75 µg /mL
Spectrophotometry [297]	2.00 µg/mL
Derivative spectrophotometry [298]	0.211µg/mL
Capillary electrophoresis [299]	0.40 µg/mL
Chemiluminescence Flow Injection Analysis [300]	0.02 µg/mL
Flow Injection Analysis using UV-Detection [301]	0.1384 µg/mL
Flow injection Chemiluminescence method [302]	0.03 µg/mL
High Performance Liquid Chromatography (HPLC) with Diode Array Detection [303]	0.163 µg/mL
HPLC with UV detection [304]	0.05 µg/mL
HPLC and on-line postcolumn derivatisation [305]	0.133 µg/mL
HPLC with fluorimertic detection [306]	0.02 µg/mL in gastric juice 0. 3 µg/mL in plasma
HPLC with UV detection [307]	0.05 µg/mL
HPLC Electrospray ionisation mass spectrometry [308]	0.04 µg/mL
Isocratic reversed phase HPLC using UV detection [309]	15 ng/mL
Liquid Chromatography using a Tandem Solid-Phase Extraction Method [310]	0.10 µg/mL
Postcolumn derivatisation with Fluram [311]	2.5 µg / mL
Voltammetry using polyglutamic acid/glutaraldehyde film [312]	0.3858 µg/mL
Voltammetry using a poly (*N*-vinyl imidazole) modified carbon paste electrode [313]	0.3405 µg/mL
Adsorptive Stripping Voltammetry [314]	0.0839 µg/mL
Present method using MWNT/AuNP/GCE	7.170 ng/mL
Present method using MWNT/PtNP/GCE	19.47 ng/mL

Table 8.2 Study of the effect of foreign species on the anodic peak current of 1×10^{-3} M AMX at MWNT/AuNP/GCE and MWNT/PtNP/GCE

Foreign species	Signal change (%)	
	MWNT/AuNP sensor	MWNT/PtNP sensor
Urea	+1.522	-1.811
Glucose	-0.827	+0.952
Lactose	+2.095	-3.468
Na^+	+1.226	+1.641
K^+	+0.935	-1.488
Cl^-	+1.226	+1.641
SO_4^{2-}	+0.935	-1.488
Ascorbic acid	+15.36	+17.85

Table 8.3 Determination of AMX in pharmaceutical preparation

Sample	Declared amount (mg/tablet)	Method adopted	Found* (mg/tablet)	S.D*	C.V*
Pressmox (Citadel Aurobindo Biotech Ltd.)	500	MWNT/AuNP/GCE	497	1.54	1.24
		MWNT/PtNP/GCE	498	1.86	1.41
		Standard method	502	2.11	1.55

*****Average of six replicates

Table 8.4 Determination of AMX in urine sample

Type of sensor	Added (M)	Found (M)	Recovery (%)
MWNT/AuNP/GCE	4.00×10^{-4}	4.15×10^{-4}	103.8
	6.00×10^{-4}	5.82×10^{-4}	97.00
	8.00×10^{-4}	7.91×10^{-4}	98.88
MWNT/PtNP/GCE	6.00×10^{-5}	6.16×10^{-5}	102.7
	8.00×10^{-5}	7.83×10^{-5}	97.88
	1.00×10^{-4}	1.01×10^{-4}	101.0

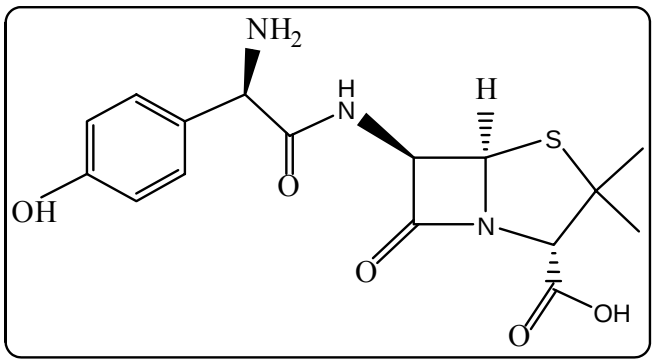

Figure 8.1 Structure of AMX

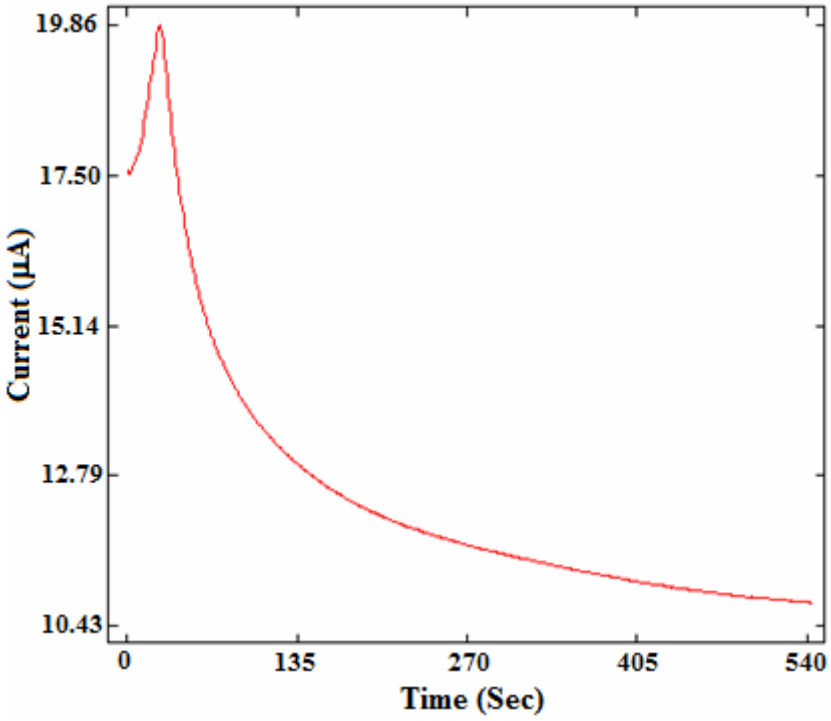

Figure 8.2 Electrodeposition of PtNP

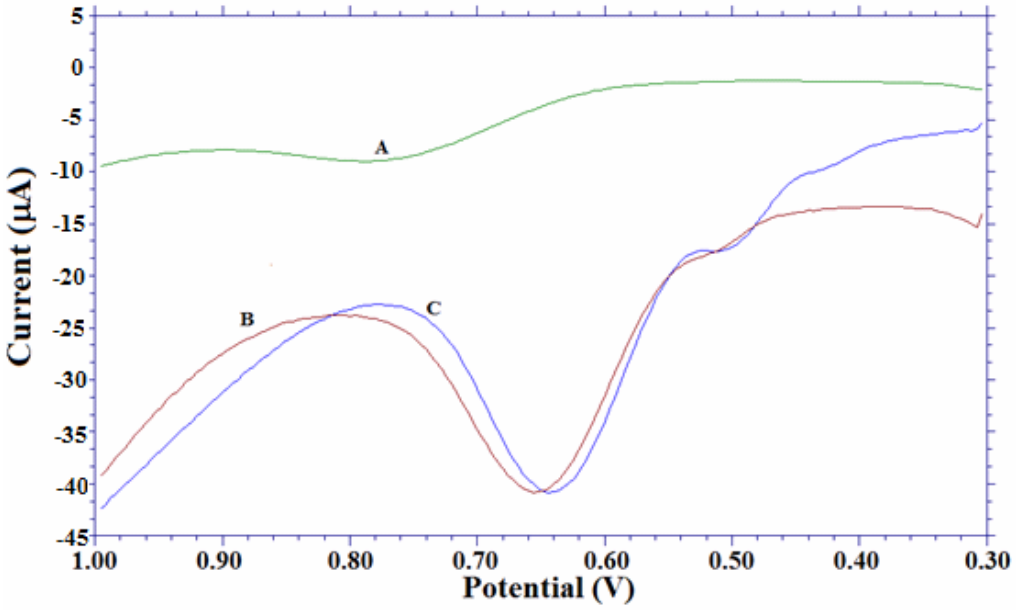

Figure 8.3 Electrochemical response of AMX on (A) bare GCE (B) MWNT/AuNP modified GCE (C) MWNT/PtNP modified GCE

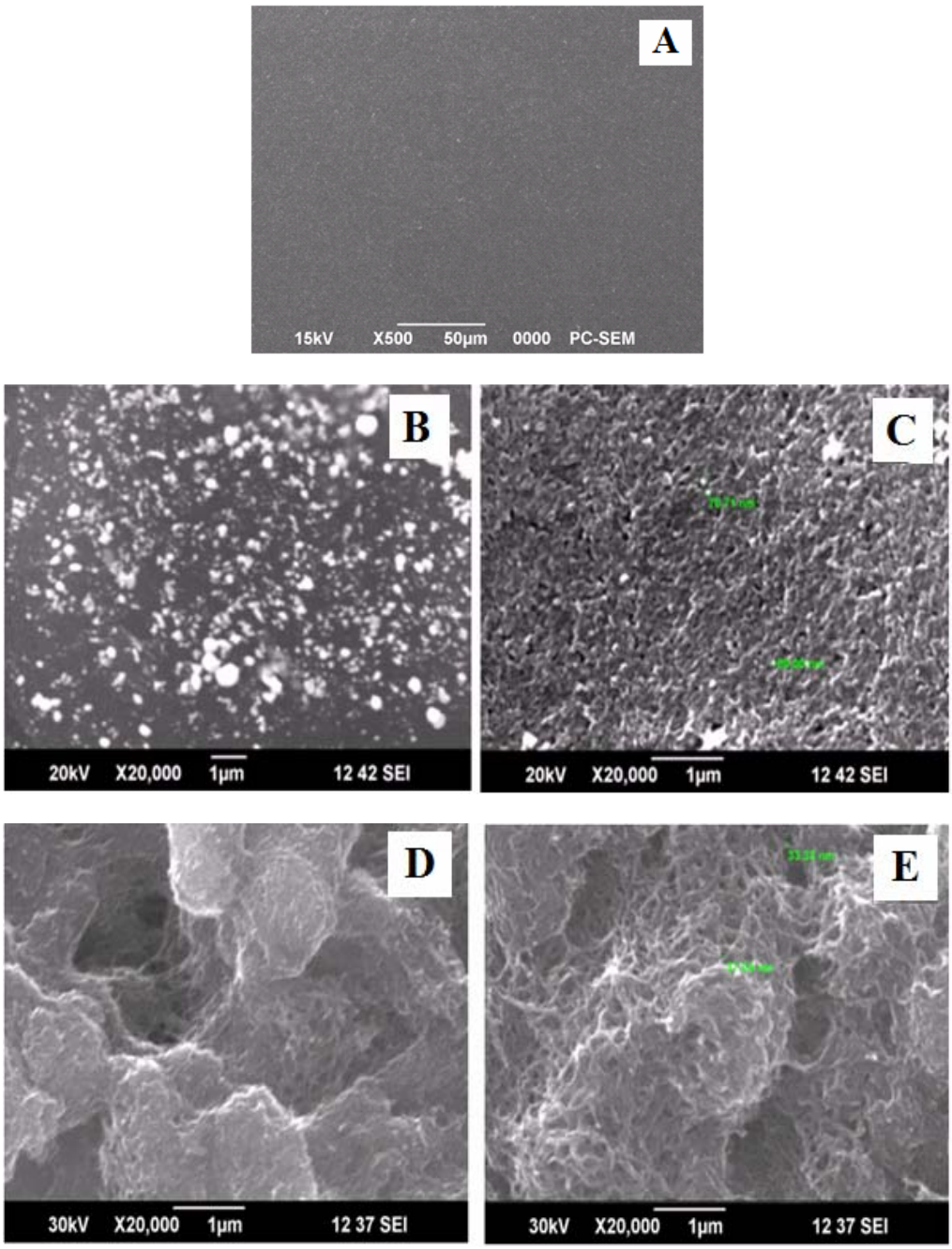

Figure 8.4 SEM images of (A) bare GCE (B) AuNP modified GCE (C) PtNP modified GCE (D) MWNT/AuNP modified GCE (E) MWNT/PtNP modified GCE

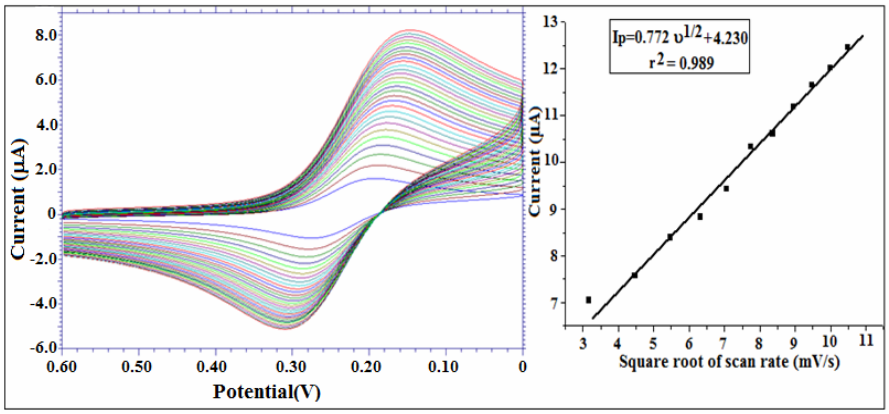

(A)

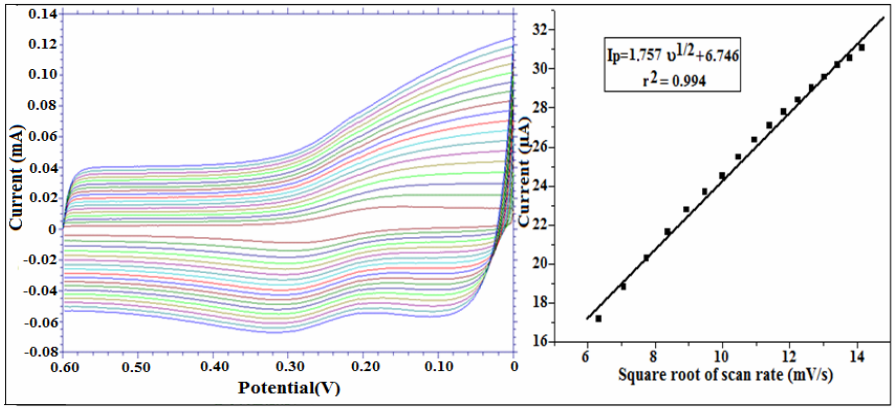

(B)

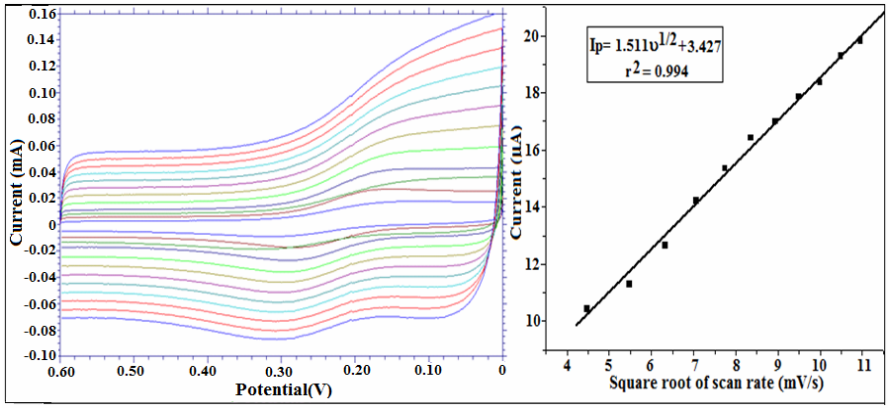

(C)

Figure 8.5 Surface area studies at (A) bare GCE (B) MWNT/AuNP/GCE (C) MWNT/PtNP/GCE and inset are plot of peak currents as a function of the square root of scan rates

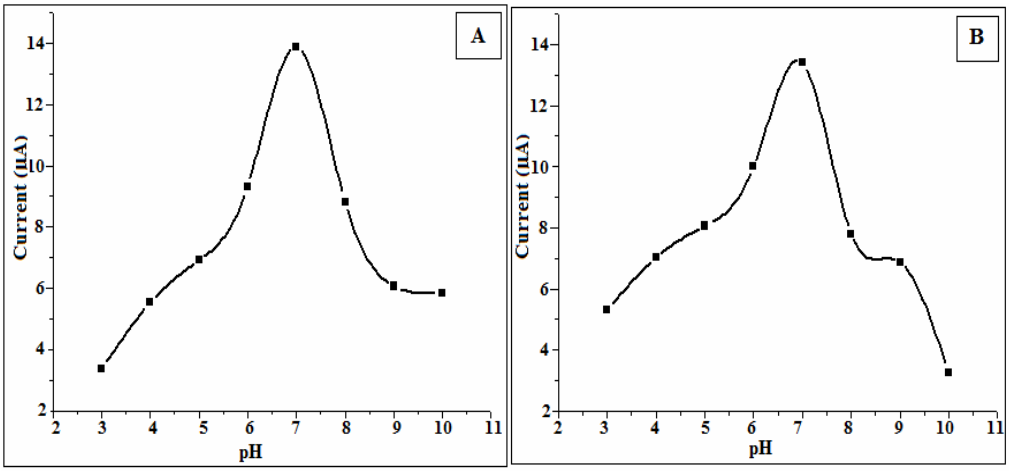

Figure 8.6 Relationship between anodic peak current and pH of the medium at (A) MWNT/AuNP/GCE (B) MWNT/PtNP/GCE

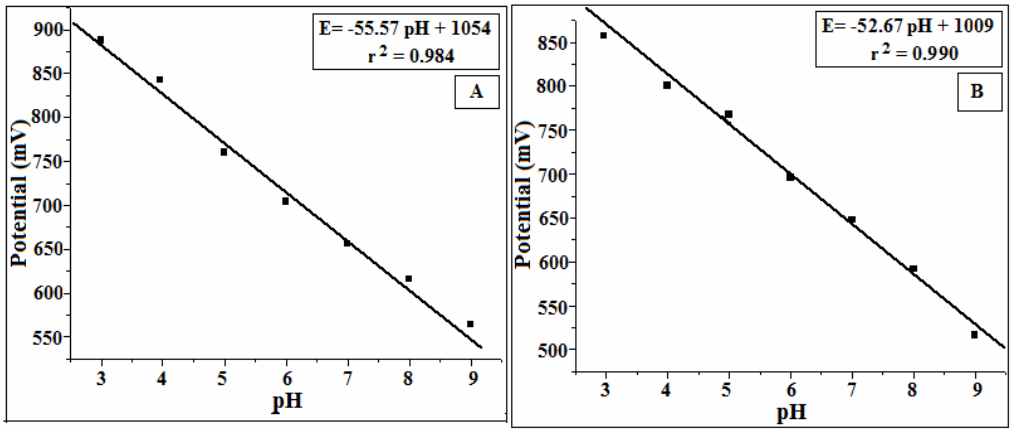

Figure 8.7 Plot of anodic peak potential of 1×10^{-3} M AMX versus pH of the medium at (A) MWNT/AuNP/GCE (B) MWNT/PtNP/GCE

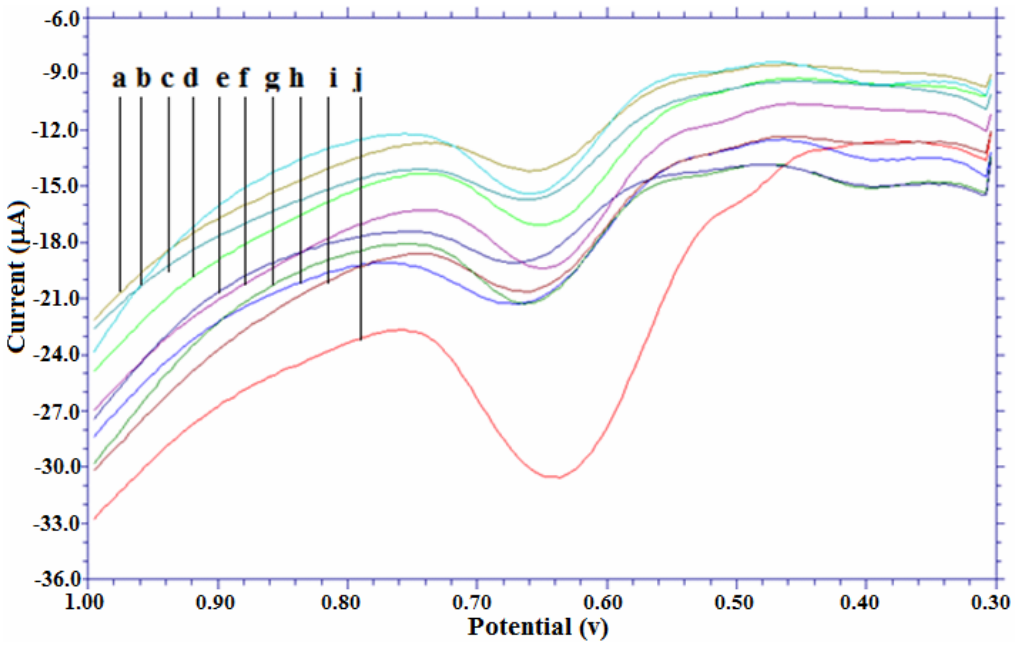

Figure 8.8 Differential pulse voltammograms of AMX at different electrodeposition cycles (a) 100 cycles (b) 10 cycles (c) 90 cycles (d) 20 cycles (e) 80 cycles (f) 30 cycles (g) 60 cycles (h) 50 cycles (i) 70 cycles (j) 40 cycles

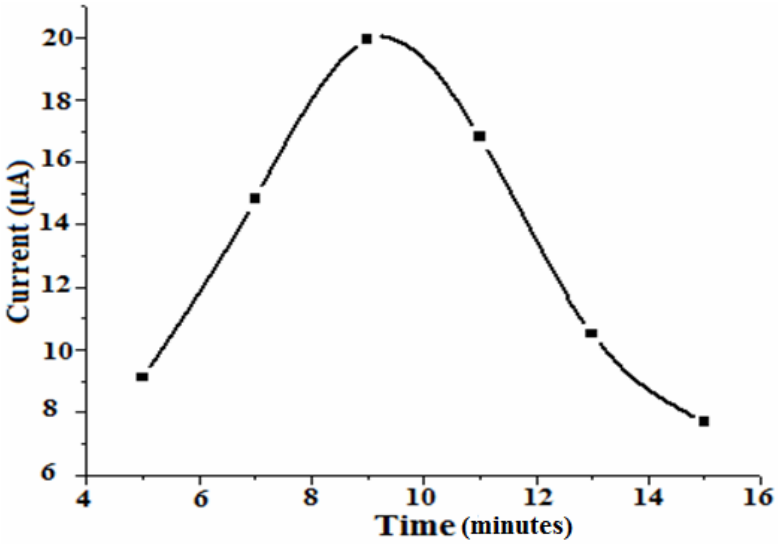

Figure 8.9 Effect of electrodeposition time of PtNP

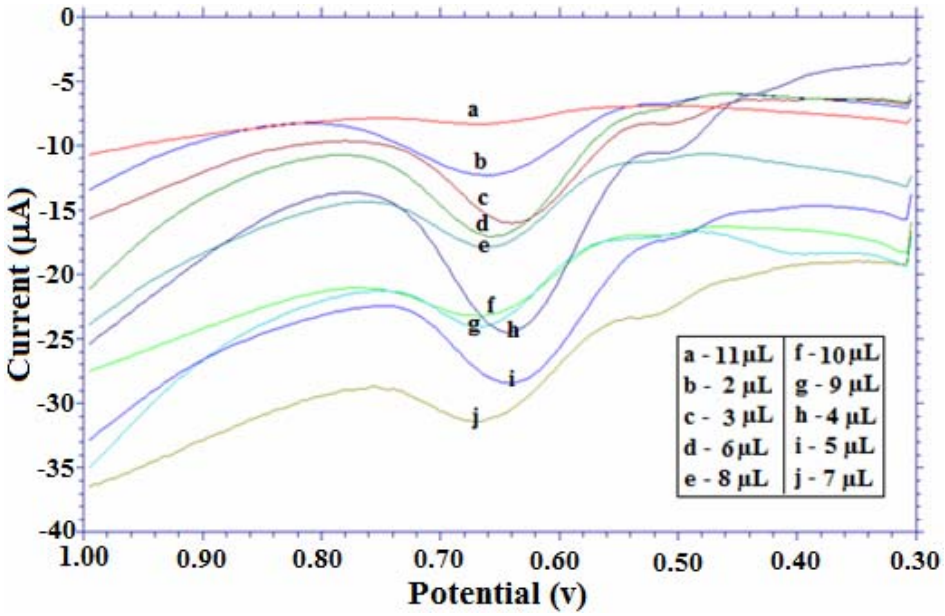

(A)

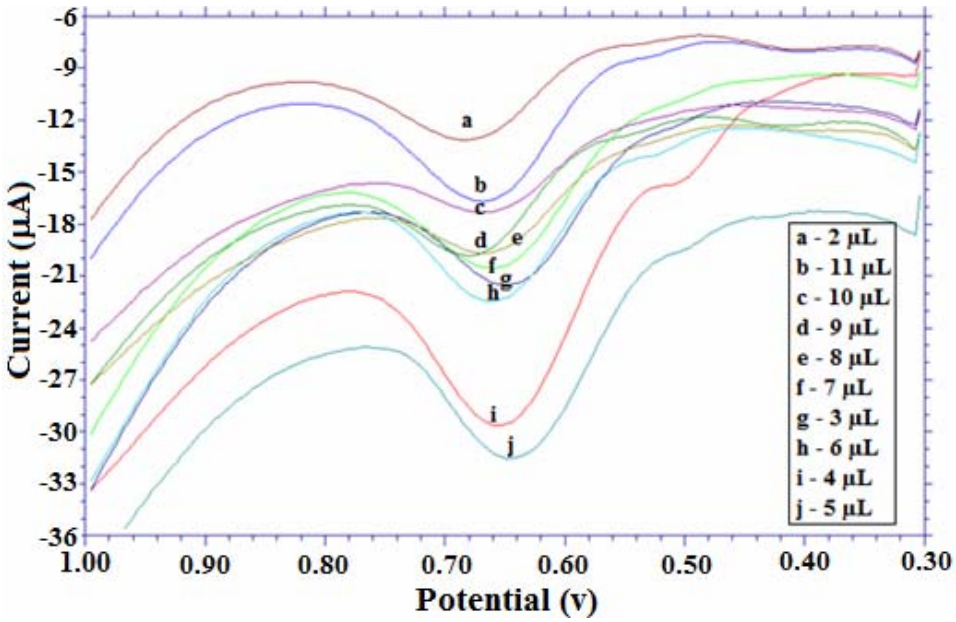

(B)

Figure 8.10 Effect of the amount of MWNT dispersion at (A) AuNP/GCE (B) PtNP/GCE

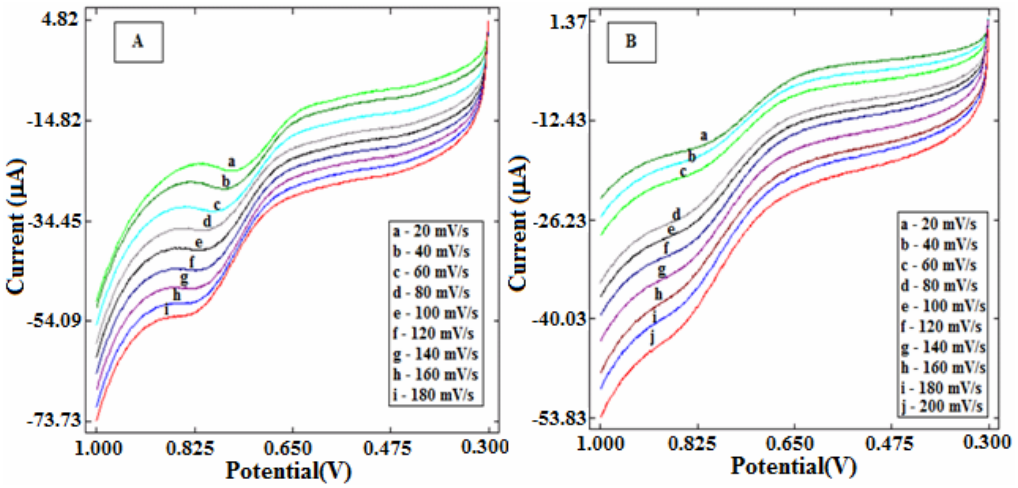

Figure 8.11 Overlay of linear sweep voltammograms of 1×10^{-3} M AMX at (A) MWNT/AuNP/GCE (B) MWNT/PtNP/GCE in 0.1 M PBS at different scan rates.

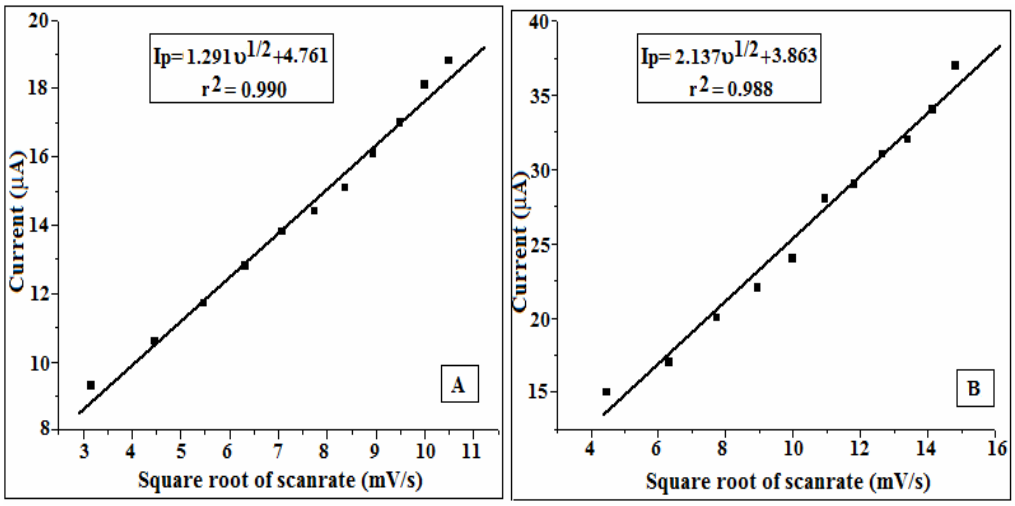

Figure 8.12 Variance of anodic peak current of AMX with scan rate at (A) MWNT/AuNP/GCE (B) MWNT/PtNP/GCE

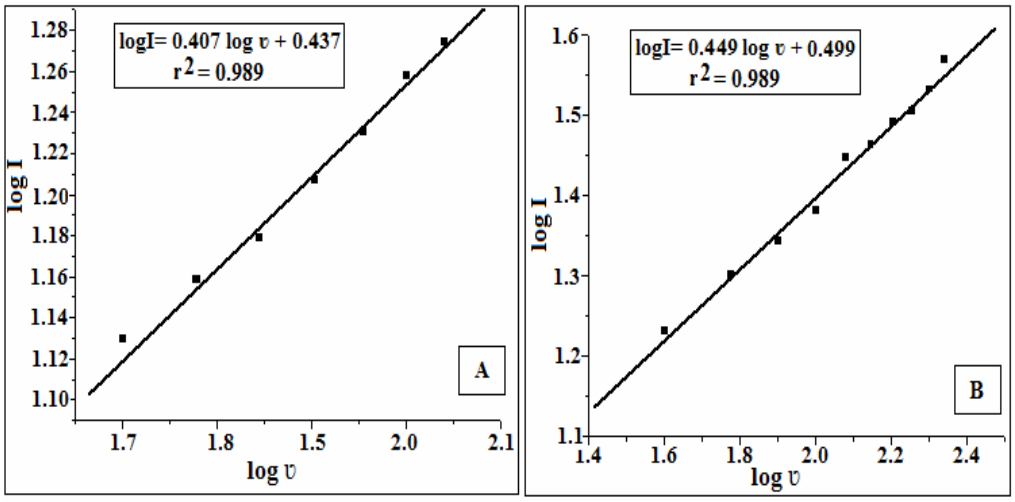

Figure 8.13 Plot of log I versus log ν at (A) MWNT/AuNP/GCE (B) MWNT/ PtNP/GCE sensors

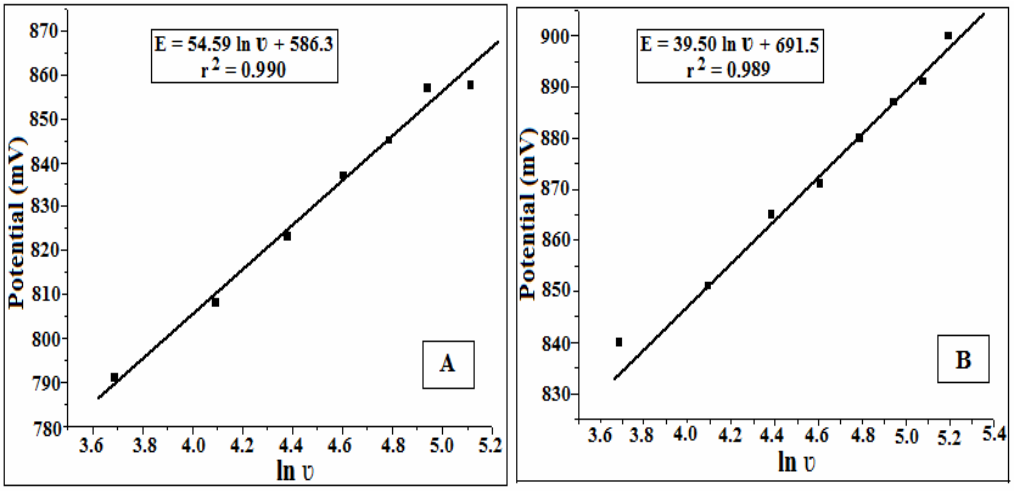

Figure 8.14 Plot of peak potential against ln scan rate at (A) MWNT/AuNP/ GCE (B) MWNT/PtNP/GCE sensors

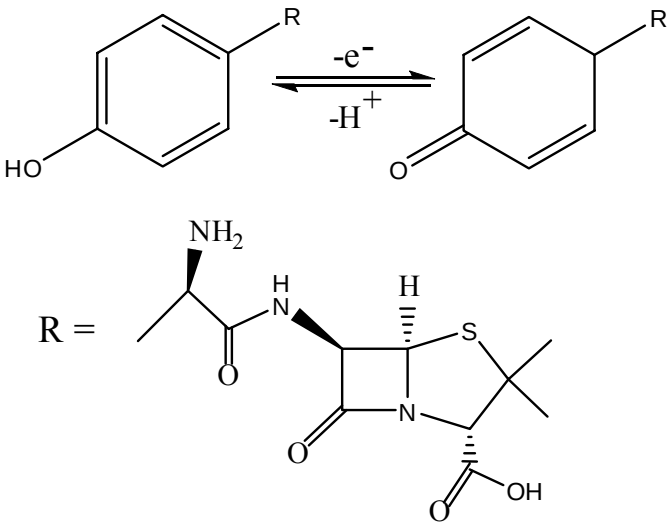

Figure 8.15 Mechanism of oxidation of AMX

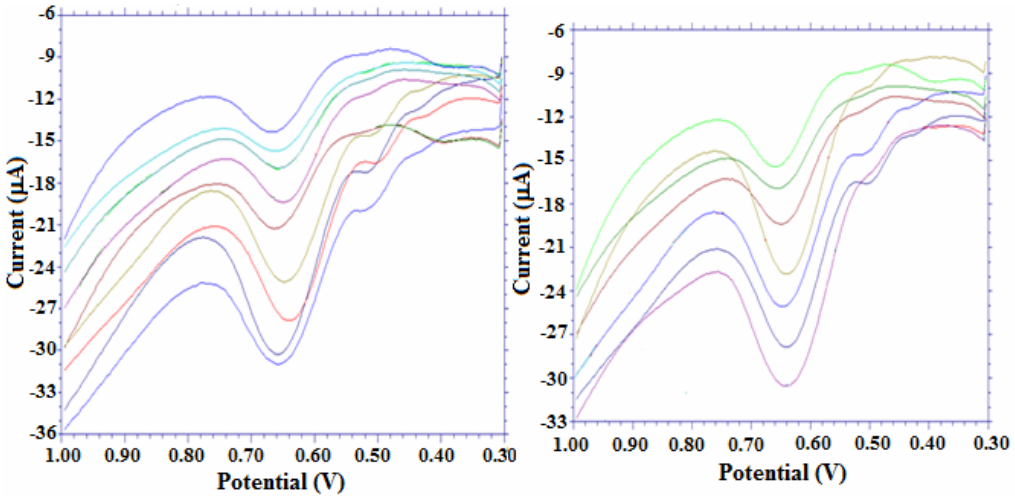

(A) **(B)**

Figure 8.16 Differential pulse voltammograms of AMX at different concentrations, 10^{-3} - 10^{-6} M (from bottom to top) on (A) MWNT/AuNP/GCE (B) MWNT/PtNP/GCE

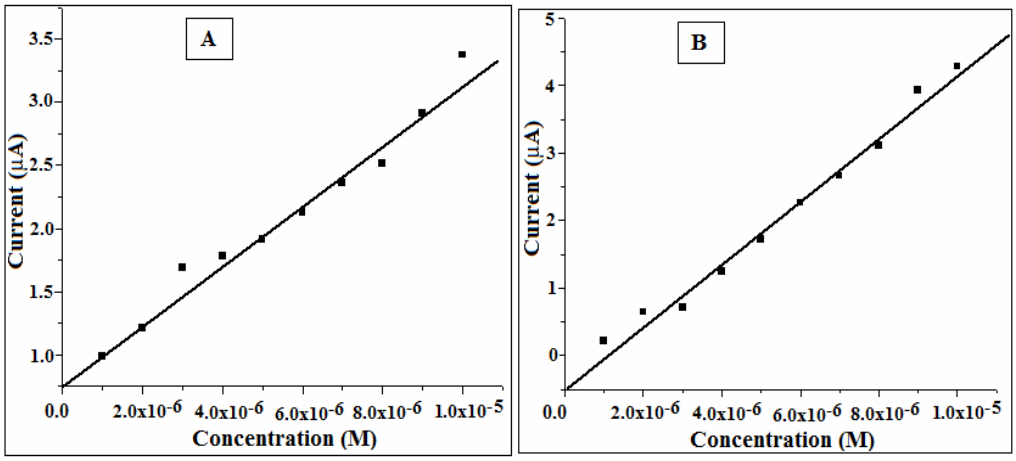

Figure 8.17 Dependence of concentration of AMX on peak current at (A) MWNT/AuNP/GCE (B) MWNT/PtNP/GCE

.....ஜ۞ஜ.....

Chapter 9

SUMMARY AND CONCLUSIONS

Contents

9.1 The objectives of the work
9.2 Summary of the work done

This chapter presents a brief summary of the important findings and results of the work. The main objectives of the investigations are also included in this chapter.

9.1 The objectives of the work

- Chemical modification of electrode surface
- Surface area calculation as an evidence for effective modification of the electrode surface and to study its surface morphology using SEM
- Fabrication of electrochemical sensors for pharmaceuticals using the chemically modified electrodes (CME)
- Optimization of electrochemical parameters of the developed sensors
- Analytical applications in pharmaceutical formulations and in real samples

Electroanalytical chemistry has come a long way from the polarographic era, when most work involved aqueous solutions and mercury electrodes. During the 1960s and 1970s, new technology was introduced that included the incorporation of operational amplifiers and computers into electrochemical

instrumentation, an expansion into nonaqueous solvents and greater use of solid electrodes made of gold, platinum, and carbon. Voltammetry is one of several important analytical techniques for the analysis of drugs in biological fluids, at concentrations of less than 10^{-6} M. The development of CMEs continues to be an area of great interest in pharmaceutical analysis due to their numerous applications in electrocatalysis. The modification techniques adopted as part of the present work includes multiwalled carbon nanotube (MWNT) based modification, electropolymerization, gold nanoparticle (AuNP) based modifications and platinum nanoparticle (PtNP) based modifications.

Modification of the electrode surface with MWNT was done by drop casting method. A homogeneous suspension of MWNT was prepared in nafion-water mixture by ultrasonication. From this suspension, suitable aliquot was dropped onto the surface and dried in air to get a thin film of MWNT on the electrode surface.

Modification of the electrode surface with polymer film was attained using electropolymerisation technique. The electrode was immersed in the solution of a suitable monomer and several cyclic scans were carried out in a suitable potential window using cyclic voltammetry.

To obtain prussian blue (PB)/MWNT hybrids, the MWNT were added to the mixture of $FeCl_3$, $K_3Fe(CN)_6$ and KCl. This dark suspension was dropped on the surface of the electrode. The PB/MWNT modified electrode was obtained just after evaporation of the solvent.

AuNP was deposited electrochemically from a solution of chloroauric acid in 0.05 M sulphuric acid to get AuNP modified electrode

PtNP was electrochemically deposited on electrode surface from a solution of chloroplatinic acid in 0.1 M HCl by controlled potential electrolysis at -250 mV.

9.2 Summary of the work done

A total of 8 sensors have been developed for the following drugs:

PAM chloride	-	MWNT/ Nafion modified platinum sensor
Tamsulosin Hydrochloride (TAM)	-	MWNT/Nafion modified glassy carbon sensor
Hesperidin Methyl Chalcone (HMC)	-	Prussain blue (PB)/MWNT nanocomposite film modified glassy carbon sensor
Guaiphenesin (Guai)	-	poly (p-ABSA) modified glassy carbon sensor and MWNT/ poly (p-ABSA) modified glassy carbon sensor
Cephalexin (Ceph)	-	AuNP modified glassy carbon sensor.
Amoxicillin trihydrate (AMX)	-	MWNT/AuNP and MWNT/PtNP modified glassy carbon sensors

The salient features of the developed sensors are summarized in the following table

Sensor developed	Supporting electrolyte used	Detection limit (M)	Linear concentration range (M)	Difference in peak potential between the bare electrode and modified electrode
MWNT/ Nafion modified Pt sensor for PAM Chloride	Phosphate buffer (pH 8)	3.03×10^{-7}	1×10^{-6}- 2×10^{-5}	Peak potential lowered by 90 mV
MWNT/Nafion modified GC sensor for TAM	Acetate buffer (pH 5)	9.80×10^{-8}	3×10^{-7}- 2×10^{-6}	Peak potential lowered by 148 mV
PB/ MWNT modified GC sensor for HMC	Acetate buffer (pH 2)	7.16×10^{-8}	3×10^{-7}- 1×10^{-6}	Reduction peak appears at -972 mV
poly (p-ABSA) modified GC sensor for Guai	0.1 M HCl	9.55×10^{-7}	2×10^{-6} – 1×10^{-5}	Peak potential lowered by 64 mV
MWNT/poly (p-ABSA) modified GC sensor for Guai	0.1 M HCl	1.47×10^{-8}	2×10^{-6} – 1×10^{-5}	Peak potential lowered by 148 mV
poly (p-ABSA) modified SPCE sensor for Guai	0.1 M HCl	9.35×10^{-5}	2×10^{-4}– 1×10^{-3}	Even though the potential remains the same,0.517 mA increase in peak current
MWNT/poly (p-ABSA) modified SPCE sensor for Guai	0.1 M HCl	1.53×10^{-6}	7×10^{-6}– 2×10^{-6}	Even though the potential remains the same,1.09 mA increase in peak current
AuNP modified GC sensor for Ceph	0.1 M NaOH	1.33×10^{-8}	1×10^{-6}- 1×10^{-5}	Peak potential lowered by 80 mV
MWNT/AuNP modified GC sensor for AMX	Phosphate buffer (pH 7)	1.71×10^{-8}	1×10^{-6}- 1×10^{-5}	Peak potential lowered by 132 mV
MWNT/PtNP modified GC sensor for AMX	Phosphate buffer (pH 7)	4.64×10^{-8}	1×10^{-6}- 1×10^{-5}	Peak potential lowered by 138 mV

The development of chemical and biological sensors is currently one of the most active areas of analytical chemistry research. Sensors are small devices that incorporate a recognition element with a signal transducer. Such devices can be used for direct measurement of the analyte in the sample matrix. There are a variety of combinations of recognition elements and signal transducers. Electrochemical sensors, in which an electrode is used as the transducer element, represent an important subclass of chemical sensors. Such devices hold a leading position among sensors presently available and have found a vast range of important applications in the fields of clinical, industrial, environmental and agricultural analyses. The field of sensors, in general and electrochemical sensors in particular is interdisciplinary and future advances are likely to occur from progress in several disciplines.

.....ꕥ.....

References

[1] J. A. Plambeck, *Electroanalytical Chemistry, Basic Principles and Application,* Wiley Interscience Pub., USA (1982).

[2] T. A. Nieman, D. A. Skoog and F. J. Holler, *Principles of instrumental analysis*, Pacific Grove, California (1998).

[3] P. T. Kissenger and W. R. Heineman, *Laboratory Techniques in Electroanalytical Chemistry*, 2nd Edn., Marcel Dekker, New York (1996).

[4] J. Wang, *Electroanalytical Chemistry*, 3rd Edn., Wiley-VCH Pub., New Jersey (2006).

[5] M. R. Smyth and J. G. Vos, *Analytical Voltammetry*. XXVII, Elsevier Science Pub., Amsterdam (1992).

[6] S. A. Ozkan, B. Uslu and H. Y. Aboul-Enein, *Crit. Rev. Anal. Chem*., **33**, 155 (2003).

[7] J. Bard and L. R. Faulkner, *Electrochemical Methods. Fundamentals and Applications,* 2nd Edn., John Wiley &Sons Inc., New York (2001).

[8] R. Kellner, J. M. Mermet, M. Otto, M. Valcarcel and H. M. Widmer, *Analytical Chemistry: A Modern Approach to Analytical Science*, 2nd Edn., Wiley-VCH Pub., Weinheim (2004).

[9] J. P. Hart, *Electroanalysis of Biologically Important Compounds*, Ellis Horwood Pub., New York (1990).

[10] Uslu and S. A. Ozkan, *Anal. Lett*., **40**, 817 (2007).

[11] B. Uslu and S. A. Ozkan, *Comb. Chem. High Through. Screen.,* **10**, 495 (2007).

[12] J. Wang, B. Tian, J. Wang, J. Lu, C. Olsen, C. Yarnitzky, K. Olsen, D. Hammerstrom and W. Bennett, *Anal. Chim. Acta,* **385**, 429 (1999).

[13] K. Z. Brainina and E. Neyman, *Electroanalytical Stripping Methods.* 26, John Wiley&Sons Inc., New York (1993).

[14] J. Wang, *Electroanalytical Techniques in Clinical Chemistry and Laboratory Medicine.* Wiley-VCH Pub., New York (1988).

[15] D. Harvey, *Modern Analytical Chemistry*, McGrawHill Company, Boston (2000).

[16] S. A. Ozkan, *Curr. Pharm. Anal.,* **5**, 127 (2009).

[17] X. Zhang, H. Ju and J. Wang, *Electrochemical sensors, biosensors and their biomedical applications*, Elsevier, Academic press (2008).

[18] Joseph, Z. Stetter, W. R. Penrose and S. Yao, *J .Electrochem. Soc.*, **150**, S11 (2003).

[19] R. W. Cattrall, *Chemical Sensors,* Oxford Chemistry Premiers, New York (1997).

[20] M. Whitfield, and D. Jagner, *Marine electrochemistry: A practical introduction,* John Wiley &Sons Inc., (1981).

[21] S. P. Kounaves *"Voltammetric Techniques" in Handbook of Instrumental Techniques for Analytical Chemistry*, Upper saddle river, NJ (1997).

[22] C. C. Liu, *"Electrochemical Sensors." The Biomedical Engineering Handbook,* 2nd Edn., CRC Press LLC, (2000).

[23] W. Bott, *Current Separations*, **14**, 64 (1995).

[24] M. A. T. Gilmartin and J. P. Hart, *Analys*t, **120**, 1029 (1995).

[25] C. M. A. Brett and A. M. O. Brett, *Electroanalysis,* Oxford University Press, Oxford (1998).

[26] C. M. A. Brett, *Electroanal.*, **11**, 1013 (1999).

[27] H. Shirakawa, E. J. Louis, A. G. MacDiarmid, C. K. Chiang and A. J. Heeger, *J. Chem. Soc., Chem. Commun.,* **474**, 578 (1977).

[28] M. Delamar, P. C. Lacaze, J. S. Dumousseau and J. E. Dubois, *Electrochim. Acta,* **27**, 61 (1982).

[29] G. E. Wnek, J. C. W. Chien, F. E. Karasz and C. P. Lillya, *Polymer,* **20**, 1441 (1979).

[30] F. Diaz, K. K. Kanazawa and G. P. Gardini, *J. Chem. Soc., Chem. Commun.,* **1**4, 635 (1979).

[31] G. Tourillon and F. Garnier, *J. Electroanal. Chem.,* **135**, 173 (1982).

[32] F. Diaz and J. A. Logan, *J. Electroanal. Chem.,* **111**, 111 (1980).

[33] D. T. McQuade, A. E. Pullen and T. M. Swager, *Chem. Rev.,* **100**, 2537 (2000).

[34] Y. Wang, H. Xu, J. Zhang and G. Li, *Sensors,* **8**, 2043 (2008).

[35] N. Shipway, E. Katz and I. Willner, *Chem. Phys. Chem.*, **1**, 18 (2000).

[36] N. L. Rosi and C. A. Mirkin, *Chem. Rev.*, **105**, 1547 (2005).

[37] S. Agasti, S. Rana, M. H. Park, C. K. Kim, C. C. You and V. M. Rotello, *Adv. Drug Delivery Rev.*, **62**, 316 (2010).

[38] P. Alivisatos, *Nat. Biotechnol.*, **22**, 47 (2004).

[39] Asefa, C. T. Duncan and K. K. Sharma, *Analyst*, **134**, 1980 (2009).

[40] M. M. C. Cheng, G. Cuda, Y. L. Bunimovich, M. Gaspari, J. R. Heath, H. D. Hill, C. A. Mirkin, A. J. Nijdam, R. Terracciano, T. Thundat and M. Ferrari, *Curr. Opin. Chem. Biol.,* **10**, 11 (2006).

[41] P. Pandey, M. Datta and B. D. Malhotra, *Anal. Lett.*, **41**, 159 (2008).

[42] C. M. Niemeyer, *Angew. Chem. Int. Ed.*, **40**, 4128 (2001).

[43] N. C. Tansil and Z. Q. Gao, *Nano Today*, **1**, 28 (2006).

[44] K. Welser, R. Adsley, B. M. Moore, W. C. Chan and J. W. Aylott, *Analyst*, **136**, 29 (2011).

[45] L. West and N. J Halas, *Curr. Opin. Biotechnol.*, **11**, 215 (2000).

[46] K. Khanna, *Def. Sci. J.*, **58**, 608 (2008).

[47] Saha, S. S. Agasti, C. Kim, X. Li, and V. M. Rotello, *Chem. Rev.*, **112**, 2739 (2012).

[48] E. Boisselier and D. Astruc, *Chem. Soc. Rev.*, **38**, 1759 (2009).

[49] C. Daniel and D. Astruc, *Chem. Rev.*, **104**, 293 (2004).

[50] H. Haick, *J. Phys. D: Appl. Phys.*, **40**, 7173 (2007).

[51] Zayats, R. Baron, I. Popov and I. Willner, *Nano Lett.*, **5**, 21 (2005).

[52] Zhao, M. A. Brook and Y. F. Li, *Chem. Bio. Chem.*, **9**, 2363 (2008).

[53] U. H. F. Bunz and V. M. Rotello, *Angew. Chem. Int. Ed.*, **49**, 3268 (2010).

[54] R. A. Sperling, P. R. Gil, F. Zhang, M. Zanella and W. J. Parak, *Chem. Soc. Rev.*, **37**, 1896 (2008).

[55] S. H. Radwan and H. M. E. Azzazy, *Expert Rev. Mol. Diagn.*, **9**, 511 (2009).

[56] S. W. Zeng, K. T. Yong, I. Roy, X. Q. Dinh, X. Yu and F. Luan, *Plasmonics*, **6**, 491, (2011).

[57] R. Wilson, *Chem. Soc. Rev.*, **37**, 2028 (2008).

[58] E. Scavetta, S. Stipa and D. Tonelli, *Electrochem. Commun.,* **9**, 2838 (2007).

[59] Chu, D. Duan, G. Shen and R. Yu, *Talanta*, **71**, 2040 (2007).

[60] K. B. Male, S. Hrapovic and J. H. T. Luong, *Analyst*, **132,** 1254 (2007).

[61] Yang, Y. Yang, Y. Liu, G. Shen and R. Yu, *Biosens. Bioelectron.*, **21**, 1125 (2006).

[62] H. F. Cui, J. S. Ye, W. D. Zhang, C. M. Li, J. H. T. Luong and F. S. Sheu, *Anal. Chim. Acta*, **594**, 175 (2007).

[63] F. Qu, M. Yang, G. Shen and R. Yu, *Biosens. Bioelectron.*, **22**, 1749 (2007).

[64] J. Li and X. Lin, *Biosens. Bioelectron.,* **22**, 2898 (2007).

[65] D. Harvey, *Analytical Chemistry 2.0*: Chapter 11: Electrochemical Methods, saylor.org,

[66] C. R. Raj, T. Okajima and T. Ohsaka, *J. Electroanal. Chem.,* **543**, 127 (2003).

[67] K. C. Ho, C. Y. Chen, H. C. Hsu, L. C. Chen, S. C. Shiesh and X. Z. Lin, *Biosens. Bioelectron.,* **20**, 3 (2004).

[68] F. H. Wu, G. C. Zhao, X. W. Wei, and Z. S. Yang, *Microchim. Acta,* **144**, 243 (2004).

[69] Qiao and S. F. Wang, *Microchim. Acta,* **151,** 47 (2005).

[70] D. Sun, H. Wang and K. Wu, *Microchim. Acta*, **152**, 255 (2006).

[71] L. Wang, J. Bai, P. Huang, H. Wang, L. Zhang and Y. Zhao, *Electrochem. Commun.,* **8**, 1035 (2006).

[72] Yang, G. Hu, X. Chen, J. Zhao and G. Zhao, *Colloids Surf., B*, **54,** 230 (2007).

[73] L. Wang, P. Huang, J. Bai, H. Wang, L. Zhang and Y. Zhao, *Chem. Anal. (Warsaw),* **52**, 25 (2007).

[74] L. Zhang, C. Zhang and J. Lian, *Biosens. Bioelectron.,* **24**, 690 (2008).

[75] Ya, D. Luo, G. Zhan, and C. Li, *Bull. Korean Chem. Soc*., **29**, 928 (2008).

[76] K. J. Huang, X. Liu, W. Z. Xie and H. X Yuan, *Colloids Surf., B*, **64**, 269 (2008).

[77] U. Yogeswaran and S. M. Chen, *Sensor. Actuat. B: Chem.,* **130,** 739 (2008).

[78] K. J. Huang, X. Liu, W. Z. Xie and H. X. Yuan, *Microchim. Acta*, **162**, 227 (2008).

[79] C. Yang, S. Zhang, Y. Liu and W. Huang, *Front. Chem. China.*, **3**, 353 (2008).

[80] G.P. Jin, J. Li and X. Peng, *J. Appl. Electrochem.,* **39**, 1889 (2009).

[81] S. Issac and K. Girish Kumar, *Drug Test. Anal.*, **1,** 350 (2009).

[82] S. Yang, L. Qu, G. Li, R. Yang and C. Liu, *J. Electroanal. Chem.,* **645**, 115 (2010).

[83] M. Behpour, E. Honarmand, and S. M. Ghoreishi, *Bull. Korean Chem. Soc.*, **31**, 845 (2010).

[84] M. Behpour, S. M. Ghoreishi and E. Honarmand, *Int. J. Electrochem. Sci.,* **5**, 1922 (2010).

[85] X. Chen, Z. Wang, F. Zhang, L. Zhu, L. Yanhui and Yanzhi XI, *Chem. Pharm. Bull.* **58**, 475 (2010).

[86] S. Yang, L. Qu, R. Yang, J. Li and L. Yu, *J. Appl. Electrochem.,* **40**,1371 (2010).

[87] R. C. Carvalho, C. C. Gouveia and C. M. A. Brett, *Anal. Bioanal. Chem.*, **398**, 1675 (2010).

[88] B. Habibi, H. Phezhhan and M. P. Azar, *J. Iran. Chem. Soc.,* **7**, 103, (2010).

[89] S. Yang, R. Yang, G. Li, J. Li and L. Qu, *J. Chem. Sci.*, **122**, 919 (2010).

[90] H. K. Maleh, M. Keyvanfard, K. Alizad, M. Fouladgar, H. Beitollahi, A. Mokhtari and F. G. Orimi, *Int. J. Electrochem. Sci.*, **6**, 6141 (2011).

[91] H. M. Moghaddam and H. Beitollahi, *Int. J. Electrochem. Sci.,* **6**, 6503 (2011).

[92] D. B. Kul and M. A. Christopher, *International Journal of Electrochemistry*, 1 (2011).

[93] F. Atta, A. Galal and S. M. Azab, *Int. J. Electrochem. Sci.,* **6**, 5082 (2011).

[94] S. Adekunle, J. G. Ayenimo, X. Y. Fang, W. O. Doherty, O. A. Arotiba and B. B. Mamba, *Int. J. Electrochem. Sci.,* **6**, 2826 (2011).

[95] M. B. Gholivand, A. Azadbakht and A. Pashabadia, *Electroanal.*, **23**, 2771 (2011).

[96] M. L. Ye, B. Xu and W. D. Zhang, *Microchim. Acta*, **172**, 439 (2011).

[97] S. H. Yu and G. C. Zhao, *International Journal of Electrochemistry*, Article ID 431253 **1**,1 (2012).

[98] E. Nagles, P. Alvarez, V. Arancibia, M. Baez, V. Garreton and N. Ehrenfeld, *Int. J. Electrochem. Sci.*, **7**, 11745 (2012).

[99] S. Shahrokhiana and S. Rastgara, *Electrochim. Acta,* **78**, 422 (2012).

[100] K. Li, X. Zhu and Y. Liang, *Pharmacology & Pharmacy*, **3,** 275 (2012).

[101] X. Tian, C. Cheng, H. Yuan, J. Du, D. Xiao, S. Xie and M. F. C. Martin, *Talanta*, **93,**79 (2012).

[102] M. Sadikoglu, G. Taskin, F. G. Demirtas, B. Selvi and M. Barut, *Int. J. Electrochem. Sci.,* **7**, 11550 (2012).

[103] X. Sun, S. Du and X. Wang, *Eur. Food Res. Technol*., **235**, 469 (2012)

[104] H. Beitollahi, A. Mohadesi, S. K. Mahani, H. K. Maleh and A. Akbari, *Turk. J. Chem.*, **36**, 526 (2012).

[105] S. Kumar and V. V. Beckett, *Beilstein J. Nanotechnol.*, **3**, 388 (2012).

[106] B. Unnikrishnan, P. C. Hsu and S. M. Chen, *Int. J. Electrochem. Sci.,* **7**, 11414 (2012).

[107] H. K. Maleh, M. Keyvanfard, K. Alizad, V. Khosravi and M. Asnaashariisfahani, *Int. J. Electrochem. Sci.,* **7**, 6816 (2012).

[108] J. Zhou, F. Wang, K. Zhang, G. Song, J. Liu and B. Ye, *Microchim. Acta,* **178**,179 (2012).

[109] K. S. Ngai, W. T. Tan, Z. Zaina, R. B. M. Zawawi and M. Zidan, *Int. J. Electrochem. Sci.,* **7**, 4210 (2012).

[110] G. Ziyatdinova, M. Morozov and H. Budnikov, *J. Solid State Electrochem.,* **16**, 2441 (2012).

[111] W. Guo, M. Geng and L. Zhou, *Anal. Sci.*, **28**, 693 (2012).

[112] Mohadesi, *Int. J. Electrochem. Sci.*, **7**, 2430 (2012).

[113] W. C. Chen, B. Unnikrishnan and S. M. Chen, *Int. J. Electrochem. Sci.,* **7**, 9138 (2012).

[114] T. Jos, S. Issac, R. Joseph, L. Rajith and K. Girish Kumar, *Micro Nano Lett.,***7**, 854 (2012).

[115] M. R. Shahmiri, A. Bahari, H. K. Maleh, R. Hosseinzadeh and N. Mirnia, *Sensor. Actuat. B: Chem.,* **177**, 70 (2013).

[116] M. Ansari, S. Kazemi, M. A. Khalilzadeh, H. K. Maleh and M. B. P. Zanousi, *Int. J. Electrochem. Sci.,* **8**, 1938 (2013).

[117] K. Girish Kumar and L. Karpagaselvi, *Analyst*, **119**, 1375 (1994).

[118] K. Girish Kumar and R. Letha, *J. Pharm. Biomed. Anal.*, **15**, 1725 (1997).

[119] K. P. R. Chowdary and K. Girish Kumar, *Indian Drugs*, **35**, 645 (1998).

[120] G. Devala Rao, K. Girish Kumar and K. P. R. Chowdary, *J. Indian Council of Chemists*, **17**, 32 (2000).

[121] K. Girish Kumar, K. P. R. Chowdary and G. Devala Rao, *The Antiseptic*, **98**, 453 (2001).

[122] G. Karthikeyan, K. Mohanraj, K. P. Elango and K. Girish Kumar, Trans. *Metal. Chem.*, **29**, 86 (2004).

[123] K. Girish Kumar, S. John, R. Poduval and P. Augustine, *The Chinese Pharm. Jour.*, **57**, 29 (2005).

[124] G. Karthikeyan, K. Mohanraj, K. P. Elango and K. Girish Kumar, *Russ. Jour. Coordi. Chem*., **32,** 380 (2006).

[125] K. Girish Kumar, S. John, P. Augustine, R. Poduval and B. Saraswathyamma, *Anal. Sci*., **23**, 291 (2007).

[126] B. Saraswathyamma, I. Grzybowska, Cz. Orlewska, J. Radecki, W. Dehaen, K. Girish Kumar and H. Radecka, *Electroanal*., **20**, 2317 (2008).

[127] B. Saraswathyamma, M. Pajak, J. Radecki, W. Maes, W. Dehaen, K. Girish Kumar and H. Radecka, *Electroanal*., **20**, 2009 (2008).

[128] R. Joseph and K. Girish Kumar, *Anal. Lett*., **42**, 2309 (2009).

[129] L. Rajith and K. Girish Kumar, *Drug Test. Anal*., **2**, 436 (2010).

[130] S. Issac and K. Girish Kumar, *Anal. Methods*, **2**, 1484 (2010).

[131] R. Joseph and K. Girish Kumar, *Drug Test. Anal*., **2**, 278 (2010).

[132] R. Joseph and K. Girish Kumar, *Anal. Sci*., **27**, 67 (2011).

[133] L. Rajith, A K Jissy, K. Girish Kumar and Ayan Datta, *J. Phys. Chem. C*, **15**, 21858 (2011).

[134] D. Thomas, L. Lonappan, L. Rajith, S. T. Cyriac and K. Girish Kumar, *J. Fluores,* (in press), 2013.

[135] S. C. Tsang, Y. K. Chen, P. J. E. Harris and M. L. H. Green, *Nature*, **372**, 159 (1994).

[136] S. A. Kumar and S. M. Chen, *J. Mol. Catal. A-Chem*., **278**, 244 (2007).

[137] X. Dai and R. G. Compton, *Anal. Sci*., **22**, 567 (2006).

[138] Pharmacopoeia of India, 3rd Edn., Controller of India, Delhi, 407 (1985).

[139] United states pharmacopoeia, The national formulary reissue, official monographs, USP 33, 981.

[140] H. G. Brittain, *Analytical Profiles of Drug Substances and Excipients,* **25,** 153 (1998).

[141] British Pharmacopeia, Vols. landl I, H. M. Stationery Office, London, UK (1988).

[142] British Pharmacopaeia, H.M. Stationary Office, London (1993).

[143] http://www.health.state.ny.us/environmental/emergency/chemical_terrorism/nerve_ agents_tech.htm

[144] http://en.wikipedia.org/wiki/Pralidoxime

[145] K. K. Rajic, B. Stankovic, and A. Granov, *J. Pharm. Biomed. Anal.*, **8**, 735 (1990).

[146] H. Kalasz, E. Szoko, T. Tabi, G. A. Petroianu, D. E. Lorke, A. Omar, S. Alaffi, A. Jasem, and K. Tekes, *Med. Chem.,* **5**, 237 (2009).

[147] M. Bodiroga, D. Agbaba, D. Z. Stakic, and R. Popovic, *J. Pharm. Biomed. Anal.,* **12**, 127 (1994).

[148] M. S. Dresselhaus, G. Dresselhaus and P. C. Eklund, *Science of Fullerenes and Carbon Nanotubes*, Academic Press: New York (1996).

[149] J. Kong, N. R. Franklin, C. Zhou, M. G. Chapline, S. Peng, K. Cho, and H. Dai, *Science,* **287**, 622 (2000).

[150] P. G. Collins, K. Bradley, M. Ishigami, and A. Zettl, *Science*, **287**, 1801 (2000).

[151] H. Jianbo, C. Changlun, and L. Jinhuai, *Sens. Actuators B Chem.,* **99**, 1 (2004).

[152] P. G. Collins, A. Zettl, H. Bando, A. Thess, and R. E. Smalley, *Science*, **278**, 100 (1997).

[153] E. Frackowiak, K. Metenier, V. Bertagna, and F. Beguin, *Appl. Phys. Lett.*, **77**, 2421 (2000).

[154] A. C. Dillon, K. M. Jones, T. A. Bekkedahl, C. H. Kiang, D. S. Bethune, and M. J. Heben, *Nature*, **386**, 377 (1997).

[155] A. M. Rao, D. Jacques, R. C. Haddon, W. Zhu, C. Bower, and S. Jin, *Appl. Phys. Lett.,* **76**, 3813 (2000).

[156] J. Wang, M. Musameh and Y. H. Lin, *J. Am. Chem. Soc.*, **125**, 2408 (2003).

[157] A. Salimi, R. G. Compton and R. Hallaj, *Anal. Biochem.*, **333**, 49 (2004).

[158] J. Chen, J. Bao, C. X. Cai and T. H. Lu, *Anal. Chim. Acta*, **516**, 29 (2004).

[159] M. Musameh, J. Wang, A. Merkoci and Y. Lin, *Electrochem. Commun.*, **4**, 743 (2002).

[160] P. J. Britto, K. S. V. Santhanam and P. M. Ajayan, *Bioelectrochem. Bioenerg.*, **41**, 121 (1996).

[161] Q. Liang, Y. Wang, G. Luo and Z. Wang, *J Electroanal. Chem.*, **540**, 129 (2003).

[162] M. Wang, Y. Shen,Y. Liu, T. Wang, F. Zhao, B. Liu and S. Dong, *J Electroanal. Chem.*, **578**, 121 (2005).

[163] Y. Yan, W. Zheng, M. Zhang, L. Wang, L. Su and L. Mao, *Langmuir*, **21**, 6560 (2005).

[164] C. X. Cai and J. Chen, *Anal. Biochem.*, **325**, 285 (2004).

[165] A. Guiseppi-Elie, C. Lei and R. H. Baughman, *Nanotechnology*, **13**, 559 (2002).

[166] L. Qingwen, T. Z Yuntian, A. K. Ian, and H. W. Alan, *J. Phys. Chem. B*, **110**, 13926 (2006).

[167] J. E. B. Randles, *Trans. Faraday. Soc.*, **44**, 322 (1948).

[168] E. Laviron, E. Roullier and C. Degrand, *J. Electroanal. Chem.*, **112**, 11 (1980).

[169] E. Laviron, *J. Electroanal. Chem.,* **52**, 395 (1974).

[170] J. W. Bird and D. G. M. Diaper, *Can. J. Chem.*, **47**, 145 (1969).

[171] K. E. Andersson and C. Sjogren, *Prog. Neurobiol.,* **19**, 71 (1982).

[172] http://www.rxlist.com/flomax-drug/clinical-pharmacology.htm

[173] K. Raghubabu, L. Shanti swarup, B. Kalyanaramu, M. N. Rao and C. Ramdas, *Int. J. Pharm. Bio. Sci.*, **2,** 12 (2012).

[174] C. R. Chapple, *Br. J. Urol.,* **81**, 34 (1998).

[175] J. P. Hieble, D. B. Bylund and D. E. Clarke, *Pharmacol. Rev.*, **47**, 267 (1995).

[176] M. C. Michel, B. Kenny and D. A. Schwinn, *Naunyn Schmiedebergs Arch Pharmacol.*, **352**, 1 (1995).

[177] R. Foglar, K. Shibata, K. Horie, A. Hirasawa and G. Tsujimoto, *Eur. J. Pharmacol.* **288**, 201 (1995).

[178] A. Leonardi, J. P. Hieble, L. Guarneri, D.P. Naselsky, E. Poggesi, G. Sironi, A.C. Sulpizo and R.Testa, *J. Pharmacol. Exp. Ther.,* **281**, 1272 (1997).

[179] K. Taguchi, M. Saitoh, S. Sato, M. Asano and M. C. Michel, *J. Pharmacol. Exp. Ther.*, **280**, 1 (1997).

[180] S. C. Sweetman, Martindale, *The Complete Drug Reference*, 33rd Edn., Pharmaceutical Press, London, 655 (2002).

[181] Goodman and Gilman, *The Pharmacological Basis of Therapeutics*, 9th Edn., Section V, CD ROM, McGraw-Hill (1996).

[182] P. Narayan and A. Tewari, *J. Urol.*, **160**, 1701 (1998).

[183] H. Lepor, *Tamsulosin Invest. Group Urol.,* **51,** 892 (1998).

[184] M. K. Thimmaraju, V. Rao, K. Hemanth, and P. Siddartha Kumar, *JAPS*, **8**,177 **(**2011).

[185] R. N Rao, M. V. N. KTalluri, A. N Raju, D. D Shinde and G. S Ramanjaneyulu, *J. Pharm. biomed. Anal.,* **46**, 94 (2008).

[186] G. S. Kumar and B. S. Pavan Kumar, *J. B. Clin. Pharm.*, **3**, 255 (2012).

[187] D. B. Patel, N. U. Patel and B. G. Chaudhari, *der pharmacia sinica*, **2**, 172 (2011).

[188] S. A. Ozkan, B. Uslu and H. Y. A. Enein, *Talanta*, **61**, 147 (2003).

[189] K. Balasubramanian and M. Burghard, *J. Mater. Chem.*, **18**, 3071 (2008).

[190] P. Sharma and P. Ahuja, *Materials Research Bulletin*, **43**, 2517 (2008).

[191] G. N. Chen, Z. F. Zhao, X. L. Wang, J. P. Duan and H. Q. Chen, *Anal. Chim. Acta*, **452**, 245 (2002).

[192] B. T. Demircigil, S. A. Ozkan, O. Coruh and S. Yilmaz, *Electroanal.*, **14**,122 (2002).

[193] E. Bermejo, A. Zapardiel, J. A. Perez-Lopez, M. Chicharro, A. Sanchez and L. Hernandez, *J. Electroanal. Chem.*, **481**, 52 (2000).

[194] P. Dugo, M. L. Presti, M. Oehman, A. Fazio, G. Dugo and L. Mondello, *J. Sep. Sci.,* **28**, 1149 (2005).

[195] S. Gorinstein, D. Huang, H. Leontowicz, M. Leontowicz, K. Yamamoto, R. Soliva-Fortuny, O. M. Belloso, A. L. M. Ayala and S. Trakhtenberg, *Acta Chromatogr.,* **17**, 108 (2006).

[196] M. Asztemborska and J. Z. ukowski, *J. Chromatogr. A*, **17**, 95 (2006).

[197] H. W. Voigtlaender, R. Rotea and M. A. Montagut, *Cienc. Ind. Farm.*, **10**, 265 (1978).

[198] J. A. Emim, A. B. Oliveira and A. J. Lap, *J. Pharm. Pharmacol.,* **46**, 118 (1994).

[199] E. M. Galati, A. Trovato, S. Kirjavainen and A. M. Forestieri, A. Rossitto and M. T. Monforte, *Farmaco*, **51**, 219 (1996).

[200] G. Carlo, N. Mascolo, A. A. Izzo, and F. Capasso, *Life Sci.*, **65**, 337 (1999).

[201] L. Sung-Heui and L. Tae-Sook, *J. Nutr. Res.,* **19**, 1245 (1999).

[202] H. Doostdar, M. D. Burke and R. T. Mayer, *Toxicol.*, **144**, 31 (2000).

[203] M. J. Alcaraz and M. L. Ferrandiz, *J. Ethnopharm.*, **21**, 209.

[204] S. Silvestri, *Pharm. Acta. Helv.*, **45**, 390 (1970).

[205] J. Gastillo, O. Benavente and F. Borrego, *J. Chromatogr.,* **555**, 285 (1991).

[206] J. Zheng, Z. Meng and H. Zhang, *Sci. China Ser. B, Chemistry*, **48**, 20 (2005).

[207] P. J. Kulesza, K. Miecznikowski, M. Chojak, M. A. Malik, S. Zamponi and R. Marassi, *Electrochim. Acta.,* **46**, 4371 (2001).

[208] R. J. Mortimer, *Chem. Soc. Rev.,* **26**, 147 (1997).

[209] R. Koncki, T. Lenarczuk and S. Glab, *Anal. Chim. Acta,* **424**, 27 (2000).

[210] K. C. Pan, C. S. Chuang, S. H. Cheng and Y. O. Su, *J. Electroanal. Chem.,* **501**, 160 (2001).

[211] G. Zhao, J. J. Feng, Q. L. Zhang, S. P. Li and H. Y. Chen, *Chem. Mater.,* **17**, 3154 (2005).

[212] M. Jayalakshimi and F. Scholz, *J. Power Sources,* **91**, 217 (2000).

[213] A. A. Karyakin, O. V. Gitelmacher and E. E. Karyakina, *Anal. Chem.,* **67**, 2419 (1995).

[214] A. A. Karyakin and E. E. Karyakina, *Sens. Actuators B Chem.,* **57**, 268 (1999).

[215] D. Moscone, D. D'Ottavi, D. Compagnone and G. Palleschi, *Anal. Chem.*, **73**, 2529 (2001).

[216] D. Pan, J. Chen, L. Nie, W. Tao and S. Yao, *Electrochim. Acta*, **49**, 795 (2004).

[217] A. A. Karyakin, E. E. Karyakina and L. Gorton, *Anal. Chem.*, **72**, 1720 (2000).

[218] Q. Chi and S. Dong, *Anal. Chim. Acta*, **310**, 429 (1995).

[219] A. A. Karyakin, E. E. Karyakina and L. Gorton, *Talanta*, **43**, 1597 (1996).

[220] F. Ricci, A. Amine, G. Palleschi and D. Moscone, *Biosens. Bioelectron.*, **18**, 165 (2003).

[221] J. Li, T. Peng and Y. Peng, *Electroanal.*, **15**, 1031 (2003).

[222] R. Garjonyte and A. Malinauskas, *Biosens. Bioelectron.*, **15**, 445 (2000).

[223] J. M. Zen, P. Y. Chen and A. S. Kumar, *Anal. Chem.*, **75**, 6017 (2003).

[224] W. Zhao, J. J. Xu, C. G. Shi and H. Y. Chen, *Langmuir*, **21**, 9630 (2005).

[225] W. Q. Jin, A. Toutianoush, M. Pyrasch, J. Schnepf, H. Gottschalk, W. Rammensee and B. Tieke, *J. Phys. Chem. B*, **107**, 12062 (2003).

[226] X. Zhai, W. Wei, J. Zeng, X. Liu and S. Gong, *Anal. Lett.*, **39**, 913 (2006).

[227] L. Wang, S. J. Guo, X. G. Hu and S. J. Dong, *Colloids. Surf. A*, **317**, 394 (2008).

[228] Z. F. Li, J. H. Chen, W. Li, K. Chen, L. H. Nie and S. Z. Yao, *J. Electroanal. Chem.*, **603**, 59 (2007).

[229] R. J. Chen, H. C. Choi, S. Bangsaruntip, E. H. Yenilmez, X. W. Tang, Q. Wang, Y. L. Chang and H. G. Dai, *J. Am. Chem. Soc.*, **126**, 1563 (2004).

[230] G. A. Goodman, T. W. Rann and A. S. Nlies, *The Pharmacological Basis of Therapeutics*, 8th Edn., Pergamon Press, New York, 638 (1990).

[231] Martindale, *The Extra Pharmacopoeia*, Royal Pharmaceutical Society, London, 1227 (1996).

[232] O. Abdallah, *Int. J. Anal. Chem.,* **10**, 5 (2010).

[233] A. R. Lee and T.M. Hu, *J. Pharm. Biomed. Anal.,* **12**, 747 (1994).

[234] N. B. Pappano, Y. C. D. Micalizzi, N. B. Debattista and F. H. Ferretti, *Talanta*, **44**, 633 (1997).

[235] N. Dubey, S. Sahu and G. N. Singh, *Indian. J. Chemistry*, **51 B**, 1633 (2012).

[236] A. Ozdemir, H. Aksoy, E. Dinc, D. Baleanu and S. Dermis, *Rev. Roum. Chim.*, **51**, 117 (2006).

[237] M. I. Ansari, M. Kazemipour and M. Shahriar, *Ira. J. Pharmacol. Ther.,* **5**, 67 (2006).

[238] M. Senthilraja and P. Giriraj, *Asian J. Pharm. Clin. Res.,* **4**, 1315 (2011).

[239] V. Z. Shahabadi, M. Shamsipur, B. Hemmatenejad and M. Akhond, *Anal. Lett.,* **43**, 687 (2010).

[240] R. Pomponio, R. Gotti, M. Hudaib, V. Andrisano and V. Cavrini, *J. Sep.Sci.*, **24**, 258 (2001).

[241] I. Tapsoba, J. E. Begaied and K. Boujlel, *J. Pharm. Biomed. Anal.*, **38**, 162 (2005).

[242] M. B. Gholivand, A. Azadbakht and A. Pashabadi, *Electroanal.,* **23**, 2771 (2011).

[243] F. Xu, M. N. Gao, L. Wang, G. Y. Shi, W. Zhang, L. T. Jin and J. Y. Jin, *Talanta*, **55**, 329 (2001).

[244] H. Tang, G. Z. Hu, S. X. Jiang and X. Liu, *J. Appl. Electrochem.*, **39**, 2323 (2009).

[245] S. A. Kumar and S. M. Chen, *J. Mol. Catal. A, Chem.*, **278**, 244 (2007).

[246] K. J. Huang, D. F. Luo, W. Z. Xie and Y. S. Yu, *Colloids Surf. B*, **61**, 176 (2008).

[247] G. Y. Jin, F. Huang, W. Li, S. N. Yu, S. Zhang and J. L. Kong, *Talanta*, **74**, 815 (2008).

[248] F. Huang, G. Y. Jin, Y. Liu and J. L. Kong, *Talanta*, **74**, 1435 (2008).

[249] T. W. Odom, J. L. Huang, P. Kim and C. M. Lieber, *Nature*, **391**, 62 (1998).

[250] M. Hughes, G. Z. Chen, M. S. Shaffer, D. J. Fray and A. H. Windle, *Chem. Mater.*, **14**, 1610 (2002).

[251] P. F. Bolado, P. J. L. Ardisama, D. H. Santos and A. C. Garc, *Anal. Chim. Acta*, **638**, 133 (2009).

[252] O. D. Renedo, M. E. B. Calvo and M. J. A. Martinez, *Sensors*, **8**, 4201 (2008).

[253] N. McGuire, K. Honeychurch and J. Hart, *Electroanal.*, **21**, 2165 (2009).

[254] S. A. Wring and J. P. Hart, *Analyst*, **117**, 1281 (1992).

[255] J. Kulys and E. J. D'Costa, *Anal. Chim. Acta*, **243**, 173 (1991).

[256] S. A. Wring, J. P. Hart, L. Bracey and B. J. Birch, *Anal. Chim. Acta*, **231**, 203 (1990).

[257] E. G. Cookeas and C. E. Efstathiou, *Analyst*, **119**, 1607 (1994).

[258] J. W. Bird and D. G. M. Diaper, *Can. J. Chem.*, **47**, 145 (1969).

[259] L.S. Goodman and A. Gilman, *The Pharmacological Basis of Therapeutics*, 10th Edn., McGraw-Hill, New York (2001).

[260] A. P. Argekar, S. V. Raj and S. U. Kapadia, *Anal. Lett.*, **30**, 821 (1997).

[261] P. Priyanka and P. Suresh, *Asian J. Pharm.*, **2**, 120 (2008).

[262] A. B. C. Yu, C. H. Nightingale and D. R. Flanagan, *J. Pharm. Sci.*, **66**, 213 (1977).

[263] D. R. E. Wasseef, *Spectrosc. Lett.*, **40**, 797 (2007).

[264] T. Nakagawa, J. Haginaka, K. Yamaoka and T. Uno, *J. Antibiot.*, **31**, 769 (1978).

[265] D. Zendelovska, T. Stafilov and S. Petrov, *Acta. Pharm.*, **52**, 243 (2002).

[266] P. C. Falc, A. S. Cabeza, L. G. Martinez, F. B. Reig and I. M. Mansanet, *Michrochim. Acta*, **126**, 207 (1997).

[267] J. H. Mtindez, A. S. Pfirez, M. D. Zamarreno and L. V. Las, *Anal. Chim. Acta*, **160**, 335 (1984).

[268] Y. Chen, L. Huang and Q. Lin, *Int. J. Electrochem. Sci.*, **7**, 7948 (2012).

[269] O. Chailapakul, A. Fujishima, P. Tipthara, and H. Siriwongchal, A*nal. Sci*., **17**, 419, (2001).

[270] A. Dekanski, J. Stevanovic, R. Stevanovic, B. Z. Nikolic and V. M. Jovanovic, *Carbon*, **39**, 1195 (2001).

[271] D. Martel and A. Kuhn, *Electrochim. Acta*, **45**, 1829 (2000).

[272] J. H. Ye and P. S. Fedkiw, *Electrochim. Acta*, **41**, 221 (1996).

[273] A. Sarapuu, K. Tammeveski, T. T. Tenno, V. Sammelselg, K .Kontturi and D. J. Schiffrin, *Electrochem. Commun.*, **3**, 446 (2001).

[274] M. C. Daniel and D. Astruc, *Chem. Rev.*, **104**, 293 (2004).

[275] Y. Zhuo, R. Yuan, Y. Q. Chai, Y. Zhang, X. L. Li, Q. Zhu and N. Wang, *Anal. Chim. Acta*, **548**, 205 (2005).

[276] Z. M. Liu, Y. Yang, H. Wang, Y. L. Liu, G. L. Shen and R. Q. Yu, *Sensor. Actuat. B*, **106**, 394 (2005).

[277] S. S. Kumar, J. Mathiyarasu and K. L. Phani, *J. Electrochem. Chem.*, **578**, 95 (2005).

[278] L. Zhang, X. Jiang, E. K. Wang and S. J. Dong, *Biosens. Bioelectron.*, **21**, 337 (2005).

[279] X. Dai, O. Nekrassoya, M. E. Hyde and R. G. Compton, *Anal. Chem.*, **76**, 5924 (2004).

[280] L. Wang and E. K. Wang, *Electrochem. Commun.*, **6**, 49 (2004).

[281] V. V. Shumyantseva, S. Carrara, V. Bavastrello, D. J. Riley, T. V. Bulko, K. G. Skryabin, A. I. Archakov and C. Nicolini, *Biosens. Bioelectron.*, **21**, 217 (2005).

[282] Y. Ma, J. Di, X. Yan, M. Zhao, Z. Lu and Y. Tu, *Biosens. Bioelectron.*, 24, 1480 (2009).

[283] F. E. Cheick, F. Rashwan, H. Mahmoud and M. E. Rouby, *J. Solid State Electrochem.*, **14**, 1425 (2010).

[284] S. Schimpf, M. Lucas, C. Mohr, U. Rodemerck, A. Brückner, J. Radnik, H. Hofmeister and P. Claus, *Catal. Today*, **72**, 63 (2002).

[285] H. Berndt, A. Martin, I. Pitsch, U. Prüsse and K. D. Vorlop, *Catal. Today*, **191**, 91 (2004).

[286] D. B. Akolekar and S. K. Bhargava, *J. Mol. Catal. A: Chem.*, **77**, 236 (2005).

[287] H. Shi, H. Bi, B. Yao and L. Zhang, *Appl. Surf. Sci.*, **276**, 161 (2000).

[288] http://www.nlm.nih.gov/medlineplus/druginfo/medmaster/a685001.html

[289] British Pharmacopoeia, CD, ROM (2000).

[290] P. O. Erah, A. F. Goddard, D. A. Barrett, P. N. Shaw and R. C. Spiller, *J. Antimicrob. Chemother.,* **39**, 5 (1997).

[291] P. O. Erah, A. F. Goddard, D. A. Barrett, P. N. Shaw and R. Spiller, *Pharm. Sci.*, **1**, 597 (1995).

[292] A. Tsuji, E. Nakashima, S. Hamano and T. Yamana, *J. Pharm. Sci.*, **67**,1059 (1978).

[293] H. J. Mascher and C. Kikuta, *J. Chromatogr. A*, **812,** 221 (1998).

[294] H. Mascher and C. Kikuta, *J. Chromatogr. A*, **506**, 417 (1990).

[295] M. Q. A. Abachi, H. Haddi and A. M. A. Abachi, *Anal. Chim. Acta,* **554,** 184 (2005).

[296] G.G. Mohamed, *J. Pharm. Biomed. Anal.,* **24**, 561 (2001).

[297] Q. Li and Z. Yang, *Anal. Lett.,* **39**, 763 (2006).

[298] K. H. A. Saidi and S. S. Abdulameer, *Journal of Biotechnology Research*, **5**, 49 (2011).

[299] G. Pajchel, K. Pawłowski and S. Tyski, *J. Pharm. Biomed. Anal.,* **29**, 75 (2002).

[300] J. Du, Y. Li and J. Lu, *Anal. Lett.,* **35**, 2295 (2002).

[301] G. Altiokka, N. O. Can and H. Y. Aboul-Enein, *J. Liq. Chromatogr. R. T.*, **30**, 1333 (2007).

[302] Y. Sun, Y. Tang, H. Yao and Y. Li, *Anal. sci.*, **21**, 457 (2005).

[303] Q. Peia, G. P. Yang, Z. J. Li, X. D. Peng, J. H. Fan and Z. Q. Liu, *J. Chromatogr. B,* **879**, 2000 (2011).

[304] G. Hoizey, D. Lamiable, C. Frances, T. Trenque, M. Kaltenbach, J. Denis and H. Millart, *J. Pharm. Biomed. Anal.,* **30**, 661 (2002).

[305] H. J. Mascher and C. Kikuta, *J. Chromatogr. B,* **812**, 221 (1998).

[306] J. I. D. Wibawa, D. Fowkes, P. N. Shaw and D. A. Barrett, *J. Chromatogr. B,* **774**, 141, (2002).

[307] W. Li, F. Tan and K. Zhao, *J. Pharm. Biomed. Anal.,* **41**, 594 (2006).

[308] K. H. Yoon, S. Y. Lee, W. Kim, J. S. Park and H. J. Kim, *J. Chromatogr. B,* **813**, 121 (2004).

[309] S. M. Foroutan, A. Zarghi, A. Shafaati, A. Khoddam and H. Movahed, *J. Pharm. Biomed. Anal.,* **45**, 531 (2007).

[310] H. J. Nelis, J. Vandenbranden, A. D. Kruif, and A. P. D. Leenheer, *Antimicrob. Agents. Chemother.,* **36**, 1859 (1992).

[311] T. L. Lee, L. D. Arconte and M. A. Brooks, *J. Pharm. Sci.*, **68,** 454 (1979).

[312] D. P. Santos, M. F. Bergamini and M. V. B. Zanoni, *Sensor. Actuat. B; Chem.,* **133**, 398 (2008).

[313] B. Uslu and I. Biryol, *J. Pharm. Biomed. Anal.,* **20**, 591 (1999).

[314] B. Rezaei and S. Damiri , *Electroanal.,* **21**, 1577 (2009).

[315] A. N. Shipway, E. Katz and I. Willner, *Chem. Phys. Chem.*, **1**, 18 (2000).

[316] C. M. Cobley, J. Y. Chen, E. C. Cho, L. V. Wang and Y. N. Xia, *Chem. Soc. Rev.*, **40**, 44 (2011).

[317] R. D. Powell and J. F. Hainfeld, *Micron*, **42**, 163 (2011).

[318] N. Uehara, *Anal. Sci.*, **26**, 1219 (2010).

[319] J. Tashkhourian, M. R. H. Nezhad, J. Khodavesi and S. Javadi, *J. Electroanal. Chem.,* **633**, 85 (2009).

[320] W. N. Hu, D. M. Sun and W. Ma, *Electroanal.*, **22**, 584 (2010).

[321] U. Yogeswaran, S. Thiagarajan and S. M. Chen, *Anal. Biochem.,* **365**, 122 (2007).

[322] S. Thiagarajan and S. M. Chen, *Talanta*, **74**, 212 (2007).

[323] J. S. Huang, Y. Liu, H. Q. Hou and T. Y. You, *Biosens. Bioelectron*., **24**, 632 (2008).

[324] G. G. Wildgoose, C. E. Banks and R. G. Compton., *Small*, **2**, 182 (2006).

[325] A. K. Gupta and M. Gupta, *Biomater.,* **26**, 3995 (2005).

[326] H. Hong, Y. Zhang, J. Sun and W. Cai, *Nano Today*, **4**, 399 (2009).

[327] S. J. Liu and C. H. Huang, C. K. Huang and W. S. Hwang, *Chem. Commun.*, **32**, 4809 (2009).

[328] Y. Sun and Y. Xia, *Science*, **298**, 2176 (2002).

[329] C. J. Murphy, T. K. Sau, A. M. Gole, C. J. Orendorff, J. Gao, L. Gou, S. E. Hunyadi, and T. Li, *J. Phys. Chem. B*, **109**, 13857 (2005).

[330] Y. Xia, P. Yang, Y. Sun, Y. Wu, B. Mayers, B. Gates, Y. Yin, F. Kim and H. Yan, *Adv. Mater.*, **15**, 353 (2003).

[331] D. S. Kim, T. Lee and K. E. Geckeler, *Angew. Chem. Int. Ed.*, **45**, 104 (2006).

[332] N. I. Kovtyukhova, B. K. Kelley and T. E. Mallouk. *J. Am. Chem. Soc.*, **126**, 12738 (2004).

[333] J. G. Huang, T. Kunitake and S. Onoue, *Chem. Commun*., **8**, 1008 (2004).

[334] V. Georgakilas, D. Gournis, V. Tzitzios, L. Pasquato, D. M. Guldi and M. Prato, *J. Mater. Chem.*, **17**, 2679 (2007).

[335] B. Jia, L. Gao and J. Sun, *Carbon*, **45**, 1476 (2007).

[336] H. Wang, L. Cao, S. Yan, N. Huang and Z. Xiao, *Mater. Sci. Eng. B.*, **164**, 191(2009).

[337] Y. Guo, S.h. Guo, Y. Fang and S. H. Dong, *Electrochim. Acta*, **55**, 3927 (2010).

[338] H. J. Jiang, Y. Zhao, H. Yang and D. L. Akins, *Mater. Chem. Phys.,* **114**, 879 (2009).

[339] V. W. S. Hung and K. Kerman, *Electrochem. Commun.*, 13, 328 (2011).

[340] N. Alexeyeva, J. Kozlova, V. Sammelselg, P. Ritslaid, H. Mandar and K. Tammeveski, *Appl. Surf. Sci.*, **256**, 3040 (2010).

[341] F. Xiao, F. G. Zhao, J. Li, L. Liu and B. Zeng, *Electrochim. Acta,* **53**, 7781 (2008).

[342] A. I. Gopalan, K. P. Lee and D. Ragupathy, *Biosens. Bioelectron.*, **24**, 2211 (2009).

[343] M. P. N. Bui, X. H. Pham, K. N. Han, C. A. Li, E. K. Lee, H. J. Chang and G. H. Seong, *Electrochem. Commun.*, **12**, 250 (2010).

[344] T. M. Day, P. R. Unwin and J. V. Macpherson, *Nano Lett.*, **7**, 51 (2007).

[345] X. Dai, O. Nakrassova, M. E. Hyde and R. Compton, *Anal. Chem.*, **76,** 5924 (2004).

[346] U.S. Mohanty, *J. Appl. Electrochem.,* **41**, 257 (2011).

[347] G. G. Wildgoose, C. E. Banks and R. G. Compton, *Small*, 2, 182 (2006).

[348] H. S. Liu, C. J. Song, L. Zhang, J. J. Zhang, H. J. Wang and D. P. Wilkinson. *J Power Sources*, **155**, 95 (2006).

[349] X. W. Yu, P. G. Pickup, *J Power Sources*, **182**, 124 (2008).

[350] E. Antolini, *J Power Sources*, **170**, 1 (2007).

[351] H. Lee, S. E. Habas, S. Kweskin, D. Butcher, G. A. Somorjai and P. Yang, *Angew. Chem. Int. Ed.*, **45**, 7824 (2006).

[352] T. S. Ahmadi, Z. L. Wang, T. C. Green, A. Henglein and M. A. El-Sayed, *Science*, **272**, 1924 (1996).

[353] X. G. Hu, T. Wang and S. J. Dong, *J Nanosci. Nanotechnol.*, **6**, 2056 (2006).

[354] C. Wang, H. Daimon, Y. Lee, J. Kim and S. H. Sun, *J. Am. Chem. Soc.,* **129**, 6974 (2007).

[355] J. Y. Chen, T. Herricks, M. Geissler and Y. N. Xia, *J. Am. Chem. Soc.,* **126**, 10854 (2004).

[356] T. Kijima, T. Yoshimura, M. Uota, T. Ikeda, D. Fujikawa, S. Mouri and S. Uoyama, *Angew. Chem. Int. Ed.*, **43**, 228 (2004).

[357] X. W. Teng and H. Yang, *Nano Lett.*, **5**, 885 (2005).

[358] J. Y. Chen, T. Herricks and Y. N. Xia, *Angew. Chem. Int. Ed.*, **44**, 2589 (2005).

[359] E. P. Lee, Z. M. Peng, D. M. Cate, H. Yang, C. T. Campbell and Y. N. Xia, *J. Am. Chem. Soc.,* **129**, 10634 (2007).

[360] V. Lordi, N. Yao and J. Wei, *Chem. Mater.,* **13**, 733 (2001).

[361] M. Endo, Y. A. Kim, M. Ezaka, K. Osada, T. Yanagiswa, T. Hayashi, M. Terrones and M. S. Dresselhaus, *Nano Lett.,* **3**, 723 (2003).

[362] D. L. Boxall, G. A. Deluga, E. A. Kenik, W. D. King and C. M. Lukehart, *Chem. Mater.,* **13**, 891 (2001).

[363] S. J. Gullón, V. Montiel, A. Aldaz and J. Clavilier, *J. Electroanal. Chem.,* **491**, 69 (2000).

[364] Z. L. Liu, J. Y. Lee, M. Han, W. X. Chen and L. M. Gan, *J. Mater. Chem.,* **12**, 2453 (2002).

[365] W. Z. Li, C. H. Liang, W. J. Zhou, J. S. Qiu, Z. H. Zhou, G. Q. Sun and Q. Xin, *J. Phys. chem.,* **107**, 6292 (2003).

[366] G. Yu, .W Chen, J. Zhao and Q. Nie, *J. Appl. Electrochem.,* **36**, 1021 (2006).

[367] W. X. Chen, J. Zhao, J. Y. Lee and Z. L. Liu, *Mater. Chem. Phys.*, **91**, 124 (2005).

[368] X. H. Xue, T. H. Lu, C. P. Liu and W. Xing, *Chem. Commun.,* **12**, 1601 (2005).

[369] J. B. Goodenough, A. Hamnett, B. J. Kennedy, R. Manoharan and S. A. Weeks, *Electrochim. Acta*, **35**, 199 (1990).

[370] E. Laviron, *J. Electroanal. Chem.,* **52**, 355 (1974).

.....ꕥ.....

List of Publications

International Journals

[1] S. Mathew, L. Rajith, **L. Laina**, T. Jos, K. Girish Kumar, A lead (II) selective PVC membrane potentiometric sensor based on a tetra azamacrocyclic ligand. *J. Incl. Phenom. Macrocycl. Chem.* (*in press*), 2013.

[2] D. Thomas, **L. Laina**, L. Rajith, S. T. Cyriac, K. Girish Kumar**,** Quantum Dots (QDs) based fluorescent sensor for the selective determination of Nimesulide. *J. Fluores.* (*in press*), 2013.

[3] A.E. Vikraman, Z. Rasheeed, **L. Laina**, L. Rajith, K. Girish Kumar, MWCNT modified gold electrode sensor for the determination of propyl gallate in vegetable oils. *Food Anal. Methods, (in press), (*2013).

[4] D. Thomas, L. Rajith, **L. Laina**, S. Issac, K. Girish Kumar, Sensitive determination of nitrite in food samples using Voltammetry, *Food Anal. Methods*, **5**, 752 (2012).

[5] **L. Laina**, S.Issac, R. Joseph, D.Thomas, K. Girish Kumar, Electrochemical studies of TAM using Multiwalled carbon nanotube modified Glassy carbon sensor, *Micro Nano Lett.*, **6**, 867 (2011).

[6] **L. Laina**, K. Girish Kumar, Carbon nanotube based sensor for the differential pulse voltammetric determination of Pyridine -2- Aldoxime Methochloride, *Sensor Lett.*, **9,** 541 (2011).

.....ഌ.....

Conference papers

[1] PB/MWNT composite based sensor for the determination of hesperidin methyl chalcone. (Swadeshi Science Congress, Kasaragod, November 2012)

[2] Carbon nanotube based sensor for voltammetric determination of Hesperidin methyl chalcone (C Tric, Cochin University of Science and Technology, Kochi, March 2011).

[3] Carbon nanotube based sensor for the differential pulse voltammetric determination of PAM Chloride (National seminar on "New horizons of physics", St. Paul's college, Kalamassery, Kochi, August 2011)

[4] Carbon nanotube based sensor for the differential pulse voltammetric determination of tamsulosin hydrochloride. (1st Kerala Women's Science Congress, St.Teresa's College, Ernakulam, August 2010).

[5] The electrochemical behavior of PAM Chloride at a multiwalled carbon nanotube-nafion modified Platinum electrode. (National Seminar on Emerging Trends in Pharmaceutical Analysis, Vijayawada, February 2009).

.....ൠ.....